

MASTER THESIS

---

# Unstable Particles and Resonances

---

*Author:*  
JEROEN RODENBURG

*Supervisor:*  
Prof. dr. ERIC LAENEN

## Abstract

In the standard model all but the lightest particles are unstable. Any scattering process that proceeds by the production and subsequent decay of such an unstable particle, becomes enhanced when the center-of-mass energy  $s$  approaches its mass  $m^2$ . Since self-energy corrections are also enlarged in this phase space region, perturbation theory breaks down. Several schemes have been developed to overcome this problem, including resumming the propagator, the narrow-width approximation, the complex mass scheme and setting up an effective field theory. The aim of this thesis is to explain and compare these schemes, with an emphasis on gauge invariance and unitarity. Resumming the propagator violates gauge invariance; the other schemes respect both and are compared at accuracy and functionality. The narrow-width approximation is typically the most straightforward scheme for calculating observables sufficiently integrated over  $s$  to leading order precision, for NLO calculations the complex mass scheme is especially convenient, and for even higher order precision the effective field theory seems most promising.



Universiteit Utrecht

Institute for Theoretical Physics,  
University Utrecht



Nikhef Institute for Subatomic  
Physics

# Contents

<b>1. Preliminaries</b>	<b>5</b>
1.1. Notation and conventions . . . . .	5
1.2. Diagrams and Feynman rules . . . . .	6
<b>I. Fundamental concepts</b>	<b>9</b>
<b>2. Relation between fundamental aspects</b>	<b>10</b>
<b>3. Gauge Invariance</b>	<b>13</b>
3.1. Motivation . . . . .	13
3.2. Non-Abelian Gauge Theories . . . . .	13
3.2.1. The matter-field Lagrangian . . . . .	13
3.2.2. The gauge field Lagrangian . . . . .	16
<b>4. Ward identity</b>	<b>18</b>
4.1. Relation with Gauge Invariance . . . . .	18
4.1.1. Current conservation . . . . .	18
4.1.2. From current conservation to the Ward Identity . . . . .	20
4.2. Diagrammatic proof of the Ward identity . . . . .	23
<b>5. Unitarity</b>	<b>28</b>
5.1. The scattering matrix and unitarity . . . . .	28
5.2. Cutting equations . . . . .	29
5.3. Unitarity & the Cutting Equation . . . . .	33
5.4. Summary proof of unitarity . . . . .	39
<b>6. Renormalization</b>	<b>41</b>
6.1. Renormalizability by powercounting . . . . .	41
6.2. Dimensional regularization . . . . .	42
6.3. The renormalization procedure . . . . .	43
6.4. The on-shell renormalization scheme (OSRS) . . . . .	46
<b>7. Spontaneously Symmetry Breaking</b>	<b>49</b>
7.1. Spontaneously broken symmetries . . . . .	49
7.2. SSB without choosing a gauge . . . . .	50
7.3. SSB in the unitary gauge . . . . .	52
<b>8. The electroweak sector of the Standard Model</b>	<b>54</b>
8.1. Chirality . . . . .	54
8.2. Prototype Model . . . . .	54
8.2.1. The kinetic terms and the gauge fields . . . . .	55

8.2.2. Fermion masses . . . . .	59
8.3. Structure of the Standard Model . . . . .	59
<b>II. Unstable Particles</b>	<b>63</b>
<b>9. Unstable Particles and the naïve approach</b>	<b>64</b>
9.1. Unstable Particles . . . . .	64
9.2. Masses and Decay Rates . . . . .	65
9.3. Resonances . . . . .	71
9.4. The naive approach . . . . .	73
9.5. The narrow-width approximation (NWA) . . . . .	75
<b>10. The gauge invariance problem</b>	<b>78</b>
10.1. Why resummation is fine for stable particles . . . . .	78
10.2. W-boson resonance . . . . .	79
10.2.1. Running width scheme . . . . .	82
10.2.2. Fixed width scheme . . . . .	86
10.2.3. Running width scheme + $WW\gamma$ -vertex correction . . . . .	86
10.3. Comparison of the different schemes . . . . .	87
10.4. Fermion resonance in QED . . . . .	88
10.5. Fermion resonance in the Standard Model . . . . .	96
<b>11. The Complex Mass Scheme (CMS)</b>	<b>100</b>
11.1. Definition . . . . .	100
11.2. How the CMS avoids the gauge invariance problem . . . . .	101
11.3. Relation between the CMS and the $\bar{m}$ -scheme . . . . .	102
11.4. The W-boson resonance in the CMS . . . . .	105
11.5. Unitarity in the CMS . . . . .	106
11.5.1. Decomposition of the CMS propagator . . . . .	109
11.5.2. Including the imaginary mass counterterm . . . . .	110
11.5.3. Cutting an unstable propagator off resonance . . . . .	113
11.5.4. Cutting an unstable propagator near resonance . . . . .	115
<b>12. Effective Field Theory (EFT)</b>	<b>121</b>
12.1. Introduction . . . . .	121
12.2. Expansion by regions . . . . .	122
12.2.1. A simple example . . . . .	122
12.2.2. The general procedure . . . . .	125
12.3. Setting up the EFT . . . . .	126
12.3.1. Identifying the relevant modes and factorization . . . . .	126
12.3.2. Constructing $\mathcal{L}_{\text{HSET}}$ . . . . .	130
12.3.3. The Lagrangian of the collinear modes . . . . .	133
12.3.4. Constructing $\mathcal{L}_{\text{int}}$ . . . . .	133
12.4. How the full theory is reproduced by the EFT: two example diagrams . . . . .	136
12.4.1. The full theory tree-level diagram . . . . .	136
12.4.2. Full theory self-energy correction and ordering into gauge invariant pieces . . . . .	137
12.5. Checking the Ward identity at tree-level . . . . .	138
12.6. Unitarity in the EFT . . . . .	140

12.7. Calculating quantum corrections: the forward scattering amplitude to NLO . . .	141
<b>13. Comparing the NWA, CMS and EFT</b>	<b>144</b>
13.1. Advantages and drawbacks . . . . .	144
13.1.1. NWA . . . . .	144
13.1.2. CMS . . . . .	144
13.1.3. EFT . . . . .	145
13.2. Accuracies for single-top production . . . . .	146
<b>14. Conclusion</b>	<b>150</b>
<b>A. Calculation of <math>I(k^2, m_1^2, m_2^2)</math></b>	<b>151</b>
<b>B. Calculation of <math>\Gamma_h^{1\text{-loop}}</math></b>	<b>154</b>
<b>C. Calculation of loop corrections in the EFT</b>	<b>157</b>

# 1. Preliminaries

## 1.1. Notation and conventions

This thesis will mostly follow the conventions used by de Wit, Laenen and Smith [1]. This includes the Einstein summation convention, meaning that whenever the same index appears twice in the same term, a summation over all possible values is implied. Greek indices ( $\mu, \nu, \rho, \dots$ ) denote space-time components and latin indices ( $i, j, k \dots$ ) space components only. So a summation over the index, say,  $j$  runs from 1 to 3. The time component will be the 0th component of four-vectors. For the indices corresponding to (gauge) groups latin letters are used as well, but those from the beginning of the alphabet ( $a, b, c \dots$ ). Finally, spinor-indices will be greek indices from the beginning of the alphabet ( $\alpha, \beta, \gamma \dots$ ).

### Metric

The used metric is

$$\eta_{\mu\nu} = \eta^{\mu\nu} = \text{diag}(-1, 1, 1, 1), \quad (1.1)$$

such that a vector  $v_\mu$  is related to  $v^\mu$  by  $(v_0, v_j) = v_\mu = \eta_{\mu\nu} v^\nu = (-v^0, v^j)$ . The scalar product of two four-vectors  $v$  and  $w$  then takes the form  $v \cdot w = \eta_{\mu\nu} v^\mu w^\nu = -v^0 w^0 + v^j w^j$ . The derivate operator  $\partial_\mu$  has its index ‘naturally lowered’. That is to say  $\partial_\mu = (\frac{\partial}{\partial x^\mu}, \frac{\partial}{\partial x^j})$ . This implies for example that  $\partial_\mu v^\mu = \frac{\partial v^0}{\partial x^0} + \frac{\partial v^j}{\partial x^j}$ . The Levi-Civita tensor  $\epsilon^{\mu\nu\rho\sigma}$  is defined by  $\epsilon^{0123} = 1$  and complete anti-symmetry. Equation (1.1) then implies that  $\epsilon_{0123} = -1$ .

### Fourier Transformations

A function  $f(x)$  and its Fourier transform  $f(k)$  are related by

$$f(x) = \int d^4k e^{ik \cdot x} f(k), \quad f(k) = \int \frac{d^4x}{(2\pi)^4} e^{-ik \cdot x} f(x).$$

### Field expansions

A scalar field  $\phi(x)$  can be expanded in terms of creation and annihilation operators  $a_{\vec{k}}$  and  $a_{\vec{k}}^\dagger$  as follows

$$\phi(x) = \int \frac{d^3k}{(2\pi)^3} \frac{1}{2\omega_{\vec{k}}} (a_{\vec{k}} e^{ik \cdot x} + a_{\vec{k}}^\dagger e^{-ik \cdot x}), \quad (1.2)$$

where  $\omega_{\vec{k}} := \sqrt{|\vec{k}|^2 + m^2}$ . Similar expansions hold for other fields. The physical states created by the creation operators,  $|\vec{k}\rangle = a_{\vec{k}}^\dagger |0\rangle$  etc, are normalized to one.

### Gamma matrices

The gamma matrices  $\gamma^\mu$  satisfy the Clifford algebra

$$\{\gamma^\mu, \gamma^\nu\} = \gamma^\mu \gamma^\nu + \gamma^\nu \gamma^\mu = 2\eta_{\mu\nu} \mathbf{1}, \quad (1.3)$$

with our metric (1.1). We can then consistently pick  $\gamma^0$  to be anti-hermitian and  $\gamma^j$  hermitian. The Dirac conjugate field  $\bar{\psi}$  is related to the Dirac field  $\psi$  as

$$\bar{\psi} = i\psi^\dagger\gamma^0. \quad (1.4)$$

These fields, together with the following combinations of gamma matrices

$$\gamma^5 = \gamma_5 = \frac{1}{24}i\epsilon_{\mu\nu\rho\sigma}\gamma^\mu\gamma^\nu\gamma^\rho\gamma^\sigma = -i\gamma^0\gamma^1\gamma^2\gamma^3, \quad \sigma^{\mu\nu} = -\frac{1}{2}i(\gamma^\mu\gamma^\nu - \gamma^\nu\gamma^\mu), \quad (1.5)$$

can be used to obtain the following useful, hermitian, fermionic bilinears

$$\begin{aligned} \bar{\psi}\psi &: \text{ scalar} \\ i\bar{\psi}\gamma^5\psi &: \text{ pseudoscalar} \\ i\bar{\psi}\gamma^\mu\psi &: \text{ vector} \\ i\bar{\psi}\gamma^\mu\gamma^5\psi &: \text{ axial vector} \\ i\bar{\psi}\sigma^{\mu\nu}\psi &: \text{ tensor.} \end{aligned}$$

## Units

Following most textbooks in the field, we conveniently set

$$\hbar = c = 1. \quad (1.6)$$

This implies for the units that

$$[\text{energy}] = [\text{mass}] = [\text{length}]^{-1} = [\text{time}]^{-1}. \quad (1.7)$$

When desired, one can reintroduce  $\hbar$  and  $c$  in the equations on dimensional grounds.

## 1.2. Diagrams and Feynman rules

### Feynman rules

We shall not extensively explain the Feynman rules, since the general idea is always the same, but we do note some aspects that may very well be different in other texts.

- Propagators carry a factor  $\frac{1}{i(2\pi)^4}$ . For example, the propagator for a scalar field reads  $\Delta(p) = \frac{1}{i(2\pi)^4} \frac{1}{p^2 + m^2 - i\epsilon}$ .
- Every vertex carries a factor  $i(2\pi)^4$  in addition to the constants of the corresponding interaction term in the Lagrangian.
- A derivative of a field in an interaction term in the Lagrangian gives rise to a factor  $ip_\mu$  at the resulting vertex in the diagram. Here  $p_\mu$  denotes the momentum of the propagator corresponding to that field that is *incoming* at the vertex.
- External lines are to be put on-shell and - except for scalar fields - to be contracted with the appropriate polarization vectors. Unless stated otherwise, no extra factor (e.g. a residue) is implied for the external lines.

If one sums all possible connected diagrams, with a certain number of incoming lines with momenta  $\{p_i\}$  and a certain number of outgoing lines with momenta  $\{q_j\}$ , calculated by these Feynman rules, then one obtains  $i(2\pi)^4\delta^4(\sum_i p_i - \sum_j q_j)\mathcal{M}(\{p_i\} \rightarrow \{q_j\})$ . Here  $\mathcal{M}$  is the *invariant amplitude* of the process. In other words, to obtain  $\mathcal{M}$ , one must sum all possible allowed diagrams and extract a factor  $i(2\pi)^4$  as well as the momentum-conserving delta function.

The invariant amplitude for a process with only one incoming and one outgoing particle (both with momentum  $p$ ) is called the *self-energy*  $\Sigma(p)$ . It appears in the resummed propagator of a scalar field as

$$\Delta^{\text{res}}(p) = \frac{1}{i(2\pi)^4} \frac{1}{p^2 + m^2 - \Sigma(p)}. \quad (1.8)$$

### Relation with scattering matrix

Starting from the interaction terms in the Hamiltonian  $\mathcal{H}^{\text{int}}$ , one can obtain the elements of the scattering matrix  $\langle p|\mathcal{S}|q\rangle$ . Here  $|p\rangle$  generally denotes the physical state characterized by a set of particles with on-shell momenta  $\{p_i\}$  at  $t = \infty$ . Part of the contributions to this matrix element  $\langle p|\mathcal{S}|q\rangle$  come from particles that freely propagate from their initial to their final states. One could therefore argue these do not actually describe scattering. To filter out these contributions we decompose  $\mathcal{S} = \mathbb{1} + i\mathcal{T}$  and consider the matrix elements  $\langle p|i\mathcal{T}|q\rangle$ . These can be calculated [2, chapter 4.6] as

$$\langle p|i\mathcal{T}|q\rangle = \langle p| T\left(e^{-i\int d^4x \mathcal{H}^{\text{int}}(x)}\right)|q\rangle_A. \quad (1.9)$$

The subscript A indicates that the external particles of the resulting expression are to be amputated. The  $T$  in (1.9) denotes time-ordering; the time-ordering of the exponential is defined by

$$T\left((e^{-i\int d^4x \mathcal{H}^{\text{int}}(x)})|q\rangle := 1 + \sum_{n=1}^{\infty} \frac{1}{n!} \int d^4x_1 \dots \int d^4x_n T\left(\mathcal{H}^{\text{int}}(x_1), \dots, \mathcal{H}^{\text{int}}(x_n)\right). \quad (1.10)$$

To calculate the matrix elements (1.9), one can substitute the field expansions in terms of creation and annihilation operators (analogous to (1.2)) for the fields that are contained in  $\mathcal{H}^{\text{int}}$ . The resulting expression can be worked out by using Wick's theorem, resulting in the LSZ reduction formula [2]. The result can be summarized as an (infinite series of) amputated Feynman diagrams. These diagrams obey the same Feynman rules that were outlined above for the calculation of an invariant amplitude, apart from one difference. The difference is that that external lines are to be multiplied by their propagator residue. This residue is (for diagonal propagators) generally of the form  $\left(\frac{Z(p_i)}{(2\pi)^3 2\omega_{\vec{p}_i}}\right)^{\frac{1}{2}}$ , where  $Z(p_i)$  is some function of the momentum of the external line. To be clear: whenever we draw diagrams, the Feynman rules as outline above are implied. Whenever these extra factors have to be included, this shall be indicated explicitly. The relation between the scattering matrix elements and the invariant amplitude is thus

$$\langle p|i\mathcal{T}|q\rangle = i(2\pi)^4\delta^4(\sum_i p_i - \sum_j q_j) \mathcal{M}(\{p_i\} \rightarrow \{q_j\}) \prod_n \left(\frac{Z(k_n)}{\sqrt{(2\pi)^3 2\omega_{k_n}}}\right)^{\frac{1}{2}}, \quad (1.11)$$

where the product runs over the external lines carrying momentum  $k_n$ .

It should be mentioned that there is one Feynman diagram that does not contribute to

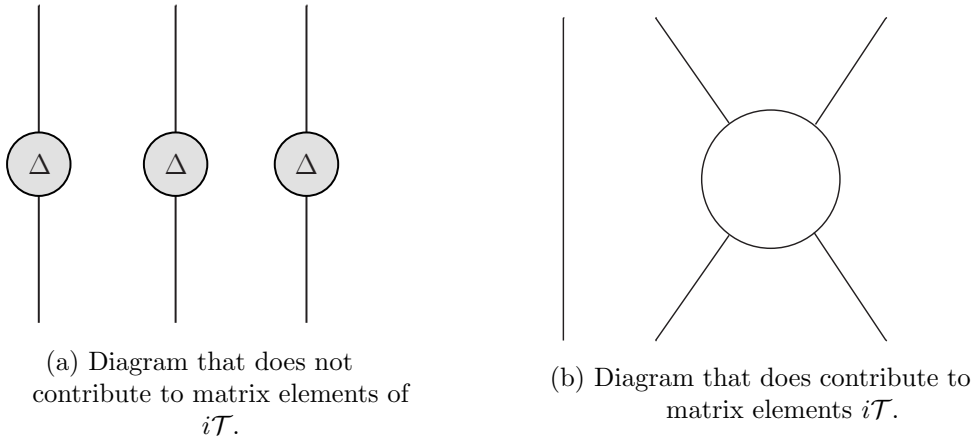


Figure 1.1.

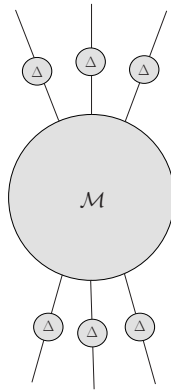


Figure 1.2.: How  $\mathcal{M}$  represents scattering.

(1.9). This is the diagram in which every incoming external line is connected to only one outgoing line as in figure 1.1a. This completely disconnected diagram precisely represents the ‘non-scattering’ process that is included in  $\mathcal{S}$  via the  $\mathbf{1}$ . It is therefore not contained in  $i\mathcal{T}$ . Notice that that we *do* include ‘partly disconnected’ diagrams such as the one shown in figure 1.1b. The diagram in the figure consists of two disconnected pieces. Both pieces will acquire a momentum-conserving delta function by the Feynman rules. In order to obtain the invariant amplitude  $\mathcal{M}$  corresponding to this diagram, one overall momentum conserving delta function has to be extracted. Therefore,  $\mathcal{M}$  will still contain a delta function guaranteeing momentum conservation of one of the disconnected pieces of the diagram. More generally, the invariant amplitude  $\mathcal{M}$  of a diagram consisting of  $n$  disconnected pieces will contain  $n - 1$  momentum conserving delta functions. As a last remark, it is also understood that we do not consider diagrams containing vacuum bubbles, for these only contribute to a shift in the energy of the vacuum state [2, p. 113].



**Part I.**

**Fundamental concepts**

## 2. Relation between fundamental aspects

The ultimate test for any physical theory is comparison with experiments. Indeed, the success of the Standard Model is largely due to its excellent agreement with experimental data. On a more basic level, in order for a quantum field theory to make any physical sense, it needs to satisfy the following *fundamental properties*.

- As quantum field theory is designed to describe quantum mechanics in a special relativistic way, it needs to be *Lorentz invariant*.
- It needs to be *causal*, i.e. it should guarantee that information cannot travel faster than the speed of light.
- it needs to be *unitary*, or more precisely, the scattering matrix should be so. As we shall see, this condition is equivalent to *conservation of probability*, which is essential for the physical interpretation of the theory.
- It needs to be *renormalizable* in order to be able to extract finite physical observables from the theory.

The first part of this thesis is devoted to obtaining a better understanding of some of these aspects. Before discussing these in more detail, we outline below how these fundamental properties are guaranteed to be satisfied in the Standard Model.

*Lorentz invariance* is to a large extent ascertained by starting out with a Lorentz invariant action. However, when describing particles with spin the situation is a bit more subtle. It turns out that in this case *gauge invariance* is crucial to guarantee Lorentz invariance. Let us explain why. Any non-scalar field can be decomposed in terms of polarization vectors. The polarization vectors can for example be chosen to represent particles with a certain spin. Under Lorentz transformations, the polarization vectors transform in a certain representation of the Lorentz group. We now specialize to spin-1 particles. These are usually described by a vector field  $V_\mu(x)$  transforming as  $V_\mu \rightarrow V'_\mu = L_\mu^\nu V_\nu$ , where  $L_\mu^\nu$  is a 4x4 matrix describing the Lorentz transformation. We know that a *massive* spin-1 particle can have only three different spins, yet  $V_\mu(x)$  has four components. Therefore, we need a condition on  $V_\mu$  to remove one component. Since we want this component to disappear in every reference frame, we should make sure this condition is Lorentz invariant. The usual choice is to impose  $\partial_\mu V^\mu(x) = 0$ , or equivalently  $k_\mu V^\mu(k) = 0$  in Fourier space. This condition projects out the component of  $V^\mu$  in the direction of  $k^\mu$ . The Lagrangian (the Proca Lagrangian) is constructed in such a way that this condition is set by the equations of motion for  $V^\mu$ . For *massless* spin-1 particles (e.g. photons), the situation is a bit different. There exist only *two* photon polarizations, so if we are to describe photons by a vector field  $A_\mu$ , we need to dispose of *two* components. Another complication is that the energy of the photon is given by  $k^0 = |\vec{k}|$ , implying that  $k_\mu k^\mu = 0$ . Consequently, using the relation  $k_\mu A^\mu(k) = 0$  to project out one component as before leaves  $k^\mu$  as one of the three allowed polarizations. However, any polarization vector  $\epsilon(k)$  needs to be normalized to 1 (in our conventions). The reason is that  $|\epsilon(k)|^2$  is the probability for a particle with momentum

$k$  to become the same particle with the same momentum in a non-interacting theory. Clearly, this probability has to be 1. The fact that  $k_\mu k^\mu = 0$  means that the polarization  $\epsilon^\mu(k) = k^\mu$  cannot be normalized. This is the problem that is solved by the Lagrangian exhibiting *gauge symmetry*, which implies that the polarization  $k^\mu$  is *unphysical* and does *not* describe a real particle. The other two polarizations, the transverse polarizations  $\epsilon^1(k)$  and  $\epsilon^2(k)$ , *do* represent physical photons. This does, however, not solve all the problems as such, for we can think of Lorentz transformations under which the transverse polarizations mix with the unphysical  $k^\mu$  polarization. This would mean that physical particles in one reference frame are suddenly (partly) described by the unphysical polarization vector in a different frame. Fortunately, this problem is also solved by gauge invariance, for gauge invariance leads, as we will see in chapter 4, to the *Ward identity*. The Ward identity essentially states that  $k_\mu \mathcal{M}^\mu(k) = 0$  for any process involving an external photon with momentum  $k^\mu$ . Since polarization vectors  $\epsilon^\mu$  enter the expressions by contractions with the invariant amplitude  $\epsilon_\mu \mathcal{M}^\mu$ , the Ward identity ensures that the unphysical polarization  $\epsilon_\mu(k) = k_\mu$  is excluded from the game in *every* Lorentz frame. Seen in this light, gauge invariance is essential for a Lorentz invariant description of photons.

Lorentz invariance is not the only reason that we need gauge invariance: the Ward identity also serves to ascertain that QED (and hence the standard model) is *unitary*. This will be explained in chapter 5.

A convenient way to make sure that a theory is *renormalizable*, is to ensure that it is renormalizable *by powercounting*. This will be explained in the chapter 6. Interesting in this respect is the electroweak sector of the Standard Model, which incorporates three massive vector bosons. As mentioned above, the usual way to describe these particles is by a vector field described by the Proca Lagrangian. However, naively introducing the massive vector bosons in this way leads to a theory that is *not* guaranteed to be renormalizable by powercounting. Therefore, the massive vector bosons are introduced in a different way. One starts with a gauge invariant Lagrangian describing four *massless* gauge fields that *is* renormalizable by powercounting. One then assumes that three of the four symmetries are spontaneously broken. This will result in three of the gauge fields becoming massive, as we will see in the chapter 7. This mechanism of spontaneously symmetry breaking, the *Higgs mechanism*, thus guarantees that the theory is renormalizable.

Summarizing, we can say that gauge symmetry really plays a crucial role. It allows for a Lorentz invariant description of photons and it serves, by means of the Ward identity, to prove that the theory is unitary. Also, by building a theory where the gauge symmetry is (partly) broken, we can introduce massive spin-1 particles in a way that guarantees our theory to be renormalizable. Of course this is only one way of looking at how the fundamental concepts are linked together. Perhaps one can think of a coherent story relating them in a different way. The point is really that the theory satisfies all the properties listed above at the same time. The relations between the important concepts are shown diagrammatically in figure 2.1.

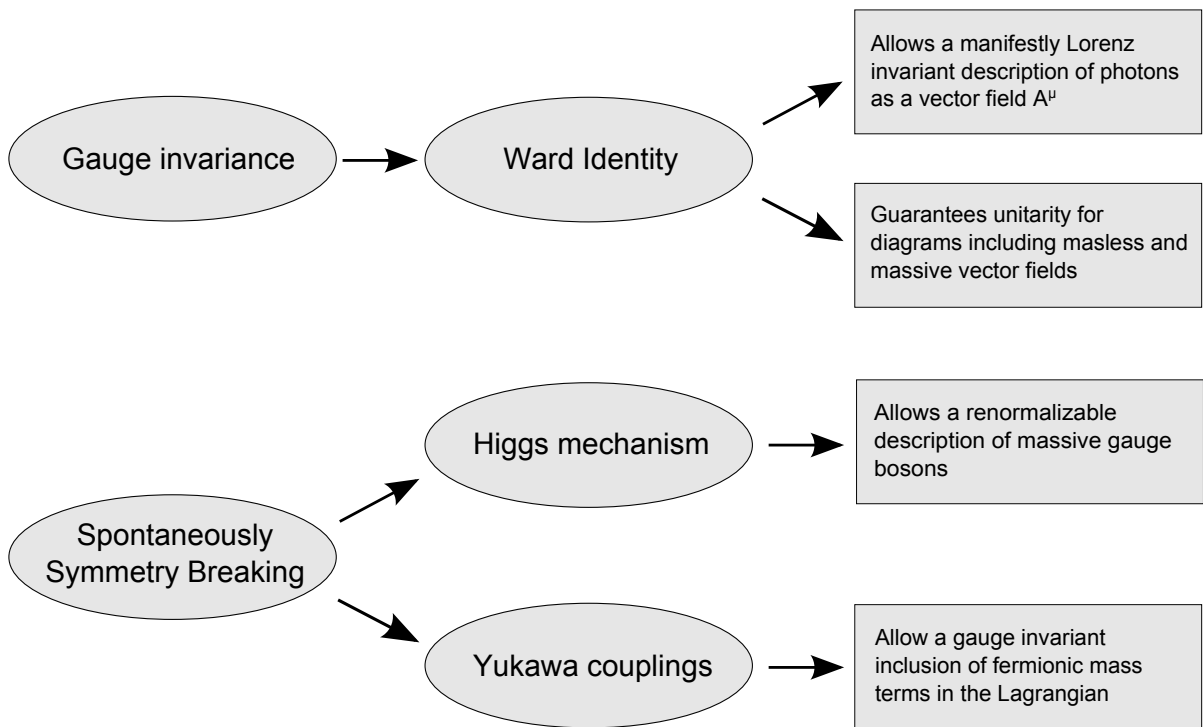


Figure 2.1.: Relations between fundamental concepts

## 3. Gauge Invariance

### 3.1. Motivation

Symmetries play an important role in quantum field theory. The reason for abandoning ordinary quantum mechanics and switching to quantum field theory has been to allow for the (special) relativistic description of quantum mechanics, so it comes as no surprise that the actions we encounter are invariant under Lorentz transformations. Indeed, any theory describing special relativity is required to exhibit this symmetry.

There is another important symmetry that we encounter in present-day Lagrangians: *gauge symmetry*. The inspiration for introducing this symmetry comes from the success of the theory of quantum electrodynamics (QED), which is described by the Lagrangian

$$\mathcal{L}_{\text{QED}} = -\frac{1}{4}F_{\mu\nu}F^{\mu\nu} - \bar{\psi}\not{\partial}\psi - m\bar{\psi}\psi + iqA_\mu\bar{\psi}\gamma^\mu\psi, \quad (3.1)$$

where  $F_{\mu\nu} = \partial_\mu A_\nu - \partial_\nu A_\mu$  is the electromagnetic field strength tensor. This Lagrangian is invariant under the combined transformations of the fields

$$\begin{cases} \psi(x) & \rightarrow e^{iq\xi(x)}\psi \\ A_\mu(x) & \rightarrow A_\mu(x) + \partial_\mu\xi(x). \end{cases} \quad (3.2)$$

This transformation is called a *gauge transformation*. To be more precise, it is a *local* gauge transformation, meaning that the transformation itself is a function of spacetime. In the case of (3.2) this means that  $\xi$  is a function of  $x$ . Transformations that do not depend on the spacetime coordinates are called global. Here we focus on local transformations. The gauge symmetry implies that the fields can be altered without changing  $\mathcal{L}_{\text{QED}}$ , so without changing the physics. The degrees of freedom in the fields that are associated with the gauge transformations are therefore *unphysical*.

The Lagrangian (3.1), with its gauge symmetry, turned out to be so successful in describing QED, that other Lagrangians with other gauge symmetries were sought after, in the hope of describing other particles and their interactions. This has eventually led to the Standard Model, which is outlined in chapter 8. As it turns out, an important feature of the transformations described by (3.2) (which form a group), is that they form an *abelian* group. This means that the order of applying two subsequent gauge transformations does not matter. The aim of the next paragraph is to describe more general, *non-abelian*, gauge transformations. These play a key role in the Standard Model.

### 3.2. Non-Abelian Gauge Theories

#### 3.2.1. The matter-field Lagrangian

In this section we shall construct a Lagrangian that is invariant under a non-abelian gauge transformations. It features  $N$  matter fields  $\{\phi_i, 1 \leq i \leq N\}$  which can in principle be complex. For illustrational purposes, we assume the field to be scalar fields with equal mass, but

the approach can be generalized to other fields. As before, we are interested in local gauge transformations. To ensure that the transformations depend on the spacetime coordinates in a smooth manner they are assumed to be elements  $U(x)$  of a  $N$ -dimensional representation of a Lie group  $G$ . A Lie group is a continuous group that can be parameterized by a finite number of parameters in an analytic way. The fields then transform as

$$\Phi(x) \rightarrow \Phi'(x) = U(x)\Phi(x), \quad \text{where} \quad \Phi := \begin{pmatrix} \phi_1 \\ \phi_2 \\ \vdots \\ \phi_N \end{pmatrix}. \quad (3.3)$$

The standard free Lagrangian for these matter fields is

$$\mathcal{L}_{\text{matter}}^{\text{free}} = -\partial_\mu \Phi^\dagger \partial^\mu \Phi - m^2 \Phi^\dagger \Phi. \quad (3.4)$$

Now we aim to build a Lagrangian invariant under gauge transformations  $U(x) \in G$ . If we take unitary transformations  $U$ , then the second term transforms as  $\Phi^\dagger \Phi \rightarrow \Phi^\dagger U^\dagger U \Phi = \Phi^\dagger \Phi$ . This mass term is thus invariant. The same does not hold for the kinetic term. This is due to the fact that  $\partial_\mu \Phi$  does not transform as simply as  $\Phi$  does, for

$$\partial_\mu \Phi \rightarrow \partial_\mu (U\Phi) = (\partial_\mu U)\Phi + U(\partial_\mu \Phi). \quad (3.5)$$

It is because of the transformations being local that we pick up the term containing the derivative of the transformation itself. Our strategy to obtain a Lagrangian invariant under the transformation (3.3) will be to modify  $\partial_\mu \Phi$  and obtain a quantity  $D_\mu \Phi$ , called the *covariant derivative* of  $\Phi$ . This covariant derivative will be *defined* by the requirement that it transforms in the same way as  $\Phi$  does, i.e. as  $D_\mu \Phi \rightarrow U D_\mu \Phi$ . This will then guarantee the invariance of the kinetic term in  $\mathcal{L}$  under the transformation, just as the transformation rule of  $\Phi$  guarantees the invariance of the mass term.

To construct the covariant derivative we follow Peskin and Schroeder [2]. First we consider the derivative of  $\Phi$  in the direction of a 4-vector  $n$ . It transforms under a gauge transformation as follows

$$n^\mu \partial_\mu \Phi(x) = \lim_{\epsilon \rightarrow 0} \frac{1}{\epsilon} [\Phi(x + \epsilon n) - \Phi(x)] \rightarrow \lim_{\epsilon \rightarrow 0} \frac{1}{\epsilon} [U(x + \epsilon n)\Phi(x + \epsilon n) - U(x)\Phi(x)]. \quad (3.6)$$

Once again we see that this quantity does not transform covariantly, the reason being that  $U(x)$  works on  $\Phi(x)$  differently on different space-time coordinates. A way to fix this is to introduce a function  $U(x, y)$  of 2 space-time variables, which is required to transform as

$$U(x, y) \rightarrow U'(x, y) = U(x)U(x, y)U^{-1}(y). \quad (3.7)$$

The covariant derivative on  $\Phi$  in the direction of  $n$  can then be defined as

$$n^\mu D_\mu \Phi = \lim_{\epsilon \rightarrow 0} \frac{1}{\epsilon} [\Phi(x + \epsilon n) - U(x + \epsilon n, x)\Phi(x)]. \quad (3.8)$$

This does indeed transform in the required way, for

$$\begin{aligned} n^\mu D_\mu \Phi(x) &\rightarrow \lim_{\epsilon \rightarrow 0} \frac{1}{\epsilon} [U(x + \epsilon n)\Phi(x + \epsilon n) - U(x + \epsilon n)U(x + \epsilon n, x)U^{-1}(x)U(x)\Phi(x)] \\ &= \lim_{\epsilon \rightarrow 0} U(x + \epsilon n) \cdot \lim_{\epsilon \rightarrow 0} \frac{1}{\epsilon} [\Phi(x + \epsilon n) - U(x + \epsilon n, x)\Phi(x)] \\ &= U(x) n^\mu D_\mu \Phi(x). \end{aligned} \quad (3.9)$$

So  $D_\mu \Phi \rightarrow U D_\mu \Phi$ , exactly as required. Since the only thing we require of  $U(x, y)$  is its transformation property (3.7),  $U(x, y)$  can consistently be restricted to take values in the representation of our Lie group  $G$ , i.e.  $U(x, y) \in G$ . The transformation rule (3.7) then guarantees  $U'(x, y) \in G$  as well. Furthermore, we can consistently set  $U(x, x) = \mathbb{1}$ , for this will transform according to  $\mathbb{1} = U(x, x) \rightarrow U(x)U(x, x)U^{-1}(x) = \mathbb{1}$ .

Assuming that the Lie group is compact, every group element can be written as  $U(\xi^a(x)) = \exp(g\xi_a(x)t^a)$ . Every element  $U(x)$  is thus characterized by a set of functions  $\{\xi^a(x), 1 \leq a \leq \dim(G)\}$ . Since  $U$  is unitary, the generators  $\{t^a, 1 \leq a \leq \dim(G)\}$  are anti-hermitian.  $g$  is simply a dimensionless constant.

Since  $U(x + \epsilon n, x)$  it can be expanded as

$$\begin{aligned} U(x + \epsilon n, x) &= U(x, x) + \epsilon n^\mu (\partial_\mu U)(x, x) + \mathcal{O}(\epsilon^2) \\ &= \mathbb{1} + \epsilon \cdot g n^\mu W_\mu(x) + \mathcal{O}(\epsilon^2). \end{aligned} \quad (3.10)$$

Here  $W_\mu(x) := (\partial_\mu U)(x, x)$  lives in the Lie algebra, i.e.  $W_\mu(x) = W_\mu^a(x)t_a$ . Since the generators  $t_a$  are anti-hermitian and the fields  $W_\mu^a$  are real,  $W_\mu$  is anti-hermitian as well. Inserting the expression (3.10) into the definition of the covariant derivative (3.8) yields

$$\begin{aligned} n^\mu D_\mu \Phi(x) &= \lim_{\epsilon \rightarrow 0} \frac{1}{\epsilon} [\Phi(x + \epsilon n) - \Phi(x)] - \lim_{\epsilon \rightarrow 0} \frac{\epsilon}{\epsilon} g n^\mu W_\mu \Phi(x) \\ &= n^\mu \partial_\mu \Phi(x) - g n^\mu W_\mu \Phi(x). \end{aligned} \quad (3.11)$$

Or in short

$$D_\mu \Phi(x) = (\partial_\mu - g W_\mu) \Phi(x). \quad (3.12)$$

The new fields  $W_\mu^a$  (contained in  $W_\mu = W_\mu^a t_a$ ) have thus entered the covariant derivative. The way these fields transform under gauge transformations follows from applying the transformation rule (3.7) to  $U(x + \epsilon n, x)$  expanded again as in (3.10).

$$\begin{aligned} \mathbb{1} + \epsilon \cdot g W_\mu(x) n^\mu + \mathcal{O}(\epsilon^2) &\rightarrow [U(x) + \epsilon \cdot n^\mu (\partial_\mu U)(x) + \mathcal{O}(\epsilon^2)] [\mathbb{1} + \epsilon \cdot g W_\mu(x) n^\mu + \mathcal{O}(\epsilon^2)] U^{-1}(x) \\ &\Rightarrow W_\mu \rightarrow U W_\mu U^{-1} + \frac{1}{g} (\partial_\mu U) U^{-1}, \end{aligned} \quad (3.13)$$

where the second line follows from the part of the first line of first-order in  $\epsilon$ .

Let us summarize what we have done. We have constructed the covariant derivative as the ordinary derivative plus an extra field. This extra field transforms in a such way that it precisely cancels the part of  $\partial_\mu \Phi$  that does not transform covariantly. To be more precise, the second term of the transformation (3.13) precisely cancels the second term of the transformation (3.5), such that  $D_\mu \Phi$  transforms covariantly. Explicitly,

$$\begin{aligned} D_\mu \Phi &= \partial_\mu \Phi - g W_\mu \Phi \rightarrow (\partial_\mu \Phi)' - g W_\mu' (U \Phi) \\ &\stackrel{(3.5), (3.13)}{=} U \partial_\mu \Phi + (\partial_\mu U) \Phi - g U W_\mu \Phi - (\partial_\mu U) \Phi \\ &= U (\partial_\mu - g W_\mu) \Phi \\ &= U (D_\mu \Phi). \end{aligned} \quad (3.14)$$

Having found an expression for the covariant derivative, we can easily write down a gauge invariant matter-field Lagrangian. This is done by simply taking the free matter field Lagrangian  $\mathcal{L}_{\text{matter}}^{\text{free}}$  (3.4) and making the replacement  $\partial_\mu \rightarrow D_\mu$ . The full matter Lagrangian obtained in this way is

$$\begin{aligned}\mathcal{L}_{\text{matter}} &= -(D_\mu \Phi)^\dagger D^\mu \Phi - m^2 \Phi \\ &= -\Phi^\dagger (\overleftarrow{\partial}_\mu + gW_\mu)(\partial^\mu - gW^\mu)\Phi - m^2 |\Phi|^2 \\ &= -|\partial_\mu \Phi|^2 - m^2 |\Phi|^2 - gW_\mu [\Phi^\dagger \partial^\mu \Phi - (\partial^\mu \Phi)^\dagger \Phi] + g^2 W_\mu W^\mu |\Phi|^2.\end{aligned}\tag{3.15}$$

We now recognize  $\mathcal{L}_{\text{matter}}$  as the free matter Lagrangian  $\mathcal{L}_{\text{matter}}^{\text{free}}$  (3.4) plus additional interaction terms between the gauge fields and the matter fields.

To obtain the full Lagrangian we also need terms quadratic in the gauge fields. These terms give rise to the propagators of the gauge fields. The next section is devoting to constructing the piece of the Lagrangian  $\mathcal{L}_{\text{gauge}}$  that contains only gauge fields;  $\mathcal{L}_{\text{gauge}}$  thus includes these quadratic terms. The full Lagrangian is then be given by  $\mathcal{L} = \mathcal{L}_{\text{matter}} + \mathcal{L}_{\text{gauge}}$ .

### 3.2.2. The gauge field Lagrangian

$\mathcal{L}_{\text{gauge}}$  is to depend on the gauge fields in a way that is both Lorentz invariant and gauge invariant, and in a way that gives us a renormalizable theory. We follow the approach of de Wit, Laenen and Smith [1] to construct a suitable  $\mathcal{L}_{\text{gauge}}$ .

In order to build a gauge invariant Lagrangian, a useful object to consider is the operator  $[D_\mu, D_\nu]$ . To see what this operator does, we let it work on  $\Phi(x)$ .

$$\begin{aligned}[D_\mu, D_\nu]\Phi &= (\partial_\mu - gW_\mu)(\partial_\nu - gW_\nu)\Phi - (\partial_\nu - gW_\nu)(\partial_\mu - gW_\mu)\Phi \\ &= g\left(-\partial_\mu(W_\nu\Phi) - W_\mu\partial_\nu\Phi + \partial_\nu(W_\mu\Phi) + W_\nu\partial_\mu\Phi\right) + g^2[W_\mu, W_\nu]\Phi \\ &= -g\left((\partial_\mu W_\nu - \partial_\nu W_\mu) - g[W_\mu, W_\nu]\right)\Phi \\ &= -gG_{\mu\nu}\Phi,\end{aligned}\tag{3.16}$$

where we defined the field strength tensor  $G_{\mu\nu} := \partial_\mu W_\nu - \partial_\nu W_\mu - g[W_\mu, W_\nu]$ . Since all the derivatives of  $\Phi$  cancel,  $[D_\mu, D_\nu]$  can simply be viewed as the object  $-gG_{\mu\nu}$ .  $G_{\mu\nu}$  lives in the Lie algebra; explicitly

$$\begin{aligned}G_{\mu\nu} &= G_{\mu\nu}^a t_a = (\partial_\mu W_\nu^a - \partial_\nu W_\mu^a)t_a - W_\mu^b W_\nu^c [t_b, t_c] \\ &= (\partial_\mu W_\nu^a - \partial_\nu W_\mu^a - f_{bc}^a W^{\mu b} W^{\nu c})t_a.\end{aligned}\tag{3.17}$$

In obtaining the second line we used the fact that the commutator of two generators of a Lie group is a linear combination of generators of the same group, i.e.  $[t_a, t_b] = f_{ab}^c t_c$ . The factors  $f_{ab}^c$  are called the structure constants of  $G$ . To find out how  $G_{\mu\nu}$  transforms under gauge transformations, we use the transformation rule of  $D_\mu \Phi$ , expressed by equation (3.14). Since multiple covariant derivatives of  $\Phi$  transform in the same way

$$[D_\mu, D_\nu]\Phi \rightarrow U[D_\mu, D_\nu]\Phi.\tag{3.18}$$

Combining this with  $G_{\mu\nu}\Phi \rightarrow G'_{\mu\nu}U\Phi$  and (3.16) yields

$$G_{\mu\nu} \rightarrow UG_{\mu\nu}U^{-1}.\tag{3.19}$$



Because of its convenient transformation property (3.19),  $G_{\mu\nu}$  can be used to construct gauge invariant quantities. To understand this, first note that any product of field strength tensors will transform in the same way:  $G_{\mu\nu}G_{\rho\sigma}\cdots G_{\tau\nu} \rightarrow UG_{\mu\nu}G_{\rho\sigma}\cdots G_{\tau\nu}U^{-1}$ . Due to its cyclic property, the trace of such a product is then a gauge invariant quantity.

To obtain quantities that are Lorentz invariant is straightforward: simply contract the Lorentz indices. That only leaves the third requirement to be met: renormalizability. As will be explained in chapter 6, in order to guarantee renormalizability by powercounting all terms in the Lagrangian need to have coupling constants with nonnegative mass dimension. Since  $g$  is by definition a dimensionless constant, equation (3.12) reveals that the mass dimension of  $W_\mu$  is 1. This implies that  $G_{\mu\nu}$  has mass dimension 2. Since the action  $S = \int d^4x \mathcal{L}$  is dimensionless,  $\mathcal{L}$  has mass dimension 4. To guarantee renormalizability by powercounting, we thus only include terms in  $\mathcal{L}_{\text{gauge}}$  that contain  $G_{\mu\nu}$  only once or are quadratic in  $G_{\mu\nu}$ . The anti-symmetry of  $[D_\mu, D_\nu]$  implies that  $G_{\mu\nu}$  is anti-symmetric as well, hence  $G_\mu^\mu = 0$ . This leaves  $\text{Tr}[G^{\mu\nu}G_{\mu\nu}]^1$  as a suitable term in the Lagrangian. Introducing a factor  $\frac{1}{4}$  for convenience, the gauge field Lagrangian is defined as

$$\mathcal{L}_{\text{gauge}} = \frac{1}{4}\text{Tr}[G_{\mu\nu}G^{\mu\nu}] = \frac{1}{4}G_{\mu\nu}^a G^{\mu\nu b} \text{Tr}[t_a, t_b]. \quad (3.20)$$

It can be shown for unitary representations of compact Lie groups that one may use  $\text{Tr}[t_a t_b] = -\delta_{ab}$  [1]. Thereby the Lagrangian for the gauge fields reads

$$\begin{aligned} \mathcal{L}_{\text{gauge}} &= -\frac{1}{4}G_{\mu\nu}^a G_a^{\mu\nu} \\ &= -\frac{1}{4}\left(\partial_\mu W_\nu^a - \partial_\nu W_\mu^a - gf_{cd}^a W_\mu^c W_\nu^d\right)\left(\partial^\mu W_a^\nu - \partial^\nu W_a^\mu - gf_{efa} W^{\mu e} W^{\nu f}\right) \\ &= -\frac{1}{4}(\partial_\mu W_\nu^a - \partial_\nu W_\mu^a)(\partial^\mu W_a^\nu - \partial^\nu W_a^\mu) \\ &\quad - gf_{cd}^a W_\mu^c W_\nu^d \partial^\mu W_a^\nu + \frac{1}{4}g^2 f_{cd}^a f_{efa} W_\mu^c W^{\mu e} W_\nu^d W^{\nu f}. \end{aligned} \quad (3.21)$$

That does it: a Lagrangian invariant under a general (unitary) representation of a compact Lie group can thus be obtained by adding  $\mathcal{L}_{\text{gauge}}$  (3.21) to a free matter field Lagrangian with the replacement  $\partial_\mu \rightarrow D_\mu$ .

Now we are in the position to see how the special case of QED follows from this prescription. In this case the fields transform in the fundamental representation of the  $U(1)$  gauge group. This leads to considerable simplifications: since  $U(1)$  is 1-dimensional, the latin indices can only take one value and are hence ignored. For the same reason, the gauge fields  $W_\mu^a$  constitute only one gauge field, which is called  $A_\mu$ . The only generator is  $i$ , which is indeed anti-hermitian. Furthermore,  $U(1)$  is an abelian group. Infinitesimal gauge transformations therefore commute, implying that  $[t_a, t_b] = 0$ . Consequently, the structure constants vanish.  $G_{\mu\nu}$  thus reduces to  $F_{\mu\nu}$  and the gauge Lagrangian (3.21) reduces to the first term in (3.1). Renaming  $g \rightarrow q$ , the rest of the QED Lagrangian (3.1) follows by the substitution  $\partial_\mu \rightarrow D_\mu = \partial_\mu - iqA_\mu$  in the free Lagrangian for fermions, i.e.

$$\mathcal{L}_{\text{matter}}^{\text{free}} = -\bar{\psi}\not{\partial}\psi - m\bar{\psi}\psi \rightarrow \mathcal{L}_{\text{matter}} = -\bar{\psi}(\not{\partial} - iqA_\mu\gamma^\mu)\psi - m\bar{\psi}\psi. \quad (3.22)$$

This does indeed yields the remaining terms of (3.1). Therefore, QED does indeed follow as a special case of this general treatment.

<sup>1</sup>Actually,  $\epsilon^{\mu\nu\rho\sigma}\text{Tr}[G_{\mu\nu}G_{\rho\sigma}]$  is also a possibility, but it can be shown to equal a total derivative. Therefore, it disappears from the Lagrangian in perturbation theory [1, p. 265].

## 4. Ward identity

Closely related to the principle of gauge invariance is the Ward identity. For an *abelian* gauge theory this identity states the following. Suppose  $\mathcal{M}_\mu(k)$  is an invariant amplitude in Fourier space with an arbitrary number of external lines, at least one external photon line, and with *all* external lines truncated. Then contracting this amplitude with an external photon moment  $k_\mu$  yields

$$k_\mu \mathcal{M}^{\diamond\mu}(k) = 0, \quad (4.1)$$

provided that the external lines, except the photons, are taken on their mass shell. This last requirement is indicated by the  $\diamond$  in (4.1). The Ward identity (4.1) holds order by order in perturbation theory. This is because the identity holds for every possible value of the perturbation parameter  $g$  (or  $q$  for QED). *All* diagrams of a certain order in  $g$  contributing to  $\mathcal{M}^\mu$  have to be summed; individually they do not usually satisfy the Ward identity.

An important point is that the Ward identity is satisfied *as a result of gauge invariance*. Gauge invariance leads to current conservation which leads to the Ward identity. This will be shown in section 4.1. In section 4.2 an alternative proof is presented for QED, using explicit diagram manipulations.

### 4.1. Relation with Gauge Invariance

#### 4.1.1. Current conservation

The route from gauge invariance to the Ward identity proceeds via current conservation. The existence of a conserved current follows from Noether's theorem. Noether's theorem states that for every continuous, *rigid* symmetry of the action parameterized by a transformation parameter  $c_a$ , there exists a corresponding conserved current  $J_\mu^a(x)$ . The fact that the current is conserved means that  $\partial^\mu J_\mu^a = 0$ .

We consider a general abelian gauge theory with general matter fields  $\Phi(x)$  and gauge fields  $A_\mu^a(x)$ . We shall show that the interaction terms in the Lagrangian  $\mathcal{L}^{\text{int}}(\Phi, A_\mu^a)$  are then related to the conserved currents by

$$\frac{\partial \mathcal{L}^{\text{int}}}{\partial A_\mu^a(x)} = J_\mu^a(x). \quad (4.2)$$

Before deriving this equation, we point out a consequence of (4.2): it provides an alternative method to obtain a gauge invariant theory. The prescription to obtain a gauge invariant theory given in chapter 3 was the following. Start with the free matter-field Lagrangian  $\mathcal{L}_{\text{matter}}^{\text{free}}(\partial_\mu \Phi, \Phi)$ , which we shall abbreviate somewhat as  $\mathcal{L}^{\text{free}}(\partial_\mu \Phi, \Phi)$ , and substitute  $\partial_\mu \rightarrow D_\mu = \partial_\mu - g A_\mu^a t_a$ . The substitution transforms this Lagrangian as

$$\mathcal{L}^{\text{free}}(\partial_\mu \Phi, \Phi) \rightarrow \mathcal{L}^{\text{free}}(D_\mu \Phi, \Phi) = \mathcal{L}^{\text{free}}(\partial_\mu \Phi, \Phi) + \mathcal{L}^{\text{int}}(\Phi, A_\mu^a) \quad (4.3)$$

and thus gives rise to interaction terms  $\mathcal{L}^{\text{int}}(\Phi, A_\mu^a)$ . To obtain the full Lagrangian one then adds the gauge field Lagrangian  $\mathcal{L}_{\text{gauge}}(A_\mu^a)$ . Equation (4.2) provides another way of obtaining

the interaction terms as follows. First find  $J_\mu^a$  by Noether's theorem from the *rigid* symmetry of the free matter-field Lagrangian  $\mathcal{L}^{\text{free}}(\partial_\mu\Phi, \Phi)$  (note that this  $\mathcal{L}^{\text{free}}$  *does* have a rigid symmetry, it is the corresponding *local* symmetry that it lacks). Then integrate  $J_a^\mu$  over  $A_\mu^a$  to find  $\mathcal{L}^{\text{int}}$  by (4.2). In the case of QED this is particularly easy: the current is given by  $J^\mu = iq\bar{\psi}\gamma^\mu\psi$ , such that  $\mathcal{L}_{\text{int}} = A_\mu J^\mu$ .

Incidentally, equation (4.2) also reveals that the Noether current appears in the equation of motion of the gauge field. In the abelian case  $\mathcal{L}_{\text{gauge}} = -\frac{1}{4}F_{\mu\nu}^a F_a^{\mu\nu}$ , such that the equation of motion reads<sup>1</sup>

$$\partial^\nu F_{\mu\nu}^a = J_\mu^a. \quad (4.4)$$

To derive equation (4.2), we first find the Noether current that corresponds to the rigid symmetry of the free matter-field Lagrangian  $\mathcal{L}^{\text{free}}(\partial_\mu\Phi, \Phi)$ . Then we show it satisfies (4.2). Let an infinitesimal (rigid) symmetry transformation of  $\mathcal{L}^{\text{free}}$  be parameterized by constants  $c^a$ , then

$$\begin{aligned} 0 &= \delta_c \mathcal{L}^{\text{free}}(\partial_\mu\Phi, \Phi) \\ &= \frac{\partial \mathcal{L}^{\text{free}}}{\partial(\partial_\mu\Phi_j)} \cdot \delta_c(\partial_\mu\Phi_j) + \frac{\partial \mathcal{L}^{\text{free}}}{\partial\Phi_j} \cdot \delta_c\Phi_j \\ &= \left( \frac{\partial \mathcal{L}^{\text{free}}}{\partial\Phi_j} - \partial_\mu \frac{\partial \mathcal{L}^{\text{free}}}{\partial(\partial_\mu\Phi_j)} \right) \cdot \delta_c\Phi_j + \partial_\mu \left( \frac{\partial \mathcal{L}^{\text{free}}}{\partial(\partial_\mu\Phi_j)} \cdot \delta_c\Phi_j \right). \end{aligned} \quad (4.5)$$

Note that the second line is where we use the fact we are dealing with an *abelian* gauge theory. Both the Lagrangian and the variations of the fields contain the generators of the symmetry group. It is only if the group is abelian that we have the freedom to use the chain rule and arrange them in the order shown in the second line. Now, in the last line, the first term in parentheses equals 0 if the Euler-Lagrange equations are satisfied. Equation (4.5) then implies

$$0 = -\partial_\mu \left( \frac{\partial \mathcal{L}^{\text{free}}}{\partial(\partial_\mu\Phi_j)} \delta_c\Phi_j \right) = -c^a \partial_\mu \left( \frac{\partial \mathcal{L}^{\text{free}}}{\partial(\partial_\mu\Phi_j)} g(t_a\Phi)_j \right). \quad (4.6)$$

Since the  $c^a$  are arbitrary (infinitesimal) constants, equation (4.6) implies that

$$\partial_\mu J_a^\mu = 0, \quad \text{where} \quad J_a^\mu := -\frac{\partial \mathcal{L}^{\text{free}}(\partial_\mu\Phi, \Phi)}{\partial(\partial_\mu\Phi_j)} g(t_a\Phi)_j. \quad (4.7)$$

Equation (4.7) expresses *conservation of the Noether current*. Now that we have found the Noether current, we show that it does indeed satisfy (4.2) by

$$\begin{aligned} \frac{\partial \mathcal{L}^{\text{int}}(\Phi, A_\nu^b)}{\partial A_\mu^a} &\stackrel{(4.3)}{=} \frac{\partial \mathcal{L}^{\text{free}}(D_\mu\Phi(\partial_\mu\Phi, A_\nu^b), \Phi)}{\partial A_\mu^a} = \frac{\partial \mathcal{L}^{\text{free}}(D_\mu\Phi, \Phi)}{\partial(D_\mu\Phi_j)} \cdot \frac{\partial(D_\mu\Phi_j)}{\partial A_\mu^a} \\ &= \frac{\partial \mathcal{L}^{\text{free}}(\partial_\mu\Phi, \Phi)}{\partial(\partial_\mu\Phi_j)} \left( -g(t_a\Phi)_j \right) = J_a^\mu. \end{aligned} \quad (4.8)$$

In the third step the fact was used that  $A_\mu^a$  appears via  $D_\mu\Phi = (\partial_\mu - A_\mu^a t_a)\Phi$ ; this is where the fact is used that we are dealing with a theory invariant under *local* gauge transformations. Therefore, equation (4.2) (and thus the fact that in QED  $A_\mu$  couples to a conserved current), is a consequence of gauge invariance!

---

<sup>1</sup>As is very typical for the abelian case, we have renamed  $G_{\mu\nu}^a \rightarrow F_{\mu\nu}^a$ . In QED, where the gauge group is one-dimensional, the index  $a$  can take only value and is therefore omitted.

### 4.1.2. From current conservation to the Ward Identity

In this paragraph it is shown how the fact that the conserved current couples to the gauge fields (in the sense of equation (4.2)), leads to the Ward identity (4.1). This requires some explanation on how the interaction terms in  $\mathcal{L}$  give rise to invariant amplitudes for scattering processes. This explanation is given first.

Let us consider a scattering process with incoming particles with momenta  $\{p_i\}$  and outgoing particles with momenta  $\{q_j\}$ . The corresponding states are abbreviated as  $|p\rangle := |\{p_i\}\rangle$  and  $|q\rangle := |\{q_i\}\rangle$ . As revealed by equations (1.9) and (1.11), a way to see how the Feynman rules for the invariant amplitude arise is by writing out  $\langle p|T\left(\exp\left(-i\int d^4x\mathcal{H}^{\text{int}}(x)\right)\right)|q\rangle_A$ . Apart from some factors for the external lines and an overall momentum-conserving delta function, to  $n$ -th order in perturbation theory this yields

$$\mathcal{M}^{(n)}(\{p_i\} \rightarrow \{q_j\}) = \int d^4x_1 \dots \int d^4x_n \langle p|T\left(\mathcal{H}^{\text{int}}(x_1), \dots, \mathcal{H}^{\text{int}}(x_n)\right)|q\rangle_A. \quad (4.9)$$

We shall use QED as an example for now; then  $\mathcal{H}^{\text{int}}(x) = -\mathcal{L}^{\text{int}}(x) = -iqA_\mu(x)\bar{\psi}(x)\gamma^\mu\psi(x)$ . This expression can be plugged into (4.9), together with the expansion of the fields terms of their creation and annihilation operators, e.g

$$\psi(x) = \int \frac{d^3k}{(2\pi)^3 2\omega_{\vec{k}}} \sum_\lambda \left( u^\lambda(\vec{k}) a_{\vec{k}} e^{-ik\cdot x} + v^\lambda(\vec{k}) b_{\vec{k}} e^{ik\cdot x} \right), \quad (4.10)$$

where  $\lambda$  labels the different polarizations. Plugging (4.10) and the analogous expansions for

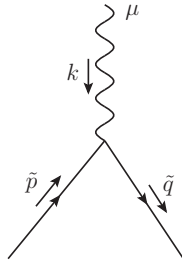


Figure 4.1.: The only vertex in QED

$\bar{\psi}(x)$  and  $A_\mu(x)$  into (4.9) gives rise to the Feynman rules. We shall not perform this substitution explicitly here, but only outline some ingredients of the resulting rules that are important to us. Every term in  $\mathcal{H}^{\text{int}}(x)$  becomes associated with a vertex in Feynman diagrams. In this case the only vertex is shown in figure 4.1. Every such a vertex is characterized by

- the lines emanating from the vertex. These correspond to the fields in the associated interaction-term; in this case we have one photon line and two fermion lines.
- some prefactors; in this case  $i(2\pi)^4(-iq\gamma^\mu)$ . The vertex can thus carry an index; in this case the index  $\mu$ .
- momentum conservation at the vertex, meaning that all incoming momenta at the vertex add up to zero. This is expressed by a delta function of these momenta. The delta function

results from the integral over the coordinate of the interaction term. For the vertex of figure 4.1 it follows as

$$\int d^4x e^{i\tilde{p}\cdot x} e^{ik\cdot x} e^{-i\tilde{q}\cdot x} = \int d^4x e^{ix\cdot((\tilde{p}+k)-\tilde{q})} = (2\pi)^4 \delta^4((\tilde{p}+k)-\tilde{q}). \quad (4.11)$$



Figure 4.2.: The Feynman diagrams are found by connecting the lines in all possible ways.

The invariant amplitude to  $n$ -th order (4.9) is then found as follows. Draw all external lines (with momenta  $\{p_i\}$  and  $\{q_j\}$ ) together with any  $n$  vertices, as shown in figure 4.2. Then connect *all* the lines of the vertices to *all* the external lines and each other. Every possible way to do this, for every combination of vertices, gives a Feynman diagram contributing to the invariant amplitude.

With this background we are ready to understand why the Ward identity (4.1) holds. First the reasoning is explained for QED; afterwards it shall be explained how to generalize the reasoning to other abelian gauge theories. The starting point is current conservation  $\partial_\mu J^\mu = 0$ . This is an operator identity, so replacing  $\mathcal{H}^{\text{int}}(x_1)$  in (4.9) by  $\partial_\mu J^\mu(x_1)e^{ik\cdot x_1}$  renders the expression 0. We now claim that

$$\begin{aligned} \int d^4x_1 \dots \int d^4x_n \langle p|T\left((\partial_\mu J^\mu(x_1)e^{ik\cdot x_1}, \mathcal{H}^{\text{int}}(x_2), \dots, \mathcal{H}^{\text{int}}(x_n))\right)|q\rangle \Big|_{C\&A} \\ = i(2\pi)^4 \frac{1}{n} ik_\mu \mathcal{M}^{\diamond\mu}(\{p_i\} + k \rightarrow \{q_j\}). \end{aligned} \quad (4.12)$$

Since the left-hand side is 0, (4.12) proves the Ward identity (4.1). So let us prove the claim (4.12). What changes under the replacement  $\mathcal{H}^{\text{int}}(x_1) \rightarrow \partial_\mu J^\mu(x_1)e^{ik\cdot x_1}$  is one of the vertices of every diagram. In QED  $\mathcal{H}^{\text{int}}(x) = -A_\mu(x)J^\mu(x)$ , where  $J^\mu = iq\bar{\psi}\gamma_\mu\psi$ . This means that the new vertex differs from the old one in that it does not have an external photon line. It will thus be a diagram looking like the left-hand side of figure 4.3. We now discuss the other characteristics of the vertex. The exponential factors resulting from the field expansions read  $e^{i\tilde{p}\cdot x} e^{-i\tilde{q}\cdot x}$ , such that the derivative  $\partial_\mu$  brings down a factor  $i(\tilde{p}-\tilde{q})_\mu$ . The integral over  $x_1$  then gives

$$\int d^4x e^{i\tilde{p}\cdot x_1} e^{-i\tilde{q}\cdot x_1} e^{ik\cdot x_1} = \int d^4x e^{ix_1\cdot((\tilde{p}+k)-\tilde{q})} = (2\pi)^4 \delta^4((\tilde{p}+k)-\tilde{q}). \quad (4.13)$$

If we interpret this as momentum conservation, it is as if a momentum  $k$  ‘magically’ appears at the vertex! This interpretation is shown graphically in figure 4.3. Due to this delta function,

Figure 4.3.: The vertex generated by  $\partial_\mu J^\mu(x)e^{ik\cdot x}$ ; for QED set  $m = 1$ .

the prefactor brought down by the derivative is  $i(\tilde{p} - \tilde{q})_\mu = -ik_\mu$ . Apart from this  $-ik_\mu$ , the prefactors are the same as for the usual QED vertex of figure 4.1. Since momentum conservation applies in the same manner as well, the only difference between the vertex drawn on the right-hand side of 4.3 and the QED vertex is that the QED vertex has a photon line emerging from it. All the diagrams contributing to the left-hand side of the claimed equation (4.12) are then found by connecting the lines in figure 4.4a in all possible ways<sup>2</sup> and contracting with  $-ik_\mu$ . The diagrams contributing to  $i(2\pi)^4 \mathcal{M}^\mu(\{p_i\} + k \rightarrow \{q_j\})$ , which is in the right-hand side of the claimed equation (4.12), are found by connecting the lines in figure 4.4b in all possible ways. In the last case, there are  $n$  possible ways to connect the external photon line with momentum  $k_\mu$  to a photon line emerging from a vertex. This factor  $n$  cancels against the  $\frac{1}{n}$  in (4.12). The remaining connections that have to be made are the same as the connections that have to be made in figure 4.4a! This proves the claimed equality (4.12) for QED.

There is one detail that has yet gone unmentioned. The  $\diamond$  in equation (4.12) serves to indicate that the external matter lines are to be taken on-shell and that  $\mathcal{M}$  is to be contracted with their polarization vectors. These requirements are a consequence of the fact that we had to invoke the equations of motion for the matter fields after equation (4.5) in order to derive current conservation, which was a crucial ingredient of our derivation.



(a) Contributions to the left-hand side of (4.12)



(b) Contributions to the right-hand side of equation (4.12)

Figure 4.4.

It is not too hard to generalize this proof to other abelian gauge theories. In fact, we did not really use the fact that we were dealing with QED; the same argument can be repeated with general vertices, the newly constructed vertex will still satisfy the relation shown in figure 4.3, and the claimed equation (4.12) will still hold. There is only one aspect that changes in the proof. In paragraph 4.1.1 it was pointed out that QED is special in the sense that the conserved current does not depend on the gauge field, such that  $\mathcal{L}^{\text{int}} = A_\mu J^\mu$ . In general,  $\mathcal{L}^{\text{int}}$  is a polynomial in the gauge fields  $A_\mu^a$ . Every term in the polynomial thus gives rise to a term in  $J_\mu^a$  as dictated by equation (4.2). The same argument as above can then be applied to every term separately to show that equation (4.12) holds, which in turn proves the Ward identity. So let us focus on one term in  $\mathcal{L}^{\text{int}}$ :  $\mathcal{L}^{(m)} \sim A^m$ , which includes QED for  $m = 1$ . Then (4.2) implies that  $J_\mu^a A_a^\mu = m\mathcal{L}^{\text{int}}$ , which involves an extra factor  $m$  as compared to the QED case. This results in the extra factor  $m$  in figure 4.3, which contributes to the left-hand side of equation (4.12). There is another change. When connecting the external photon line with momentum  $k_\mu$  in figure 4.4b to a photon line of a vertex as before, there are now  $n \cdot m$  possibilities instead of  $n$ , since every vertex now carries  $m$  photon lines instead of 1. This extra factor of  $m$  contributes to the right-hand side (4.12). Both sides of (4.12) thus obtain an extra

<sup>2</sup>To be clear here, the dotted line should *not* be connected, it is only there to denote the ‘magically appearing’ momentum  $k$ . Furthermore, the external states  $\{p_i\}$  and  $\{q_i\}$  are now assumed to be the ones appearing in figure 4.4a, so together they comprise  $3n - 1$  particles.

factor of  $m$ , such that the equation is still satisfied and hence so is the Ward Identity.

## 4.2. Diagrammatic proof of the Ward identity

Following the approach of Peskin and Schroeder [2, chapter 7.4], we now show in that the Ward identity (4.1) is satisfied in QED by an alternative proof that uses explicit Feynman diagram manipulations. To this end, we first prove a more general identity for QED, called the *Ward-Takahashi identity*. To state it, some notation has to be introduced. Let  $\mathcal{M}'^\mu(k; p_1 \cdots p_n; q_1 \cdots q_n)$  denote an arbitrary correlation function with  $n$  incoming fermions with momenta  $p_1 \cdots p_n$ ,  $n$  outgoing fermions with momenta  $q_1 \cdots q_n$ , and with at least one external photon line with momentum  $k^\mu$ . The ' serves to indicate that *only* its external photon lines are assumed to be truncated, its external fermion lines are *not*. The notation  $\mathcal{M}$  *without* a prime is reserved for fully truncated correlation functions. Similarly, let  $\mathcal{M}'^0(p_1 \cdots p_n; q_1 \cdots q_n)$  denote a correlation function with one external photon less, but with the same number of incoming and outgoing fermions and also with only its external photon lines truncated. Then the Ward-Takahashi identity states

$$k_\mu \mathcal{M}'^\mu(k; p_1 \cdots p_n; q_1 \cdots q_n) = e \sum_i \left( \mathcal{M}'^0(p_1 \cdots p_n; \cdots q_i - k \cdots) - \mathcal{M}'^0(\cdots p_i + k \cdots; q_1 \cdots q_n) \right). \quad (4.14)$$

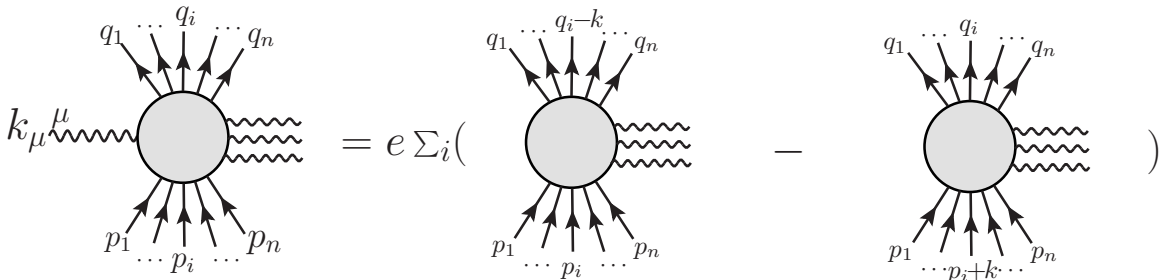


Figure 4.5.: The Ward-Takahashi identity (4.14)

The identity is graphically depicted in figure 4.5.

As a side remark, sometimes the term Ward-Takahashi identity is used to refer to equation (4.14) for the special case that  $\mathcal{M}'^\mu$  is the (full) photon-fermion-fermion amplitude; the special case with only 1 outgoing photon line, 1 incoming fermion line and 1 outgoing fermion line.  $\mathcal{M}'^0$  is in this case the (full) fermion propagator.

Now we prove the identity (4.14) to every order in perturbation theory, that is, to every order in  $q$ . Figure 4.6 shows the Feynman rules for QED. Let us consider a fixed order in perturbation theory and a fixed number  $n$  of incoming and outgoing external fermion lines. Also we consider a fixed number of external photons for  $\mathcal{M}'^\mu$  (at least one) and consider the corresponding  $\mathcal{M}'^0$  with one external photon less. Obviously, if we would remove the external photon line with momentum  $k$  from a diagram contributing to  $\mathcal{M}'^\mu$ , we would get a diagram contributing to  $\mathcal{M}'^0$ . This could for example be the diagram shown in figure 4.7.

Typically this is not the only diagram contributing to  $\mathcal{M}'^0$ ; there will be more. If we attach an external photon line (with momentum  $k$ ) to a fermion line in any such a  $\mathcal{M}'^0$ -diagram, we obtain

$$\begin{array}{ll}
\begin{array}{c} \xrightarrow{p} \\ \hline \end{array} & \frac{1}{i(2\pi)^4} [i\gamma_\mu p^\mu + m]^{-1} \\
\begin{array}{c} \mu \quad k \quad \nu \\ \sim \sim \sim \sim \sim \sim \end{array} & \frac{1}{i(2\pi)^4} [\eta_{\mu\nu} - (1 - \lambda^{-2}) \frac{k_\mu k_\nu}{k^2}] \\
\begin{array}{c} \mu \\ \sim \\ \swarrow \quad \searrow \\ \hline \end{array} & i(2\pi)^4 i q \gamma^\mu
\end{array}$$

Figure 4.6.: Feynman Rules for QED, omitting the momentum-conserving delta function for the vertex. The photon propagator is obtained by adding the gauge fixing term

$$-\frac{1}{2}(\lambda\partial^\mu A_\mu)^2 \text{ to } \mathcal{L}_{\text{QED}}.$$

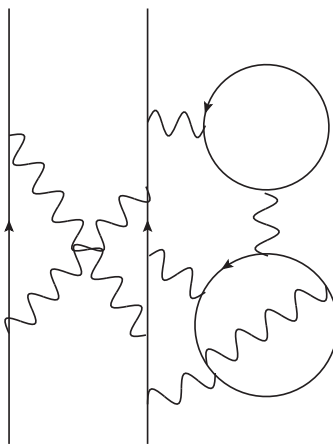


Figure 4.7.: Example diagram contributing to  $\mathcal{M}^0$

a diagram contributing to  $\mathcal{M}^\mu$  again. Since the only vertex in QED is the three-point-vertex shown in figure 4.6, every diagram contributing to  $\mathcal{M}^\mu$  can be obtained in this way. Thus, a procedure to generate all diagrams contributing to  $\mathcal{M}^\mu$  is:

1. Consider one diagram contributing to  $\mathcal{M}^0$  and attach a photon line in every possible way. Sum the results.
2. Repeat step 1 for all diagrams contributing to  $\mathcal{M}^0$  and sum the results. This will give you  $\mathcal{M}^\mu$ .

In order to prove the identity (4.14), we follow this procedure while performing the contraction with the momentum of the attached photon momentum  $k_\mu$  already at step 1. We shall show that the contribution to  $k_\mu \mathcal{M}^\mu$  obtained after step 1 satisfies the Ward-Takahashi identity by itself. Since this will be true for every contribution, equation (4.14) then follows immediately. So let us consider one diagram contributing to  $\mathcal{M}^0$  (for example the one shown in figure 4.7), apply step 1, and contract with  $k_\mu$ . The only place where we can attach a photon line is at a fermion line. Since the fermion lines are continued at every vertex they cannot end; therefore



they either form a continued line connecting an incoming external line with an outgoing line, or they form an internal loop. First we consider first what happens if we connect the photon line at all places along one continued fermion line. We shall do the same for a fermion loop afterwards.

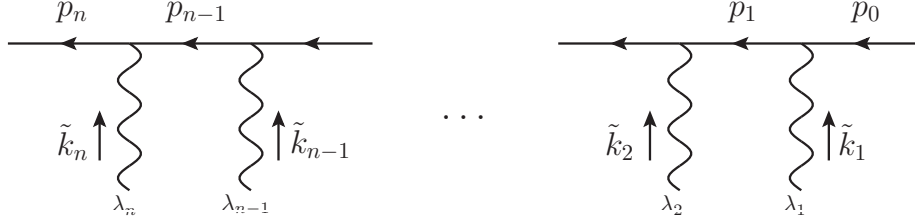


Figure 4.8.: One continued fermion line inside a diagram contributing to  $\mathcal{M}'^0$ . The fermion momenta are defined as  $p_i = p + \sum_{j=0}^i \tilde{k}_j$  with  $1 \leq i \leq n$ , where  $p$  is the incoming fermion momentum.

Before the photon line is attached, the part of the diagram containing the continued fermion line looks like figure 4.8, decoding the algebraic expression

$$\frac{(-ie)^n}{i(2\pi)^4} \left( [i\not{p}_n + m]^{-1} \gamma^{\lambda_n} [i\not{p}_{n-1} + m]^{-1} \gamma^{\lambda_{n-1}} \dots \gamma^{\lambda_2} [i\not{p}_1 + m]^{-1} \gamma^{\lambda_1} [i\not{p} + m]^{-1} \right). \quad (4.15)$$

To obtain the whole diagram this has to be multiplied with the algebraic expression for the

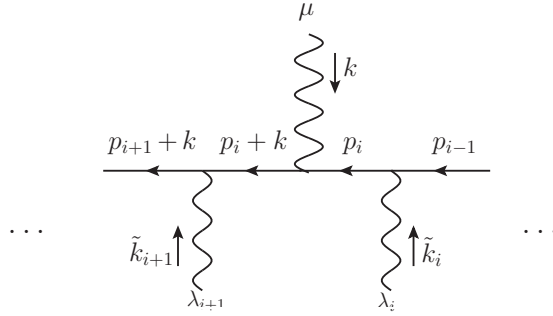


Figure 4.9.: A photon attached to the fermion line

rest of the diagram. Now we attach a photon with momentum  $k^\mu$  after the  $i$ -th photon line as shown in figure 4.9, and contract with  $k^\mu$ . The diagram in figure 4.9 then reads

$$\dots [i(\not{p}_{i+1} + \not{k}) + m]^{-1} \gamma^{\lambda_{i+1}} [i(\not{p}_i + \not{k}) + m]^{-1} (-ie) \not{k} [i\not{p}_i + m]^{-1} \gamma^{\lambda_i} [i\not{p}_{i-1} + m]^{-1} \dots \quad (4.16)$$

Using

$$-ie\not{k} = (-e) \left[ (i(\not{p}_i + \not{k}) + m) - (i\not{p}_i + m) \right], \quad (4.17)$$

this can be rewritten as

$$(-e) \left( \dots [i(p_{i+1} + k) + m]^{-1} \gamma^{\lambda_{i+1}} \quad [ip_i + m]^{-1} \quad \gamma^{\lambda_i} [ip_{i-1} + m]^{-1} \dots - \dots [i(p_{i+1} + k) + m]^{-1} \gamma^{\lambda_{i+1}} \quad [i(p_i + k) + m]^{-1} \quad \gamma^{\lambda_i} [ip_{i-1} + m]^{-1} \dots \right), \quad (4.18)$$

which is graphically depicted in figure 4.10. The dotted line is there again to depict a ‘magically

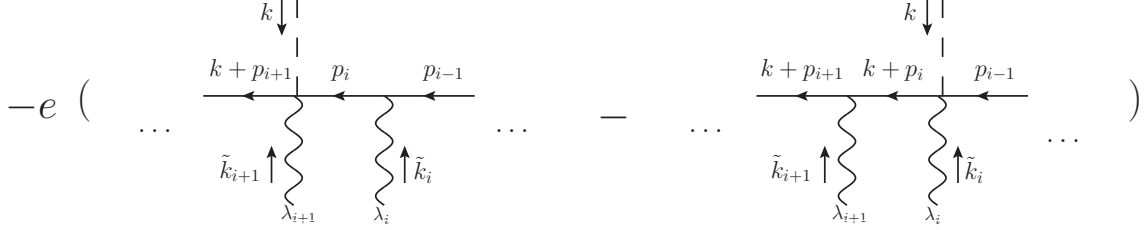


Figure 4.10.: Expression (4.18)

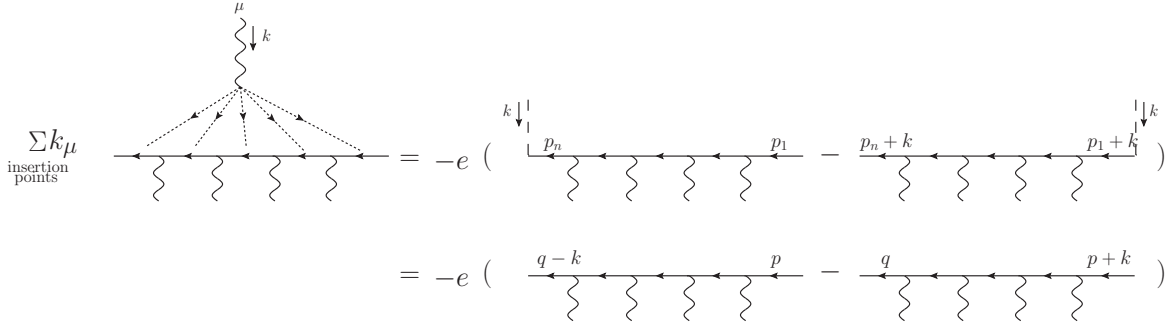


Figure 4.11.: The result of summing over the insertion points.

incoming’ momentum  $k$ . Now, if we sum the diagrams with different insertion points (that is, sum figure 4.10 over  $i$ ), then the first term obtained at every insertion point gets canceled by the second term obtained at the next insertion point. This leaves us only with the first term obtained at the last insertion point and the second term obtained at the first insertion point, as shown in figure 4.11. In figure 4.11 we defined  $q = p_n + k$  for comparison with the momenta of  $\mathcal{M}^\mu$  later on. Of course, the diagrams in figure 4.11 are still to be multiplied with the algebraic expression of the rest of the diagrams, which have not changed by attaching the photon line and contracting with  $k_\mu$ .

Now we can repeat the same procedure, but attaching the photon at all possible points along a fermion *loop*. The expression for a photon loop is equal to equation (4.15) (figure 4.8), with the modification that now the beginning and ending of the line are connected. Therefore we have  $p = p_n$  and  $\sum_{j=1}^n \tilde{k}_j = 0$  by momentum conservation of the diagram. In addition, the whole expression is now integrated over one loop-momentum, say over  $p$ . Despite these changes, we can perform the very same trick: we attach the photon line at all possible places along the loop, contract with  $k^\mu$  and sum the results; we do again obtain two terms for every insertion point, but since we are considering a loop instead of a line, *all* terms do now cancel when summing the diagrams. Therefore, the only contribution to  $k_\mu \mathcal{M}^\mu$  comes from attachments along

continued fermion lines, rather than from attachments to fermion loops.

To complete step 1 of the procedure we now sum over the insertion points of *all* continued lines of the particular diagram that we are considering. The result is the right-hand side of figure 4.5 (or equation (4.14)), with the modification that the blob ( $\mathcal{M}^0$ ) is supposed to denote the particular diagram contributing to  $\mathcal{M}^0$  under consideration. Performing step 2, that is summing over all possible diagrams contributing to  $\mathcal{M}^0$ , we obtain the true equation, where  $\mathcal{M}'^\mu$  and  $\mathcal{M}^0$  contain all contributing diagrams. This proves the Ward-Takahashi identity in QED.

The last step is to prove the Ward identity (4.1). Recall the difference between  $k_\mu \mathcal{M}'^\mu$  and  $k_\mu \mathcal{M}^{\diamond\mu}$ : to obtain the latter from the former, we need to amputate the external fermions, put them on-shell and contract with the appropriate fermion spinors. The external fermion lines of  $k_\mu \mathcal{M}'^\mu$  are amputated by multiplying from the right with the inverse propagators  $(i\not{q}_j + M)$  and from the left with  $(i\not{p}_j + m)$  for every  $1 \leq j \leq n$ . For the moment we assume to be dealing with fermions, not with anti-fermions. According to the right-hand side of the Ward-Takahashi identity (figure 4.5), almost all these inverse propagators cancel against propagators that are present in  $k_\mu \mathcal{M}'^\mu$ . There is one exception in every term, namely the inverse propagator that corresponds to the external fermion with the ‘anomalous’ momentum  $p_i + k$  or  $q_i - k$ . It is the survival of this inverse propagator that ensures that the corresponding term vanishes when it is contracted with the corresponding fermion spinor  $u_i(p_i)$  or  $\bar{u}(q_i)$ . The vanishing of these terms occurs by either the relation  $(i\not{p}_i + m)u(p_i) = 0$  or by  $\bar{u}(q_i)(i\not{q}_i + m) = 0$ . If external lines correspond to anti-fermions an analogous argument applies. In that case the momenta acquire a minus sign such that the inverse propagators read  $(-i\not{q}_j + m)$  and  $(-i\not{p}_j + m)$ . The surviving inverse propagators are then contracted with spinors representing anti-fermions and cancel by the relations  $(-i\not{p} + m)v(p) = 0$  and  $\bar{v}(q)(-i\not{q} + m) = 0$ . This completes the diagrammatic proof of the Ward identity (4.1).

# 5. Unitarity

## 5.1. The scattering matrix and unitarity

In this section the scattering matrix is introduced and it is explained why it *has to be* unitary. The rest of this chapter is devoted to *proving* its unitarity.

In particle physics we are typically interested in scattering experiments. In a very general sense, the scattering of particles describes anything happening to them between their initial state at time  $t = -\infty$  and their final state at  $t = \infty$ . At these initial and final times the particles are assumed to be infinitely far apart<sup>1</sup> such that they are described by a free, non-interacting theory. For such a theory the complete Hilbert space is spanned by the basis consisting of all possible vectors created by letting the the creation operators work any number of times on the vacuum state. This basis thus consists of states  $|p\rangle = a^\dagger(p)|0\rangle$ ,  $|p, q\rangle = a^\dagger(p)a^\dagger(q)|0\rangle$  etc. Such a basis can be built both for  $t = -\infty$  and  $t = +\infty$ . Basis vectors of the ‘initial state basis’ are denoted as  $|p\rangle_{\text{in}}$ ,  $|p, q\rangle_{\text{in}}$ , ...; basis vectors of the ‘final state basis’ as  $|p\rangle_{\text{out}}$ ,  $|p, q\rangle_{\text{out}}$ , ... Since both bases are orthonormal, they are related to each other by an (infinite-dimensional) unitary matrix  $\mathcal{S}$ . More concretely,  $|p\rangle_{\text{out}} = \mathcal{S}|p\rangle_{\text{in}}$ ,  $|p, q\rangle_{\text{out}} = \mathcal{S}|p, q\rangle_{\text{in}}$  etc. The matrix  $\mathcal{S}$  is called the *scattering matrix*. Its matrix elements are closely related to probabilities of scattering processes: the probability for an incoming configuration  $a$  to scatter into an outgoing configuration  $b$  is given by

$$|{}_{\text{out}}\langle b|a\rangle_{\text{in}}|^2 = |{}_{\text{in}}\langle a|b\rangle_{\text{out}}|^2 = |{}_{\text{in}}\langle a|\mathcal{S}|b\rangle_{\text{in}}|^2 = |S_{a,b}|^2, \quad (5.1)$$

where  $S_{a,b}$  denotes the scattering matrix element in the in-basis.

To be able to interpret scalar products as probabilities, it is essential that the  $\mathcal{S}$  matrix is unitary. This can be understood as follows. The probability that a state with configuration  $a$  at  $t = \infty$  has configuration  $b$  at that same time is clearly 0; unless  $a = b$  in which case the probability is 1. We thus need

$${}_{\text{out}}\langle b|a\rangle_{\text{out}} = \delta_{ab}. \quad (5.2)$$

This explains why the ‘final state basis’ *has* to be orthonormal in order for the probability interpretation to make any sense. On the other hand we have

$${}_{\text{out}}\langle b|a\rangle_{\text{out}} = {}_{\text{in}}\langle b|\mathcal{S}^\dagger\mathcal{S}|a\rangle_{\text{in}} = (\mathcal{S}^\dagger\mathcal{S})_{ab}. \quad (5.3)$$

This shows that we really need  $\mathcal{S}^\dagger\mathcal{S} = \mathbf{1}$  in order to fulfill (5.2). If the scattering matrix would *not* be unitary, then the complete probability interpretation would break down at  $t = \infty$ .

At this point one may wonder why we are stressing the point that  $\mathcal{S}$  needs to be unitary. After all, if it is defined as a matrix relating two orthonormal bases then it is unitary *by construction*. In practice, scattering amplitudes are calculated by evaluating Feynman diagrams using the corresponding Feynman rules, rules derived from a hermitian interaction Hamiltonian  $\mathcal{H}^{\text{int}}$ .

---

<sup>1</sup>Clearly this is not the case for quarks, which form bound states due to the strong force. In this thesis we ignore this complication; that is, we ignore the complication of quantum chromodynamics.

And indeed, one can ‘derive’ in the operator-formalism that this is equivalent to calculating scalar products between ‘in’ and ‘out’ states as in (5.1). This would thus guarantee that the corresponding scattering matrix is unitary. *However*, this ‘derivation’ is far from perfect. On the contrary, there exists a formal proof that an important object used in the derivation does not exist [3]! This setback turns out *not* to be a reason to abandon the approach of calculating scattering matrix elements by Feynman diagrams. The reason is simply that the results turn out to agree very well with experiments. It *does* mean however that we cannot rely upon the mentioned ‘derivation’ to guarantee the unitarity of the scattering matrix. Therefore, we shall need some other means of establishing its unitarity. This then is the aim of the rest of this chapter. Following Veltman [3], the cutting equations for Feynman diagrams are derived in section 5.2. In section 5.3 these are shown to imply that the scattering matrix *is* unitary.

## 5.2. Cutting equations

This section concerns the derivation of the cutting equations. They are derived using a generalized kind of Feynman rules, known as cutting rules, which have been formulated by Cutkosky in 1960 [4]. First we show the derivation for a scalar field. Generalizations to other fields are discussed afterwards.

### Another form of the propagator

As a first step, we show that the Feynman propagator for a scalar field can be rewritten as

$$\Delta(x) = \frac{1}{i(2\pi)^4} \int d^4k \frac{e^{ik \cdot x}}{k^2 + m^2 - i\epsilon} \quad (5.4)$$

$$= \theta(x^0)\Delta^+(x) + \theta(-x^0)\Delta^-(x), \quad (5.5)$$

where

$$\Delta^\pm(x) := \frac{1}{(2\pi)^3} \int d^4k e^{ik \cdot x} \theta(\pm k^0) \delta(k^2 + m^2). \quad (5.6)$$

This relation will be shown working backwards, i.e. we will manipulate (5.5) to obtain (5.4). Firstly, the theta-functions in (5.5) can be written as

$$\theta(x^0) = \frac{1}{i(2\pi)} \int_{-\infty}^{\infty} d\tau \frac{e^{i\tau x^0}}{\tau - i\epsilon}. \quad (5.7)$$

This equation can be understood by writing the integral as a contour integral in the complex  $\tau$ -plane. It can be closed for  $x^0 > 0$  by a large arc in the upper half-plane and for  $x^0 < 0$  by one in the lower half-plane. Since the pole is located at  $\tau = i\epsilon$ , Cauchy’s residue theorem tells us that we only get a contribution for  $x^0 > 0$ , in which case the integral becomes  $2\pi i$  and the result is indeed 1. Plugging (5.7) into (5.5) yields

$$\Delta(x) = \frac{1}{i(2\pi)^4} \int d^4k d\tau e^{ik \cdot x + i\tau x^0} \delta(k^2 + m^2) \left\{ \frac{\theta(k^0)}{\tau - i\epsilon} + \frac{\theta(-k^0)}{-\tau - i\epsilon} \right\}. \quad (5.8)$$

In order to dispose of the  $\tau$  in the exponential, we shift the integration variable  $k^0 \rightarrow k'^0 = k^0 - \tau$ . This results in

$$\Delta(x) = \frac{1}{i(2\pi)^4} \int d^4k d\tau e^{ik \cdot x} \delta(-(k^0 + \tau)^2 + |\vec{k}|^2 + m^2) \left\{ \frac{\theta(k^0 + \tau)}{\tau - i\epsilon} + \frac{\theta(-(k^0 + \tau))}{-\tau - i\epsilon} \right\}. \quad (5.9)$$

To perform the integral over  $\tau$ , the delta function can be regarded as a function of  $k^0 + \tau$  in order to use the identity

$$\delta(f(x)) = \sum_i \frac{\delta(x - x_i)}{|f'(x_i)|}. \quad (5.10)$$

The sum in (5.10) is over the  $i$ 's labelling the  $x_i$ 's that solve  $f(x_i) = 0$ . In our case the  $(k^0 + \tau)_i$ 's are  $\pm\omega_{\vec{k}} = \pm\sqrt{|\vec{p}|^2 + m^2}$  and  $|f'(\pm\omega_{\vec{k}})| = 2\omega_{\vec{k}}$ . Equation (5.9) then becomes

$$\begin{aligned} \Delta(x) &= \frac{1}{i(2\pi)^4} \int d^4k e^{ik \cdot x} \frac{1}{2\omega_{\vec{k}}} \left\{ \frac{1}{-k^0 + \omega_{\vec{k}} - i\epsilon} + \frac{1}{k^0 + \omega_{\vec{k}} - i\epsilon} \right\} \\ &= \frac{1}{i(2\pi)^4} \int d^4k \frac{e^{ik \cdot x}}{k^2 + m^2 - i\epsilon}, \end{aligned} \quad (5.11)$$

which is the same as (5.4), as promised. Note that, according to (5.6),

$$(\Delta^\pm)^*(x) = \Delta^\mp(x), \quad (5.12)$$

such that the complex conjugated Feynman propagator (5.5) can be written as

$$\Delta^*(x) = \theta(x^0)\Delta^-(x) + \theta(-x^0)\Delta^+(x). \quad (5.13)$$

### The Largest Time Equation

Now consider an arbitrary, truncated Feynman diagram in real space-time. It has  $n$  vertices, all of which carry a coordinate  $x_i$ . We call the diagram  $D(x_1, x_2, \dots, x_n)$ . Furthermore, we call the coordinate with the largest time-component  $x_m$ . Equation (5.5) then tells us that we can write any propagator connecting the vertex  $x_m$  to another vertex  $x_i$  as  $\Delta(x_m - x_i) = \Delta^+(x_m - x_i)$  (and  $\Delta(x_i - x_m) = \Delta^-(x_i - x_m)$ ). To exploit this idea further we introduce new Feynman rules, involving the possibility to *circle* diagrams. These rules are the following.

- A circled vertex equals  $-1$  times the usual, uncircled vertex.
- A propagator between two uncircled vertices  $x$  and  $y$  still denotes  $\Delta(y - x)$ .
- A propagator between two circled vertices  $x$  and  $y$  now denotes  $\Delta^*(y - x)$ .
- If only one of the two vertices is circled, then the propagator denotes  $\Delta^+(y - x)$  if  $y$  is circled and  $\Delta^-(y - x)$  if  $x$  is circled.

Any number of vertices of  $D(x_1 \cdots x_n)$  can be circled, giving rise to  $2^n$  possible circlings of that diagram.

Consider now one such circling. This circling still has  $x_m^0$  as largest time. Then changing the circling of  $x_m$  (that is, circle it if uncircled and uncircle if circled) will return the same diagram times  $-1$ . It can be understood as follows. Note first of all that changing the circling of  $x_m$  will introduce the factor  $-1$  by the first listed Feynman rule. Now suppose that  $x_m$  is uncircled. For a propagator connecting an *uncircled* vertex  $x_i$  to  $x_m$ , we can write  $\Delta(x_m - x_i) = \Delta^+(x_m - x_i)$ , by (5.5). This  $\Delta^+(x_m - x_i)$  is precisely what the propagator becomes by circling  $x_m$ . This idea is shown in the first line of figure 5.1. For a propagator connecting a *circled* vertex  $x_j$  to  $x_m$ , we can write  $\Delta(x_m - x_j) = \Delta^*(x_m - x_j)$ , by (5.13). Again, this  $\Delta^*(x_m - x_j)$  is precisely what the propagator becomes by circling  $x_m$ . This is shown in the second line of figure 5.1. So we have now established that if  $x_m$  is uncircled, then changing its circling it yields the same diagram times  $-1$ . Along the same lines it can be shown that this is true if we start out with a circled

$$\begin{array}{lcl}
x_i \text{ --- } x_m & = \Delta(x_m - x_i) = \Delta^+(x_m - x_i) = & x_i \text{ --- } \textcircled{x_m} \\
\textcircled{x_j} \text{ --- } x_m & = \Delta^-(x_m - x_j) = \Delta^*(x_m - x_j) = & \textcircled{x_j} \text{ --- } \textcircled{x_m}
\end{array}$$

Figure 5.1.

$x_m$ .

A consequence of this is that if we take an arbitrary circling of  $D(x_1 \cdots x_m)$ , and add to it the same diagram *with the opposite circling of  $x_m$* , then we get zero. This is true for *any* possible way of circling all non- $x_m$ -vertices. So if we consider *all*  $2^{n-1}$  possible circlings which have  $x_m$  uncircled to their counterparts which have  $x_m$  circled, then we get zero. But then we are simply summing all possible circlings of  $D(x_1 \cdots x_m)$ . So

$$\sum_{\text{circlings}} D(x_1 \cdots x_n) = 0. \tag{5.14}$$

This is called the *Largest Time Equation (LTE)*.

### From circling to cuttings

We now move on to consider the diagram in Fourier space: this is done by integrating over all vertex coordinates, which results in energy-momentum conservation at every vertex. The propagators are then substituted by their Fourier transform. Furthermore, we attach external lines to the diagram. Since the diagrams will be identified with a scattering matrix element later on, we put the external lines on-shell and add their residue factors  $(\pm 2\pi)^3 2\omega_{\vec{k}}^{-\frac{1}{2}}$ . The resulting diagram will be denoted as  $D(a \rightarrow b)$ , where  $a$  is short for the incoming momenta  $\{k_a\}$  and  $b$  for the outgoing momenta  $\{k_b\}$ .  $D(a \rightarrow b)$  still satisfies (5.14).

A nice feature of this construction is that, by (5.6),  $\Delta^+(k)$  only carries on-shell momentum with positive energy and  $\Delta^-(k)$  only on-shell momentum with negative energy. Because of our new Feynman rules, this implies that a propagator connecting an uncircled vertex to a circled vertex transports positive energy towards that circled vertex (or negative energy towards the uncircled vertex). Since  $\Delta$  and  $\Delta^*$  are combinations of  $\Delta^+$  and  $\Delta^-$  (by (5.5) and (5.13)), between two circled or between two uncircled vertices energy can flow either way.

Consider now a region of connected circled vertices in our diagram, bordered by only un-

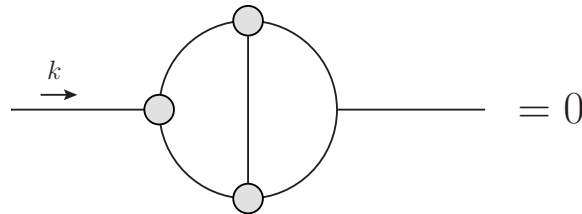


Figure 5.2.: This diagram vanishes because the circled region is not connected to an outgoing external line.

circled vertices. Both internal and external lines can connect to this region. The *internal* lines connect this region to the bordering uncircled vertices. Therefore, they transport energy *into*

the region. If there is at least one *outgoing external* line connecting to this region this is fine: then energy can flow out again. However, if there are only *incoming* external lines connecting to the region, then energy *cannot* flow out. As a result, energy-momentum conservation cannot be satisfied in this region, such that the particular circling of this diagram gives zero. Figure 5.2 shows an example of such a situation. Similarly, a region of uncircled vertices (bordered by only circled ones) can only exist if an *incoming* external line connects to it to provide an inflow of energy.

This concept becomes more illuminating if we introduce some new notation. By conven-

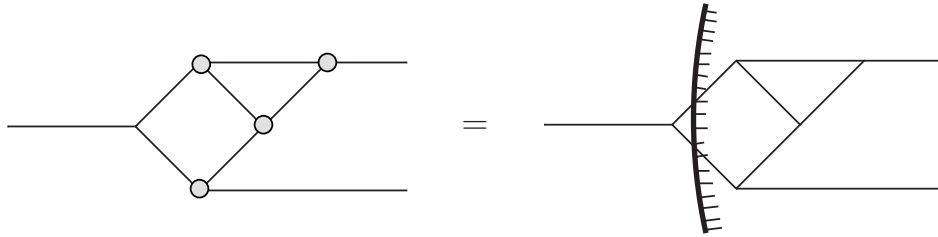


Figure 5.3.: The energy flow is through the cutting line to the right.

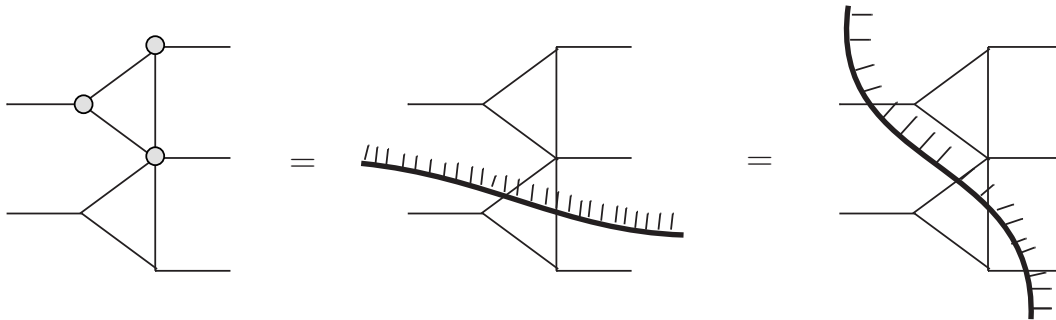


Figure 5.4.: Every cut can be written as a vertical cut.

tion, we draw the *incoming* external lines on the left-hand side of the diagram and the *outgoing* external lines on the right-hand side. Then the main point: we stop drawing circles around vertices. Instead, we draw a thick line cutting through the internal lines that separate circled regions from uncircled regions. The fact that energy flows from the uncircled region towards the circled region is indicated by small ‘teeth’ on the line, indicating the direction of energy flow. An example of this notation is shown in figure 5.3.

It turns out that every non-zero circling of a diagram can be written as a diagram with a single ‘vertical’ cut as the one in figure 5.3. The reasoning explaining this is as follows. Since we cannot have regions that are not connected to any external lines (that would violate energy-conservation), we will not have any diagrams with the cutting lines forming loops. Therefore, any cutting line will enter the diagram at some point and leave it another. If we allow the cutting lines to cut through external lines as well (we do), again in a manner consistent with the energy flow, then we can make sure that every cutting line enters a diagram at the bottom and leaves it at the top. Every cutting line then cuts the diagram ‘vertically’. This idea is illustrated in figure 5.4. Furthermore, a diagram can be cut only by one such a ‘vertical cutting’. If you would have two, then the region in between would not be connected to any external lines and violate energy conservation again, as shown in figure 5.5.



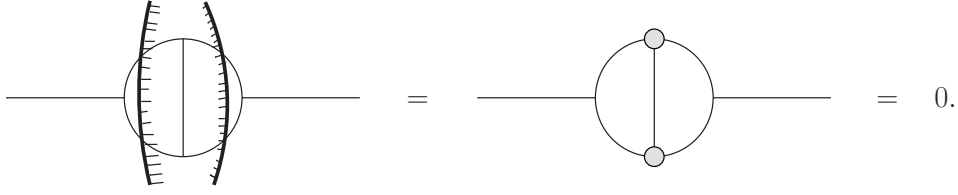


Figure 5.5.: A diagram with two vertical cuttings vanishes.

So in this notation, every non-vanishing circling in equation (5.14) (in Fourier space and with external lines attached) is uniquely characterized by one vertical cut. Only the fully uncircled and fully circled diagram can both be drawn without a cut. The fully uncircled diagram is equal to the original diagram  $D(a \rightarrow b)$ . Its fully circled counterpart we will denote by  $\bar{D}(a \rightarrow b)$ . Moving both these diagrams to the other side of equation (5.14) yields the *cutting equation*

$$D(a \rightarrow b) + \bar{D}(a \rightarrow b) = - \sum_{\text{cuttings}} D(a \rightarrow b). \quad (5.15)$$

Before showing how the cutting equation is related to unitarity, let us think about what the fully circled diagram  $\bar{D}(a \rightarrow b)$  actually embodies. Recall that in *real space* the fully circled diagram is obtained from  $D(x_1 \cdots x_n)$  by complex conjugating all the internal propagators and multiplying by  $-1$  for every vertex. In *Fourier space* this means that every internal propagator has to be replaced by its complex conjugate propagator *with reversed momentum*, e.g.  $\Delta(k) \rightarrow \Delta^*(-k)$ . Also, the minus signs have to be taken into account; these can be incorporated by changing the vertex factors  $i(2\pi)^4 \rightarrow -i(2\pi)^4$ . Both these modifications will be used later to identify  $\bar{D}(a \rightarrow b)$  with a complex conjugated diagram.

### 5.3. Unitarity & the Cutting Equation

This section explains how the cutting equation relates to unitarity. More precisely, it proves that the cutting equation (5.15) is equivalent to the condition that the scattering matrix be unitary. The proof is shown for scalar fields. For fermions, the proof proceeds analogously [3]. For photons, the situation is a bit more involved; this will be discussed afterwards.

As explained in section 5.1, a quantum field theory is said to be unitary if the scattering matrix is, so if  $\mathcal{S}^\dagger \mathcal{S} = \mathbf{1}$ . Decomposing  $\mathcal{S} = \mathbf{1} + i\mathcal{T}$ , the equivalent relation for  $\mathcal{T}$  is

$$i(\mathcal{T} - \mathcal{T}^\dagger) = -\mathcal{T}^\dagger \mathcal{T}. \quad (5.16)$$

Equation (5.16) has to hold for all matrix elements of  $\mathcal{T}$ . Denoting a general ‘in-basis’ state by  $|a\rangle := |\{k_a\}\rangle$  and a general ‘out-basis’ state by  $|b\rangle := |\{k_b\}\rangle$ , (5.16) implies

$$\begin{aligned} i(\langle b|\mathcal{T}|a\rangle - \langle b|\mathcal{T}^\dagger|a\rangle) &= - \sum_c \langle b|\mathcal{T}^\dagger|c\rangle \langle c|\mathcal{T}|a\rangle \\ \Leftrightarrow i(\langle b|\mathcal{T}|a\rangle - \langle a|\mathcal{T}|b\rangle^*) &= - \sum_c \langle c|i\mathcal{T}|a\rangle \langle c|i\mathcal{T}|b\rangle^*. \end{aligned} \quad (5.17)$$

It is this equation that we will identify the cutting equation (5.15) with. Or actually, we shall identify it with the cutting equation (5.15) summed over all diagrams contributing to the

scattering process  $a \rightarrow b$ . For later reference, equation (1.11) can be used to rewrite (5.17) in terms of invariant amplitudes as

$$\mathcal{M}(a \rightarrow b) - \mathcal{M}(b \rightarrow a)^* = \sum_n \prod_{i=1}^n \left( \int d^3 q_i \frac{Z_i}{(2\pi)^3 2\omega_{\vec{q}_i}} \right) \mathcal{M}^*(b \rightarrow \{q_i\}) \mathcal{M}(a \rightarrow \{q_i\}) i(2\pi)^4 \delta(\sum_i q_i - \sum k_a). \quad (5.18)$$

### Equivalence of the left-hand-sides

We start by showing that the left-hand-sides of equation (5.17) and (5.15) (summed over all relevant diagrams) are the same. In order to do so we need the Hamiltonian of our system to be hermitian; this is a condition for the theory to be unitary! The reason is that the hermiticity of the hamiltonian implies, as we shall discuss below, that

$$\bar{D}(a \rightarrow b) = D^*(b \rightarrow a). \quad (5.19)$$

Here  $D(b \rightarrow a)$  denotes the same diagram as  $D(a \rightarrow b)$ , but with all arrows on the internal lines<sup>2</sup> reversed, and all momenta (internal and external) reversed: it describes the time-reversed process. Recall that we put the external momenta in our diagrams on-shell and attached the appropriate residue factors, so our diagrams really contribute to scattering amplitudes. By (5.19) the equivalence of the left-hand-sides then follows swiftly, for summing the LHS of (5.15) over the diagrams  $D$  contributing to the process  $a \rightarrow b$  gives

$$\begin{aligned} \sum_D \left( D(a \rightarrow b) + \bar{D}(a \rightarrow b) \right) &= \sum_D D(a \rightarrow b) + \sum_D D^*(b \rightarrow a) \\ &= \langle b | i\mathcal{T} | a \rangle + (\langle a | i\mathcal{T} | b \rangle)^* \\ &= i(\langle b | \mathcal{T} | a \rangle - \langle a | \mathcal{T} | b \rangle^*). \end{aligned} \quad (5.20)$$

This proves the equivalence of the left-hand sides.

So how does the Hamiltonian  $\mathcal{H}$  being hermitian guarantee (5.19)? Well, if  $\mathcal{H}$  contains only real fields, then the hermiticity of  $\mathcal{H}$  implies that all the coupling constants in the interaction terms are real. Therefore, the expressions for the vertices entering our diagrams are real as well, apart from the usual  $i(2\pi)^4$ . Recall that  $\bar{D}(a \rightarrow b)$  follows from  $D(a \rightarrow b)$  by complex conjugating the internal propagators, reversing their momenta and complex conjugating the vertex factors  $i(2\pi)^4$ . Since the other vertex constants are real, this means that  $\bar{D}(a \rightarrow b)$  is equal to  $D^*(a \rightarrow b)$  with all internal momenta reversed. This means that  $\bar{D}(a \rightarrow b)$  is equal to the complex conjugate of the reversed process, as expressed by (5.19).

If  $\mathcal{H}$  contains complex fields the story is a bit more complicated. Propagators corresponding to complex fields carry an arrow in Feynman diagrams. To see what happens to the vertices under complex conjugation in this case, let us consider a three-point vertex as an example. Suppose  $\mathcal{L}^{\text{int}} = gA^*BC + \dots$ , where  $A$ ,  $B$  and  $C$  are complex (scalar) fields. The corresponding vertex is shown in figure 5.6a. It shows that a  $B$ -particle and a  $C$ -particle can interact to form an  $A$ -particle. In order for  $\mathcal{L}^{\text{int}}$  (and thus  $\mathcal{H}^{\text{int}}$ ) to be hermitian, the complex conjugated interaction term,  $g^*AB^*C^*$ , must also be present in  $\mathcal{L}^{\text{int}}$ . The vertex that corresponds to this term is the one in 5.6b. Comparing this to the first vertex, we note that the propagator-arrows are reversed, the momenta are reversed and that the coupling constant (which enters the Feynman diagram) is complex conjugated. Figure 5.6b shows the reversed process of figure

<sup>2</sup>Here we refer to the arrows that are associated with complex fields.

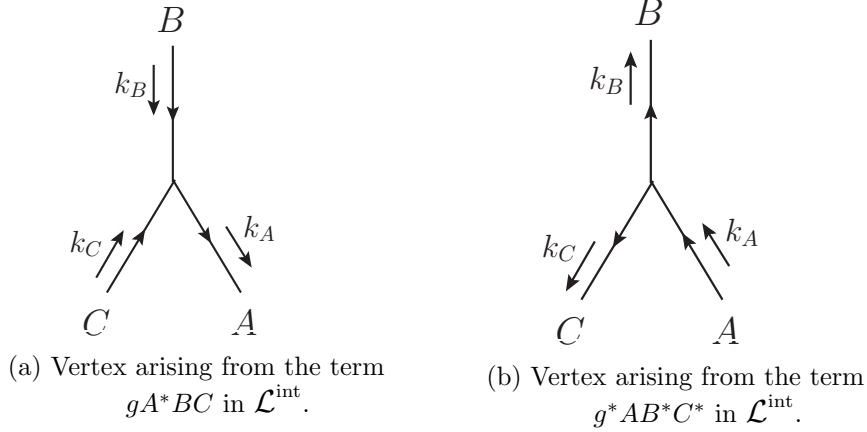


Figure 5.6.

5.6a: an  $A$ -particle decaying into an  $B$  and  $C$ -particle, instead of  $B$  and  $C$  annihilating to form an  $A$ -particle. Now if the first vertex is part of a fully uncircled diagram  $D$  then the corresponding vertex factors are  $i(2\pi)^4g$ . In the corresponding fully *circled* diagram  $\bar{D}$ , the vertex factors will acquire a minus sign and thus be equal to  $-i(2\pi)^4g$ . This is the complex conjugate of  $i(2\pi)^4g^*$ , which are the vertex factors arising from the vertex of the reversed process of figure 5.6b in a fully uncircled diagram! The hermiticity of  $\mathcal{H}$  guarantees that this vertex of the reversed process does indeed exist. The fully circled diagram  $\bar{D}(a \rightarrow b)$  also has all its internal propagators complex conjugated (meaning that the propagator-arrows are reversed) and its internal momenta reversed. Together this implies that  $\bar{D}(a \rightarrow b)$  equals the complex conjugate of the reversed process  $D^*(b \rightarrow a)$ , which is again precisely (5.19). The hermiticity of  $\mathcal{H}$  guarantees that the reversed diagram does indeed exist.

### Equivalence of the right-hand-sides

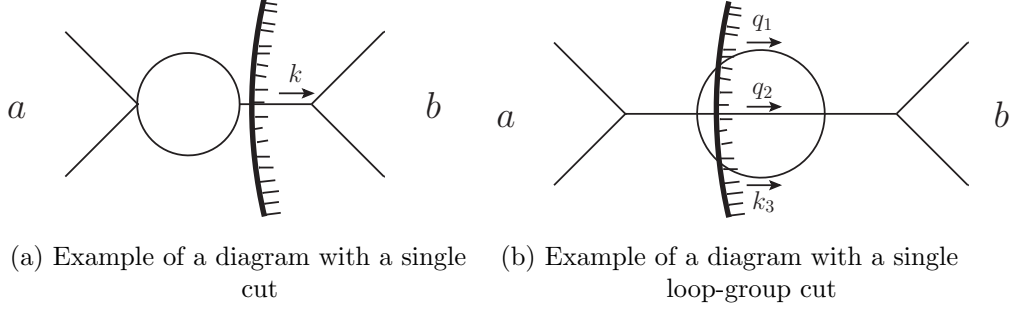
As for the right-hand sides, we start by showing that that the RHS of the cutting equation (5.15) gives a contribution to the RHS of the unitarity condition (5.17) for the case where only one internal line is being cut, as in figure 5.7a. The momentum of the cut line,  $k$ , is equal to the total incoming momenta and outgoing momenta:  $k = \sum k_a = \sum k_b$ . In this case, the cut diagram can be decomposed as

$$D_{\text{single cut}}(a \rightarrow b) = D_{\text{left}}(a \rightarrow k)\Delta^+(k)\bar{D}_{\text{right}}(k \rightarrow b)\delta^4(\sum k_a - \sum k_b). \quad (5.21)$$

This decomposition can be regarded as the definition of  $D_{\text{left}}$  and  $D_{\text{right}}$ . We wrote  $\bar{D}_{\text{right}}$  with the bar because all its vertices are circled.  $D_{\text{left}}$  and  $D_{\text{right}}$  do not represent contributions to scattering matrix elements (yet), for 1. the momentum  $k$  is not on-shell, 2. the residue factor  $((2\pi)^3 2\omega_{\vec{k}})^{-\frac{1}{2}}$  is missing and 3. they do not contain a momentum conserving delta function (note that the overall delta function has been factored out in equation (5.21)). The presence of  $\Delta^+(k)$  is going to take care of all three issues. The trick is to rewrite  $\Delta^+(k)$  as follows

$$\Delta^+(k) = \frac{1}{(2\pi)^3}\theta(k^0)\delta(k^2 + m^2) = \int d^4q \frac{1}{(2\pi)^3}\theta(q^0)\delta(q^2 + m^2)\delta^4(q - k) \quad (5.22a)$$

$$= \int d^3q \frac{1}{(2\pi)^3} \frac{1}{2\omega_{\vec{q}}}\delta^4(q - k) \Big|_{q_0=\omega_{\vec{q}}}, \quad (5.22b)$$



where in the last step the integral over  $q^0$  was used to integrate out the delta function  $\delta(q^2 + m^2)$ . Inserting (5.22b) into (5.21) yields

$$\begin{aligned}
D_{\text{single cut}} &= \int d^3q \, D_{\text{left}}(a \rightarrow k) [(2\pi)^3 2\omega_{\vec{q}}]^{-1} \delta^4(q - k) \Big|_{q^0 = \omega_{\vec{q}}} \bar{D}_{\text{right}}(k \rightarrow b) \delta^4(\sum k_a - \sum k_b) \\
&= \int d^3q \left\{ D_{\text{left}}(a \rightarrow q) [(2\pi)^3 2\omega_{\vec{q}}]^{-\frac{1}{2}} \delta^4(q - \sum k_a) \Big|_{q^0 = \omega_{\vec{q}}} \right\} \\
&\quad \left\{ D_{\text{right}}^*(b \rightarrow q) [(2\pi)^3 2\omega_{\vec{q}}]^{-\frac{1}{2}} \delta^4(q - \sum k_b) \Big|_{q^0 = \omega_{\vec{q}}} \right\}
\end{aligned} \tag{5.23}$$

In the last step we used equation (5.19). Now the terms between brackets *are* contributions to  $\langle q | i\mathcal{T} | a \rangle$  and  $\langle q | i\mathcal{T} | b \rangle^*$ , where  $|q\rangle$  denotes a *single particle* state with momentum  $q$ . Indeed, the appropriate residue factors and delta functions are now provided and  $q$  is on-shell by  $q^0 = \omega_{\vec{q}}$ . Note that we integrate over all possible momenta  $q$  of the single particle. If we then sum over all possible diagrams  $D$  for the process  $a \rightarrow b$ , and sum over all possible ways to cut a single internal line of these, then we obtain

$$\sum_{D, \text{ single cuts}} D(a \rightarrow b) = \sum_{\text{single part. states } c} \langle c | i\mathcal{T} | a \rangle \langle c | i\mathcal{T} | b \rangle^* . \tag{5.24}$$

This is starting to look like an equivalence between the RHS's of (5.15) (summed over  $D$ ) and (5.17).

Now we generalize to other cuttings. Suppose that we do not cut a single line, but a group of lines which are connected by loops, for example as in figure 5.7b. We shall call such a group of lines a *loop-group*. Note that the single line we had before is a special case of a loop-group. The loop-group cut again divides the diagram into two pieces. If the loop-group consists of  $n$  lines, then it contains  $n - 1$  loops. We can choose the momenta of  $n - 1$  of the cut lines to be the loop momenta  $q_1 \cdots q_{n-1}$  that are integrated over. If we choose these momenta in the direction of energy flow through the cut, then the momentum of the  $n$ -th cut line,  $k_n$ , will be given by  $k_n = \sum k_a - \sum_{i=1}^{n-1} q_i$ . We can use the same tricks as before to rewrite the diagram with one loop-group (LG) cut.

$$\begin{aligned}
D_{\text{LGcut}}(a \rightarrow b) &= \int d^4 q_1 \dots \int d^4 q_{n-1} \quad D_{\text{left}}(a \rightarrow q_1 \dots q_{n-1}, k_n) \Delta^+(q_1) \dots \Delta^+(q_{n-1}) \Delta^+(k_n) \\
&\quad \bar{D}_{\text{right}}(q_1 \dots q_{n-1}, k_n \rightarrow b) \delta^4(\sum k_a - \sum k_b) \\
&= \int d^4 q_1 \dots \int d^4 q_n \quad D_{\text{left}}(a \rightarrow q_1 \dots q_n) \prod_{i=1}^n \frac{\theta(q_i^0)}{(2\pi)^3} \delta(q_i^2 + m^2) \delta^4(k_n - q_n) \\
&\quad \bar{D}_{\text{right}}(q_1 \dots q_n \rightarrow b) \delta^4(\sum_i^n q_i - \sum k_b) \\
&= \int d^3 q_1 \dots \int d^3 q_n \quad \left\{ D_{\text{left}}(a \rightarrow \{q\}) \prod_{j=1}^n [(2\pi)^3 2\omega_{\vec{q}_j}]^{-\frac{1}{2}} \delta^4(\sum k_a - \sum_i^n q_i) \Big|_{q_i^0 = \omega_{\vec{q}_i}} \right\} \\
&\quad \left\{ D_{\text{right}}^*(b \rightarrow \{q\}) \prod_{j=1}^n [(2\pi)^3 2\omega_{\vec{q}_j}]^{-\frac{1}{2}} \delta^4(\sum k_b - \sum_i^n q_i) \Big|_{q_i^0 = \omega_{\vec{q}_i}} \right\}.
\end{aligned} \tag{5.25}$$

In the second step we rewrote  $\Delta^+(k^n)$  according to (5.22a) and in the last step we performed all the integrals over  $q_i^0$ . The terms between brackets are contributions to  $\langle \{q\} | i\mathcal{T} | a \rangle$  and  $\langle \{q\} | i\mathcal{T} | b \rangle^*$ . We integrate over all possible momenta of the states  $|\{q\}\rangle$ . If we then sum over all diagrams  $D$  for the process  $a \rightarrow b$  and over all possible cuts through single loop-groups (LGcuts), then we obtain

$$\sum_{D, \text{LGcuts}} D_{\text{LGcut}}(a \rightarrow b) = \sum_c \langle c | i\mathcal{T} | a \rangle \Big|_{\text{FC}} \langle a | i\mathcal{T} | b \rangle^* \Big|_{\text{FC}}, \tag{5.26}$$

where the subscript FC serves to indicate that we only obtain the fully connected diagrams in  $\langle c | i\mathcal{T} | a \rangle$  and  $\langle c | i\mathcal{T} | b \rangle^*$ .

We can generalize this to general cuts, which can cut through multiple loop-groups. For every extra loop-group that is being cut, an extra disconnected piece of a diagram will be produced. An example is shown in figure 5.8: four loop-groups are being cut instead of one, and as a result five separate pieces are produced instead of two. We can perform the exact same manipulations as above for every cut loop-group. We will obtain an integral over the momentum of every cut line, the residue factor for every cut line and for every cut loop-group there will be a momentum-conserving delta function. Together with the overall delta function already present in the original diagram, we will then have a momentum conserving delta function for every separate piece of the cut diagram. In figure 5.8, four delta functions result from the four loop-group cuts. Together with the overall delta function this gives five delta functions, each expressing momentum conservation for one of the five disconnected pieces. If we then again sum over all possible diagrams (for the process  $a \rightarrow b$ ) and all possible cuts of those diagrams, then we obtain all possible diagrams contributing to the RHS of the unitarity condition (5.17). That is

$$\sum_{D, \text{cuttings}} D(a \rightarrow b) = \sum_c \langle c | i\mathcal{T} | a \rangle \langle c | i\mathcal{T} | b \rangle^*. \tag{5.27}$$

This concludes the proof that, for scalar fields, the perturbation theory we set up is indeed unitary for scalar fields.

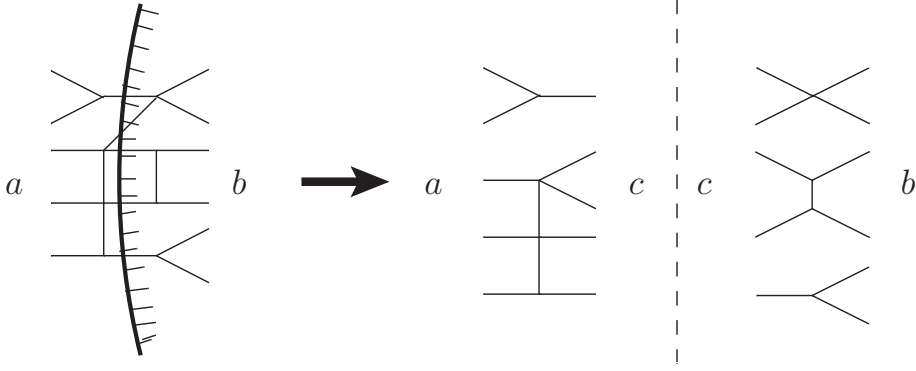


Figure 5.8.: Four loop-group cuts lead to five separate pieces.

### Other fields

If we have other fields carrying more degrees of freedom, then the question whether we can generalize the proof presented for scalar fields hinges on two factors. Firstly, can we find a decomposition of the propagator  $\Delta_{ij}$  into  $\Delta_{ij}^+$  and  $\Delta_{ij}^-$  analogous to (5.5)? The indices  $i$  and  $j$  here can denote any kind of index appropriate. Secondly, obtaining scattering matrix elements will now also involve the contraction of the diagrams with (physical) polarization vectors of the external lines. The sum over all possible states  $c$  in the unitarity condition (5.17) thus involves a sum over all possible polarization vectors, i.e.

$$\sum_{\lambda} \epsilon_i^{\lambda}(\vec{k}) \epsilon_j^{\lambda}(\vec{k}). \quad (5.28)$$

In order to identify the RHS of the unitarity condition (5.17) with the RHS of the cutting equation (5.15), we need the expression (5.28) to be present in the numerators of  $\Delta^+$  and  $\Delta^-$ . This is the second issue.

For fermions both issues work out well [3]. For photons the story does not proceed as smoothly, as we shall discuss now. To start with the second issue, the sum over the two physical polarizations yields for photons

$$\sum_{\lambda=1}^2 \epsilon_{\mu}^{\lambda}(\vec{k}) \epsilon_{\nu}^{\lambda}(\vec{k}) = \eta_{\mu\nu} - \frac{k_{\mu} \tilde{k}_{\nu} + \tilde{k}_{\mu} k_{\nu}}{k \cdot \tilde{k}} \Big|_{k^0 = \omega_{\vec{k}}}, \quad (5.29)$$

where  $\tilde{k}_{\mu}$  is defined by  $\tilde{k}_{\mu} = (-k_0, k_j)$ : it is equal to  $k_{\mu}$  with the time component reversed.  $\tilde{k}_{\mu}$  not a Lorentz covariant vector. This can be seen for example by the fact that  $\tilde{k}_{\mu} k^{\mu} = \omega_{\vec{k}}^2 + |\vec{k}|^2 = 2|\vec{k}|^2$ . Since  $|\vec{k}|^2$  can vary under Lorentz transformations (boosts in the  $\vec{k}$  direction) and since  $k^{\mu}$  is Lorentz contravariant, this implies that  $\tilde{k}_{\mu}$  does *not* transform Lorentz covariantly. This implies that (5.29) is *not* a Lorentz tensor. It is hard to imagine that such a quantity should be included in  $\Delta_{\mu\nu}^+$  and  $\Delta_{\mu\nu}^-$ , which is what unitarity would require.

This is where the Ward identity comes to the rescue: by the virtue of  $k_{\mu} \mathcal{M}^{\mu}(k) = 0$ , the troublesome part of (5.29) vanishes when contracted with invariant amplitudes. So if we can show that  $\Delta_{\mu\nu}^+$  and  $\Delta_{\mu\nu}^-$  carry  $\eta_{\mu\nu}$  in their numerator (plus possible factors containing  $k_{\mu}$  which will vanish due to the Ward identity), then unitarity is satisfied, for this  $\eta_{\mu\nu}$  then equals to the non-vanishing part of (5.29). This brings us to the first issue: can we make a sensible decomposition of  $\Delta_{\mu\nu}$ ? To calculate the photon propagator one usually adds the gauge fixing term  $\mathcal{L}_{\text{gf}} = -\frac{1}{2}(\lambda \partial_{\mu} A^{\mu})^2$  to the Lagrangian. This does not affect the physical predictions of

the theory and one is free to choose whatever value for  $\lambda$  one finds convenient. The propagator then becomes

$$\Delta_{\mu\nu}(k) = \frac{1}{i(2\pi)^4} \frac{1}{k^2} \left( \eta_{\mu\nu} - (1 - \lambda^{-2}) \frac{k_\mu k_\nu}{k^2} \right). \quad (5.30)$$

Decomposing this analogous to (5.5) does not work very well, because the  $k_\mu k_\nu$ -term gives rise to so-called contact terms [3, chapter 8.5]. However, we can simply pick  $\lambda = 1$  (the Feynman gauge), such that this term vanishes! The photon propagator  $\Delta_{\mu\nu}$  is then just the scalar propagator  $\Delta$  (with zero mass) times  $\eta_{\mu\nu}$ . Therefore, the decomposition into  $\Delta_{\mu\nu}^\pm$  is easily made as  $\Delta_{\mu\nu}^\pm = \Delta^\pm \eta_{\mu\nu}$ . The  $\eta_{\mu\nu}$  is exactly the part of (5.29) that we needed. This proves that the scattering matrix is unitary when photons are involved! Note that this result does not depend on our choice of  $\lambda$ , since the scattering matrix is a physical quantity and does therefore not depend  $\lambda$ . Summarizing, we can say that we really need gauge invariance to ensure, by means of the Ward identity, that a theory involving photons is unitary!

## 5.4. Summary proof of unitarity

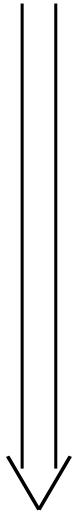
Figure 5.9 shows a summary of the presented proof of unitarity (for a scalar field). There is one more piece of terminology that has to be explained here: the notion of cut structure. We have seen that we can represent circled diagrams by cut diagrams. Only diagrams with a single vertical cut, consistent with the overall energy flow, survive. In our terminology, these diagrams are said to obey the cut structure; other diagrams are said to violate the cut structure.

$$1. \begin{cases} \Delta(x) = \theta(x)\Delta^+(x) + \theta(-x)\Delta^-(x) & (5.5) \\ \Delta^\pm(x) = (\Delta^\pm)^*(x) & (5.12) \end{cases}$$



**Largest Time Equation:**

$$D(a \rightarrow b) + \bar{D}(a \rightarrow b) = - \sum_{\substack{\text{other} \\ \text{circlings}}} D(a \rightarrow b) \quad (5.14)$$



**2.a)** Circled regions are the complex conjugate of their time-reversed process, e.g.  $\bar{D}(a \rightarrow b) = D^*(b \rightarrow a) = \langle a | iT | b \rangle$ .

This follows from  $\mathcal{L}_{\text{int}}^\dagger = \mathcal{L}_{\text{int}}$ .

**2.b)** Only cuts obeying the cut structure survive.

$$\text{This is because } \Delta^\pm(k) = 2\pi\theta(\pm k^0)\delta(k^2 - m^2) \quad (5.6)$$

represents an on-shell particle with purely positive/negative energy.

**Unitarity:**

$$i(\langle b | \mathcal{T} | a \rangle - \langle a | \mathcal{T} | b \rangle^*) = - \sum_c \langle c | iT | a \rangle \langle c | iT | b \rangle^* \quad (5.17)$$

*Reminders on notation:*

- $D(a \rightarrow b)$  denotes a diagram contributing to the invariant amplitude of the process  $a \rightarrow b$ .
- $\bar{D}(a \rightarrow b)$  denotes the same diagram with all vertices circled.

Figure 5.9.: The steps of the unitarity proof.



## 6. Renormalization

An important feature of quantum field theory is that it gives to rise infinities. Any loop appearing in a Feynman diagram denotes an integral which may diverge. This can occur due to the behaviour of the integrand at large loop momenta, in which case we speak of an *ultraviolet divergence*, or due to its behaviour at small loop momenta, in which case the resulting divergence is called an *infrared divergence*, or it may be due to both. In this chapter we restrict ourselves to discussing ultraviolet divergences. An example of a diagram giving rise to an ultraviolet divergence is the one loop correction to the QED vertex shown in figure 6.1b. The corresponding invariant amplitude is

$$\Lambda^\mu(p, q) = \frac{e^3}{(2\pi)^4} \int d^4k \gamma^\nu \frac{-i(\not{q} + \not{k}) + m}{(q+k)^2 + m^2} \gamma^\mu \frac{-i(\not{p} + \not{k}) + M}{(p+k)^2 + m^2} \gamma^\rho \frac{1}{k^2} \left( \eta_{\rho\nu} - (1 - \lambda^{-2}) \frac{k_\rho k_\nu}{k^2} \right). \quad (6.1)$$

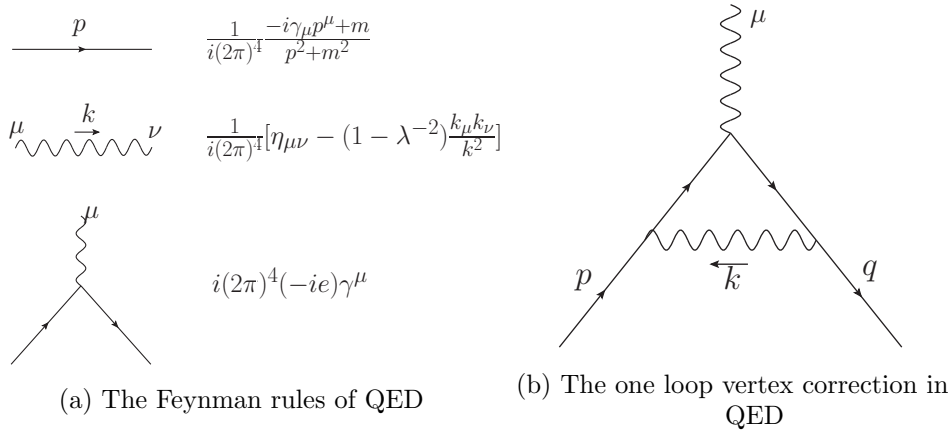
For large loop momentum  $k$  the integrand behaves as  $\frac{1}{k}$ , which means that this integral is logarithmically divergent.

Of course, the physical quantities that the theory predicts should be finite. The idea to deal with the divergencies is to interpret the parameters in the Lagrangian - the bare Lagrangian - merely as parameters, without bearing any kind of physical relevance. For example, the ‘fermion mass’  $m$  appearing in  $\mathcal{L}_{\text{QED}}$  is *not* the real fermion mass. It is just a parameter in the Lagrangian. The idea of renormalization is that these parameters must in fact be infinite in precisely such a way that the physical quantities of the theory (such as the *real* fermion mass) *are* finite. Modifying the parameters like this to cure the theory is called *renormalizing* the theory. The way to go about this is as follows. First one adopts a *regularization method*: one modifies the theory in such a way that it does not yield any divergent quantities. An example of a regularization method is *dimensional regularization*, which adjusts the dimension of the theory such that all integrals become finite. It is only at the end of the renormalization procedure that one returns to the original theory, e.g. to four dimensions. The second step is to calculate the regularized invariant amplitudes and to identify the pieces that would diverge in the original theory (e.g. in four dimensions). Then one adds terms to the Lagrangian, called *counterterms*, which precisely cancel these pieces. At the level of the Lagrangian, the counterterms can be interpreted as containing the infinite parts of the bare Lagrangian. When a theory can be renormalized by adding only a finite number of counterterms to  $\mathcal{L}$  the theory is said to be *renormalizable*.

Before discussing the regularization of the theory in section 6.2, and how to adjust the Lagrangian to cancel the infinities in section 6.3, we first discuss a way to determine whether the theory at hand is renormalizable at all.

### 6.1. Renormalizability by powercounting

An easy way to test whether a theory is renormalizable or not, is by simply looking at the mass dimensions of the coupling constants in the Lagrangian. Under the assumption that all



propagators in the theory behave as  $1/k^2$  for large momentum  $k$ , three categories of theories can be distinguished.

- Theories in which all coupling constant have *positive* mass dimension are called *super-renormalizable*. In these theories there is only a finite number of diverging invariant amplitudes and divergencies only occur up to a certain order in perturbation theory.
- Theories in which all coupling constant have *nonnegative* mass dimension are called *renormalizable*. Again, there is only a finite number of divergent invariant amplitudes, but divergencies occur at any order in perturbation theory.
- Theories in which at least one coupling constant has a *negative* mass dimension. In this case the number of divergent invariant amplitudes is infinite.

Theories falling in the first two categories can be renormalized by adding a finite number of counterterms to  $\mathcal{L}$  and are thus guaranteed to be renormalizable. The converse, however, is not necessarily true: theories of the last category may still be renormalizable, for example owing to cancelling divergencies due to symmetries of the theory. These theories are just not guaranteed to be renormalizable *by powercounting*. For a proof we refer to [2, chapter 10.1].

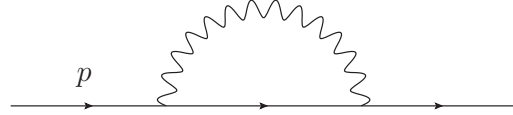
## 6.2. Dimensional regularization

There are many ways to regularize a theory. One way is by introducing a *cut-off*: instead of integrating the loop-momenta from  $-\infty$  to  $\infty$  one sets a lower and upper bound and instead integrates from  $-a$  to  $a$ . This can be interpreted as modelling space as a lattice; there will exist a minimum wavelength related to  $a$ . This renders the integrals finite. One can return to the original theory by taking  $a \rightarrow \infty$ . A drawback of this method is that breaking up space as a lattice is not Lorentz invariant; the length  $a$  for example can change under boosts by length contraction. If one then starts adjusting the theory for finite  $a$  (by adding counterterms), one cannot be sure to obtain a Lorentz invariant theory back after taking  $a \rightarrow \infty$ . For this reason it is preferable to exploit a regularization method that preserves all the important symmetries of the theory.

This is why dimensional regularization is such a popular regularization method: it does preserve the symmetries of the theory. The idea of dimensional regularization is that we do not work



(a) The one loop contribution to the vacuum polarization  $\Pi_{\mu\nu}(k)$



(b) The one loop contribution to the self-energy  $\Sigma(p)$

in four dimensions, but in  $n = 4 - \epsilon$  dimensions, where  $\epsilon$  is small. At the very end of the renormalization procedure we take the limit  $\epsilon \rightarrow 0$  to return to the original theory. As an example, consider the vertex correction  $\Lambda^\mu$  of equation (6.1). For large  $k$  it behaves as the integral  $\int d^{4-\epsilon} k \frac{1}{k^4}$ , which converges for finite  $\epsilon > 0$ . The idea is then to expand  $\Lambda^\mu$  in  $\epsilon$  and neglect all  $\mathcal{O}(\epsilon)$ -terms, since these terms will eventually cancel in the limit  $\epsilon \rightarrow 0$  anyway. In general, terms that diverge for  $\epsilon \rightarrow 0$  then arise as poles  $(\frac{1}{\epsilon})^m$ .  $\Lambda_\mu$  for example becomes

$$\Lambda^\mu(p, q) = \frac{1}{\epsilon} \cdot \frac{ie^3 \mu^\epsilon}{8\pi^2 \lambda^2} \gamma^\mu + \Lambda_f^\mu(p, q), \quad (6.2)$$

where  $\Lambda_f^\mu$  is now a function that does not depend on  $\epsilon$  and is thus finite in  $n = 4$  dimensions. The  $\mu$  in the expression is an arbitrary mass parameter, which has to be introduced on dimensional grounds somewhere along the way. It also appears in  $\Lambda_f^\mu$ . The idea of renormalization is to include minus the infinite part of (6.2) as a counterterm in the Lagrangian. There is an ambiguity here: one is free to add any finite part to this counterterm, for this will still yield a finite renormalized quantity. The fact that both terms depend on the arbitrary mass parameter  $\mu$  illustrates this ambiguity.

### 6.3. The renormalization procedure

To illustrate how the divergencies of physical quantities can be accounted for in the Lagrangian of the theory, we first discuss how to renormalize QED to one loop order, following [1, chapter 9.3]. After that the example shall be summarized and placed in a broader perspective, by outlining the renormalization procedure in more general terms.

There are three divergent one loop diagrams in QED: the vertex correction of figure 6.1 that we already encountered, and the vacuum polarization and self-energy graphs shown in figures 6.2a and 6.2b. In dimensional regularization the expressions for these diagrams can be written as

$$\begin{cases} \Pi_{\mu\nu}(k) &= e^2 \left( k^2 \eta_{\mu\nu} - k_\mu k_\nu \right) \left[ \frac{1}{\epsilon} \cdot \Pi_{\text{inf}} + \Pi_f(k^2) \right] \\ \Sigma(p) &= e^2 \left\{ \left[ \frac{1}{\epsilon} \cdot A_{\text{inf}} + A_f(p^2) \right] m + \left[ \frac{1}{\epsilon} \cdot B_{\text{inf}} + B_f(p^2) \right] i\not{p} \right\} \\ \Lambda^\mu(p, q) &= e^3 \left[ \frac{1}{\epsilon} \cdot \Lambda_{\text{inf}} \gamma^\mu + \Lambda_f^\mu(p, q) \right]. \end{cases} \quad (6.3)$$

Note that  $\Pi_{\mu\nu}$  is transverse, such that it satisfies the Ward identity, as it should. An important point here is that the separation of  $\Pi_{\mu\nu}$  into  $\Pi_{\text{inf}}$  and  $\Pi_f$  is not unique. In (6.3),  $\Pi_{\text{inf}}$  is allowed to have terms linear in  $\epsilon$ , such that  $\epsilon^{-1} \Pi_{\text{inf}}$  can also contain finite terms. (To be clear: we do *not* allow  $\Pi_f$  to have poles in  $\epsilon$ :  $\Pi_f$  is really finite in 4 dimensions). This means that we can pick the finite part of  $\Pi_{\text{inf}}$  freely, for this can be compensated by picking  $\Pi_f$  appropriately. Exactly the same freedom exists in decomposing  $\Sigma$  and  $\Lambda$ .

The idea is now to add counterterms to the Lagrangian that give rise to diagrams that,

at this order in perturbation theory, cancel the infinite parts of these diagrams. We thus add the counterterms

$$\begin{cases} \Delta\mathcal{L}_1 = -\frac{e^2}{4}\epsilon^{-1}\Pi_{\text{inf}}(\partial_\mu A_\nu - \partial_\nu A_\mu)^2 \\ \Delta\mathcal{L}_2 = -e^2\epsilon^{-1}A_{\text{inf}}m\bar{\psi}\psi \\ \Delta\mathcal{L}_3 = -e^2\epsilon^{-1}B_{\text{inf}}\bar{\psi}\not{\partial}\psi \\ \Delta\mathcal{L}_4 = -e^3\epsilon^{-1}\Lambda_{\text{inf}}\bar{\psi}\gamma^\mu\psi A_\mu. \end{cases} \quad (6.4)$$

These terms give rise to the diagrams shown in figure 6.3, which are precisely minus the diverging terms in (6.3). If you want to renormalize the theory to a higher order in perturbation theory, say to second loop order, then you should first add all the counterterms to cancel the divergencies of one loop diagrams, and *then* calculate all two loop diagrams and see what counterterms you need to cancel those. The reason is that the counterterms needed for one loop diagrams will also appear in two and higher order loop diagrams. So first the theory should be renormalized to first order, then to second order and so on.

$$\begin{aligned} \Delta\mathcal{L}_1 : & \quad \text{Diagram 1} & = -e^2(k^2\eta_{\mu\nu} - k_\mu k_\nu)\epsilon^{-1}\Pi_{\text{inf}} \\ \Delta\mathcal{L}_2 + \Delta\mathcal{L}_3 : & \quad \text{Diagram 2} & = -e^2(m\epsilon^{-1}A_{\text{inf}} + i\gamma_\mu p^\mu\epsilon^{-1}B_{\text{inf}}) \\ \Delta\mathcal{L}_4 : & \quad \text{Diagram 3} & = -e^3\epsilon^{-1}\Lambda_{\text{inf}}\gamma^\mu \end{aligned}$$

Figure 6.3.: Vertices arising from  $\Delta\mathcal{L} = \Delta\mathcal{L}_1 + \Delta\mathcal{L}_2 + \Delta\mathcal{L}_3 + \Delta\mathcal{L}_4$

The parameters that appeared so far in our expressions (such as  $m$  and  $e$ ) have been finite. We have seen that the Lagrangian  $\mathcal{L}_{\text{finite}}$  containing these parameters gives rise to infinite physical quantities and can, therefore, not describe a physical theory. To cancel these divergencies, we need to add infinite counterterms to  $\mathcal{L}_{\text{finite}}$ . We then obtain a physical theory described by the Lagrangian  $\mathcal{L}_{\text{phys}} = \mathcal{L}_{\text{finite}} + \Delta\mathcal{L}$ . Equation (6.4) shows that the counterterms contain the fields in exactly the same way as  $\mathcal{L}_{\text{finite}}$  does, so we can combine these terms with the terms in  $\mathcal{L}_{\text{finite}}$ .  $\mathcal{L}_{\text{phys}}$  will then have the standard form of a QED Lagrangian, but with parameters (and fields) which are infinite. Usually we call  $\mathcal{L}_{\text{phys}}$  the *bare* Lagrangian  $\mathcal{L}_0$  and  $\mathcal{L}_{\text{finite}}$  just  $\mathcal{L}$ , such that

$$\mathcal{L}_0 = \mathcal{L} + \Delta\mathcal{L}. \quad (6.5)$$

The parameters and fields of  $\mathcal{L}_0$  are called bare as well and also carry the subscript 0. They are related to the finite parameters and fields (which do not carry a subscript) appearing in  $\mathcal{L}$ , by

$$\begin{cases} A_0^\mu = \sqrt{Z_A}A^\mu \\ \psi_0 = \sqrt{Z_\psi}\psi \end{cases}, \quad \text{and} \quad \begin{cases} e_0 = Z_e e \\ m_0 = Z_m m \\ \lambda_0 = Z_\lambda \lambda. \end{cases} \quad (6.6)$$

The finite quantities are called *renormalized* quantities. The interpretation is that the physical Lagrangian of our theory,  $\mathcal{L}_0$ , contains fields and parameters that are infinite in precisely such a way that the physical predictions of the theory are finite. These infinite fields and parameters are related to finite ones by the *renormalization constants*, the  $Z$  factors in (6.6). To determine these renormalization constants we note

$$\begin{aligned}\mathcal{L}_0 &= -\frac{1}{4}(\partial^\mu A_0^\nu - \partial^\nu A_0^\mu)^2 - \frac{1}{2}(\lambda_0 \partial_\mu A_0^\mu)^2 - \bar{\psi}_0(\not{\partial} + m_0)\psi - ie_0 A_0^\mu \bar{\psi}_0 \gamma_\mu \psi_0 \\ &= -\frac{1}{4}Z_A(\partial^\mu A^\nu - \partial^\nu A^\mu)^2 - \frac{1}{2}Z_\lambda^2 Z_A(\lambda \partial_\mu A^\mu)^2 - Z_\psi \bar{\psi}(\not{\partial} + Z_m m)\psi \\ &\quad - ieZ_e \sqrt{Z_A} A^\mu \bar{\psi} \gamma_\mu \psi\end{aligned}\tag{6.7}$$

$$\begin{aligned}&= \mathcal{L} + \Delta\mathcal{L} \\ &= -\frac{1}{4}\left(1 + e^2 \frac{1}{\epsilon} \Pi_{\text{inf}}\right)(\partial^\mu A^\nu - \partial^\nu A^\mu)^2 - \frac{1}{2}(\lambda \partial_\mu A^\mu)^2 \\ &\quad - \left(1 + e^2 \frac{1}{\epsilon} B_{\text{inf}}\right)\bar{\psi}\not{\partial}\psi - \left(1 + e^2 \frac{1}{\epsilon} A_{\text{inf}}\right)m\bar{\psi}\psi - ie\left(1 + e^2 \frac{1}{\epsilon} \Lambda_{\text{inf}}\right)A^\mu \bar{\psi} \gamma_\mu \psi + \mathcal{O}(e^4).\end{aligned}\tag{6.8}$$

The renormalization constants are found by comparing (6.7) and (6.8), resulting in

$$\left\{\begin{array}{l} Z_A = 1 + e^2 \frac{1}{\epsilon} \Pi_{\text{inf}} \quad + \mathcal{O}(e^4) \\ Z_\psi = 1 + e^2 \frac{1}{\epsilon} B_{\text{inf}} \quad + \mathcal{O}(e^4) \\ Z_e = 1 + e^2 \frac{1}{\epsilon} \left[\Lambda_{\text{inf}} - \frac{1}{2} \Pi_{\text{inf}}\right] + \mathcal{O}(e^4) \\ Z_m = 1 + e^2 \frac{1}{\epsilon} \left[A_{\text{inf}} - B_{\text{inf}}\right] + \mathcal{O}(e^4) \\ Z_\lambda = 1 - \frac{e^2}{2} \frac{1}{\epsilon} \Pi_{\text{inf}} \quad + \mathcal{O}(e^4). \end{array}\right.\tag{6.9}$$

Since there was the ambiguity in determining the counterterms, the  $Z$ 's are not uniquely defined either. So neither the bare parameters, nor the renormalized parameters in  $\mathcal{L}$  carry any physical meaning.

Now that we have shown how to perform the renormalization of QED at one loop order, we shall outline the renormalization procedure in more general terms, broadly following Denner [5, chapter 3]. This should also clarify how we can relate the parameters in  $\mathcal{L}$  to real physical quantities. The renormalization procedure consists of the following steps.

- Start by picking a set of  $n$  independent parameters in the Lagrangian. In QED this could for example be  $e, m$ , and  $\lambda$  as above. Express all parameters in  $\mathcal{L}$  in terms of these parameters.
- Calculate the divergent diagrams to a certain order in perturbation theory using a regularization method.

- Add counterterms to the Lagrangian to cancel the infinite parts of the diagrams. An arbitrary finite part can be added to every counterterm. This finite part can be fixed by choosing certain conditions you impose, called *renormalization conditions*. We will encounter an example of these in section 6.4.
- The counterterms can be accommodated by splitting the bare fields and parameters in  $\mathcal{L}_0$  into renormalization constants and renormalized fields and parameters. The Lagrangian then splits into a renormalized, finite part, plus counterterms:  $\mathcal{L}_0 = \mathcal{L}_{\text{finite}} + \Delta\mathcal{L}$ .
- Find relations between physical observables and the  $n$  renormalized parameters, for example by calculating cross sections.
- Use  $n$  *experimental* values of these observables in these relations to determine the  $n$  renormalized parameters. The remaining relations can then be used to predict other observables: this constitutes the predictive power of the theory.

In the first and third step there are some choices to be made: the choice of what parameters to use and the choice of renormalization conditions together define the *renormalization scheme* that is being used. The choice of such a scheme boils down to the choice of how to split up the bare Lagrangian  $\mathcal{L}_0$  into  $\mathcal{L}_{\text{finite}}$  and  $\Delta\mathcal{L}$ .

An interesting consequence of this is the following. Suppose you calculate values for physical observables at a certain order in perturbation theory in different renormalization schemes. Then the results can be different. This is already evident at tree-level: there the counterterms do not contribute to physical observables yet, so the expression of physical observables in terms of the renormalized parameters will be the same in any renormalization scheme. Yet the renormalized parameters themselves will be different! For example, consider electron-electron scattering in QED. This process happens at tree-level through the exchange of a virtual photon. The diagram will therefore be proportional to  $e^2$ , where  $e$  is the renormalized electron charge. Suppose now we switch to a renormalization scheme where  $e$  is renormalized differently. Then the expression for the amplitude in terms of  $e$  will still be the same, for counterterms do not contribute at tree-level. However,  $e$  itself has changed, and thereby the resulting value for the physically observable cross section! Since renormalization starts at the one-loop level, the difference between the two values of  $e$  is  $\mathcal{O}(\alpha)$ . That is, resulting change in the physical observable (the cross section) is of higher order in perturbation theory. This is true in general: if one calculates a physical observable to order  $\alpha^n$  in different renormalization schemes, then the difference between the results is  $\mathcal{O}(\alpha^{n+1})$ . This is a consequence of the fact that the bare Lagrangian  $\mathcal{L}_0 = \mathcal{L}_{\text{phys}}$  is independent of the renormalization scheme chosen, which implies that to the order in which we are doing perturbation theory the different schemes should yield consistent results.

Furthermore, the fact that  $\mathcal{L}_0$  is *gauge* invariant (for any  $\alpha$ ), implies that the physical observables are gauge invariant, order by order in perturbation theory, in *any* renormalization scheme. This means that by adopting a different renormalization scheme, one can change the  $\mathcal{O}(\alpha^{n+1})$  part of the observables *in a gauge invariant manner*. This feature will be exploited by the complex mass scheme in chapter 11n.

## 6.4. The on-shell renormalization scheme (OSRS)

An example of a renormalization scheme is the on-shell renormalization scheme (OSRS). In the OSRS we pick the independent parameters in the Lagrangian to be parameters that represent,

at least naively, physical observables. Also the necessary gauge fixing constants are used as an independent parameter. In QED this means that  $e$ ,  $m$  and  $\lambda$  are used. In the standard model the used independent parameters are the bosons masses  $M_W$ ,  $M_Z$ , and  $M_H$ ; the fermion masses; the elements  $V_{ij}$  of the quark mixing matrix; and the gauge fixing constants. So the coupling constants such as  $g$  or  $G$ , as well as the vacuum expectation value  $v$  are considered functions of these.

At tree-level, the renormalized versions of these parameters really correspond to the associated physical observable. For example,  $m$  in QED really describes the mass of the fermion in QED at tree-level, for the full propagator at tree-level is just the bare propagator

$$\Delta^{\text{tree}}(p) = \frac{1}{i(2\pi)^4} \frac{-i\not{p} + m}{p^2 + m^2}, \quad (6.10)$$

which has a pole at  $p^2 = -m^2$ . This is the case in any renormalization scheme. If radiative corrections are included this generally ceases to be the case, for the full propagator changes. The denominator of the full propagator can generically be written as

$$\Delta^{\text{full}}(p) \sim \frac{1}{p^2 + m^2 - \Sigma(p^2, m^2)}, \quad (6.11)$$

where  $\Sigma(p^2, m^2)$  is a scalar function that is either equal to or very closely related to the self-energy. The second argument of  $\Sigma(p^2, m^2)$  is there to emphasize that the self-energy generally depends on the fermion mass  $m^2$  used in the calculation of the loop diagrams and counterterms. We can check that the full propagator does indeed have such a denominator structure for our QED example. After subtracting the counterterms, the self-energy to order  $\alpha$  is given by (6.3) with  $A_{\text{inf}} = B_{\text{inf}} = 0$ . In chapter 10 it will be shown how to resum the self-energy corrections in order to obtain the full propagator. The result is

$$\Delta_{\text{fermion}}^{\text{full}} = \frac{1}{i(2\pi)^4} \frac{-i\not{p}(1 - e^2 B_f(p^2)) + m(1 - e^2 A_f(p^2))}{p^2(1 - e^2 B_f(p^2)) + m^2(1 - e^2 A_f(p^2))}, \quad (6.12)$$

which indeed has the denominator structure (6.11) upon identifying

$$\Sigma_{\text{fermion}}(p^2, m^2) = -e^2 (p^2 B_f(p^2) + m^2 A_f(p^2)). \quad (6.13)$$

As will be explained in chapter 9,  $\Sigma$  is in general a complex quantity; for stable particles it will be purely real if evaluated on-shell.

Equation (6.11) does not assume a particular renormalization scheme, therefore  $m$  can still be any renormalized mass. Now we are ready to define the OSRS. The renormalized mass in this scheme we call  $M$ . The OSRS is defined by requiring  $p^2 = -M^2$  to be the value where the real part of the denominator of the full propagator vanishes (to any order in perturbation theory). This makes it the pole of the propagator for stable particles, so for stable particles  $M$  is the physical mass at any order of perturbation theory. The OSRS is thus defined by requiring

$$[p^2 + M^2 - \text{Re}\Sigma(p^2, M^2)]_{p^2=-M^2} = 0 \quad \Leftrightarrow \quad \text{Re}\Sigma(-M^2, M^2) = 0 \quad (6.14)$$

Using (6.14), (6.11) can be expanded around  $p^2 = -M^2$  to yield

$$\begin{aligned} \Delta^{\text{full}} &\sim \frac{1}{p^2 + M^2 - (p^2 + M^2)\text{Re}\Sigma'(-M^2, M^2) - \text{Im}\Sigma(-M^2, M^2)} \\ &= \frac{Z}{p^2 + M^2 - Z\text{Im}\Sigma(-M^2, M^2)}, \end{aligned} \quad (6.15)$$

where

$$Z := \frac{1}{1 - \text{Re}\Sigma'(p^2, M^2)}, \quad \text{and} \quad \Sigma'(p^2) := \frac{\partial}{\partial p^2} \Sigma(p^2). \quad (6.16)$$

Furthermore, the OSRS requires  $Z = 1$  for convenience.

Summarizing, the renormalization of the mass and of the fields in the OSRS is defined by requiring

$$\begin{cases} \text{Re } \Sigma(-M^2, M^2) = 0 \\ \text{Re } \Sigma'(-M^2, M^2) = 0. \end{cases} \quad (6.17)$$

This guarantees that the renormalized mass  $M$  is the physical mass for stable particles and that the residue  $Z = 1$ . The denominator structure of the full propagator in this scheme is then

$$\Delta^{\text{full}}(p^2) \sim \frac{1}{p^2 + M^2 - \text{Im } \Sigma(-M^2, M^2)}. \quad (6.18)$$

Although this scheme is very convenient for stable particles, it is less so for unstable ones, for their self-energy has a non-vanishing imaginary part. One can think of a renormalization scheme where the *complete* self-energy vanishes for unstable particles. This scheme is called the complex mass scheme and is the subject of chapter 11.



# 7. Spontaneously Symmetry Breaking

The masses of unstable particles play an important role in the description of these particles. We shall therefore describe how these masses enter the Standard Model. The massive vector bosons of the Standard Model, the W bosons and the Z boson, arise by the so called *Higgs-mechanism*, which is closely related to the phenomenon of spontaneously symmetry breaking (SSB). This chapter aims to explain SSB and the Higgs-mechanism, and why the Higgs mechanism is in fact necessary to describe massive vector bosons. The next chapter outlines how these principles are implemented in the Standard Model.

## 7.1. Spontaneously broken symmetries

To illustrate the meaning of *spontaneously broken symmetries*, let us begin with a simple Lagrangian describing only one scalar field  $\phi(x)$

$$\mathcal{L} = -\partial_\mu\phi\partial^\mu\phi - V(\phi). \quad (7.1)$$

The ground state of the system is the field  $\phi(x)$  for which  $V(\phi)$  is minimal. For simplicity we assume here that this field is constant in space-time: let us call it  $v$ . Since the ground state corresponds to the vacuum,  $v$  is called the vacuum expectation value. It would be nice, however, to have a field which is zero in the ground state. That is, we would like to describe our Lagrangian in terms of a field  $\tilde{\phi}$  by expanding  $\phi$  around  $v$  as  $\phi(x) = v + \tilde{\phi}(x)$ . Of course, if  $v = 0$  this does not change anything; if  $v \neq 0$  however, it may have important consequences. For suppose that the Lagrangian (7.1) is invariant under transformations of  $\phi$  in a representation of a gauge group  $G$ , then it may be the case that the vacuum expectation value is not invariant under some of these transformations. These transformations are called spontaneously broken symmetries.

In general, gauge transformations applied to  $v$  will make it sweep out an orbit. All the values that  $v$  can attain under gauge transformations are denoted by  $G(v)$ . The orbit  $G(v)$  forms an equipotential submanifold in the space that  $\phi$  lives in, for gauge transformations leave the potential invariant. In general, *some* transformations do not change  $v$ . For example, if  $v = 0$ , *all* transformations leave  $v$  invariant. These transformations form a subgroup  $H_v \in G$ , such that  $H_v(v) = v$ .  $H_v$  is called the stability subgroup, or isotropy group, of  $v$ . The dimension of the orbit plus the dimension of the stability subgroup equals the dimension of the full gauge group:  $\dim[H_v] + \dim[G(v)] = \dim[G]$ . We illustrate these concepts by two examples.

- Suppose that  $\phi(x)$  is a complex scalar field transforming in the fundamental representation of  $G = U(1)$ . Furthermore, suppose that  $V(\phi) = V(|\phi|)$  is a mexican hat potential, with a whole circle of points in the complex plane of  $\phi$  as its minimum. Then in the ground state, the system spontaneously ‘chooses’ one of these values  $\phi = v \neq 0$  that minimizes  $V$ , without any preference for which one. Now, any such  $v$  is not invariant under  $U(1)$  transformations (which correspond to rotations in the complex plane), so the  $U(1)$ -symmetry is spontaneously broken.  $H_v$  is in this case the 0-dimensional subgroup

$H_v = \mathbb{1}$ , and the orbit  $G(v)$  is the circle in the complex plane with radius  $|v|$ . Their dimensions do indeed add up to the dimension of  $G$ , which is 1.

- Suppose that  $\phi(x)$  is a 3-dimensional real vector transforming in the fundamental representation of  $SO(3)$  (3-dimensional rotations). Furthermore, suppose again that  $V(\phi)$  acquires a minimum for some nonzero value of  $\phi(x) = v$ . Then the orbit  $G(v)$  is the surface of the sphere around the origin with radius  $|v|$ , which is a 2-dimensional surface. Any rotation that moves  $v$  over this orbit is a broken symmetry transformation.  $H_v$  comprises the 1-dimensional group of rotations around the axis through the point  $v$  (and the origin). Indeed, such rotations clearly leave  $v$  invariant. Again, the dimensions add up as  $\dim(H_v) + \dim(G(v)) = 1 + 2 = 3 = \dim(SO(3))$ .

After the SSB, that is *after* having rewritten the Lagrangian (7.1) by using  $\phi(x) = v + \tilde{\phi}(x)$ , the remaining symmetries of the theory are the unbroken ones, thus the gauge transformations of  $H_v$ . The reason is that the vacuum expectation value  $v$  is then considered *fixed*, it is not considered to change anymore under gauge transformations. A general infinitesimal transformation  $\delta\phi$  that leaves the *original* Lagrangian (7.1) invariant can be written as

$$\delta\phi = \delta(v + \tilde{\phi}) = \delta v + \delta\tilde{\phi}. \quad (7.2)$$

After the SSB, we thus ignore  $\delta v$ . This implies that symmetries  $\delta\phi$  of the original Lagrangian only remain symmetries  $\delta\tilde{\phi}$  after the SSB if they are symmetries for which  $\delta v = 0$  anyway. So indeed, the remaining symmetries of the Lagrangian are the ones corresponding to  $H_v$  - the unbroken symmetries, which is an appropriate term indeed.

## 7.2. SSB without choosing a gauge

We now focus on the implications of SSB for *local* gauge symmetries. First we show that every such broken symmetry gives rise to a *massive* gauge field. To this end, let us again consider scalar fields and let us take them real. This is no restriction, for  $n$  complex fields can be described as  $2n$  real ones. In order to make the standard mass term  $-\frac{1}{2}m^2\Phi^2$  in the Lagrangian invariant under gauge transformations, we assume that  $\Phi$  is a  $N$ -dimensional vector transforming in the fundamental representation of (a subgroup of)  $G = O(N)$ . This means that the generators of the symmetry group are anti-symmetric:  $t_a^T = -t_a$ . Chapter 3 has taught us how to construct the corresponding gauge invariant Lagrangian. The result is

$$\mathcal{L} = -\frac{1}{4}\text{Tr}\left[\left(G(W)_{\mu\nu}\right)^2\right] - \frac{1}{2}\left(D_\mu\Phi\right)^2 - V(\Phi). \quad (7.3)$$

We wrote  $G(W)_{\mu\nu}$  to emphasize that the field strength  $G$  is a function of the gauge fields  $W$ . The term involving this field strength gives rise to quadratic terms describing *massless* gauge fields  $W_\mu^a$ . However, if there are spontaneously broken symmetries, the second term of (7.3) also rise to more terms quadratic in  $W_\mu^a$  - mass terms. We work out the second term to see this happening.

$$\begin{aligned} -\frac{1}{2}\left(D_\mu\Phi\right)^2 &= -\frac{1}{2}\left(\partial_\mu\Phi - gW_\mu^a(t_a\Phi)\right)^2 \\ &= -\frac{1}{2}(\partial_\mu\Phi)^2 + g\partial_\mu\Phi_i W_\mu^a(t_a\Phi)_i - \frac{1}{2}g^2 W_\mu^a W^{\mu b}(t_a\Phi)_i(t_b\Phi)_i. \end{aligned} \quad (7.4)$$

Upon performing the expansion  $\Phi = v + \tilde{\Phi}$  equation (7.4) becomes

$$-\frac{1}{2}(D_\mu\Phi)^2 = -\frac{1}{2}(\partial_\mu\tilde{\Phi})^2 + gW_\mu^a\partial^\mu\tilde{\Phi}_i(t_av)_i - \frac{1}{2}g^2W_\mu^aW^{\mu b}(t_av)_i(t_bv)_i + (\tilde{\Phi}, W)^{3\text{ or }4}, \quad (7.5)$$

where the last term denotes terms that are cubic or quartic in the fields  $\tilde{\Phi}$  and/or  $W$ . Three terms appear in the quadratic part of (7.5): the standard kinetic term for  $\tilde{\Phi}$ , a term coupling the matter fields  $\tilde{\Phi}$  and the gauge fields  $W_\mu^a$ , and - as claimed - a term quadratic in the gauge fields  $W_\mu^a$ . We analyze this third term. First of all, note that  $t_av$  gives 0 if  $t_a$  generates a transformation in the stability subgroup  $H_v$ ; this is the case for a number of  $\dim[H_v]$  generators. The other generators move  $v$  along the orbit  $G(v)$  and thus yield nonzero - these are the generators associated with the spontaneously broken symmetries. The third term can thus be written as  $-\frac{1}{2}(m^2)^{a'b'}W_{\mu a'}W_{\nu b'}$ , where the primes on the indices indicate that they should only run over the  $\dim[G(v)]$  indices that correspond to the generators of these broken symmetries. We also defined  $(m^2)^{a'b'} = g^2(t^a v)_i(t^{b'} v)_i$ . This matrix  $m^2$  can be interpreted as the square of the mass matrix of  $\dim[G(v)]$  gauge fields. Switching to a basis where this matrix is diagonal yields the (squared) masses of these fields. Note that  $(m^2)^{a'a'} = g^2(t_{a'} v)^2 > 0$  (no sum intended) as required for real masses. Every spontaneously broken symmetry thus gives rise to a gauge field with a nonzero mass! This mechanism is called the *Higgs mechanism*.

We now analyze the second term of (7.5) - the quadratic coupling between  $\tilde{\Phi}$  and the gauge fields. The term contains the dot product of  $\partial_\mu\tilde{\Phi}$  and  $t_av$ . Since we are assuming  $v$  to be  $x$ -independent this product can be rewritten as  $\partial_\mu(\tilde{\Phi}_i(t_av)_i)$ , which involves the dot product of  $\tilde{\Phi}$  and  $t_av$ . Again, this only gives contributions for the infinitesimal transformations  $t_av$  in a direction of  $G(v)$ , so the dot product filters out the components of  $\tilde{\Phi}$  along this orbit  $G(v)$ . The particles corresponding to these components are called *Goldstone bosons*. The second term of (7.5) thus couples every goldstone boson to the field  $W_{\mu a'}$  that corresponds to the generator  $t_{a'}$  associated with that particular Goldstone boson. That is, the goldstone bosons couple to exactly those gauge bosons that have acquired a mass by the third term of (7.5). The other  $\dim[H_v]$  gauge fields remain massless. The coupling between these  $\tilde{\Phi}$  and  $W$ -fields implies that these fields can propagate into one another. Indeed, the coupling gives rise to the vertex of figure 7.1. This does not seem very physical, which should not come as a surprise. Since we started out with a gauge symmetry, there are unphysical degrees of freedom in our fields. Under a gauge transformation, the field  $\Phi$  is moved along the orbit  $G(\Phi)$ , which means that the components of  $\tilde{\Phi}$  in the direction of this orbit are unphysical. Since these components represent the goldstone bosons, the goldstone bosons are unphysical! Notice that it are precisely these components that can 'propagate into' other gauge fields. Because they are unphysical, these bosons are sometimes called *would-be Goldstone bosons*. Actually, in concluding that gauge bosons acquired a mass just by looking at the third term of (7.5), we skated over the fact that these gauge bosons couple to the would-be Goldstone bosons. This coupling affects the mass, for the vertex of figure 7.1 gives a contribution to the self-energy of these bosons by the diagram of figure 7.2. This diagram is of order  $g^2$  - the same order as the third term of (7.5). We shall not go further into this issue here, since the picture will be much more clear in the unitary gauge.

An advantage of not choosing a gauge is that it yields (bare) propagators behaving as  $1/k^2$  for large momentum  $k$  [2, Chapter 21.1] [1, Chapter 19.3]. We shall not show this here, we only mention the steps that have to be taken to find these propagators. The prescription to find the propagators is to rewrite the quadratic part of the Lagrangian in Fourier space and then invert the terms multiplying the fields. However, since the Lagrangian exhibits gauge symmetry, this inverse propagator will have eigenvectors with eigenvalue 0 and can therefore

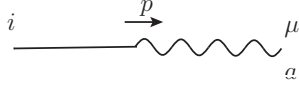


Figure 7.1.:  $\Phi$ - $W_\mu^a$  vertex



Figure 7.2.: Diagram contributing to the gauge boson self-energy at order  $g^2$  in perturbation theory

not be inverted. To circumvent this problem one can add a gauge fixing term to  $\mathcal{L}$  and then calculate the propagators. In fact, also ghost fields will have to be introduced. The behaviour of the propagators for large  $k$  means that, provided the potential  $V(\Phi)$  in the Lagrangian (7.3) does not contain any terms with negative mass dimension, we know that the theory is renormalizable by power counting. The drawback of the approach of not choosing a gauge is that it is not very clear which fields represent physical particles. In the next section we therefore take a different approach: instead of leaving the gauge invariance we shall impose a gauge condition and work in the unitary gauge. All the fields will then be physical such that the physical content of the theory will be much more transparent. The drawback will be propagators behaving as  $k^0$  for large momentum  $k$ . This makes it hard to renormalize the theory in the unitary gauge, which is required for extracting finite physical quantities.

### 7.3. SSB in the unitary gauge

In this section we shall redefine our fields in a way that makes the distinction between physical and unphysical fields more clear. Recall that gauge transformations move the field  $\Phi(x)$  along the orbit  $G(\Phi)$ . On every such orbit  $G(\Phi)$  we can pick a convenient point  $\rho(x)$  such that all  $\Phi(x)$ 's on that orbit are related to  $\rho(x)$  by a gauge transformation  $Y(x)$ , i.e.  $\Phi(x) = Y(x)\rho(x)$ . Note that  $Y(x)$  is not specified uniquely: one can freely multiply  $Y(x)$  with any transformation  $H(x) \in H_\rho$  since  $H(x)\rho(x) = 0$ . By construction  $\rho$  does not transform under a gauge transformation  $U(x) \in G(x)$ ,  $\rho(x)$  is therefore a physical field.  $Y$  on the other hand transforms as  $Y \rightarrow UY$  (ensuring  $\Phi \rightarrow U\Phi$ ) and thus contains all the unphysical degrees of freedom of  $\Phi(x)$ . We also define new gauge fields  $\hat{W}_\mu^a$  as

$$\hat{W}_\mu = \hat{W}_\mu^a t_a = Y^{-1}W_\mu Y + \frac{1}{g}(\partial_\mu Y^{-1})Y. \quad (7.6)$$

The fields  $\hat{W}_\mu^a$  are also gauge invariant, as can be checked by combining the transformation rules for  $Y$  and  $W_\mu$  (3.6). Therefore, these fields are also physical. Next we rewrite  $\mathcal{L}$  (equation (7.3)) in terms of the new fields  $Y(x)$ ,  $\rho(x)$  and  $\hat{W}_\mu^a$ . Since  $\mathcal{L}$  is gauge invariant and since all the gauge dependence of the new fields is in  $Y(x)$  (which is completely gauge dependent), we know that  $\mathcal{L}$  does not depend on  $Y(x)$ . Therefore, we may as well pick a convenient value for it: let us take  $Y(x) = \mathbb{1}$ . This means that we are moving all the fields  $\Phi$  on the orbit  $G(\Phi)$  to the chosen point  $\rho$ , i.e.  $\Phi(x) = \rho(x)$ . This gauge choice is called the *unitary gauge*. Choosing  $Y(x) = \mathbb{1}$  leads to another simplification, namely  $\hat{W}_\mu = W_\mu$ . After having specified this gauge, we expand  $\rho$  around its vacuum expectation value as  $\rho(x) = v + \tilde{\rho}(x)$ . The resulting Lagrangian is the same as (7.3) upon the replacements  $W \rightarrow \hat{W}$  and  $\tilde{\Phi} \rightarrow \rho$ . In particular, the second term

in the analogue of equation (7.5) contains the dot product  $\tilde{\rho}_i(t_a v)_i$ . As before,  $t_a v$  only yields vectors directed along  $G(v)$  for certain values of  $a$ , otherwise it gives 0. But the components of  $\Phi$  in this direction reside in  $Y(x)$ , not in  $\rho(x)$ , and hence not in  $\tilde{\rho}(x)$  either. Therefore, this term vanishes completely - there is *no* quadratic term in  $\mathcal{L}$  coupling  $\tilde{\rho}(x)$  and  $W_\mu^a$ . Putting it all together yields the Lagrangian

$$\mathcal{L} = -\frac{1}{4}\text{Tr}\left[\left(G(\hat{W})_{\mu\nu}\right)^2\right] - \frac{1}{2}(m^2)^{a'b'}\hat{W}_{\mu a'}\hat{W}^{\mu}_{b'} - \frac{1}{2}(\partial_\mu\tilde{\rho})^2 - V(\tilde{\rho}) + (\tilde{\rho}, \hat{W})^3\text{or}^4. \quad (7.7)$$

This time the physical content of the theory is clear:  $\text{dim}[G(v)]$  of the vector fields have acquired masses (recall that the primed indices can only take on  $\text{dim}[G(v)]$  values), while the other  $\text{dim}[H_v]$  vector fields remain massless. Furthermore, there is the (physical) scalar field  $\tilde{\rho}$  interacting with both itself and with the vector fields. The goldstone bosons (which were contained in  $Y(x)$ ) have disappeared from the theory. They were, as explained before, unphysical.

This clearness of the physical content of the theory is the advantage of working in the unitary gauge. It is a distinct feature of SSB that we can choose a gauge without sacrificing Lorentz invariance or locality of the theory [1, p. 571]. The reason is that choosing the unitary gauge is in this case completely equivalent to a formal redefinition of the fields: we *could* have obtained the Lagrangian (7.7) by just rewriting all the fields in our original Lagrangian (7.3) in terms of our new fields  $\tilde{\rho}(x)$ ,  $Y(x)$  and  $\hat{W}_{\mu a}$ ; we only used the gauge condition  $Y = \mathbb{1}$  because it was an *easier* way to obtain the same result. Working in the unitary gauge also has a drawback. The part of  $\mathcal{L}$  quadratic in the massive gauge fields is equal to the Proca Lagrangian. Therefore, the propagator for these fields is the Proca propagator

$$\Delta_{\mu\nu}^{proca}(k) = \frac{1}{i(2\pi)^4} \frac{1}{k^2 + m^2} \left( \eta_{\mu\nu} + \frac{k_\mu k_\nu}{m^2} \right). \quad (7.8)$$

For large momenta this propagator behaves as  $(k^2)^0$  and not as  $1/k^2$ . This makes it hard to renormalize the theory and thus to calculate finite physical quantities in this gauge. We *do* know that the theory is renormalizable. This was clear from the approach taken in the previous section. This is why the Higgs mechanism is such an important mechanism: it provides a *renormalizable* theory containing massive vector bosons. If one would include massive vector bosons by including a Proca Lagrangian for the corresponding fields by hand, there would be no guarantee that the theory should be renormalizable. Indeed, in the next chapter we will see that the massive vector bosons acquire their mass by the Higgs mechanism in the Standard Model. The scalar field that spontaneously breaks the symmetry is the *Higgs field*.

# 8. The electroweak sector of the Standard Model

## 8.1. Chirality

This chapter introduces the electroweak sector of the Standard Model. The Standard Model treats left- and right-handed fermions differently. This notion of left- and right-handedness is closely related to chirality, which is introduced in this section.

One can define the gamma matrix  $\gamma_5 = \gamma^5 = -i\gamma^0\gamma^1\gamma^2\gamma^3$ , satisfying the property  $(\gamma^5)^2 = \mathbf{1}$ . The eigenvalues of  $\gamma^5$  are thus  $\pm 1$  and are called the *chirality* of the corresponding eigenstates. It turns out that the eigenvectors corresponding to either eigenvalue span a 2-dimensional subspace. Projection operators projecting spinor states onto these subspaces are

$$P_{L/R} = \frac{1}{2}(\mathbf{1} \pm \gamma^5). \quad (8.1)$$

The fact that these operators are projection operators is confirmed by the relations

$$P_L P_R = P_R P_L = 0, \quad P_L + P_R = \mathbf{1}, \quad P_L^2 = P_L, \quad P_R^2 = P_R. \quad (8.2)$$

The fact that  $\gamma^5 P_{L/R} = \pm P_{L/R}$  shows that they do indeed project onto the mentioned subspaces. A fermion  $\psi_L = P_L \psi$  with chirality  $+1$  is called a *left-handed* fermion and a fermion  $\psi_R = P_R \psi$  with chirality  $-1$  is called a *right-handed* fermion.

There is one more thing to note here: if one writes down a mass-term for a fermion  $\psi$  in the standard way, one finds that the left- and right-handed components of  $\psi$  couple, for

$$-m\bar{\psi}\psi = -m(\bar{\psi}_L\psi_R + \bar{\psi}_R\psi_L). \quad (8.3)$$

We shall come back to this issue in paragraph 8.2.2. In the kinetic term this does not happen. Due to the presence of the gamma-matrix in  $\not{\partial} = \gamma^\mu \partial_\mu$  the kinetic term can be written as

$$-\bar{\psi}\not{\partial}\psi = -\bar{\psi}_L\not{\partial}\psi_L - \bar{\psi}_R\not{\partial}\psi_R. \quad (8.4)$$

## 8.2. Prototype Model

This section discusses a prototype model that contains the gauge bosons, the Higgs field and two fermions. This model captures the basics of the electroweak interactions of the standard model. The complete standard model essentially consists of a number of copies of this prototype model, as will be discussed in section 8.2.2. Our approach follows de Wit, Laenen and Smith [1, chapter 20].

We denote the two fermion fields as  $p$  and  $n$  and decompose them into  $p_L, p_R, n_L$  and  $n_R$ . The prototype model contains three gauge bosons. One of them is massless - the photon, responsible for electromagnetic interactions. The other two bosons - the Z and W boson, mediating the weak force - are massive. The W boson is charged electromagnetically and is therefore described by a complex field. This means that there are actually two W-bosons, the positively charged  $W^+$  and its anti-particle  $W^-$ . That makes a total of four gauge fields. The gauge *group* under which the fields transform must therefore be four-dimensional. This group turns out to be  $U(1) \times SU(2)$ . The generator of  $U(1)$  is  $i$ . We call the corresponding gauge field  $B_\mu$  and the corresponding coupling constants  $\frac{1}{2}q$  and  $\frac{1}{2}q_j$  ( $j = 1, 2, 3$ ). The  $SU(2)$ -generators are given by  $t_a = \frac{1}{2}i\sigma_a$  ( $a = 1, 2, 3$ ), where  $\sigma_a$  denote the Pauli matrices. We denote the corresponding gauge fields as  $W_\mu^a$  and the coupling constant as  $g$ . The structure constants are the components of the Levi-Civita tensor, i.e.  $f_{abc} = \epsilon_{abc}$ . Three of the gauge fields will need to acquire a mass, which happens by the Higgs mechanism explained in chapter 7. To accommodate this we introduce two scalar fields,  $\phi_1$  and  $\phi_2$ . These scalar fields will spontaneously break three of the four symmetries and thereby ‘give’ three of the gauge bosons their masses.

We now describe how the matter fields transform under the gauge transformations. Consider first a transformation  $U_2 \in SU(2)$ . The left-handed fermion components are combined into a doublet  $\psi_L$ , which transforms in the fundamental representation of  $SU(2)$ . The right-handed components on the other hand are just singlets transforming in the trivial representation of  $SU(2)$ . In other words, they do not transform at all. This is where the Standard Model makes an obvious distinction between left- and right-handedness. Finally, the scalar fields are also combined in a doublet  $\Phi$  transforming in the fundamental representation of  $SU(2)$ . Summarizing, the matter fields transform as

$$\Phi = \begin{pmatrix} \phi_1 \\ \phi_2 \end{pmatrix} \rightarrow U_2 \Phi, \quad \psi_L = \begin{pmatrix} p_L \\ n_L \end{pmatrix} \rightarrow U_2 \psi_L, \quad p_R \rightarrow p_R, \quad n_R \rightarrow n_R. \quad (8.5)$$

Under a  $U(1)$ -transformation, parameterized by  $\xi$ , the matter fields change as follows

$$\Phi \rightarrow e^{\frac{1}{2}iq\xi}\Phi, \quad \psi_L \rightarrow e^{\frac{1}{2}iq_1\xi}\psi_L, \quad p_R \rightarrow e^{\frac{1}{2}iq_2\xi}p_R, \quad n_R \rightarrow e^{\frac{1}{2}iq_3\xi}n_R. \quad (8.6)$$

In other words, every matter field transforms into  $e^{\frac{1}{2}iqY\xi}$  times itself, where  $Y = 1, q_1/q, q_2/q$  and  $q_3/q$  for respectively  $\Phi, \psi_L, p_R$  and  $n_R$ .  $Y$  is called the *hypercharge*.

The gauge invariant Lagrangian is then given by:

$$\mathcal{L}^{\text{PT}} = \mathcal{L}_{\text{gauge}}^{\text{PT}} - \frac{1}{2}|D_\mu\Phi|^2 - V(\Phi) - \bar{\psi}_L \not{D}\psi_L - \bar{p}_R \not{D}p_R - \bar{n}_R \not{D}n_R + \text{fermion mass-terms}. \quad (8.7)$$

The superscript  $PT$  is short for ‘prototype’.  $\mathcal{L}_{\text{gauge}}^{\text{PT}}$  is the standard gauge field Lagrangian for the fields  $B_\mu$  and  $W_\mu^a$ . The fermion mass-terms are the subject of paragraph 8.2.2.

### 8.2.1. The kinetic terms and the gauge fields

Now we discuss the spontaneous symmetry breaking. We assume that  $\Phi(x)$  has a nonzero vacuum expectation value. This spontaneously breaks some of the symmetries. To figure out

which, we follow the approach of section 7.3 and write  $\Phi$  as

$$\Phi(x) = Y(x) \frac{1}{\sqrt{2}} \begin{pmatrix} 0 \\ \rho(x) \end{pmatrix}. \quad (8.8)$$

Any  $\Phi(x)$  can be written in the form (8.8) for some  $Y(x) \in U(1) \times SU(2)$ . The gauge dependent components of  $\Phi(x)$  reside in  $Y(x)$ . The physical part of  $\Phi(x)$  resides in the field  $\rho(x)$ . We then adopt the unitary gauge by choosing  $Y(x) = \mathbb{1}$ , such that

$$\Phi(x) = \frac{1}{\sqrt{2}} \begin{pmatrix} 0 \\ \rho(x) \end{pmatrix}. \quad (8.9)$$

This choice of gauge leaves a residual symmetry; it leaves (8.9) invariant under transformations of the stability subgroup  $H_v \subset U(1) \times SU(2)$ . To find this residual symmetry, we consider an arbitrary gauge transformation  $U \in U(1) \times SU(2)$  and then find its most general form that leaves (8.9) invariant. Since  $U \in U(1) \times SU(2)$ , it can be written as the product of a  $U_1(\xi) \in U(1)$  and a  $U_2(r, \theta, \xi^3) \in SU(2)$ . The transformation  $U$  is thus characterized by the parameters  $\xi$ ,  $r$ ,  $\theta$  and  $\xi^3$ , where  $\xi$  characterizes a transformation generated by  $i$  and  $\xi^3$  characterizes a transformation generated by  $t_3$ . Explicitly

$$\begin{aligned} U(\xi, r, \theta, \xi^3) &= U_1(\xi) \cdot U_2(r, \theta, \xi^3) \\ &= e^{\frac{1}{2}iq\xi} \mathbb{1} \cdot \begin{pmatrix} r e^{\frac{1}{2}ig\xi^3} & \sqrt{1-r^2} e^{\frac{1}{2}i\theta} \\ \sqrt{1-r^2} e^{-\frac{1}{2}i\theta} & r e^{-\frac{1}{2}ig\xi^3} \end{pmatrix} \\ &= \begin{pmatrix} r e^{\frac{1}{2}i(g\xi^3+q\xi)} & \sqrt{1-r^2} e^{\frac{1}{2}i(\theta+q\xi)} \\ \sqrt{1-r^2} e^{-\frac{1}{2}i(\theta+q\xi)} & r e^{\frac{1}{2}i(-g\xi^3+q\xi)} \end{pmatrix}. \end{aligned} \quad (8.10)$$

In order to leave (8.9) invariant, the upper right entry of (8.10) must be 0 and the lower right entry must be 1. The former requirement is achieved by setting  $r = 1$ , leaving transformations

$$U(\xi, \xi^3) = \begin{pmatrix} e^{\frac{1}{2}i(g\xi^3+q\xi)} & 0 \\ 0 & e^{\frac{1}{2}i(-g\xi^3+q\xi)} \end{pmatrix}. \quad (8.11)$$

Note that this  $U$  is two-dimensional. We still need the lower right entry to equal 1, that is, we need  $-g\xi^3 + q\xi = 0$ . This reduces the number of components of a transformation  $U$  that leaves (8.9) invariant to 1. This means that the stability subgroup  $H_v$  is one-dimensional. This is precisely what we need, for we need one gauge field - the photon - to remain massless. Indeed, we shall find that the residual symmetry is a  $U(1)$  symmetry, which is the symmetry associated with electromagnetism. The other three symmetries are broken, which results in the other three gauge bosons becoming massive, as discussed in chapter 7.

We would like to associate one parameter  $\xi^{EM}$  with the residual symmetry - the electromagnetic symmetry. The superscript  $EM$  is short for electromagnetism. Therefore, instead of the parameters  $g$  and  $q$  we shall characterize the transformation (8.11) by two new parameters  $\xi^{EM}$  and  $\xi^Z$ . These are related to the old parameters  $\xi^3$  and  $\xi$  by a rotation, to ensure that they are orthogonal. To make sure that the part of the transformation that is characterized by  $\xi^{EM}$  leaves (8.9) invariant, we associate the lower-right entry of (8.10) - the part of (8.11) that alters (8.9) - with  $\xi^Z$ . We therefore define  $-\xi^Z := \frac{1}{\sqrt{g^2+q^2}}(-g\xi^3 + q\xi)$ . This implies that the change of variables that we are after is the rotation

$$\begin{pmatrix} \xi^Z \\ \xi^{EM} \end{pmatrix} = \begin{pmatrix} \cos(\theta_W) & -\sin(\theta_W) \\ \sin(\theta_W) & \cos(\theta_W) \end{pmatrix} \begin{pmatrix} \xi^3 \\ \xi \end{pmatrix}, \quad \text{where} \quad \begin{cases} \cos(\theta_W) = \frac{g}{\sqrt{g^2+q^2}} \\ \sin(\theta_W) = \frac{q}{\sqrt{g^2+q^2}} \end{cases}. \quad (8.12)$$



The angle  $\theta_W$  is called the *weak mixing angle*. Using (8.12), the transformation (8.11) can then be rewritten in terms of  $\xi^{EM}$  and  $\xi^Z$ , as follows.

$$U(\xi^{EM}, \xi^Z) = \begin{pmatrix} e^{ig\sin(\theta_W)\xi^{EM}} & 0 \\ 0 & 1 \end{pmatrix} \cdot \begin{pmatrix} e^{\frac{1}{2}i(g\cos(\theta_W)-q\sin(\theta_W))\xi^Z} & 0 \\ 0 & e^{-\frac{1}{2}i\frac{g}{\cos(\theta_W)}\xi^Z} \end{pmatrix}. \quad (8.13)$$

Equation (8.13) shows that the transformation  $U(\xi^{EM}, \xi^Z)$  is a product of two transformations, one characterized by  $\xi^{EM}$  and one by  $\xi^Z$ , both of which are equivalent to a  $U(1)$ -transformation. The transformation that is characterized by  $\xi^{EM}$  (that is a transformation (8.13) with  $\xi^Z = 0$ ) does indeed leave (8.9) invariant, as we wanted.

We redefine the gauge fields analogous to (8.12), that is

$$\begin{pmatrix} A_\mu \\ Z_\mu \end{pmatrix} = \begin{pmatrix} \cos(\theta_W) & -\sin(\theta_W) \\ \sin(\theta_W) & \cos(\theta_W) \end{pmatrix} \begin{pmatrix} W_\mu^3 \\ B_\mu \end{pmatrix}. \quad (8.14)$$

As a result,  $A_\mu$  corresponds to the gauge transformations of the stability subgroup  $H_v$  and thus represents the massless particle. That is,  $A_\mu$  describes the photon. The covariant derivative (working on any matter field) can now be rewritten in terms of these new fields as

$$\begin{aligned} D_\mu &= \partial_\mu - \frac{1}{2}iqB_\mu - gW_\mu^a t_a \\ &= \partial_\mu - eA_\mu t^{EM} - \frac{g}{\cos(\theta_W)} Z_\mu t^Z - g(W_\mu^1 t_1 + W_\mu^2 t_2), \end{aligned} \quad (8.15)$$

where we defined  $e = g\sin(\theta_W)$ . We also defined new generators corresponding to the new fields  $A_\mu$  and  $Z_\mu$  by

$$\begin{aligned} t^{EM} &= \frac{1}{2}i(\sigma_3 + Y) \\ t^Z &= \frac{1}{2}i\sigma_3 - \sin^2(\theta_W)t^{EM}. \end{aligned} \quad (8.16)$$

The generator  $t^{EM}$  defines the *electric charge*  $Q$  (in units of  $e$ ) of the various matter fields by

$$t^{EM} \begin{pmatrix} 0 \\ \rho \end{pmatrix} = iQ_{\text{Higgs}} \begin{pmatrix} 0 \\ \rho \end{pmatrix}, \quad t^{EM} \begin{pmatrix} p_L \\ n_L \end{pmatrix} = i \begin{pmatrix} Q_{p_L} p_L \\ Q_{n_L} n_L \end{pmatrix}, \quad t^{EM} p_R = iQ_{p_R} p_R \quad t^{EM} n_R = iQ_{n_R} n_R. \quad (8.17)$$

In a bit more sloppy notation, the relation between the electric charge  $Q$  and the hypercharge  $Y$  can be summarized as

$$eQ = \frac{1}{2}(\sigma_3 + Y). \quad (8.18)$$

Equation (8.18) shows that the Higgs-boson is electrically neutral, for  $Q_{\text{Higgs}} = \frac{1}{2}(-1 + 1) = 0$ . Note that in order for the left- and right-handed components of the fermions  $p$  and  $n$  to have the same electric charge (i.e. in order to have  $Q_{p_L} = Q_{p_R}$  and  $Q_{n_L} = Q_{n_R}$ ), their hypercharges must be related by  $q_1 = q_2 - q$  and  $q_3 = q_1 - q$ . We shall see that these relations are precisely guaranteed by equation (8.27), which is a necessary condition to include mass-terms for the fermions.

Now we can finally expand the scalar around its ground state as

$$\Phi(x) = \frac{1}{\sqrt{2}} \begin{pmatrix} 0 \\ \rho(x) \end{pmatrix} = \frac{1}{\sqrt{2}} \begin{pmatrix} 0 \\ v + \tilde{\rho}(x) \end{pmatrix}. \quad (8.19)$$

Note that from (8.19) it is obvious that  $t^{\text{EM}}$  does indeed leave the ground state invariant, for  $t^{\text{EM}} \begin{pmatrix} 0 \\ v \end{pmatrix} \stackrel{(8.16)}{=} 0$ . In chapter 7 we saw that the gauge fields that correspond to the other generators acquire masses by the third term in equation (7.5). The situation there was slightly different, for the field  $\Phi$  in that case was a real field and all the gauge fields had equal coupling constant (c.c.). Luckily, the result is easily generalized: the masses of the gauge fields arise by the following terms in the Lagrangian.

$$\text{gauge field mass-terms} = -\frac{1}{2}(\text{c.c.})_a(\text{c.c.})_b \left( t_a \begin{pmatrix} 0 \\ v \end{pmatrix} \right)_i^* \left( t_b \begin{pmatrix} 0 \\ v \end{pmatrix} \right)_i (\text{gauge field})^a (\text{gauge field})^b.$$

Performing the implied sum over the new gauge fields and their corresponding generators yields

$$\text{gauge field mass-terms} = -\frac{1}{2}M_Z^2 Z^\mu Z_\mu - \frac{1}{2}M_W^2 \left( (W_\mu^1)^2 + (W_\mu^2)^2 \right), \quad (8.20)$$

where the masses are given by

$$M_Z = \frac{1}{2} \frac{gv}{\cos(\theta_W)} \quad \text{and} \quad M_W = \frac{1}{2}gv. \quad (8.21)$$

As a last step in a series of redefinitions, the fields  $W_\mu^1$  and  $W_\mu^2$  can be combined into one complex field as  $W_\mu = \frac{1}{\sqrt{2}}(W_\mu^1 - iW_\mu^2)$ . This field  $W_\mu$  is charged electromagnetically. This can be seen by deriving that  $W_\mu$  changes under an infinitesimal residual gauge transformation parameterized by  $\xi^{\text{EM}}$  as  $W_\mu \rightarrow W_\mu + ie\xi^{\text{EM}}$  [1, p. 593]. This is precisely the infinitesimal electromagnetic  $U(1)$  transformation of a gauge boson with charge  $e$ . In terms of this complex field  $W_\mu$  the covariant derivative reads

$$\begin{aligned} D_\mu &= \partial_\mu - \frac{1}{2}iqB_\mu - gW_\mu^a t_a \\ &= \partial_\mu - eA_\mu t^{\text{EM}} - \frac{g}{\cos(\theta_W)} Z_\mu t^Z - \frac{g}{\sqrt{2}}(W_\mu t_+ + \bar{W}_\mu t_-), \end{aligned} \quad (8.22)$$

where  $\bar{W}_\mu$  denotes the complex conjugate of  $W_\mu$  and where we defined the new generators  $t_\pm = t_1 \pm it_2 = \frac{1}{2}i(\sigma_1 \pm i\sigma_2)$ . We can also rewrite  $\mathcal{L}_{\text{gauge}}^{\text{PT}}$  - the part of the Lagrangian containing the kinetic terms for the gauge fields - in terms of the new fields  $A_\mu$ ,  $Z_\mu$  and  $W_\mu$ . The result is

$$\begin{aligned} \mathcal{L}_{\text{gauge}}^{\text{PT}} &= -\frac{1}{4} \left( G_{\mu\nu}(B) \right)^2 - \frac{1}{4} \sum_{a=1}^3 \left( G_{\mu\nu}(W_\mu^a) \right)^2 \\ &= -\frac{1}{2} |\partial_\mu^{\text{EM}} W_\nu - \partial_\nu^{\text{EM}} W_\mu|^2 - \frac{1}{4} (\partial_\mu Z_\nu - \partial_\nu Z_\mu)^2 \\ &\quad - \frac{1}{4} (\partial_\mu A_\nu - \partial_\nu A_\mu)^2 + \mathcal{O}(A_\mu, Z_\nu, W_\rho, \bar{W}_\sigma)^{3 \text{ or } 4}, \end{aligned} \quad (8.23)$$

where  $\partial_\mu^{\text{EM}} W_\nu := (\partial_\mu - ieA_\mu)$  can be interpreted as the covariant derivative corresponding to the residual  $U(1)$  symmetry. This notation makes explicit the invariance of the kinetic terms in  $\mathcal{L}_{\text{gauge}}^{\text{PT}}$  under this residual symmetry. The last term in (8.23) denotes interaction terms that are cubic or quartic in the gauge fields.

### 8.2.2. Fermion masses

This section deals with the fermionic mass-terms in  $\mathcal{L}^{PT}$ . They cannot be included as the standard terms  $-m_p \bar{p}p$  and  $-m_n \bar{n}n$ . The reason is that (8.3) implies that these are not gauge invariant, for left- and right-handed fermions transform differently. Therefore we adopt an alternative approach: we couple the fields  $p$  and  $n$  to the scalar field  $\Phi$  in a gauge invariant way, by couplings that are called *Yukawa couplings*. We shall couple them in such a way that mass-terms for the fermions arise upon the expanding  $\Phi$  around its (nonzero) expectation value. We start with the following two quantities that are invariant under  $SU(2)$  transformations.

$$\begin{cases} \psi_1 := \sqrt{2}\Phi^\dagger\psi_L & \rightarrow \sqrt{2}\Phi U^\dagger U\psi_L & = \psi_1 \\ \psi_2 := -\sqrt{2}\det(\Phi\psi^T) & \rightarrow -\sqrt{2}\det(U\Phi\psi^T U^T) = -\sqrt{2}\det(U)\det(U^T)\det(\Phi\psi^T) = \psi_2. \end{cases} \quad (8.24)$$

Under  $U(1)$  these quantities transform as

$$\begin{cases} \psi_1 \rightarrow \psi'_1 = e^{\frac{1}{2}i(q_1-q)}\psi_1 \\ \psi_2 \rightarrow \psi'_2 = e^{\frac{1}{2}i(q_2-q)}\psi_2. \end{cases} \quad (8.25)$$

Now we switch to the unitary gauge, i.e. we write  $\Phi(x) = \frac{1}{\sqrt{2}} \begin{pmatrix} 0 \\ \rho(x) \end{pmatrix}$ . Then  $\psi_1(x) = \rho(x)n_L(x)$  and  $\psi_2(x) = \rho(x)p_L(x)$ . Keeping in mind that we need terms coupling left- and right-handed components according to (8.3), such that masses then arise upon the expansion  $\rho(x) = v + \tilde{\rho}(x)$ , we introduce the following mass-terms in  $\mathcal{L}^{PT}$ .

$$\begin{cases} \mathcal{L}_n^{\text{mass}} = -G_n(\bar{n}_R\psi_1 + \bar{\psi}_1 n_R) = -G_n\rho(\bar{n}_R n_L + \bar{n}_L n_R) \\ \mathcal{L}_p^{\text{mass}} = -G_p(\bar{p}_R\psi_2 + \psi_2 p_R) = -G_p\rho(\bar{p}_R p_L + \bar{p}_L p_R). \end{cases} \quad (8.26)$$

These terms then give rise to the fermion masses  $m_p = G_p v$  and  $m_n = G_n v$ . Note that the terms (8.26) are still invariant under  $SU(2)$ -transformations, since the right-handed fermion components do not transform under these. In order for these terms to be invariant under the  $U(1)$ -transformation as well, we need to impose

$$\begin{cases} q_2 = q_1 + q \\ q_3 = q_1 - q. \end{cases} \quad (8.27)$$

Equation (8.27) implies that if we call the hypercharge of the left-handed fermions  $y$ , then the hypercharges  $Y$  of the right-handed components are given by  $y + 1$  in the case of  $p$  and by  $y - 1$  in the case of  $n$ . Equation (8.18) then allows us to calculate the charge. The resulting hypercharges and charges of the fermions are summarized in table 8.1.

## 8.3. Structure of the Standard Model

The standard model is built up in the same way as the prototype model, except it does not contain *one* pair of fermions  $n$  and  $p$ , but *several*, all with different masses. These masses can be accounted for in the prototype model by picking the appropriate value for  $G_p$  and  $G_n$  in equation (8.26). We distinguish between two different types of fermions, *quarks* and *leptons*. We

	Y	Q
$p_L$	$y$	$\frac{1}{2}(y+1)$
$p_R$	$y+1$	
$n_L$	$y$	$\frac{1}{2}(y-1)$
$n_R$	$y-1$	

(a) general case

	Y	Q
$p_L$	$\frac{1}{3}$	$\frac{2}{3}$
$p_R$	$\frac{4}{3}$	
$n_L$	$\frac{1}{3}$	$-\frac{1}{3}$
$n_R$	$-\frac{2}{3}$	

(b) hadronic case ( $y = \frac{1}{3}$ )

	Y	Q
$p_L$	$-1$	$0$
$p_R$	$0$	
$n_L$	$-1$	$-1$
$n_R$	$-2$	

(c) leptonic case ( $y = -1$ )

Table 8.1.: Hypercharge  $Y$  and charge  $Q$  of the fermions

call the corresponding prototype model versions the *hadronic* version and the *leptonic* version respectively. In the hadronic version the hypercharges and charges of the quarks are characterized by  $y = \frac{1}{3}$  (where  $y$  is still the hypercharge of the left-handed fermions in the model version), whereas in the leptonic version of the model we have  $y = -1$ . The resulting (hyper)charges are summarized in tabel 8.1. Note that the resulting  $p$ -lepton does not have a charge and does therefore not couple to the photon. This  $p$ -lepton is called the *neutrino* and is denoted by  $p = \nu$ .

The prototype model only includes electroweak interactions by the  $U(1) \times SU(2)$  gauge symmetry. Actually, the full gauge group of the standard model is  $SU(3) \times SU(2) \times U(1)$ . The extra  $SU(3)$  transformations give rise to another kind of gauge boson, the *gluon*, mediating the *strong* nuclear force. Of the fermions, only the quarks transform under the  $SU(3)$ -transformations. Therefore they acquire a new index corresponding to the (3-dimensional)  $SU(3)$ -group. We say that every quark can have three possible *colours*: red, blue or green. Leptons on the other hand do not transform under the  $SU(3)$ -transformations - they are insensitive to the strong force. This is another important difference between leptons and quarks.

So far three *generations* of particles have been found, every generation comprising one pair of leptons and one pair of quarks, which can come in any of the three colours. Therefore every generation consists of four copies of our prototype-model, whereby the three copies corresponding to the quarks can mix through strong interactions. Since every generation contains four particles (two leptons and two quarks), that makes a total of twelve fermions. Figure 8.1 summarizes all the particles in and the structure of the standard model. The up-, charm- and top-quarks are described in the prototype model by  $p$ -fermions. The other quarks - the down-, strange- and bottom-quarks - correspond to  $n$ -fermions. As for the leptons, the electron, muon and tau are the  $p$ -fermions and their corresponding neutrino's are the  $n$ -fermions. With every generation the particles become heavier. The particles of the first generation are stable and make up ordinary matter. The particles of the higher generations are unstable (except for the neutrino's) and are therefore much less common. It is mainly by high-energy experiments that these particles can be detected. It is therefore not surprising that these particles were discovered later than the particles of the first generation.

It turns out that the different generations are not completely independent. Although the leptons of different generations are, quarks of different generations can actually interact through

weak interactions. In fact, the quarks of the second and third generation are unstable and decay into up- and down-quarks. So whereas the lepton number of every separate generation is conserved, this is not true for the baryon number; one can only say that the *total* baryon number is conserved. The weak force is thus not completely captured within one prototype model; when including all generations one has to make a slight generalization to accommodate weak interactions between fermions of different generations. We will not do this here.

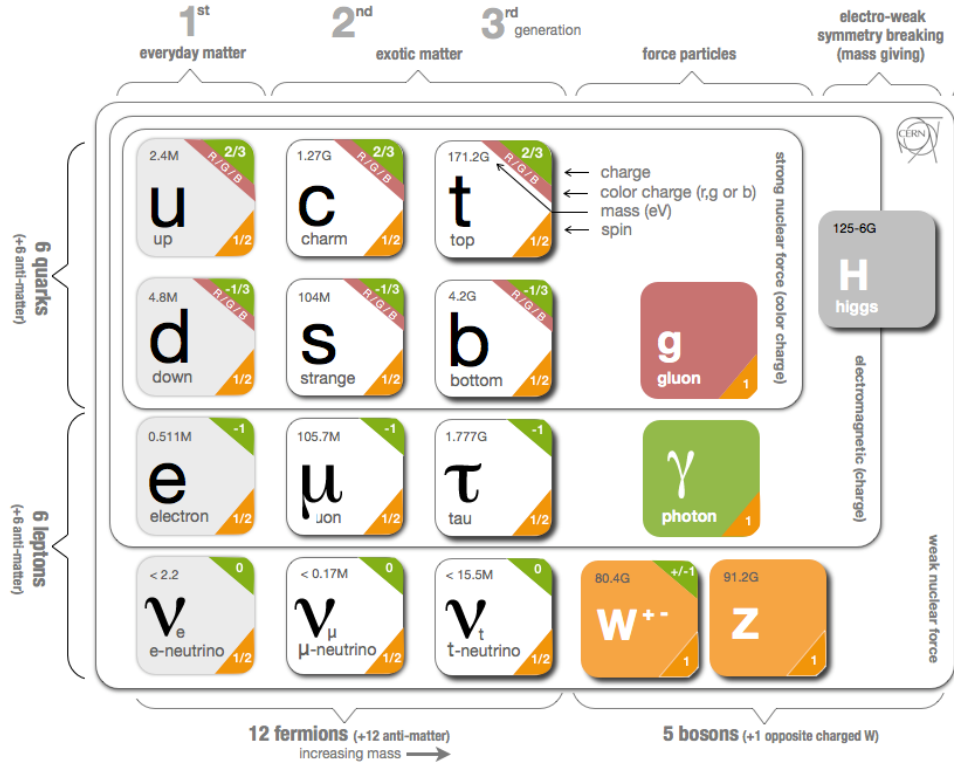


Figure 8.1.: Structure of the Standard Model. Source: <http://astrophysics.pro/particle-physics/standard-model>.

As we introduced it, the organization of the standard model into different generations and the assignments of the hypercharges ( $y = 1/3$  for quarks and  $y = -1$  for leptons) seems completely random. There is actually a theoretical ‘reason’ explaining some of the set-up: the *cancellation of the chiral anomaly*. We sketch this reason here. As shown by equation (8.5), only the left-handed components of fermions transform under the  $SU(2)$  transformations of the standard model. The infinitesimal  $SU(2)$  transformation of a complete fermion field  $\psi$  (which can denote either  $p$  or  $n$ ) can be written as

$$\psi \rightarrow \psi + ig\xi_a t^a \psi_L = \left( 1 + ig\xi_a t^a \left( \frac{1 + \gamma^5}{2} \right) \right) \psi, \quad (8.28)$$

where the  $t^a$ 's are the  $SU(2)$ -generators and where we used the fact that  $P_L = \frac{1}{2}(1 + \gamma^5)$ . We have seen before that a gauge symmetry leads to a conserved current. In this case the following currents should be conserved

$$j^{\mu a} = \bar{\psi} \gamma^\mu \left( \frac{1 + \gamma^5}{2} \right) t^a \psi. \quad (8.29)$$

However, it can be shown that, at the quantum level, these currents are *not* conserved, which is related to the fact that it is troublesome to generalize the matrix  $\gamma^5$  to more than four dimensions. This is a problem one runs into if one tries to renormalize the quantum theory by using dimensional regularization. Other regularization methods will run into other difficulties; the result is inevitably the non-conservation of the currents (8.29). Such a current that is conserved at the classical level but not at the quantum level is called an *anomaly*; this specific anomaly is called the *chiral anomaly*. It turns out that the chiral anomaly destroys the renormalizability of the theory [1, p. 603]. Fortunately, the theory is saved. The fact that every generation consists of four copies of the prototype model with these specific hypercharge assignments ( $y = 1/3$  and  $y = -1$ ) makes sure that the diagrams giving rise to the anomaly precisely cancel each other! This phenomenon is called *anomaly cancellation*. So every generation is organized in such a way that the theory *is* renormalizable.

**Part II.**

# **Unstable Particles**

# 9. Unstable Particles and the naïve approach

## 9.1. Unstable Particles

By ‘unstable particles’ we refer to elementary particles that can decay by themselves, without interacting with another particle, into other elementary particles. In other words, an elementary particle is unstable if a free particle of that type can decay into other particles. This definition is not practical for quarks, which are bound together by the strong force as hadrons, meaning that we do not usually encounter free quarks. The one exception is the top quark. Due to its high mass it is so short-lived (the predicted mean lifetime is  $5 \cdot 10^{-25} s$  [6]) that it does not have the time to hadronize. Therefore, the top quark only exists as a free quark, although for an extremely short time. It is well known that ordinary matter is made up of protons and neutrons, which both consist of only up- and down-quarks. This indicates that not only the top quark is unstable, but so are the charm-, strange- and bottom-quarks. However, to describe these one really needs quantum chromodynamics, a complication that is not adressed in this thesis. Of the other particles in the Standard Model, the stable particles are the electron, the neutrino’s, the photon and the gluon. This means that the muon, the tau, the W-bosons, the Z-boson and the Higgs boson are unstable. Mean lifetimes of the unstable particles range from the order of  $10^{-6} s$  for muons to  $10^{-25} s$  for the W-bosons, the Z-boson and the top-quark. Particle properties of the mentioned unstable particles (mass, width and mean lifetime) are shown in table 9.1. By this definition, a particle A (with momentum  $p_A$  and physical mass  $m_A$ ) is unstable if the Lagrangian allows for a diagram (figure 9.1) describing the decay of A into a set of particles (with momenta  $q_i$  and masses  $m_i$ ) whose total mass is smaller than  $m_A$ , i.e. with  $m_A > \sum_i m_i$ . This last requirement is necessary to satisfy energy conservation, which reads in the rest frame of A

$$m_A = \sum_i \sqrt{q_i^2 + m_i^2} \geq \sum_i m_i. \quad (9.1)$$

An unstable particle is characterized by having an on-shell self-energy with a nonzero imaginary part. This follows from the cutting equations, which can be used to write the imaginary part

	mass $M$	width $\Gamma$	mean lifetime $\tau$	$\Gamma/M$
muon	106 MeV	$3.00 \cdot 10^{-10}$ eV	$2.20 \cdot 10^{-6}$ s	$2.82 \cdot 10^{-21}$
tau	1.78 GeV	$2.27 \cdot 10^{-3}$ eV	$290 \cdot 10^{-15}$ s	$1.28 \cdot 10^{-15}$
W	80.4 GeV	2.09 GeV	$3.16 \cdot 10^{-25}$ s	0.0260
Z	91.2 GeV	2.50 GeV	$2.64 \cdot 10^{-25}$ s	0.0274
Higgs	126 GeV	4.15 MeV <sup>a</sup>	$1.59 \cdot 10^{-22}$ s	$3.31 \cdot 10^{-5}$
top	173 GeV	2.0 GeV	$3.3 \cdot 10^{-25}$ s	0.012

Table 9.1.: Properties of unstable particle [9]

<sup>a</sup>This is the Standard Model prediction for the Higgs width [7]. Experiments have constrained the Higgs width to be  $\Gamma_H < 17$  MeV at the 95% confidence level [8].



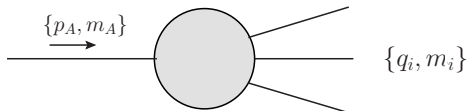


Figure 9.1.: A decay process

of the self-energy as a sum over all cuttings. To see this, we use equation (5.18) for the special case where the invariant amplitude  $\mathcal{M}$  is a self-energy, i.e.

$$\Sigma_I(p_A^2) = \frac{(2\pi)^4}{2} \sum_n \prod_{i=1}^n \left( \int d^3 q_i \frac{Z_i}{(2\pi)^3 2\omega_{\vec{q}_i}} \right) |\mathcal{M}(p_A \rightarrow \{q_i\})|^2 \delta^4(p_A - \sum_i q_i). \quad (9.2)$$

We used the shorthand  $\Sigma_I(x) := \text{Im}(\Sigma(x))$ ; similarly, we shall use  $\Sigma_R(x) := \text{Re}(\Sigma(x))$ . In (9.2), it is understood that the momenta  $\{q_i\}$  in  $\mathcal{M}$  are to be taken on-shell, yet  $p_A$  can still be arbitrary. The diagrams contributing to  $\mathcal{M}(p_A \rightarrow \{q_i\})$  are diagrams describing the decay of A into other particles, i.e. diagrams such as the one in figure 9.1. The upshot of (9.2) is then that, starting from the value of  $s_A := -p_A^2$  where such a decay process becomes kinematically possible for the first time,  $\Sigma_I(-s_A)$  acquires an imaginary part. This value of  $s_A$  is called the *threshold*. Equation (9.1) shows that the threshold is equal to  $(\sum_i m_i)^2$ . The masses  $m_i$  are now understood to denote the produced masses of the decay process that requires the lowest energy, i.e. of the decay process with the smallest total outgoing mass. So we see that the on-shell self-energy  $\Sigma_I(-s_A = -m_A^2)$  becomes nonzero if and only if  $m_A > \sum_i m_i$ , that is, precisely if A is an unstable particle. In the next section we shall see that the fact that  $\Sigma_I(-m_A^2) \neq 0$  for an unstable particle indeed makes sure that the field excitation representing that particle decays with time. In fact, it shall turn out that  $\Sigma_I(-m_A^2)$  is closely related to the decay rate of the particle.

## 9.2. Masses and Decay Rates

Several definitions of the mass and decay rate of an unstable particle - with several notations - can be found in the literature [10–15]. Besides the bare mass and a general renormalized mass, there are the mass and decay rate as defined by the on-shell renormalization scheme (OSRS); the mass and decay rate as defined by the complex mass scheme (CMS); and the physical mass and decay rate. The notation adopted in this thesis is summarized in table 9.2. Something to point out here is that the decay rate is not a Lorentz invariant quantity and thus depends on the momentum  $\vec{k}$  of the unstable particle. To make this explicit we shall always write  $\Gamma(\vec{k})$  - or  $\Gamma_{\text{phys}}(\vec{k})$  or  $\bar{\Gamma}(\vec{k})$  - when referring to the decay rate. Whenever  $\vec{k}$ -dependence is omitted, we are referring to the decay rate *at rest*, which *is* Lorentz invariant and the common quantity in the

renormalized mass:	$m$		
physical mass:	$m_{\text{phys}}$	physical decay rate:	$\Gamma_{\text{phys}}$
OSRS mass:	$M$	OSRS decay rate:	$\Gamma$
real CMS mass:	$\bar{m}$	CMS decay rate:	$\bar{\Gamma}$
complex CMS mass:	$\hat{m}$		

Table 9.2.: masses and decay rates

literature.

### Physical mass and decay rate

Our definitions of the physical mass  $m_{\text{phys}}$  and decay rate  $\Gamma_{\text{phys}}$  were first proposed as physical by Willenbrock and Valencia [11]. They were proven to be the correct physical definitions by Bohm and Harshmann [10]. Here we motivate the definitions following and generalizing the approach of de Wit, Laenen and Smith [1, chapter 2].

We consider a scalar field  $\phi(x)$  for this analysis. The essential ingredient of the argument is the denominator structure of the full propagator. Since this structure is of the form (6.11) for *any* field the argument will hold for other types of fields as well. The full propagator for our scalar field is given by

$$\begin{aligned} \Delta^{\text{full}}(k) &= \frac{1}{i(2\pi)^4} \frac{1}{k^2 + m^2 - \Sigma(k^2, m^2) - i\epsilon} \\ &= \frac{1}{i(2\pi)^4} \frac{1}{-(k^0)^2 + |\vec{k}|^2 + m^2 - \Sigma_R(k^2, m^2) - i\Sigma_I(k^2, m^2) - i\epsilon}. \end{aligned} \quad (9.3)$$

The mass  $m$  can still be any renormalized mass; in fact, it may as well be the bare mass. The complete field excitation due to a point source  $J(y) = \delta^4(y)$  is then

$$\begin{aligned} \delta\phi(x) &= \int d^4y i\Delta^{\text{full}}(x-y)J(y) \\ &= i\Delta^{\text{full}}(x) \\ &= i \int d^3k e^{i\vec{k}\cdot\vec{x}} \int dk^0 e^{-ik^0t} \Delta^{\text{full}}(k^0, \vec{k}). \end{aligned} \quad (9.4)$$

A field excitation that we may associate with a free, physical particle, is one that survives in the limit  $t \rightarrow \infty$ . Therefore we focus on the  $k^0$ -integral for large  $t$ . Since we are considering a positive time we can close the integration in the complex  $k^0$ -plane as shown in figure 9.2.

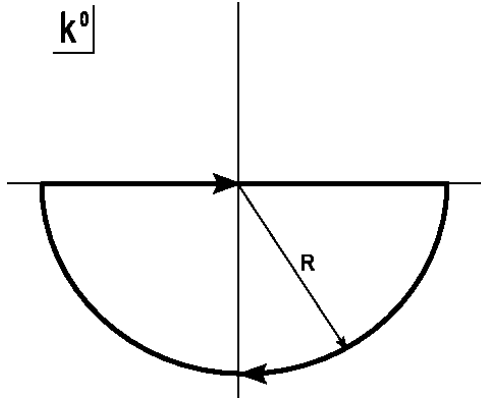


Figure 9.2.: The integration contour of (9.4) is equivalent to this contour in the limit  $R \rightarrow \infty$ , for the integrand vanishes as  $R^{-2}$  or faster on the arc.

According to Cauchy's theorem, the integral becomes

$$\int dk^0 e^{-ik^0t} \Delta^{\text{full}}(k^0, \vec{k}) = -2\pi i \sum_P e^{\text{Im}(k_P^0)t} e^{-i\text{Re}(k_P^0)t} \text{Res} \left[ \Delta^{\text{full}}(k_P^0, \vec{k}) \right], \quad (9.5)$$

where  $P$  labels all the poles  $k^0 = k_P^0$  enclosed by the contour. Since the contour encloses the lower half plane,  $\text{Im}(k_P^0)$  is negative. Therefore,  $e^{\text{Im}(k_P^0)t}$  shows a suppression with time of magnitude  $|\text{Im}(k_P^0)|$ . Since we are interested in the asymptotic behaviour for  $t \rightarrow \infty$ , the leading contribution will come from the pole in the lower half plane that is closest to the real axis. It can be seen from (9.3) that this pole, which we label by  $P = p$ , satisfies

$$k_p^2 = -m^2 + \Sigma(k_p^2, m^2) + i\epsilon \quad \Rightarrow \quad k_p^0 = \left[ |\vec{k}|^2 + m^2 - \Sigma_R(k_p^2, m^2) - i\Sigma_I(k_p^2, m^2) \right]^{1/2} + i\epsilon, \quad (9.6)$$

where  $k_p := (k_p^0, \vec{k})$ . One should realize that there is a solution for every  $\vec{k}$ , so  $k_p^0$  is really a function of  $\vec{k}$ . The field excitation for large time then reads

$$\delta\phi(x) \stackrel{t \rightarrow \infty}{\cong} 2\pi \int d^3k \text{Res} \left[ \Delta^{\text{full}}(k_p) \right] e^{\text{Im}(k_p^0)t} e^{-i\text{Re}(k_p^0)t} e^{i\vec{k}\cdot\vec{x}}. \quad (9.7)$$

Equation (9.7) shows that the field excitation representing a physical particle is a superposition of plane waves with decaying amplitude. The more negative  $\text{Im}(k_p^0)$ , the faster the suppression. Therefore, this quantity should be proportional to the decay rate. Indeed, the physical decay rate is defined by

$$\Gamma_{\text{phys}}(\vec{k}) := -2 \text{Im}(k_p^0). \quad (9.8)$$

Equation (9.6) shows it is due to the imaginary part of the self-energy that  $k_p^0$  acquires an imaginary part and thus that  $\Gamma_{\text{phys}}(\vec{k})$  becomes nonzero. This confirms once again that unstable particles have to have a self-energy with a nonzero imaginary part. We can now identify the physical mass of the particle as well. We see that the plane waves  $e^{i(-\text{Re}(k_p^0)t + \vec{k}\cdot\vec{x})}$  in (9.7) are characterized by the momentum four-vector  $(\text{Re}(k_p^0), \vec{k})$ . Therefore, one might be tempted to define the physical mass as

$$-\tilde{m}_{\text{phys}}^2 = -[\text{Re}(k_p^0)]^2 + |\vec{k}|^2, \quad (9.9)$$

according to the usual dispersion relation of a free particle. However, one should realize that the true momentum four-vector  $k_p$  is now complex and consequently that the dispersion relation is in this case *not* given by (9.9). This is why we put a tilde on  $\tilde{m}_{\text{phys}}$ : to distinguish it from the *true* physical mass  $m_{\text{phys}}$ . The reason that (9.9) cannot be the dispersion relation is that this  $\tilde{m}_{\text{phys}}$  would depend on  $\vec{k}$ , which cannot be the case for a physical rest mass. The fact that  $\tilde{m}_{\text{phys}}$  would depend on  $\vec{k}$  can be understood by considering  $k_p^2$ , which is determined by the first equality in (9.6) and therefore independent of  $\vec{k}$ .

$$\begin{aligned} k_p^2 &= -(k_p^0)^2 + |\vec{k}|^2 = -[\text{Re}(k_p^0)]^2 + |\vec{k}|^2 + [\text{Im}(k_p^0)]^2 - 2i \text{Re}(k_p^0) \text{Im}(k_p^0) \\ &= -\tilde{m}_{\text{phys}}^2 + \frac{1}{4}\Gamma_{\text{phys}}^2(\vec{k}) + i\sqrt{\tilde{m}_{\text{phys}}^2 + |\vec{k}|^2}\Gamma_{\text{phys}}(\vec{k}). \end{aligned} \quad (9.10)$$

Now, if  $\tilde{m}_{\text{phys}}$  were to be independent of  $\vec{k}$ , then  $\Gamma_{\text{phys}}(\vec{k})$  would have to be independent of  $\vec{k}$  in order to make  $\text{Re}(k_p^2)$  independent of  $\vec{k}$ . But this would render  $\text{Im}(k_p^2) = \sqrt{\tilde{m}_{\text{phys}}^2 + |\vec{k}|^2}\Gamma_{\text{phys}}(\vec{k})$   $\vec{k}$ -dependent, which contradicts the fact that  $k_p^2$  is  $\vec{k}$ -independent. Therefore,  $\tilde{m}_{\text{phys}}$  does indeed depend on  $\vec{k}$  and cannot be the physical mass. To proceed, we have to determine the physical mass in a different way. We shall exploit something else that we know about the dispersion

relation: we *do* know that when the particle is at rest, the energy of the plane wave is given by the mass of the particle, i.e.

$$m_{\text{phys}} = \text{Re}(k_p^0) \Big|_{\vec{k}=\vec{0}}. \quad (9.11)$$

This *is* a proper definition of the physical mass.

Incidentally, we can now also find the *true* dispersion relation. By using the fact that  $k_p^2$  is independent of  $\vec{k}$ , we can write

$$\begin{aligned} k_p^2 = k_p^2 \Big|_{\vec{k}=\vec{0}} &= -(k_p^0)^2 \Big|_{\vec{k}=\vec{0}} = -[\text{Re}(k_p^0) + i\text{Im}(k_p^0)]^2 \Big|_{\vec{k}=\vec{0}} \\ &= -\left[m_{\text{phys}} - i\frac{1}{2}\Gamma_{\text{phys}}\right]^2 \\ &= -m_{\text{phys}}^2 + \frac{1}{4}\Gamma_{\text{phys}}^2 + i m_{\text{phys}} \Gamma_{\text{phys}} \\ &= -(k_p^0)^2 + |\vec{k}|^2 \\ &= -[\text{Re}(k_p^0)]^2 + \frac{1}{4}\Gamma_{\text{phys}}^2(\vec{k}) + |\vec{k}|^2 + i\text{Re}(k_p^0)\Gamma_{\text{phys}}(\vec{k}). \end{aligned} \quad (9.12)$$

We emphasize again that  $\Gamma_{\text{phys}}$  is the decay rate as seen in the rest frame, whereas  $\Gamma_{\text{phys}}(\vec{k})$  is the decay rate of a particle with momentum  $\vec{k}$ . The real and imaginary parts of the third and fifth line have to be equal, giving us two equations to relate the quantities  $m_{\text{phys}}, \Gamma_{\text{phys}}, \text{Re}(k_p^0)$  and  $\Gamma_{\text{phys}}(\vec{k})$ . These can be solved to give

$$\left\{ \begin{array}{l} [\text{Re}(k_p^0)]^2 = \left[ 1 + \frac{|\vec{k}|^2}{m_{\text{phys}}^2 + \frac{1}{4}\Gamma_{\text{phys}}^2} \right] m_{\text{phys}}^2 \\ \Gamma_{\text{phys}} = \left[ 1 + \frac{|\vec{k}|^2}{m_{\text{phys}}^2 + \frac{1}{4}\Gamma_{\text{phys}}^2} \right]^{1/2} \Gamma_{\text{phys}}(\vec{k}). \end{array} \right. \quad (9.13)$$

The first relation is the exact dispersion relation for the unstable particle; the second relates the decay rate to the decay rate in the rest frame.

In summary, we can say that the physical mass and decay rate (in the rest frame) are defined by the pole of the propagator as

$$k_p^2 = -\left[m_{\text{phys}} - i\frac{1}{2}\Gamma_{\text{phys}}\right]^2 = -m^2 + \Sigma(k_p^2, m^2). \quad (9.14)$$

### The OSRS mass and decay rate

The mass of the Z-boson was very accurately determined by the LEP in the late eighties and early nineties [16]. The definition of its mass adopted in the determination was the OSRS mass. The definition of the OSRS mass  $M$  is basically obtained by sending  $\Sigma_I(k_p^2, m^2) \rightarrow 0$  in equation (9.14). That is,  $M$  is defined by

$$-M^2 = -m^2 + \Sigma_R(-M^2, m^2). \quad (9.15)$$

This mass is the renormalized mass in the OSRS. Indeed, if one requires the renormalized mass to be  $m = M$ , then (9.15) states one needs  $\Sigma_R(-M^2, M^2) = 0$ , which is precisely the renormalization condition (6.14) of the OSRS. This mass is gauge dependent at order  $\mathcal{O}(\alpha^2)$

[12, 13]. Although a gauge dependent definition seems unnatural - and certainly not physical - in principle there is nothing wrong with using a gauge dependent definition of the mass, as long as one specifies the gauge in which the mass is calculated [15]. Some gauge choices can be considered better than others, depending on how important the gauge dependent loop effects are [12].

If  $k^2$  is close to  $-M^2$ , then we can expand the denominator of the propagator (9.3) as

$$\begin{aligned}\Delta^{\text{full}}(k) &= \frac{1}{i(2\pi)^4} [k^2 + m^2 - \Sigma_R(k^2, m^2) - i\Sigma_I(k^2, m^2)]^{-1} \\ &\stackrel{(9.15)}{\simeq} \frac{1}{i(2\pi)^4} [k^2 + M^2 - (k^2 + M^2)\Sigma'_R(-M^2, m^2) - i\Sigma_I(-M^2, m^2)]^{-1} \\ &= \frac{1}{i(2\pi)^4} \frac{Z}{k^2 + M^2 - iZ\Sigma_I(-M^2, m^2)}, \quad \text{where: } Z = \frac{1}{1 - \Sigma'_R(-M^2, m^2)}.\end{aligned}\quad (9.16)$$

The OSRS decay rate  $\Gamma$  is defined as

$$M\Gamma = Z\Sigma_I(-M^2, m^2) = \frac{\Sigma_I(-M^2, m^2)}{1 - \Sigma'_R(-M^2, m^2)}.\quad (9.17)$$

So,  $M$  and  $\Gamma$  are defined by the complex pole  $\tilde{k}_p^2$  of the approximate full propagator near  $k^2 = -M^2$  (9.16), as

$$\tilde{k}_p^2 = -M^2 + iM\Gamma.\quad (9.18)$$

### The CMS mass and decay rate

As we shall see in chapter 11, the complex mass scheme allows for a complex mass  $\hat{m}$ . It is equal to the genuine complex pole  $k_p^2$  as defined in (9.6). It also defines a *real* mass  $\bar{m}$  and decay rate  $\bar{\Gamma}$  by

$$-\hat{m}^2 = -\bar{m}^2 + i\bar{m}\bar{\Gamma} = k_p^2 \stackrel{(9.6)}{=} -m^2 + \Sigma(k_p^2, m^2).\quad (9.19)$$

Since the pole  $k_p^2$  is a fundamental property of the S-matrix, it is a gauge invariant quantity, guaranteeing that  $\bar{m}$  and  $\bar{\Gamma}$  are also gauge invariant.

### Comparison of the different definitions

The different real masses and decay rates actually only differ at two-loop order  $\mathcal{O}(\alpha^2)$ , making the difference between the definitions very small. If we consider the Z-boson for example, the different masses compare as [10, 11, 14]

$$M^Z > m_{\text{phys}}^Z = M^Z - 26\text{MeV} > \bar{m}^Z = M^Z - 34\text{MeV},\quad (9.20)$$

which are indeed very close if one takes into account that  $M^Z = 91\text{GeV}$ . However, comparing it with the experimental accuracy achieved for the Z-boson mass, this difference is significant [9]. As stated before,  $M^Z$  is gauge dependent, so we must specify the gauge in which  $M^Z$  was calculated to obtain the result (9.20). The gauge adopted is the Feynman-'t Hooft gauge. Since the difference of 26MeV is relatively small, this can be considered a 'good' gauge choice [15].

We shall now show that the different masses and decay rates are indeed the same up to order  $\alpha$ . First we will show that the difference between the physical definitions and the CMS definitions

is  $\mathcal{O}(\alpha^2)$ ; then we shall show this for the difference between the CMS and OSRS definitions. This then implies that all three definitions coincide to one-loop order. We shall use the scalings

$$\frac{\Sigma_R}{M} \sim \frac{\Sigma_I}{M} \sim \frac{\Gamma_{\text{phys}}}{M} \sim \frac{\Gamma}{M} \sim \frac{\bar{\Gamma}}{M} \sim \alpha. \quad (9.21)$$

These follow from the fact that the lowest-order diagrams in  $\Sigma$  contain one loop and any decay rate (in the rest frame) is proportional to  $\Sigma_I$ . Note that we included the mass  $M$  for dimensional reasons ( $\alpha$  is dimensionless). We could also have used the mass  $m_{\text{phys}}$  or  $\bar{m}$  in any of the lines, since the masses are of the same magnitude. Furthermore, we did not write the self-energy with any arguments for we did not have to. In the remainder of this chapter it is understood that the second argument of  $\Sigma$  is always  $m^2$ ; therefore we will drop it.

The physical definitions and CMS definitions are easily compared by equating the real and imaginary parts of equations (9.14) and (9.19).

$$\begin{cases} -m_{\text{phys}}^2 + \frac{1}{4}\Gamma_{\text{phys}}^2 = -\bar{m}^2 \\ m_{\text{phys}}\Gamma_{\text{phys}} = \bar{m}\bar{\Gamma} \end{cases} \Rightarrow \begin{cases} \bar{m} = \sqrt{m_{\text{phys}}^2 - \frac{1}{4}\Gamma_{\text{phys}}^2} & = m_{\text{phys}}(1 + \mathcal{O}(\alpha^2)) \\ \bar{\Gamma} = \Gamma_{\text{phys}} \left(1 - \frac{1}{8} \frac{\Gamma_{\text{phys}}}{m_{\text{phys}}} + \dots\right) & = \Gamma_{\text{phys}} (1 + \mathcal{O}(\alpha^2)). \end{cases} \quad (9.22)$$

So indeed, these definitions coincide up to order  $\alpha$ . Incidentally, the first equality here also shows that  $m_{\text{phys}}$  and  $\Gamma_{\text{phys}}$  are gauge invariant because  $\bar{m}$  and  $\bar{\Gamma}$  are. This is of course required for physical quantities.

Now we compare the CMS definitions with the OSRS definitions, following [17, Appendix D]. We start from (9.19).

$$\begin{aligned} -\bar{m}^2 + i\bar{m}\bar{\Gamma} &= -m^2 + \Sigma_R(-\bar{m}^2 + i\bar{m}\bar{\Gamma}) + i\Sigma_I(-\bar{m}^2 + i\bar{m}\bar{\Gamma}) \\ &= -m^2 + \Sigma_R(-\bar{m}^2) + i\Sigma_I(\bar{m}^2) + \mathcal{O}(\alpha^2). \end{aligned} \quad (9.23)$$

By taking the real and imaginary parts of (9.23) we find

$$\begin{cases} -\bar{m}^2 = -m^2 + \Sigma_R(-\bar{m}^2) + \mathcal{O}(\alpha^2) \\ \bar{m}\bar{\Gamma} = \Sigma_I(-\bar{m}^2) + \mathcal{O}(\alpha^2). \end{cases} \quad (9.24)$$

We can eliminate  $-m^2$  in the first line by using (9.15).

$$\begin{aligned} -\bar{m}^2 &= -M^2 - \Sigma_R(-M^2) + \Sigma_R(-\bar{m}^2) + \mathcal{O}(\alpha^2) = -M^2 + \mathcal{O}(\alpha) \\ &= -M^2 - \Sigma_R(-M^2) + \Sigma_R(-M^2 + \mathcal{O}(\alpha)) + \mathcal{O}(\alpha^2) = -M^2 + \mathcal{O}(\alpha^2). \end{aligned} \quad (9.25)$$

This confirms that

$$\bar{m} = \sqrt{M^2 + \mathcal{O}(\alpha^2)} = M + \mathcal{O}(\alpha^2). \quad (9.26)$$

This only leaves to show that  $\bar{\Gamma}$  and  $\Gamma$  coincide to order  $\mathcal{O}(\alpha)$ . Equation (9.17) reveals that

$$M\Gamma = \Sigma_I(-M^2) + \mathcal{O}(\alpha^2). \quad (9.27)$$

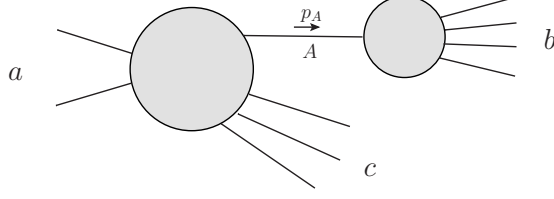


Figure 9.3.: This process becomes enhanced when the internal propagator with momentum  $p_A$  comes close to being on its mass shell.

Using this in the second line of (9.24), we find

$$\begin{aligned}
 \bar{m}\bar{\Gamma} &= M\Gamma + \Sigma_I(-\bar{m}^2) && - \Sigma_I(-M^2) + \mathcal{O}(\alpha^2) \\
 &= M\Gamma + \Sigma_I(-M^2 + \mathcal{O}(\alpha^2)) - \Sigma_I(-M^2) + \mathcal{O}(\alpha^2) && (9.28) \\
 &= M\Gamma && + \mathcal{O}(\alpha^2),
 \end{aligned}$$

which does indeed imply that

$$\bar{\Gamma} = \Gamma \frac{M}{\bar{m}} = \Gamma \frac{M}{M + \mathcal{O}(\alpha^2)} = \Gamma + \mathcal{O}(\alpha^2). \quad (9.29)$$

### 9.3. Resonances

Suppose we are doing a scattering experiment where two particles  $a_1$  and  $a_2$  (summarized by  $a$ ) scatter into two collections of particles called  $b$  (comprising  $n_b$  particles) and  $c$  (comprising  $n_c$  particles). We consider a diagram in which the  $b$ -collection emerges from a single internal propagator corresponding to a virtual particle A. This is shown in figure 9.3. The internal propagator has momentum  $p_A$ , renormalized mass  $m$  and OSRS mass  $M$ . Due to momentum conservation,  $p_A$  will be equal to the outgoing momenta of the  $b$ -particles:  $p_A = \sum p_b$ . If we would (naively, as we will see) calculate the invariant amplitude  $\mathcal{M}(a \rightarrow b + c)$  for this process up to a certain order in perturbation theory and put the external momenta on-shell, as we usually do, then the results cannot be trusted when the internal propagator comes close to being on-shell. That is, if  $-p_A^2 = -(\sum p_b)^2 := s_A$  comes close to  $m^2$ . The phase-subspace where  $-(\sum p_b)^2 = s_A = -m^2$  precisely holds is called the *resonance* of the process. The reason that the results cannot be trusted in the region of phase-space close to the resonance, is that in this region the contribution of the internal propagator,  $(p_A^2 + m^2)^{-1}$ , becomes large. If we go to higher orders of perturbation theory, there will be diagrams contributing that contain corrections to the internal propagator such as the corrections shown in figure 9.4. These diagrams contain *multiple* factors of  $(p_A^2 + m^2)^{-1}$ . If these factors becomes big, then truncating the expansion in the coupling constants gives unreliable results, for higher order terms then contribute significantly and should therefore not be neglected. In effect, perturbation theory breaks down in the resonance region. Perturbation theory is still ok for values of  $s_A$  for which

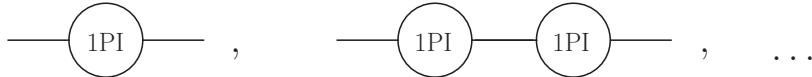


Figure 9.4.: Propagator corrections. The ‘1PI’-blob denotes one-particle irreducible diagrams.

$$\left| \frac{\Sigma(-s_A)}{s_A - m^2} \right| \ll 1, \quad (9.30)$$

but when this ratio becomes of order 1 for example, then perturbation theory can definitely not be trusted. Every diagram with a single internal propagator falls into one of the following regimes<sup>1</sup>:

1.  $\mathbf{m_A} \leq \sum_b \mathbf{m_b}$ .

This regime always applies if  $A$  is stable; indeed, if  $A$  were unstable it could decay into  $b$ . This is also the regime if  $A$  is an unstable particle with threshold  $\sum_i m_i$  smaller than  $\sum_b m_b$ , such that  $A$  can decay in the particles with masses  $m_i$  but not into  $b$ . This situation thus occurs if  $\sum_i m_i < m_A \leq \sum_b m_b$ . We can now distinguish two possibilities:

a)  $(\sum_b \mathbf{m_b})^2 - \mathbf{m_A}^2 \gg |\Sigma(-s_A)|$ .

In this case, in the rest frame of  $A$

$$s_A = (p_A^0)^2 = (\sum_b q_b^0)^2 = \left( \sum_b \sqrt{m_b^2 + |\vec{q}_b|^2} \right)^2 \geq (\sum_b m_b)^2, \quad (9.31)$$

such that

$$s_A - m_A^2 \gg |\Sigma(-s_A)| \quad \Rightarrow \quad \left| \frac{\Sigma(-s_A)}{s_A - m_A^2} \right| \ll 1. \quad (9.32)$$

This means that perturbation theory is still fine; the resonance region is not contained in the phase space.

b)  $(\sum_b \mathbf{m_b})^2 - \mathbf{m_A}^2 \lesssim |\Sigma(-s_A)|$ .

Since it is kinematically possible that  $s_A \sim (\sum_b m_b)^2$ , we can have in this case that

$$s_A - m_A^2 \lesssim |\Sigma(-s_A)| \quad \Rightarrow \quad \left| \frac{\Sigma(-s_A)}{s_A - m_A^2} \right| \gtrsim 1. \quad (9.33)$$

In this case perturbation theory does break down, because the phase space does probe the resonance region.

We emphasize that this regime can include stable particles. This can for example occur when the  $b$ -particles are the particles with smallest total mass that  $A$  can couple to, i.e.  $\sum_b m_b = \sum_i m_i$ . Then  $(\sum_b m_b)^2$  is the threshold, and  $m_A \leq \sum_b m_b$  ensures that no decay process is kinematically possible and therefore that  $A$  is stable.

2.  $\mathbf{m_A} > \sum_b \mathbf{m_b}$ .

This automatically implies that  $A$  is unstable, for the on-shell decay process  $A \rightarrow b$  is kinematically possible. Since  $s_A - (\sum_b m_b)^2 = \left( \sum_b \sqrt{m_b^2 + |\vec{q}_b|^2} \right)^2 - (\sum_b m_b)^2$  can be tuned to be *any* positive number by picking the external momenta  $\vec{q}_b$  appropriately,

$$s_A - m_A^2 = \left( s_A - (\sum_b m_b)^2 \right) - \left( m_A - (\sum_b m_b)^2 \right)$$

can be tuned to be 0. This means that the phase space contains the resonance, where perturbation theory breaks down.

---

<sup>1</sup>In the scattering experiment described in the foregoing, we suggested that the  $b$ -particles were all outgoing particles. Resonances can in fact also occur when some of the  $b$ -particles are incoming. In the distinction of the regimes we stick to the case that all  $b$ -particles are outgoing, which is the situation that we will mainly be dealing with in this thesis.



## 9.4. The naive approach

A way to circumvent the problem of the failure of perturbation theory is to resum the internal propagator. The procedure is as follows. Let us suppose in this discussion that the diagram shown in figure 9.3 is a tree-level diagram, and suppose we want to include quantum corrections to order, say,  $\alpha^2$ . The usual procedure is as follows. One both replaces the two grey blobs - which can be thought of as effective vertices - by the corresponding effective vertices calculated to order  $\alpha^2$ , *and* one replaces the internal bare propagator by the two-point function calculated to order  $\alpha^2$ . This two-point function consists of the bare propagator plus corrections, which are of the form of the first two diagrams shown in figure 9.4. All these three quantities - the two effective vertices and the two-point function - are second-order polynomials in  $\alpha$ . These are then multiplied out, and the resulting  $\mathcal{O}(\alpha^3)$ -terms are discarded. As we have just discussed, this procedure is not valid anymore in the resonance region, because the higher order terms cannot be neglected.

Therefore, we do not only include the order  $\alpha$  and  $\alpha^2$  corrections to the two-point function. Instead, we calculate  $\Sigma^{(2)}(p_A^2)$ , the self-energy up to order  $\alpha^2$ . We then include the *entire series* of corrections suggested in figure 9.4, where the ‘1PI-blobs’ now denote  $\Sigma^{(2)}(p_A^2)$ . This is referred to as *resumming the propagator*. By doing so we include the same corrections of order  $\alpha$  and order  $\alpha^2$  as before, *plus* a subset of all the  $\mathcal{O}(\alpha^3)$  corrections to the two-point function. We will show below that including all these corrections yields the two-point function shown in equation (9.3) (where the self-energy  $\Sigma$  is now really  $\Sigma^{(2)}$ ). As shown by (9.3), the  $\alpha$ -dependence of the two-point function has now shifted to the denominator (it is contained in  $\Sigma(p_A^2)$ ), so the two-point function is not a polynomial in  $\alpha$  anymore. The virtue of this resummation is that when we would repeat this at *higher* order in perturbation theory, e.g. to order  $\alpha^3$ , then the only modification to the two-point function is the replacement  $\Sigma^{(2)}(p_A^2) \rightarrow \Sigma^{(3)}(p_A^2)$ . This *is* a small correction, and we do *not* obtain an extra factor  $(p_A^2 + m^2)^{-1}$ . As such, using a resummed internal propagator repairs perturbation theory. The reason is that all the corrections that were problematic before - the corrections containing *any* number of bare propagators - are now already included at tree-level in the resummed propagator. When calculating the entire diagram, we do again multiply the effective vertices with the two-point function. This time however, the two-point function is not a polynomial in  $\alpha$  anymore and is kept like that; it is only the effective vertices, which are still second-order polynomials in  $\alpha$ , that are multiplied out. Only their  $\mathcal{O}(\alpha^3)$ -terms are discarded. The higher order corrections to the two-point function *remain*, contained in the denominator.

At first thought the inclusion of these extra  $\mathcal{O}(\alpha^3)$  seems fine: if we are doing perturbation theory to order  $\alpha^2$ , then we are free to add terms of higher order in  $\alpha$ , since we only guarantee a result that is accurate to order  $\alpha^2$ . However, it turns out to be not as simple, for in many cases the higher order terms that we are adding turn out to introduce a gauge dependence. This problem - which is the subject of chapter 10 - is the reason that we call this approach the *naive* approach.

We now discuss how to include the entire series of corrections shown in figure 9.4. There are actually two ways to do it.

1. By performing a Dyson sum and explicitly summing all the diagrams. For a scalar field this yields

$$\Delta(p) = \frac{1}{i(2\pi)^4} \frac{1}{p_A^2 + m^2} \sum_{n=0}^{\infty} \left[ \frac{\Sigma(p_A^2)}{p_A^2 + m^2} \right]^n = \frac{1}{i(2\pi)^4} \frac{1}{p_A^2 + m^2 - \Sigma(p_A^2)}. \quad (9.34)$$

The Dyson sum yields expressions with similar denominators for other types of fields. Actually, in the last step we used the expression for the sum of a geometric series, which is only valid when  $\left| \frac{\Sigma(p_A^2)}{p_A^2 + m^2} \right| < 1$ . Consequently, near the resonance this identity can formally not be used. Instead one can

2. invert the quadratic part of the effective action in Fourier space (see e.g. [2, chapter 11]) and multiply by  $i$  (or  $\frac{1}{2}i$  for real fields) to obtain  $\Delta(p_A)$ . For our scalar field this means

$$\Delta(p_A) = i \left[ -(2\pi)^4 (p_A^2 + m^2 - \Sigma(p_A^2)) \right]^{-1} = \frac{1}{i(2\pi)^4} \frac{1}{p_A^2 + m^2 - \Sigma(p_A^2)}. \quad (9.35)$$

The second method is valid in the entire phase space. Since it agrees with the Dyson sum outside the resonance region and since the algebraic result (9.35) is the same anywhere in phase space, we may as well use the Dyson sum *inside* the resonance region as well.

In principle, we need to perform the resummation only in the resonance region, i.e. if

$$\left| \frac{s_a - m^2}{m^2} \right| \sim \left| \frac{s_A - M^2}{M^2} \right| \lesssim \left| \frac{\Sigma(-s_A)}{M^2} \right| \sim \alpha, \quad (9.36)$$

where we used that  $m^2 = M^2(1 + \mathcal{O}(\alpha^2))$ . However, it is not practical to have a propagator looking different in different regions of phase space. Therefore, the resummed propagator is used everywhere in the phase space. Also, the full momentum dependence of  $\Sigma(p_A^2)$  is not usually kept. To approximate it, one of the two following schemes is typically used for bosons.

- **Fixed width scheme**

Here the resummed propagator (9.34) is replaced by the propagator given in (9.16), i.e. by

$$\Delta(p_A) = \frac{1}{i(2\pi)^4} \frac{Z}{p_A^2 + M^2 - iM\Gamma}. \quad (9.37)$$

Equation (9.16) was obtained by an expansion around  $s_A^2 = M^2$ . Therefore, this expression is accurate inside the resonance region. Indeed, the neglected terms are of order  $\left( \frac{s_A - M^2}{M^2} \right)^2$ . According to (9.36), inside the resonance region this quantity is  $\mathcal{O}(\alpha^2) \stackrel{(9.21)}{\sim} \mathcal{O}\left(\left(\frac{\Gamma}{M}\right)^2\right)$ , which is typically very small, as shown in table 9.1.

*Outside* the resonance region this can be a very crude approximation. For instance, for  $s_A < M^2$ , the imaginary part of the self-energy should not be there at all.

In the fixed width scheme, the squared invariant amplitude of the scattering process shown in figure 9.3 can be written as

$$|\mathcal{M}^{\text{tot}}(a \rightarrow b + c)|^2 = |\mathcal{M}^p(a \rightarrow A + c)|^2 \left| \frac{Z^2}{(s_A - M^2)^2 + M^2\Gamma^2} \right|^2 |\mathcal{M}^d(A \rightarrow b)|^2. \quad (9.38)$$

Here  $\mathcal{M}^p(a \rightarrow A + c)$  is the invariant amplitude corresponding to the first grey blob of figure 9.3; that is, the amplitude for producing an on-shell particle with momentum  $\vec{p}_A$  and mass  $\sqrt{s_A}$ . Similarly,  $\mathcal{M}^d(A \rightarrow b)$  corresponds to the second grey blob; it is the invariant amplitude for the decay process of the same particle.

The form of the squared propagator in (9.38) is a so-called *Breit-Wigner shape*. It describes a resonance around  $s_A = M^2$  with a width of  $M\Gamma$ . Therefore  $\Gamma$  is also called the *decay width*.

If the diagram under consideration falls into regime 1b) of paragraph 9.3, it can be the case that the internal propagator that needs to be resummed corresponds to a stable particle. In this case  $\Gamma = 0$  and the invariant amplitude (9.38) has a singularity at  $s_A = M$ . In chapter 10 - where we will encounter an example of this type - this issue will be discussed further.

- **Running width scheme**

An approximation that is much better outside the resonance region can be made if the main contribution to the self-energy comes from loops of fermions that can be considered massless. We shall show in section 10.2 that the imaginary part of the self-energy is then proportional to  $s_A$  for  $s > 0$ ; for  $s < 0$  it vanishes. The proportionality constant is found from (9.17), resulting in

$$Z\Sigma_I(s_A) = \frac{\Gamma}{M}s \cdot \theta(s). \quad (9.39)$$

If we now adopt the OSRS, then according to (6.18) the resummed propagator is given by

$$\Delta(s_A) = \frac{1}{i(2\pi)^4} \frac{1}{-s_A + M^2 - i\frac{\Gamma}{M}s_A \cdot \theta(s_A)}. \quad (9.40)$$

## 9.5. The narrow-width approximation (NWA)

If the decay width is very small ( $\Gamma/M \ll$  required precision), such that we can take the limit  $\frac{\Gamma}{M} \downarrow 0$ , then the naive approach will actually not lead to any problems. We show in this section that in this limit we do obtain a gauge invariant cross section for the process shown in figure 9.3.

The relation between the invariant amplitude and the (differential) cross section for the total scattering process  $d\sigma^{\text{tot}}$  is

$$d\sigma^{\text{tot}}(p_a \rightarrow p_b + p_c) = \frac{1}{2\lambda^{1/2}(s_A, m_1^2, m_2^2)} (2\pi)^4 \delta^4(\sum p_a - \sum p_b - \sum p_c) |\mathcal{M}^{\text{tot}}(p_a \rightarrow p_b + p_c)|^2 \prod_b \frac{d^3 p_b Z(\vec{p}_b)}{(2\pi)^3 2\omega(\vec{p}_b)} \prod_c \frac{d^3 p_c Z(\vec{p}_c)}{(2\pi)^3 2\omega(\vec{p}_c)}. \quad (9.41)$$

The function  $\lambda$  is defined as  $\lambda(x, y, z) := x^2 + y^2 + z^2 - 2xy - 2xz - 2yz$ . Furthermore,  $m_1$  and  $m_2$  are the masses of the incoming particles  $a_1$  and  $a_2$ . The differential cross section (9.41) is a function of the incoming and outgoing four-momenta. However, we are interested in the dependence on the four-momentum of the internal virtual particle A, which is  $p_A = \sum p_b$ . We can formally introduce this dependence by defining a differential cross section  $d\tilde{\sigma}^{\text{tot}}$  as follows

$$d\tilde{\sigma}^{\text{tot}}(p_a \rightarrow p_b + p_c; p_A) := d\sigma^{\text{tot}}(p_a \rightarrow p_b + p_c) \delta^4(p_A - \sum p_b) d^4 p_A. \quad (9.42)$$

We can now obtain the cross section for the incoming particles to scatter in such a way that the internal propagator will carry a momentum  $\vec{p}_A$  and an energy determined by  $s_A = -p_A^2$ . This

is done by integrating out all outgoing momenta  $p_b$  and  $p_c$ . Explicitly

$$\begin{aligned}
\frac{d^4 \tilde{\sigma}^{\text{tot}}(p_a; p_A)}{d^3 p_A ds_A} &= \left\{ \int d^{3n_b} p_b \int d^{3n_c} p_c \frac{d\sigma^{\text{tot}}(p_a \rightarrow p_b + p_c)}{d^{3n_b} p_b d^{3n_c} p_c} \delta^4(p_A - \sum p_b) \right\} \frac{d^4 p_A}{d^3 p_A ds_A} \\
&= \left\{ \frac{1}{2\lambda^{1/2}(s_A, m_1^2, m_2^2)} \prod_b \int \frac{d^3 p_b Z(\vec{p}_b)}{(2\pi)^3 2\omega(\vec{p}_b)} \prod_c \int \frac{d^3 p_c Z(\vec{p}_c)}{(2\pi)^3 2\omega(\vec{p}_c)} \right. \\
&\quad \left. |\mathcal{M}^{\text{tot}}(a \rightarrow b + c)|^2 (2\pi)^4 \delta^4(p_a - \sum p_b - \sum p_c) \delta^4(p_a - \sum p_b) \right\} \frac{1}{2(\vec{p}_A^2 + s_A)^{1/2}} \\
&= \left\{ \left[ \frac{1}{2\lambda^{1/2}(s_a, m_a^2, m_b^2)} \frac{Z}{(2\pi)^3 2\omega(\vec{p}_A)} \prod_c \int \frac{d^{3n_c} p_c Z(\vec{p}_c)}{(2\pi)^3 2\omega(\vec{p}_c)} \right. \right. \\
&\quad \left. \left. (2\pi)^4 \delta^4(p_a - p_A - \sum p_c) |\mathcal{M}^p(a \rightarrow A + c)|^2 \right] \right. \\
&\quad \left. \left[ \frac{Z(2\pi)^4}{2\omega(\vec{p}_A)} \prod_b \int \frac{d^{3n_b} p_b Z(\vec{p}_b)}{(2\pi)^3 2\omega(\vec{p}_b)} \delta^4(p_a - \sum p_b) |\mathcal{M}^d(A \rightarrow b)|^2 \right] \right. \\
&\quad \left. \left[ \frac{\omega(\vec{p}_A)}{(s_a - M)^2 + M^2 \Gamma^2} \right] \right\} \frac{4\omega(\vec{p}_A)}{2(\vec{p}_A^2 + s_A)^{1/2}} \\
&= \frac{d^3 \sigma^p(p_a; p_A)}{d^3 p_A} \frac{\Gamma(A \rightarrow b)}{\Gamma(\vec{p}_A)} \left( \frac{1}{\pi} \frac{M\Gamma}{(s_a - M)^2 + M^2 \Gamma^2} \right) \sqrt{\frac{\vec{p}_A^2 + M^2}{\vec{p}_A^2 + s_A}}. \tag{9.43}
\end{aligned}$$

In the last line,  $\Gamma(A \rightarrow b)$  denotes a partial decay rate: the rate at which A decays into b. It is defined by restricting equation (9.2) to invariant amplitudes  $\mathcal{M}$  which only describe this specific decay process.  $\Gamma(\vec{p}_A)$  denotes the *total* decay rate of A.  $\Gamma$  is the total decay rate in the rest frame. Now we are ready to make the narrow-width approximation by taking the limit  $\frac{\Gamma}{M} \downarrow 0$ . By using the identity<sup>2</sup>

$$\frac{1}{\pi} \lim_{\epsilon \downarrow 0} \frac{\epsilon}{\eta^2 + \epsilon^2} = \delta(\eta) \tag{9.44}$$

and identifying  $\Gamma/M$  as  $\epsilon$ , the term between parentheses in the last line of (9.43) becomes

$$\left( \frac{1}{\pi} \frac{M\Gamma}{(s_A - M)^2 + M^2 \Gamma^2} \right) \xrightarrow{\frac{\Gamma}{M} \downarrow 0} \delta(s_A - M^2). \tag{9.45}$$

This delta function ensures that the internal virtual particle can only be on-shell. The NWA thus ignores the width of the resonance altogether. Instead, it approximates the Breit-Wigner shape by a delta function. We can use (9.45) to integrate out  $s_A$  in (9.43) to obtain the cross section

$$\frac{d^3 \tilde{\sigma}^{\text{tot}}(p_a; p_A)}{d^3 p_A} = \frac{d^3 \sigma^p(p_a; p_A)}{d^3 p_A} \frac{\Gamma(A \rightarrow b)}{\Gamma(\vec{p}_A)}. \tag{9.46}$$

In words: the cross section for the two particles to scatter into the particle collections  $b$  and  $c$  in such a way that the the internal propagator has momentum  $\vec{p}_A$ , is equal to the cross section

<sup>2</sup>Note that this identity only holds in the distributional sense. Strictly speaking it is only valid when considered under an integral over  $\eta$  from  $-\infty$  to  $\infty$ . Therefore, the NWA can only be expected to be a fair approximation for observables sufficiently integrated over (or independent of)  $s_A$ .

for them to scatter and produce  $c$  plus the unstable (on-shell) particle  $A$  with momentum  $\vec{p}_A$ , times the probability that this particle decays into the collection of particles  $b$ .

The important observation is that the three quantities on the right-hand side of (9.46) are gauge independent. Hence so is the cross section for the total scattering process. So, as we claimed before, the NWA does not suffer from the problem that cross sections may become gauge dependent. Since the NWA boils down to ignoring the width of the resonance (which is of the order  $\Gamma/M$ ), it can be used when the precision that is required of the theoretical prediction is small compared to  $\Gamma/M$ . However, to match the high precision of today's experiments we need a method that allows the calculation of observables involving resonances to better accuracy.

## 10. The gauge invariance problem

In chapter 9 it was discussed that ordinary perturbation theory breaks down in the resonance region of a diagram with a single internal propagator. To solve this issue, the internal propagator can be resummed. If we are working at order  $\alpha^n$ , then the resummations adds a subset of the  $\mathcal{O}(\alpha^{n+1})$ -terms to the diagram. In chapter 3 it was discussed that the fact that the Lagrangian is gauge invariant for any  $\alpha$  guarantees gauge independence of physical quantities order by order in  $\alpha$ ; if one uses the Feynman rules dictated by the Lagrangian. Subsequently, in chapter 4 it was explained that the gauge invariance of the Lagrangian also guarantees that invariant amplitudes satisfy the Ward identity; again, order by order in  $\alpha$ , under the same conditions. Since the resummation procedure adds a subset of the  $\mathcal{O}(\alpha^{n+1})$ -terms to the diagram, the resulting physical quantities are not guaranteed to be gauge independent anymore. The  $\mathcal{O}(\alpha^{n+1})$ -terms may violate the Ward identities. We should thus expect to find  $k_\mu \mathcal{M}^\mu = \mathcal{O}(\alpha^{n+1})$  instead of  $k_\mu \mathcal{M}^\mu = 0$ . In this thesis this is called *the gauge invariance problem*. At first thought it may not seem to be very problematic that the Ward identity is violated, for the violation is of higher order than  $\alpha^n$ . However, even a tiny gauge dependence can be made arbitrarily large by applying an extreme gauge transformation [14]. Therefore the gauge invariance problem is really a fundamental issue.

The aim of this chapter is to explore this problem. In order to do so, we explicitly perform the resummation and check the Ward identity for three example processes. In one of the examples, the internal propagator corresponds to a stable particle (the diagram falls into regime 1b of section 9.3, so resummation *is* necessary). We shall find that the Ward identity is still satisfied in this example. In the other two examples, the resummed propagator corresponds to an unstable particle. In both cases we shall find that the resummation violates the Ward Identity. Before turning to these example processes, we shall explain how the gauge invariance problem can *always* be avoided if the internal propagator corresponds to a stable particle.

### 10.1. Why resummation is fine for stable particles

In this section we show that the gauge invariance problem does not exist if the internal propagator corresponds to a stable particle, if one adopts the on-shell renormalization scheme (OSRS). As explained in section 6.4, the renormalized mass in this scheme equals the physical mass for stable particles:  $m = M$ . Also, the propagator residue is  $Z = 1$ . Furthermore, the self-energy of the stable particle is purely real, hence  $\Gamma = 0$ . As a result, in the OSRS the resummed propagator ((9.16) for a scalar field) will just be equal to the bare propagator. For a scalar field

$$\Delta^{\text{full}}(p) = \frac{1}{i(2\pi)^4} \frac{1}{p^2 + M^2} = \frac{1}{i(2\pi)^4} \frac{1}{p^2 + m^2} = \Delta^{\text{bare}}(p). \quad (10.1)$$

Therefore, resumming the internal propagator does actually not change anything! No extra terms are added to the diagrams, which consequently remain fully gauge invariant.

The reason that this argument fails for the resummation of unstable particles is that in this case  $\Gamma \neq 0$ . Therefore, the resummed propagator *will* be different from the bare propagator.

However, this solution *can* be extended to unstable particles by altering the renormalization scheme. This is done in chapter 11.

## 10.2. W-boson resonance

The first example process we consider is the process  $q\bar{q}' \rightarrow l\nu_l$ .  $q$  and  $\bar{q}'$  denote a pair of a quark with its conjugate anti-quark, e.g. a down and an anti-up quark. All fermions are taken to be massless for simplicity. Also, generation mixing is ignored. As shown in figure 10.1, the tree-level process proceeds via a virtual W-boson. Since the W-boson is heavier than the sum of any fermion pair, the diagram falls into category 2 of section 9.3. This means that the phase space of the process contains the resonance, hence the W-boson propagator needs to be resummed. To test whether the resulting diagram is gauge invariant, we shall actually consider the same process with one extra photon emitted, i.e. we shall consider  $q\bar{q}' \rightarrow l\nu_l\gamma$ . This allows for a test of the electromagnetic Ward identity. Baur and Zeppenfeld mention that this Ward identity is violated if one uses the running-width scheme for the resummation [18].

To test the Ward identity, we first calculate the (imaginary part of the) self-energy of the W-boson. The second step is to obtain the resummed propagator. As explained in section 9.4, we then have to choose what scheme to adopt: the fixed width scheme or the running width scheme. We shall first adopt the running width scheme to test the Ward identity. After that, we test it for a fixed width. Finally, we discuss the solution that Baur and Zeppenfeld propose for the gauge invariance problem of this process.

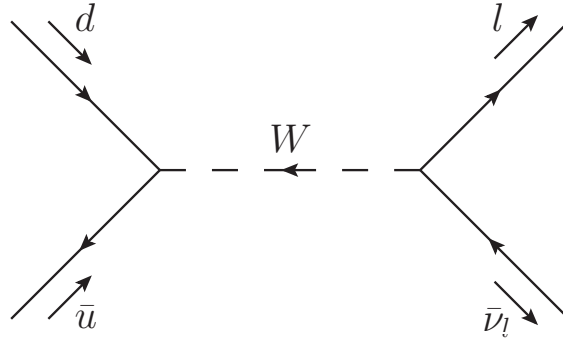


Figure 10.1.: W production. The  $d\bar{u}$  pair could be another fermion-pair as well.

### Calculation of the self-energy

We adopt the on-shell renormalization scheme for this calculation. In this scheme, the real part of the W-boson self-energy  $\Pi^{\mu\nu}(-M_W^2)$  vanishes, leaving only the imaginary part to be calculated. This can be done by using the cutting equations. The analogue of equation (9.2) for a vector boson reads

$$\Pi_{\mu\nu}^I(k) = \frac{1}{2} \sum_{\text{fermion pairs}} \int \frac{d^3q_1}{(2\pi)^3} \frac{1}{2\omega_{\vec{q}_1}} \int \frac{d^3q_2}{(2\pi)^3} \frac{1}{2\omega_{\vec{q}_2}} \mathcal{M}_\mu^*(k \rightarrow \{q_1, q_2\}) \mathcal{M}_\nu(k \rightarrow \{q_1, q_2\}) (2\pi)^4 \delta^4(k - (q_1 + q_2)), \quad (10.2)$$

where  $\Pi_{\mu\nu}^I(k^2) := \text{Im} [\Pi_{\mu\nu}(k^2)]$ . We collect some factors as  $c = \frac{g^2 N}{2^5 \pi^2}$ , where  $N$  denotes the

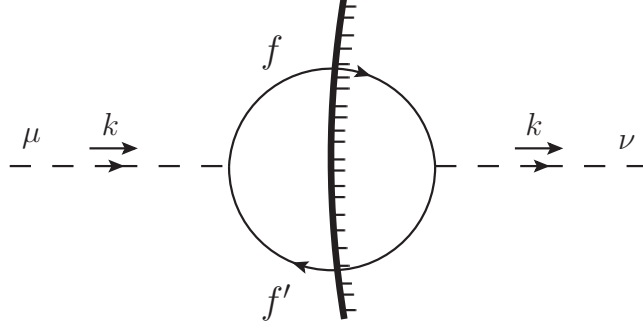


Figure 10.2.:  $\Pi_{\mu\nu}^I(k^2)$  can be obtained from this cut diagram.  $f$  and  $f'$  form a fermion pair, e.g. if  $f = u$  then  $f' = d$ . A summation over the possible internal fermion pairs is implied.

number of fermion pairs. In (10.2),  $\mathcal{M}_\mu$  and  $\mathcal{M}_\nu$  are the invariant amplitudes of the diagrams resulting from the cut shown in figure 10.2. We only consider self-energy contributions due to fermion-loops. This should not affect whether or not our diagrams satisfy the Ward identity. The reason is that the number of fermion-pairs  $N$  (and hence the number of cut diagrams of the type in figure 10.2) can in principle be chosen at will. That is, we can include *any* number  $N$  of copies of the prototype model described in section 8.2 in a gauge invariant Lagrangian. So if our answer is going to satisfy the Ward identity, it should also do so if we only include the fermion-loop contributions to the self-energy.

From figure 10.2 it is clear that  $\mathcal{M}_\mu$  and  $\mathcal{M}_\nu$  are equal to the  $W$ - $d$ - $\bar{u}$  vertex contracted with the appropriate spinors, i.e.

$$\begin{aligned}
& \mathcal{M}_\mu^*(k \rightarrow \{q_1, q_2\}) \mathcal{M}_\nu(k \rightarrow \{q_1, q_2\}) \\
&= \sum_{s, s'=1}^2 \left[ \bar{u}^s(q_1) \frac{ig}{2\sqrt{2}} \gamma_\mu (\mathbf{1} + \gamma_5) v^{s'}(q_2) \right]^* \left[ \bar{u}^s(q_1) \frac{ig}{2\sqrt{2}} \gamma_\nu (\mathbf{1} + \gamma_5) v^{s'}(q_2) \right] \\
&= \frac{-g^2}{8} \sum_{s, s'=1}^2 \bar{v}^{s'}(q_2) \gamma_\mu (\mathbf{1} + \gamma_5) u^s(q_1) \quad \bar{u}^s(q_1) \gamma_\nu (\mathbf{1} + \gamma_5) v^{s'}(q_2) \quad (10.3) \\
&= \frac{g^2}{8} \text{Tr} \left[ \gamma_\mu (\mathbf{1} + \gamma_5) \not{q}_1 \gamma_\nu (\mathbf{1} + \gamma_5) \not{q}_2 \right] \\
&= g^2 \left( q_{1\mu} q_{2\nu} + q_{1\nu} q_{2\mu} - \eta_{\mu\nu} q_1 \cdot q_2 + \epsilon_{\mu\nu\rho\sigma} q_1^\rho q_2^\sigma \right).
\end{aligned}$$

The Lorentz tensor  $\Pi_{\mu\nu}(k)$  can only include terms proportional to  $\eta_{\mu\nu}$  and  $k_\mu k_\nu$ . Consequently, it can be decomposed into a transversal and longitudinal part as

$$\Pi_{\mu\nu}(k) = H_{\mu\nu} \Pi_T(k) + \frac{k_\mu k_\nu}{k^2} \Pi_L, \quad \text{where } H_{\mu\nu} := \eta_{\mu\nu} - \frac{k_\mu k_\nu}{k^2}. \quad (10.4)$$

The transverse and longitudinal projectors satisfy some convenient relations:

$$H_{\mu\nu} k_\mu = H_{\mu\nu} k_\nu = 0, \quad H_{\mu\rho} H^\rho{}_\nu = H_{\mu\nu}, \quad \text{and} \quad \frac{k_\mu k_\rho}{k^2} \frac{k^\rho k_\nu}{k^2} = \frac{k_\mu k_\nu}{k^2}. \quad (10.5)$$

We can use these to obtain the imaginary part of  $\Pi_L$  as

$$\Pi_L^I(k) = \frac{k^\mu k^\nu}{k^2} \Pi_{\mu\nu}^I(k) = \frac{c}{k^2} \int \frac{d^3 q_1}{|\vec{q}_1|} \frac{d^3 q_2}{|\vec{q}_2|} \delta^4(k - (q_1 + q_2)) [2 q_1 \cdot k q_2 \cdot k - k^2 q_1 \cdot q_2]. \quad (10.6)$$





Figure 10.3.: The Dyson sum for the W-boson propagator.

The first equality reveals this is a Lorentz invariant quantity. We may thus as well evaluate it in the center-of-mass frame, where  $\vec{k} = \vec{0}$  and  $k^0 = \sqrt{-k^2}$ . The delta function then enforces

$$q_1 = \begin{pmatrix} q \\ \vec{q} \end{pmatrix} \quad \text{and} \quad q_2 = \begin{pmatrix} q \\ -\vec{q} \end{pmatrix}, \quad \text{where} \quad q := |\vec{q}| = \frac{1}{2}\sqrt{-k^2}. \quad (10.7)$$

Using (10.7), we can evaluate the integral

$$\begin{aligned} I(k) &:= \int \frac{d^3q_1}{|\vec{q}_1|} \frac{d^3q_2}{|\vec{q}_2|} \delta^4(k - (q_1 + q_2)) f(q_1, q_2) &= \int \frac{d^3q}{q^2} \delta(\sqrt{-k^2} - 2q) f(q_1, q_2) \\ &= \int_0^\infty dq \delta(2q - \sqrt{-k^2}) \int d\Omega_{\text{CM}} f(q_1, q_2) &= \frac{1}{2} \theta(-k^2) \int d\Omega_{\text{CM}} f(q_1, q_2), \end{aligned} \quad (10.8)$$

where it is understood that  $q_1$  and  $q_2$  in  $f(q_1, q_2)$  are now given by (10.7). With the identity (10.8), equation (10.6) becomes

$$\Pi_L^I(k) = \frac{c}{4k^2} \theta(-k^2) \int d\Omega_{\text{CM}} [(-k^2)^2 - (-k^2)^2] = 0. \quad (10.9)$$

Similarly, we can obtain the imaginary part of  $\Pi_T^I$  as

$$\begin{aligned} \Pi_T^I(k) &= \frac{1}{3} \left( \eta^{\mu\nu} - \frac{k^\mu k^\nu}{k^2} \right) \Pi_{\mu\nu}^I(k) = \frac{c}{3} \int \frac{d^3q_1}{|\vec{q}_1|} \frac{d^3q_2}{|\vec{q}_2|} \delta^4(k - (q_1 + q_2)) [-2q_1 \cdot q_2] - \Pi_L^I(k) \\ &\stackrel{(10.8)}{=} \frac{c}{6} \theta(-k^2) \int d\Omega_{\text{CM}} (-k^2) = N \frac{g^2}{48\pi^2} (-k^2) \theta(-k^2) \quad := \gamma_w \cdot (-k^2). \end{aligned} \quad (10.10)$$

Note that we adsorbed the theta-function in  $\gamma_w$ . These results agree with Baur and Zeppenfeld [18].

### Obtaining the resummed propagator

The resummed propagator can be obtained by any of the two methods that were illustrated in section 9.4 for a scalar field. We shall use both methods to obtain the resummed propagator of the W-boson in the unitary gauge.

#### 1. Dyson sum

The bare propagator in the unitary gauge is given by

$$\Delta_{\mu\nu}^0(k) = \frac{1}{i(2\pi)^4} \left[ \frac{1}{k^2 + M_W^2} H_{\mu\nu} + \frac{1}{M_W^2} \frac{k_\mu k_\nu}{k^2} \right], \quad (10.11)$$

where  $M_W$  denotes the OSRS mass of the W-boson. The full propagator can be obtained by the resummation shown in figure 10.3. Using the properties (10.5), we can define

$$\Delta'_{\mu\nu} := i(2\pi)^4 \Pi_{\mu}{}^\rho \Delta_{\rho\nu}^0 = \left[ \frac{\Pi_T}{k^2 + M_W^2} H_{\mu\nu} + \frac{\Pi_L}{M_W^2} \frac{k_\mu k_\nu}{k^2} \right], \quad (10.12)$$

such that the resummed propagator becomes

$$\begin{aligned}
\Delta_{\mu\nu}(k) &= \Delta_{\mu}^{0\rho} \left( \eta_{\rho\nu} + \Delta'_{\rho\nu} + \Delta'^{\tau\rho} \Delta'_{\tau\nu} + \Delta'^{\tau\rho} \Delta'^{\phi} \Delta'_{\phi\nu} + \dots \right) \\
&= \Delta_{\mu}^{0\rho} \left( \sum_{n=0}^{\infty} \left( \frac{\Pi_T}{k^2 + M_W^2} \right)^n H_{\rho\nu} + \sum_{n=0}^{\infty} \left( \frac{\Pi_L}{M_W^2} \right)^n \frac{k_{\rho} k_{\nu}}{k^2} \right) \\
&= \frac{1}{i(2\pi)^4} \left( \frac{1}{k^2 + M_W^2 - \Pi_T} H_{\mu\nu} + \frac{1}{M_W^2 - \Pi_L} \frac{k_{\mu} k_{\nu}}{k^2} \right).
\end{aligned} \tag{10.13}$$

## 2. Inverting the quadratic part of the effective action

The terms of the effective action that are quadratic in  $W$  are given by

$$S^{\text{eff}}[W_{\mu}] = -(2\pi)^4 \int d^4k \bar{W}_{\mu}(k) [(k^2 + M_W^2)\eta_{\mu\nu} - k_{\mu}k_{\nu} - \Pi_{\mu\nu}(k)] W_{\nu}(k). \tag{10.14}$$

These terms give rise to the full propagator

$$\begin{aligned}
\Delta_{\mu\nu}(k) &= \frac{1}{i(2\pi)^4} \left[ (k^2 + M_W^2)\eta_{\mu\nu} - k_{\mu}k_{\nu} - \Pi_T H_{\mu\nu} - \Pi_L \frac{k_{\mu}k_{\nu}}{k^2} \right]^{-1} \\
&= \frac{1}{i(2\pi)^4} \left[ (k^2 + M_W^2 - \Pi_T)H_{\mu\nu} + (M_W^2 - \Pi_L) \frac{k_{\mu}k_{\nu}}{k^2} \right]^{-1}.
\end{aligned} \tag{10.15}$$

From the relations (10.5) it is clear that (10.15) is indeed equal to (10.13).

### 10.2.1. Running width scheme

As explained in section 9.4, the running width scheme consists of approximating the self-energy as

$$\begin{cases} \Pi_L(k^2) \simeq \Pi_L^R(-M_W^2) & = 0 \\ \Pi_T(k^2) \simeq \Pi_T^R(-M_W^2) + i\gamma_w \cdot (-k^2) = i\gamma_w \cdot (-k^2), \end{cases} \tag{10.16}$$

such that the resummed propagator (10.13) can be written as

$$\Delta_{\mu\nu}(k) = \frac{1}{i(2\pi)^4} \frac{1}{k^2(1 + i\gamma_w) + M_W^2} \left[ \eta_{\mu\nu} + \frac{k_{\mu}k_{\nu}}{M_W^2} (1 + i\gamma_w) \right]. \tag{10.17}$$

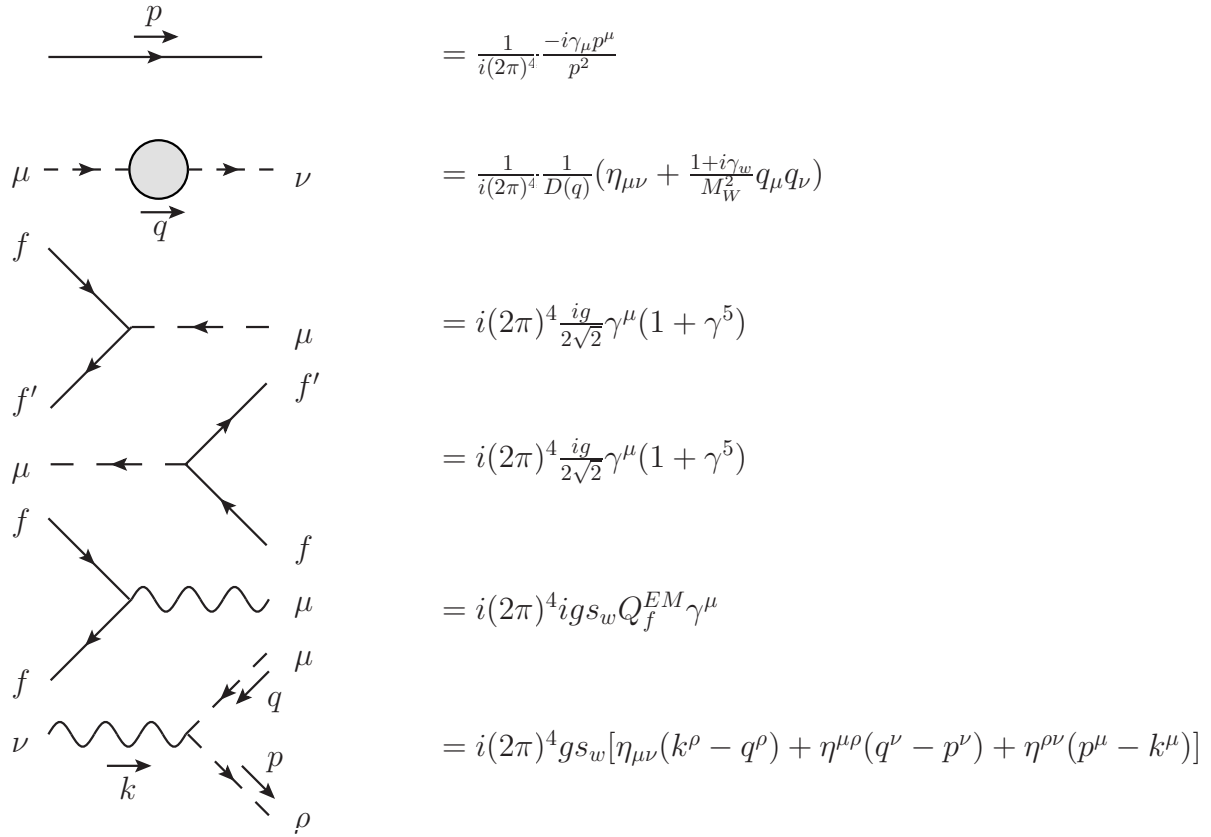
### Checking the Ward identity

The relevant Feynman rules are listed in figure 10.4, where we defined

$$D(q) := q^2(1 + i\gamma_w) + M_W^2. \tag{10.18}$$

The tree-level diagrams contributing to  $q\bar{q}' \rightarrow l\nu_l\gamma$  are obtained by attaching a photon to the diagram in figure 10.1 in all possible ways. Since the neutrino is uncharged, there are four diagrams contributing; these are shown in figure 10.5. We first calculate  $k_{\mu}\mathcal{M}^{\mu}$  for all four diagrams separately, then check whether or not they add up to 0.

$$\begin{aligned}
k_{\mu}\mathcal{M}_1^{\mu} &= c'\bar{v}(p_2)\gamma_{\nu}(1 + \gamma_5) \frac{-i(\not{p}_1 - \not{k})}{(p_1 - k)^2} \left( -\frac{1}{3} \right) \not{k}u(p_1) \\
&\quad \frac{1}{D(q_1 + q_2)} \left[ \eta^{\nu\sigma} + \frac{1 + i\gamma_w}{M_W^2} (q_1 + q_2)^{\nu} (q_1 + q_2)^{\sigma} \right] \\
&\quad \bar{u}(q_1)\gamma_{\sigma}(1 + \gamma_5)v(q_2),
\end{aligned} \tag{10.19}$$



Comments:

- A solid line represents a fermion, a wiggled line represents a photon, and a dashed line represents the W-boson.
- $Q_f^{EM}$  denotes the electromagnetic charge of the fermion  $f$ .
- $f'$  is the fermion that forms a pair with  $f$ , e.g. if  $f = u$ , then  $f' = d$ .

Figure 10.4.: Feynman Rules

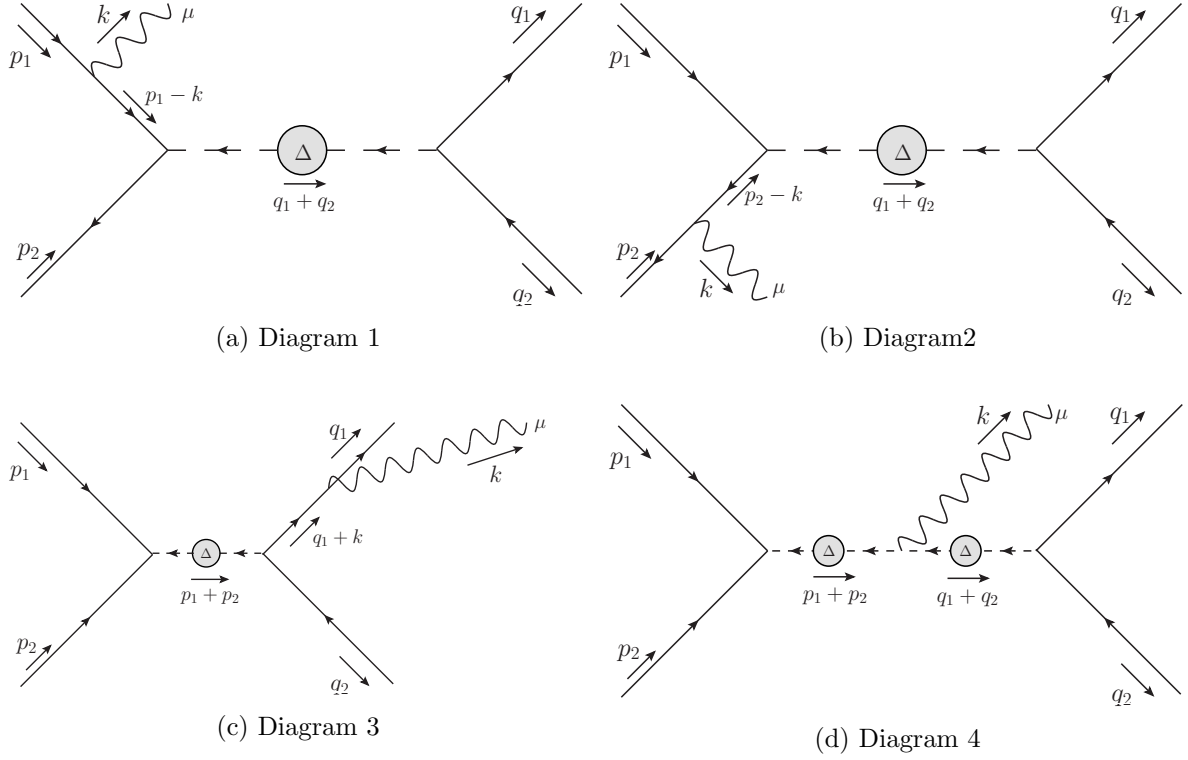


Figure 10.5.: Tree-level diagrams contributing to  $q\bar{q}' \rightarrow l\bar{\nu}_l\gamma$ . It is understood that the external fermions are the same as the ones shown in figure 10.1.

where the constant  $c'$  is defined as  $c' = -i\frac{g^3 s_w}{2^3}$ . Since the fermions are massless, we can use  $\not{p}u(p) = \not{p}v(p) = \bar{u}(p)\not{p} = \bar{v}(p)\not{p} = 0$ . Consequently, the term (10.19) that contains  $(q_1 + q_2)^\nu (q_1 + q_2)^\sigma$  vanishes. Also

$$\frac{-i(\not{p}_1 - \not{k})}{(p_1 - k)^2} \not{k} u(p_1) = \frac{-i(2p_1 \cdot k - k^2)}{-2p_1 \cdot k + k^2} u(p_1) = iu(p_1), \quad (10.20)$$

which can be used to obtain

$$k_\mu \mathcal{M}_1^\mu = \left(-\frac{1}{3}\right) \frac{1}{D(q_1 + q_2)} i c' f(p_1, p_2, q_1, q_2). \quad (10.21)$$

In (10.21) we defined

$$f(p_1, p_2, q_1, q_2) := \bar{v}(p_2) \gamma^\nu (1 + \gamma_5) u(p_1) \bar{u}(q_1) \gamma_\nu (1 + \gamma_5) v(q_2). \quad (10.22)$$

Similarly we find

$$\begin{aligned}
k_\mu \mathcal{M}_2^\mu &= c' \bar{v}(p_2) \left( \frac{2}{3} \right) \not{k} \frac{i(\not{p}_2 - \not{k})}{(p_2 - k)^2} \gamma_\nu (1 + \gamma_5) u(p_1) \\
&\quad \frac{1}{D(q_1 + q_2)} \left[ \eta^{\nu\sigma} + \frac{1 + i\gamma_w}{M_W^2} (q_1 + q_2)^\nu (q_1 + q_2)^\sigma \right] \\
&\quad \bar{u}(q_1) \gamma_\sigma (1 + \gamma_5) v(q_2) \\
&= \left( -\frac{2}{3} \right) \frac{1}{D(q_1 + q_2)} i c' f(p_1, p_2, q_2, q_2), \\
\\
k_\mu \mathcal{M}_3^\mu &= c' \bar{v}(p_2) \gamma_\nu (1 + \gamma_5) u(p_1) \\
&\quad \frac{1}{D(p_1 + p_2)} \left[ \eta^{\nu\sigma} + \frac{1 + i\gamma_w}{M_W^2} (p_1 + p_2)^\nu (p_1 + p_2)^\sigma \right] \\
&\quad \bar{u}(q_1) (-1) \not{k} \frac{-i(\not{q}_1 + \not{k})}{(q_1 + k)^2} \gamma_\sigma (1 + \gamma_5) v(q_2) \\
&= \frac{1}{D(p_1 + p_2)} i c' f(p_1, p_2, q_1, q_2), \\
\\
k_\mu \mathcal{M}_4^\mu &= -i c' \bar{v}(p_2) \gamma_\nu (1 + \gamma_5) u(p_1) \\
&\quad \frac{1}{D(p_1 + p_2)} \left[ \eta^{\nu\rho} + \frac{1 + i\gamma_w}{M_W^2} (p_1 + p_2)^\nu (p_1 + p_2)^\rho \right] \\
&\quad k_\mu [\eta^{\mu\tau} (-k^\rho + (q_1 + q_2)^\rho) + \eta^{\rho\tau} (-(q_1 + q_2)^\mu - (p_1 + p_2)^\mu) + \eta^{\mu\rho} ((p_1 + p_2)^\tau + k^\tau)] \\
&\quad \frac{1}{D(q_1 + q_2)} \left[ \eta^{\tau\sigma} + \frac{1 + i\gamma_w}{M_W^2} (q_1 + q_2)^\tau (q_1 + q_2)^\sigma \right] \\
&\quad \bar{u}(q_1) \gamma^\sigma (1 + \gamma_5) v(q_2) \\
&= \frac{2(p_1 \cdot p_2 - q_1 \cdot q_2)}{D(q_1 + q_2) D(p_1 + p_2)} i c' f(p_1, p_2, q_1, q_2).
\end{aligned} \tag{10.23}$$

$$\text{Using } \begin{cases} D(q_1 + q_2) = 2q_1 \cdot q_2 (1 + i\gamma_w) + M_W^2 \\ D(p_1 + p_2) = 2p_1 \cdot p_2 (1 + i\gamma_w) + M_W^2, \end{cases}$$

the sum of these expressions can be written as

$$\begin{aligned}
k_\mu \mathcal{M}^\mu &= k_\mu \mathcal{M}_1^\mu + k_\mu \mathcal{M}_2^\mu + k_\mu \mathcal{M}_3^\mu + k_\mu \mathcal{M}_4^\mu \\
&= \gamma_w \frac{2(p_1 \cdot p_2 - q_1 \cdot q_2)}{D(p_1 + p_2) D(q_1 + q_2)} c' f(p_1, p_2, q_1, q_2).
\end{aligned} \tag{10.24}$$

Equation (10.24) shows that the Ward identity is *not* satisfied, hence gauge invariance is broken by the resummation procedure. Since  $\gamma_w \sim \alpha$ , we see that the violation is indeed of higher order in perturbation theory.

As a check on the result (10.24), we can use the fact that the bare W-boson propagator (10.11) is obtained back from the resummed propagator (10.17) by sending  $\gamma_w \rightarrow 0$ . Therefore, in the limit  $\gamma_w \rightarrow 0$  our diagrams become the usual tree-level diagrams. So, in this limit the

Ward identity *should* thus be satisfied. Applying this idea to (10.24), we do indeed find that it gives 0 as  $\gamma_w \rightarrow 0$ . Furthermore, we wrote a FORM code [19] to calculate (10.24); the FORM result also agrees with the given result.

### 10.2.2. Fixed width scheme

Adopting the fixed width scheme amounts to approximating the self-energy as

$$\begin{cases} \Pi_L(k^2) \simeq \Pi_L(-M_W^2) = \Pi_L^R(-M_W^2) & = 0 \\ \Pi_T(k^2) \simeq \Pi_T(-M_W^2) = \Pi_T^R(-M_W^2) + \Pi_T^I(-M_W^2) = i\gamma_w M_W^2. \end{cases} \quad (10.25)$$

Under this approximation, the resummed propagator (10.13) becomes

$$\begin{aligned} \Delta_{\mu\nu}(k) &= \frac{1}{i(2\pi)^4} \left( \frac{1}{k^2 + M_W^2(1 - i\gamma_w)} H_{\mu\nu} + \frac{1}{M_W^2} \frac{k_\mu k_\nu}{k^2} \right) \\ &= \frac{1}{i(2\pi)^4} \frac{1}{k^2 + M_W^2(1 - i\gamma_w)} \left( \eta_{\mu\nu} + \frac{k^2 - iM_W\gamma_w}{M_W^2} \frac{k_\mu k_\nu}{k^2} \right). \end{aligned} \quad (10.26)$$

This is the analogous result of (9.37) for a vector boson.

### Checking the Ward identity

Checking the Ward identity in the fixed width scheme proceeds just as in the running width scheme. The only modification is that all W-boson propagators have to be replaced by (10.26). In the calculation that was performed for the running width, that the propagator terms proportional to  $\frac{k_\mu k_\nu}{k^2}$  all canceled. Therefore, the only relevant part of the propagator is the first term of (10.26) - the one proportional to  $\eta_{\mu\nu}$ . Now, if one would perform the calculation with *bare* W-propagators (so with  $\gamma_w = 0$ ), then for the same reason the only relevant part of the propagator would be

$$\Delta_{0,\mu\nu}^{\text{relevant}} = \frac{1}{i(2\pi)^4} \frac{1}{k^2 + M_W^2} \eta_{\mu\nu}. \quad (10.27)$$

This means that the relevant part of the fixed width propagator (the first term in (10.26)) can be found from the relevant part of the bare propagator (10.27) by substituting

$$M_W^2 \rightarrow M_W^2(1 - i\gamma_w). \quad (10.28)$$

Moreover, it is only through the W-propagator that  $M_W$  enters the expressions. From the fact that the calculation with bare propagators yields  $k_\mu \mathcal{M}^\mu = 0$ , we can therefore conclude that the same is true in the fixed width scheme. We thus conclude that the Ward identity *is* satisfied in the fixed width scheme.

### 10.2.3. Running width scheme + $WW\gamma$ -vertex correction

The solution proposed by Baur and Zeppenfeld to fix the gauge invariance problem of the running width scheme, is to add loop corrections to the  $WW\gamma$ -vertex of the diagram in figure 10.5d. In this subsection we show that this does indeed restore gauge invariance. Just like we only included fermion loop corrections in the resummation of our W-propagators, the only

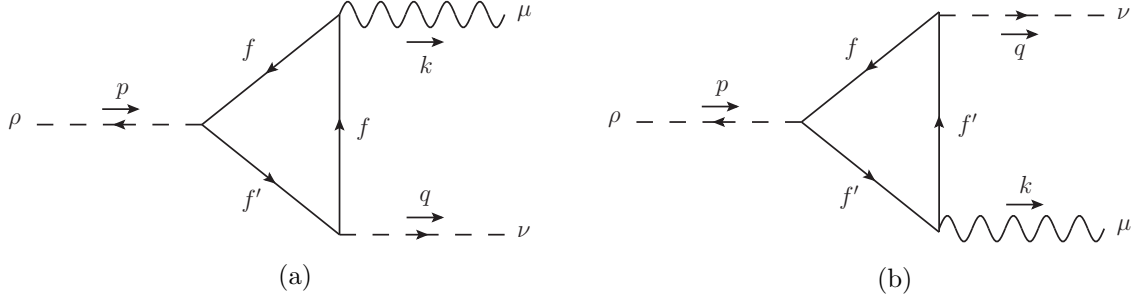


Figure 10.6.:  $WW\gamma$ -corrections

corrections added to the  $WW\gamma$ -vertex are fermion loop corrections. This is in fact the solution that is prescribed by the fermion loop scheme [20]. The corrections that have to be added to the leading order vertex are thus the ones shown in figure 10.6. Since we have only included imaginary self-energy corrections, consistency requires that we only include the imaginary parts of these triangle graphs as well. Baur and Zeppenfeld have calculated these corrections for the case that the internal fermions are again assumed to be massless. In doing so, they dropped the terms proportional to the photon momentum  $k^\mu$ . This can be understood as taking the photon on-shell ( $k^2 = 0$ ), for when checking the Ward identity the diagrams are contracted with  $k_\mu$ . Their result for the one-loop corrections  $\Gamma_1^{\mu\nu\rho}$  is

$$\Gamma_1^{\mu\nu\rho} = i\gamma_w \Gamma_0^{\mu\nu\rho}, \quad (10.29)$$

where  $\Gamma_0^{\mu\nu\rho}$  denotes the lowest order vertex, which is listed with the Feynman rules in figure 10.4. The diagram that has to be added to our running width calculation is then the diagram shown in figure 10.5d with the lowest order vertex  $\Gamma_0$  replaced by  $\Gamma_1$ . We call the invariant amplitude of this extra diagram  $\mathcal{M}'_4$ . By (10.29), we simply find that

$$k_\mu \mathcal{M}'_4{}^\mu = i\gamma_w k_\mu \mathcal{M}_4{}^\mu = -\gamma_w \frac{2(p_1 \cdot p_2 - q_1 \cdot q_2)}{D(p_1 + p_2)D(q_1 + q_2)} c' f(p_1, p_2, q_1, q_2) \stackrel{(10.24)}{=} -k_\mu \mathcal{M}^\mu. \quad (10.30)$$

This implies that  $k_\mu \mathcal{M}^\mu + k_\mu \mathcal{M}'_4{}^\mu = 0$ . Therefore, this adjustment does indeed solve the gauge invariance problem for this process.

### 10.3. Comparison of the different schemes

In this section we discuss the advantages and disadvantages of the different schemes we have encountered so far. These are summarized in table 10.1.

- **Fixed Width (FW) scheme**

In the example of the W-boson resonance the FW scheme retained  $U(1)$  gauge invariance. However, this relied heavily upon the fact that the second term of the resummed W-propagator (10.26) did not contribute to the Ward identity. Therefore, we do not have reason to believe that the FW scheme retains  $U(1)$ -invariance for more general diagrams. Another disadvantage of this scheme is that it violates  $SU(2)$  Ward identities [17].

Furthermore, there is the issue that a fixed width is generally not a good approximation outside the resonance region. For  $-p^2 < m^2$  (where  $p$  and  $m$  respectively denote the

internal propagators momentum and mass), the width is even entirely unphysical. That this inaccuracy is a serious issue for the W-boson resonance is confirmed by Baur and Zeppenfeld [18]. They state that if one considers soft photon emission, then near threshold the cross section in the fixed width scheme turns out to be at least 30% too low [18].

- **Running Width (RW) scheme**

A running width is a more accurate approximation outside the resonance region. In particular, the running width *does* vanish for spacelike momenta. However, as our example demonstrated, it violates  $U(1)$ -invariance. It also turns out to violate  $SU(2)$ -invariance [17].

- **RW +  $WW\gamma$ -vertex correction**

This is the scheme proposed by Baur and Zeppenfeld to solve the gauge invariance problem. Whereas it is generally true that it retains  $U(1)$ -invariance, it still fails to incorporate  $SU(2)$ -invariance [17].

Since neither of the schemes succeeds in retaining both  $U(1)$  and  $SU(2)$  invariance, there is need for better schemes. These are the subject of the two subsequent chapters. Before turning to these schemes, we investigate the  $U(1)$ -problem for two more examples. So far we have only focussed on internal bosons; indeed, the FW and RW schemes are defined only for bosons. In the next two sections we shall check the  $U(1)$  Ward identity for examples where the resonant propagator belongs to a fermion.

## 10.4. Fermion resonance in QED

Now that we have seen that the resummation of an internal W-boson propagator leads to a violation of the Ward identity, let us see whether this problem also occurs if the internal propagator corresponds to a fermion. In this section we consider a stable fermion in the context of QED; the next section shall concern an unstable fermion in the Standard Model.

The QED scattering process that is considered in this section is  $f\gamma \rightarrow f\gamma$  ( $f$  is for fermion). The tree-level diagrams contain only one internal propagator, which corresponds to the fermion. Since the mass of this virtual particle is equal to the total outgoing and total incoming mass, we are in regime 1b of section 9.3, meaning that the internal propagator needs to be resummed. The fact that its mass is *precisely* equal to the total outgoing (and incoming) mass makes this a special case of regime 1b: one where  $|\mathcal{M}|^2$  will have a singularity at the boundary of the phase-space. This is discussed in the box at the end of this section.

	FW	RW	RW + $WW\gamma$ -vertex correction
no width for $-p^2 < m^2$	✗	✓	✓
retains $U(1)$ gauge invariance	✓ <sup>a</sup>	✗	✓
retains $U(1)$ gauge invariance	✗	✗	✗

Table 10.1.: Comparison of the different schemes

<sup>a</sup>This table lists the properties for the considered W-boson resonance. We did not find reason to believe that the FW scheme retains  $U(1)$ -invariance in general.



To check whether or not the Ward identity is satisfied after the resummation, we shall follow the same steps: first calculate the self-energy to one-loop order, then obtain the resummed propagator, and finally check whether the Ward identity is satisfied for the tree-level diagrams with resummed internal fermion propagator.

### Calculation of the self-energy

The Feynman rules for QED have already been summarized in figure 4.6 in chapter 4. The

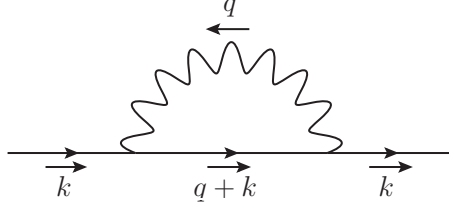


Figure 10.8.: One-loop electron self-energy in QED

electron self-energy is shown in figure 10.8. We follow [1] in its calculation. Since the integral has a linear UV-divergence, we adopt dimensional regularization to calculate and subsequently renormalize it.

$$\begin{aligned}
\Sigma(k) &= \frac{-e^2}{i(2\pi)^n} \int d^n q \frac{\gamma_\mu [-i(\not{q} + \not{k}) + m] \gamma_\nu}{(q+k)^2 + m^2} \frac{1}{q^2} \left( \eta^{\mu\nu} - \frac{q^\mu q^\nu}{q^2} \right) \\
&= ie^2 \left\{ [(n-1)m + i(n-3)\not{k}] \frac{1}{(2\pi)^n} \int d^n q \frac{1}{S(q,k)} \right. \\
&\quad + i(n-1) \frac{1}{(2\pi)^n} \int d^n q \frac{1}{S(q,k)} \not{q} \\
&\quad \left. + 2i \frac{1}{(2\pi)^n} \int d^n q \frac{k \cdot q}{q^2 S(q,k)} \not{q} \right\}, \tag{10.31}
\end{aligned}$$

where  $S(q,k) := [(q+k)^2 + m^2] q^2$ . In the two integrals over  $\not{q} = q_\mu \gamma^\mu$ ,  $\gamma^\mu$  can be pulled outside the integral. The remaining integral then has to be a Lorentz vector and can only be proportional to  $k^\mu$ . The proportionality constant is found by contracting with  $k_\mu$ , thus

$$\int d^n q f(q,k) q^\mu = A k^\mu = \frac{1}{k^2} \left( \int d^n q f(q,k) k \cdot q \right) k^\mu. \tag{10.32}$$

Using (10.32) in (10.31) yields

$$\begin{aligned}
\Sigma(k) &= ie^2 \left\{ [(n-1)m + i(n-3)\not{k}] \frac{1}{(2\pi)^n} \int d^n q \frac{1}{S} \right. \\
&\quad + i(n-1) \frac{\not{k}}{k^2} \frac{1}{(2\pi)^n} \int d^n q \frac{k \cdot q}{S} \\
&\quad \left. + 2i \frac{\not{k}}{k^2} \frac{1}{(2\pi)^n} \int d^n q \frac{(k \cdot q)^2}{S q^2} \right\}. \tag{10.33}
\end{aligned}$$

The first and third integral are finite in  $n = 4 + \epsilon$  dimensions for a small and negative  $\epsilon$ . The second integral is not; it is only defined in  $n < 3$  dimensions. Therefore, this integral is

analytically continued to higher dimensions by partial integration, using

$$n \int d^n q h(q) = \int d^n q \frac{\partial}{\partial q^\mu} [q^\mu h(q)] - \int d^n q q^\mu \frac{\partial}{\partial q^\mu} h(q). \quad (10.34)$$

The analytical continuation is then defined by dropping the boundary term. Identifying  $h(q) = \frac{k \cdot q}{S}$  yields

$$n \int d^n q \frac{k \cdot q}{S} = - \int d^n q \frac{k \cdot q}{S} + \int d^n q \frac{(2k \cdot q + 2q^2) k \cdot q}{[(k+q)^2 + m^2] S}, \quad (10.35)$$

which can be manipulated to yield

$$(n-2) \int d^n q \frac{k \cdot q}{S} = -k^2 \int d^n q \frac{1}{(q^2 + m^2)^2}. \quad (10.36)$$

By using (10.36) and some more algebra, (10.33) can be written as

$$\Sigma(k) = ie^2 \left\{ [(n-1)m + i(n-3)\not{k}] I(k^2, m^2, 0) - i\not{k} I(0, m^2, m^2) - i(k^2 + m^2) \frac{\not{k}}{k^2} J(k^2) \right\},$$

where

$$\begin{cases} I(k^2, m_1^2, m_2^2) := \frac{1}{(2\pi)^n} \int d^n q \frac{1}{[(q + \frac{1}{2}k)^2 + m_1^2][(q - \frac{1}{2}k)^2 + m_2^2]} \\ J(k^2) := \frac{1}{(2\pi)^n} \int d^n q \frac{k \cdot q}{[(q+k)^2 + m^2] q^2} \left[ \frac{1}{(q+k)^2 + m^2} + \frac{1}{q^2} \right]. \end{cases} \quad (10.37)$$

$I(k^2, m_1^2, m_2^2)$  is calculated in appendix A. The relevant results are

$$\begin{cases} I(k^2, m^2, 0) = \frac{-i\mu^\epsilon}{8\pi^2} \left\{ \frac{1}{\epsilon} + \frac{1}{2}\gamma_E + \frac{1}{2} \ln \left( \frac{m^2}{4\pi\mu^2} \right) - 1 + \frac{1}{2} \frac{k^2 + m^2}{k^2} \ln \left| \frac{k^2 + m^2}{m^2} \right| \right. \\ \qquad \qquad \qquad \left. - \frac{i\pi}{2} \frac{k^2 + m^2}{k^2} \theta(-k^2 + m^2) \right\} \\ I(0, m^2, m^2) = \frac{-i\mu^\epsilon}{8\pi^2} \left\{ \frac{1}{\epsilon} + \frac{1}{2}\gamma_E + \frac{1}{2} \ln \left( \frac{m^2}{4\pi\mu^2} \right) \right\}. \end{cases} \quad (10.38)$$

In order to calculate the two integrals appearing in  $J(k^2)$ , the product of multiple (in this case two) denominators are rewritten as one denominator by Feynman's trick

$$\frac{1}{A_1^{\alpha_1} \dots A_n^{\alpha_n}} = \frac{\Gamma(\alpha_1 + \dots + \alpha_n)}{\Gamma(\alpha_1) \dots \Gamma(\alpha_n)} \int_0^1 dx_1 \dots dx_n \frac{x_1^{\alpha_1-1} \dots x_n^{\alpha_n-1} \delta(1 - x_1 - \dots - x_n)}{(x_1 A_1 + \dots x_n A_n)^{\alpha_1 + \dots + \alpha_n}}. \quad (10.39)$$

By (10.39), the first integral of  $J(k^2)$  becomes

$$\begin{aligned} \frac{1}{(2\pi)^n} \int d^n q \frac{k \cdot q}{[(q+k)^2 + m^2]^2 q^2} &= \frac{2}{(2\pi)^n} \int_0^1 dx \int d^n q \frac{k \cdot qx}{[q^2 + 2xk \cdot q + x(k^2 + m^2)]^3} \\ &= \frac{-2k^2}{(2\pi)^n} \int_0^1 dx x^2 \int d^n q \frac{1}{(q^2 - M^2)^3}, \end{aligned} \quad (10.40)$$

where we defined  $M^2 := xm^2 + x(1-x)k^2$ . The integral over  $q$  is a standard one:

$$I_m(n, \alpha) := \int d^n q \frac{1}{(q^2 - m^2)^\alpha} = i\pi^{n/2} \frac{\Gamma(\alpha - \frac{1}{2}n)}{\Gamma(\alpha)} (m^2)^{\frac{1}{2}n - \alpha}, \quad (10.41)$$

by which the integral (10.40) becomes

$$\begin{aligned} \frac{1}{(2\pi)^n} \int d^n q \frac{k \cdot q}{[(q+k)^2 + m^2]^2 q^2} &= \frac{-ik^2}{(4\pi)^2} \int_0^1 dx \frac{x^2}{k^2 x(1-x) + m^2 x} \\ &= \frac{i}{(4\pi)^2} \left\{ 1 - \frac{k^2 + m^2}{k^2} \ln \left| \frac{k^2 + m^2}{k^2} \right| \right\}. \end{aligned} \quad (10.42)$$

Similarly, the second integral of  $J(k^2)$  becomes

$$\begin{aligned} \frac{1}{(2\pi)^n} \int d^n q \frac{k \cdot q}{[(q+k)^2 + m^2] (q^2)^2} &= \frac{-ik^2}{(4\pi)^2} \int_0^1 dx \frac{x(1-x)}{k^2 x(1-x) + m^2(1-x)} \\ &= \frac{-i}{(4\pi)^2} \left\{ 1 - \frac{m^2}{k^2} \ln \left| \frac{k^2 + m^2}{m^2} \right| \right\}. \end{aligned} \quad (10.43)$$

By putting everything together, the self-energy (10.37) becomes

$$\Sigma(k) = A(k^2) + B(k^2)i\not{k}, \quad \text{with} \quad \begin{cases} A(k^2) = \frac{e^2 \mu^\epsilon}{8\pi^2} 3 \left[ \frac{1}{\epsilon} + \frac{1}{2} \gamma_E - \frac{1}{2} \ln(4\pi) \right] + A^f(k^2), \text{ and} \\ B(k^2) = B^f(k^2) \end{cases}$$

$$\begin{cases} A^f(k^2) = \frac{e^2}{8\pi^2} \left[ -2 + 3 \ln \left( \frac{m}{\mu} \right) + \frac{3}{2} \frac{k^2 + m^2}{k^2} \ln \left| \frac{k^2 + m^2}{k^2} \right| - \frac{3}{2} i\pi \frac{k^2 + m^2}{k^2} \theta(-k^2 + m^2) \right] \\ B^f(k^2) = \frac{e^2}{8\pi^2} \left[ -\frac{1}{2} i\pi \frac{k^2 + m^2}{k^2} \theta(-k^2 + m^2) \right]. \end{cases} \quad (10.44)$$

To renormalize, a counterterm is added that cancels the  $(\frac{1}{\epsilon} + \frac{1}{2} \gamma_E - \frac{1}{2} \ln(4\pi))$ -term. The renormalized self-energy is thus given by

$$\Sigma(k^2) = A^f(k^2)m + i\not{k}B^f(k^2). \quad (10.45)$$

### Obtaining the resummed propagator

To find the resummed propagator, we shall follow the second approach explained in paragraph 9.4: we invert the quadratic part of the effective action, which is given by

$$S^{\text{eff}} = -(2\pi)^4 \int d^4 k \bar{\psi}(i\not{k} + m - \Sigma(k^2))\psi. \quad (10.46)$$

The resummed propagator then follows as

$$\begin{aligned} \Delta(k) &= \frac{1}{i(2\pi)^4} [i\not{k} + m - \Sigma(k^2)]^{-1} \\ &= \frac{1}{i(2\pi)^4} \left[ i\not{k} \left( 1 - B^f(k^2) \right) + m \left( 1 - A^f(k^2) \right) \right]^{-1}. \end{aligned} \quad (10.47)$$

To find the inverse, we use the ansatz

$$[i\not{p} + m - \Sigma]^{-1} = -i\not{k}E + mF, \quad (10.48)$$

after which we can solve for  $E$  and  $F$  by requiring

$$\begin{aligned} \mathbb{1} &\stackrel{!}{=} [i\not{k} + m - \Sigma]^{-1} [i\not{k} + m - \Sigma] \\ &= k^2 E(1 - B^f) + m^2 F(1 - A^f) + i\not{k} \left( -mE(1 - A^f) + mF(1 - B^f) \right). \end{aligned} \quad (10.49)$$

In order to satisfy (10.49), the term proportional to  $i\not{k}$  has to vanish and the remainder has to yield 1. These conditions comprise two equations that can be solved for  $E$  and  $F$ . The resulting resummed propagator reads

$$\Delta(k) = \frac{1}{i(2\pi)^4} \frac{-i\not{k}(1 - B^f) + m(1 - A^f)}{k^2(1 - B^f)^2 + m^2(1 - A^f)^2}. \quad (10.50)$$

### Checking the Ward identity

The two diagrams contributing to the process  $f\gamma \rightarrow f\gamma$  are shown in figure 10.9. The Feynman rules are summarized in figure 4.6. In order to put the external fermions on their mass shell,

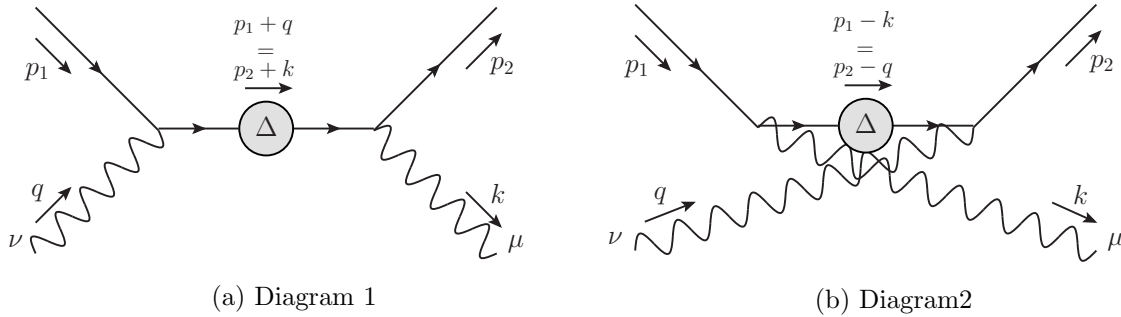


Figure 10.9.: Tree-level diagrams contributing to  $f\gamma \rightarrow f\gamma$

their physical mass has been determined. The fermion in QED is stable, thus its physical mass  $M$  is determined by the pole of (10.50), i.e.

$$-M^2 \left( 1 - B^f(-M^2) \right)^2 + m^2 \left( 1 - A^f(-M^2) \right)^2 = 0. \quad (10.51)$$

It is this mass  $M$  that appears in the spinor relations

$$i\not{p}_i u(p_i) = -M u(p_i), \quad \bar{u}(p_i) i\not{p}_i = -M \bar{u}(p_i). \quad (10.52)$$

We will *not* take the photons on-shell. The reason is that otherwise the internal virtual particle cannot become on-shell, for the momentum-conservation at the vertices would not allow it. However, if the photons are taken off-shell, the internal fermion *can* become on-shell, which guarantees that the resonance region is contained in the phase space. This justifies the resummation of the internal fermion propagator.

The aim here is to check whether this resummation violates the Ward identity, but first we establish that the Ward identity is satisfied *without* the resummation. The identity to be checked is  $k_\mu \mathcal{M}^{\mu\nu} \stackrel{?}{=} 0$ . As explained in chapter 4, in order for the Ward identity to be satisfied (without resummation),  $k$  does not have to be taken on-shell, but the other external particles do. Despite the fact that we are not taking  $q$  on-shell, we still expect the Ward identity to be satisfied without resummation. The reason can be understood by considering the diagram

in figure 10.11. We put all external momenta in figure 10.11 on-shell; the internal momentum  $q$  will then generally be off-shell. As explained in paragraph 4.2, if we attach a photon with momentum  $k^\mu$  in all possible ways to the upper fermion line and contract with  $k_\mu$ , then we get 0. The attachments of the photon along the upper fermion line yield two diagrams of which the two diagrams in figure 10.9 (without resummation) are the upper halves. By ‘upper halves’ we mean the diagrams without the fermions with momenta  $q_1$  and  $q_2$  and their vertex with the photon. These lower halves are identical for both the diagrams that are obtained by attaching the photon along the upper fermion line. Therefore, the two diagrams in figure 10.9 (without resummation) *should* (and *do*) satisfy the Ward identity, even if  $q$  is off-shell.

Now we are going to check whether this is still the case after the internal propagator has been resummed.

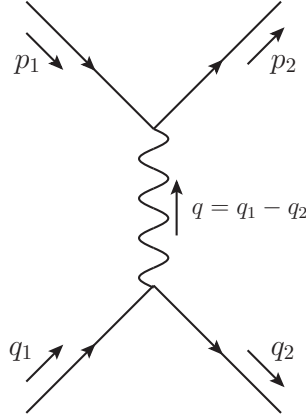


Figure 10.11.

$$\text{By defining } \begin{cases} \xi_1 := (-M^2 + 2p_1 \cdot q + q^2) (1 - B_1^f)^2 + m^2 (1 - A_1^f)^2 \\ A_1^f := A^f ((p_1 + q)^2) \\ B_1^f := B^f ((p_1 + q)^2), \end{cases} \quad (10.53)$$

the expression for the first diagram can be written as

$$\begin{aligned} k_\mu \mathcal{M}_1^{\mu\nu} &= -e^2 \bar{u}(p_2) \not{k} \frac{-i(\not{p}_2 + \not{k}) (1 - B_1^f) + m (1 - A_1^f)}{\xi_1} \gamma^\nu u(p_1), \\ &= \frac{-e^2}{\xi_1} \bar{u}(p_2) \left\{ \left[ -M (1 - B_1^f) + m (1 - A_1^f) \right] \not{k} \gamma^\nu \right. \\ &\quad \left. - i(2p_1 \cdot q + q^2) (1 - B_1^f)^2 \gamma^\nu \right\} u(p_1). \end{aligned} \quad (10.54)$$

$$\text{Similarly, using } \begin{cases} \xi_2 := (-M^2 - 2p_2 \cdot q + q^2) (1 - B_2^f)^2 + m^2 (1 - A_2^f)^2 \\ A_2^f := A^f ((p_2 - q)^2) \\ B_2^f := B^f ((p_2 - q)^2), \end{cases} \quad (10.55)$$

the second diagram yields

$$\begin{aligned}
k_\mu \mathcal{M}_2^{\mu\nu} &= -e^2 \bar{u}(p_2) \gamma^\nu \frac{-i(\not{p}_1 - \not{k}) (1 - B_2^f) + m(1 - A_2^f)}{\xi_2} \not{k} u(p_1) \\
&= -\frac{e^2}{\xi_2} \bar{u}(p_2) \left\{ \left[ -M(1 - B_2^f) + m(1 - A_2^f) \right] \gamma^\nu \not{k} \right. \\
&\quad \left. -i(2\not{p}_2 \cdot q - q^2)(1 - B_2^f) \gamma^\nu \right\} u(p_1).
\end{aligned} \tag{10.56}$$

Now we check the Ward identity

$$\begin{aligned}
k_\mu \mathcal{M}^{\mu\nu} &= k_\mu \mathcal{M}_1^{\mu\nu} + k_\mu \mathcal{M}_2^{\mu\nu} \\
&= -e^2 \bar{u}(p_2) \left\{ -i \left[ \frac{(2p_1 \cdot q + q^2)(1 - B_1^f)}{\xi_1} + \frac{(2p_2 \cdot q - q^2)(1 - B_2^f)}{\xi_2} \right] \gamma^\nu \right. \\
&\quad \left. + \frac{-M(1 - B_1^f) + m(1 - A_1^f)}{\xi_1} \not{k} \gamma^\nu \right. \\
&\quad \left. + \frac{-M(1 - B_2^f) + m(1 - A_2^f)}{\xi_2} \gamma^\nu \not{k} \right\} u(p_1).
\end{aligned} \tag{10.57}$$

If this is to vanish, all three terms need to vanish separately. This does not happen as such. The reason is that since  $A^f$  and  $B^f$  are complicated functions of their arguments (see (10.45)), such that  $A_1^f$  and  $A_2^f$  are completely independent. The same goes for  $B_1^f$  and  $B_2^f$ .

If the unstable particle was a boson, this would be the point where we would adopt either the fixed width or running width scheme as proposed in section 9.4. Since we are dealing with a fermion, the approach we shall take is to just evaluate  $A^f$  and  $B^f$  exactly at the resonance. This is analogous to the fixed width in a renormalization scheme where the propagator residue is  $Z = 1$ . We thus approximate

$$\begin{cases} A_1^f \simeq A_2^f \simeq A^f(-M^2) \\ B_1^f \simeq B_2^f \simeq B^f(-M^2) \end{cases} \stackrel{(10.51)}{\Rightarrow} \begin{cases} \xi_1 = (2p_1 \cdot q + q^2)(1 - B^f(-M^2)) \\ \xi_2 = (-2p_2 \cdot q + q^2)(1 - B^f(-M^2)) \end{cases}. \tag{10.58}$$

The last two terms in (10.57) then vanish by (10.51). The term in between brackets in the first term becomes

$$\frac{(2p_1 \cdot q + q^2)(1 - B^f(-M^2))}{(2p_1 \cdot q + q^2)(1 - B^f(-M^2))} - \frac{(2p_2 \cdot q - q^2)(1 - B^f(-M^2))}{(2p_2 \cdot q - q^2)(1 - B^f(-M^2))} = 0. \tag{10.59}$$

This means that  $k_\mu \mathcal{M}^{\mu\nu} = 0$ , i.e. the Ward identity is satisfied. In section 10.1 we argued that this *should* be the case, since the resummed propagator belongs to a stable fermion. In that section, it was argued that the Ward identity had to be satisfied in the on-shell renormalization scheme. Here we explicitly showed that the Ward identity is, for this case, satisfied in *any* renormalization scheme (for our calculation does not rely on the specific counterterms that we chose to renormalize our the self-energy with).

### On the singularity of $|\mathcal{M}^2|$

We have seen that the absence of an imaginary part of the self-energy for stable particles implies that the Ward identity is still satisfied. Another consequence of its absence is that the resummed propagator does not assume a Breit-Wigner form. Indeed, taking the absolute value squared of our process' amplitude, the denominator of the resummed propagator (10.50) enters as

$$|\mathcal{M}|^2 \sim \left| \frac{1}{s(1 - B^f(-M^2))^2 - m^2(1 - A^f(-M^2))^2} \right|^2 \stackrel{(10.51)}{\sim} \left| \frac{1}{s - M^2} \right|^2. \quad (10.60)$$

As usual  $s = -p_A^2$ , where  $p_A$  is the momentum of the internal propagator.

Let us now consider the external photons to be on-shell, making our process a physical process. The fact that the mass of the internal particle is exactly equal to the total outgoing and incoming mass (which equals the threshold of the fermion) makes this process special. The fact that its mass is not bigger means that the internal fermion is a stable particle and that its propagator does not give rise to a Breit-Wigner shape. The fact that its mass is not smaller means that the internal fermion can become arbitrarily close to being on-shell by considering arbitrarily soft photons. It cannot become exactly on-shell, for this would require photon momenta  $q = k = 0$ . In other words, the resonance lies exactly on the boundary of the phase space. If the fermion mass would be slightly smaller than the outgoing mass, the resonance would lie just outside the phase space.

To obtain a physical observable, the cross-section has to be integrated over (part of) the phase space. When integrating over the soft photon momenta, the term (10.60) would give us a divergent expression, which should not appear in a physical observable! However, if the photons are soft, then our process is almost identical to double soft bremsstrahlung of a fermion (the only difference is that one photon is incoming instead of outgoing). Since soft photons can not actually be detected by a detector, this process should - just as soft bremsstrahlung should - be regarded as a radiative correction to the fermion propagator. To obtain a *real* physical observable, our expression thus has to be added to other radiative corrections, including self-energy corrections. An example of another correction of this order is shown in figure 10.12. These corrections come with their own IR divergencies. If *all* radiative corrections at this order are included, then all divergencies will cancel to yield a finite physical observable (see e.g. [2, chapter 6] and references therein).

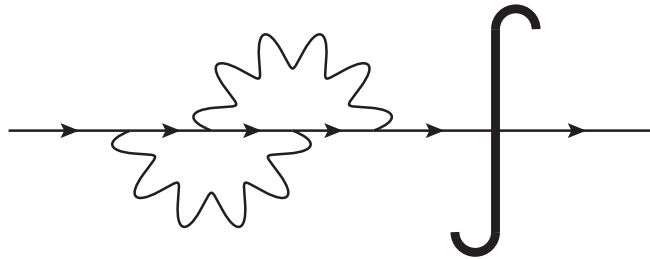


Figure 10.12.

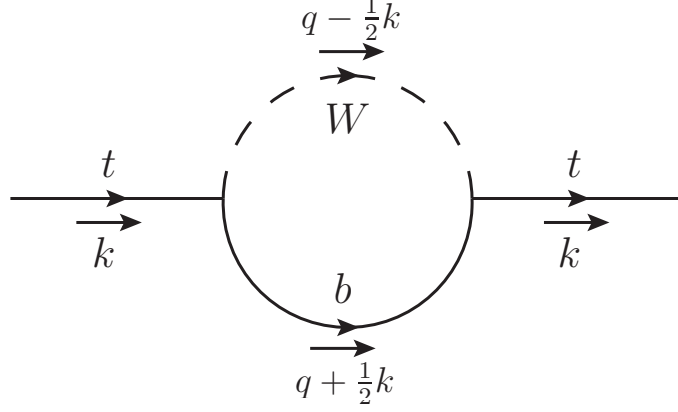


Figure 10.13.: Top-quark self-energy diagram

## 10.5. Fermion resonance in the Standard Model

Now we consider the same process, but with an *unstable* internal fermion. We choose it to be the top-quark in the context of the standard the model, so the process under consideration is  $t\gamma \rightarrow t\gamma$ .

### Calculation of the self-energy

We only consider the self-energy contribution of figure 10.13. The Feynman rules are listed in figure 10.4, except now we take the fermion to be massive. Another modification to the Feynman rules of figure 10.4 is that we adopt the Feynman gauge for the W-propagator, such that

$$\Delta_{\mu\nu}^W(k) = \frac{1}{i(2\pi)^n} \frac{\eta_{\mu\nu}}{k^2 + m_W^2}. \quad (10.61)$$

Collecting some constants as  $c = \frac{ig}{2^3}$ , the self-energy reads

$$\begin{aligned} \Sigma(k^2) &= \frac{c}{(2\pi)^n} \int d^n q \gamma^\mu (1 + \gamma^5) \frac{-i(\not{q} + \frac{1}{2}\not{k}) + m_b}{(q + \frac{1}{2}k)^2 + m_b^2} \gamma^\nu (1 + \gamma^5) \frac{\eta_{\mu\nu}}{(q - \frac{1}{2}k)^2 + m_W^2} \\ &= 2ic(1 - \gamma^5) \frac{n-2}{(2\pi)^n} \int d^n q \frac{\not{q} + \frac{1}{2}\not{k}}{[(q + \frac{1}{2}k)^2 + m_b^2][(q - \frac{1}{2}k)^2 + m_W^2]}. \end{aligned} \quad (10.62)$$

The integral over  $\not{q} = \gamma_\mu q^\mu$  can be rewritten by the use of identity (10.32). The self-energy (10.62) then becomes

$$\begin{aligned} \Sigma(k^2) &= c(1 - \gamma^5) \frac{n-2}{k^2} \left\{ (k^2 + m_W^2 - m_b^2) I(k^2, m_W^2, m_b^2) \right. \\ &\quad \left. + \frac{1}{(2\pi)^n} I_{m_W}(n, 1) - \frac{1}{(2\pi)^n} I_{m_b}(n, 1) \right\} i\not{\epsilon}. \end{aligned} \quad (10.63)$$

$I(k^2, m_1^2, m_2^2)$  is defined and calculated in appendix A.  $I_m(n, \alpha)$  is the standard integral of



equation (10.41). In  $n = 4 + \epsilon$  dimensions

$$\begin{aligned} \frac{1}{(2\pi)^n} I_m(n, 1) &= \frac{im^2\mu^\epsilon}{(4\pi)^2} \Gamma\left(-1 - \frac{1}{2}\epsilon\right) \left(\frac{m^2}{4\pi\mu^2}\right)^{\frac{1}{2}\epsilon} \\ &= \frac{im^2\mu^\epsilon}{8\pi^2} \left[ \frac{1}{\epsilon} + \frac{1}{2}\gamma_E - \frac{1}{2} + \frac{1}{2}\ln\left(\frac{m^2}{4\pi\mu^2}\right) \right], \end{aligned} \quad (10.64)$$

where the last step used

$$\Gamma(-n + \epsilon) = \frac{(-1)^n}{n!} \left[ \frac{1}{\epsilon} - \gamma_E + \sum_{r=1}^n \frac{1}{r} + \mathcal{O}(\epsilon) \right]. \quad (10.65)$$

Putting everything together and recalling that  $P_{L/R} = \frac{1 \pm \gamma_5}{2}$  yields the self-energy

$$\Sigma(k^2 = -s) = C(k^2) P_R i \not{p}, \quad (10.66)$$

with

$$\begin{aligned} C(k^2) := & \frac{g}{2^4 \pi^2} \left\{ \frac{1}{\epsilon} + \frac{1}{2}\gamma_E - \frac{1}{2} + \frac{m_W^2 - m_b^2}{2s} + \frac{1}{2}\ln\left(\frac{M_w m_b}{4\pi\mu^2}\right) \right. \\ & - \left[ \frac{1}{2} \left( \frac{m_W^2 - m_b^2}{s} \right)^2 - \frac{m_W^2}{s} \right] \ln\left(\frac{m_W}{m_b}\right) \\ & \left. + \left[ 1 - \frac{m_W^2 - m_b^2}{s} \right] \left( h(s, m_w^2, m_b^2) - i\pi \frac{\lambda^{1/2}(s, m_W^2, m_b^2)}{2s} \theta(s - (m_w + m_b)^2) \right) \right\}. \end{aligned} \quad (10.67)$$

In the on-shell renormalization scheme, we have  $\text{Re}[C(-M_t^2)] = 0$ , such that

$$C(-M_t^2) = i\tilde{\gamma}, \quad \text{with} \quad \tilde{\gamma} := -\frac{g}{2^5 \pi} \left( 1 - \frac{m_W^2 - m_b^2}{M_t^2} \right) \frac{\lambda^{1/2}(M_t^2, m_W^2, m_b^2)}{M_t^2}. \quad (10.68)$$

### Obtaining the resummed propagator

The resummed propagator will be obtained by performing the Dyson sum. As a check, we will establish that it equals the inverse of the quadratic part of the effective action. According to the Dyson sum, the resummed propagator is

$$\Delta(k) = \frac{1}{i(2\pi)^4} \frac{-i\not{k} + m_t}{k^2 + m_t^2} \left\{ 1 + \sum_{n=1}^{\infty} \left[ C(k^2) P_R i \not{k} \frac{-i\not{k} + m_t}{k^2 + m_t^2} \right]^n \right\}. \quad (10.69)$$

$$\begin{aligned} \text{By using} \quad & [P_R i \not{k} (-i\not{k} + m_t)]^2 = k^2 P_R i \not{k} (-i\not{k} + m_t) \\ \Rightarrow & [P_R i \not{k} (-i\not{k} + m_t)]^n = (k^2)^{n-1} P_R i \not{k} (-i\not{k} + m_t), \end{aligned} \quad (10.70)$$

(10.69) can be written as

$$\Delta(k) = \frac{1}{i(2\pi)^4} \frac{-i\not{k} + m_t}{k^2 + m_t^2} \left\{ 1 + \frac{1}{k^2} \sum_{n=1}^{\infty} \left( \frac{k^2 C(k^2)}{k^2 + m_t^2} \right)^n P_R i \not{k} (-i\not{k} + m_t) \right\}. \quad (10.71)$$

The summation yields 
$$\sum_{n=1}^{\infty} \left( \frac{k^2 C(k^2)}{k^2 + m_t^2} \right)^n = \frac{k^2 C(k^2)}{k^2 + m_t^2 - k^2 C(k^2)}, \quad (10.72)$$

such that the resummed propagator (10.71) becomes

$$\Delta(k) = \frac{1}{i(2\pi)^4} \frac{1}{\zeta(k^2)} \left[ m_t + \left( -1 + \frac{1}{2} C(k^2) \right) i\not{k} - \frac{1}{2} C(k^2) \gamma^5 i\not{k} \right], \quad (10.73)$$

where  $\zeta(k^2) := k^2(1 - C(k^2)) + m_t^2$ .

This should equal the inverse effective action quadratic in  $t$ . And indeed, one can check that

$$i(2\pi)^4 [i\not{k} + m_t - C(k^2) P_R i\not{k}] \cdot \Delta(k^2) = \mathbb{1}. \quad (10.74)$$

### Checking the Ward identity

The diagrams contributing to  $t\gamma \rightarrow t\gamma$  are again the ones shown in figure 10.9, where this time the fermion represents a top-quark. The internal propagator to be used is now the resummed propagator (10.73). Furthermore, we adopt the on-shell renormalization scheme, such that  $m_t = M_t$ .

As we did for the corresponding process in QED, we take the external quarks on-shell and the external photons off-shell. As explained there, the Ward identity should then be satisfied if the internal fermion is not resummed. An important difference with the QED process is that the external fermions are now unstable. This is a problem, because the LSZ-formalism cannot handle unstable external states. However, the only aim here is to get a feeling for the gauge invariance problem, so we just close our eyes for this issue and proceed. A consequence of this issue is that it is unclear what the on-shell condition is to be for the external top-quarks. We shall take two different approaches:

1. Use the relation one would use for stable particles:

$$p_j^2 = -M_t^2 \quad \Leftrightarrow \quad \begin{cases} i\not{p}_j u(p_j) = -M_t u(p_j) \\ \bar{u}(p_j) i\not{p}_j = -M_t \bar{u}(p_j). \end{cases} \quad (10.75)$$

2. Assume that  $p_j^2$  is determined by the pole of the top-quark propagator, which we take to be the resummed propagator (10.73) that is also being used for the internal fermion. That is

$$p_j^2 = -\frac{M_t^2}{1 - i\gamma} \quad \Leftrightarrow \quad \begin{cases} i\not{p}_j u(p_j) = -\frac{M_t}{\sqrt{1 - i\gamma}} u(p_j) \\ \bar{u}(p_j) i\not{p}_j = -\frac{M_t}{\sqrt{1 - i\gamma}} \bar{u}(p_j). \end{cases} \quad (10.76)$$

First we shall use the relations (10.75). If we then define

$$\begin{cases} \zeta_1 := \zeta((p_2 + k)^2) = M_t^2 C_1 + (2p_2 \cdot k + k^2)(1 - C_1) \\ C_1 := C((p_2 + k)^2), \end{cases} \quad (10.77)$$

$$\begin{aligned}
k_\mu \mathcal{M}_1^{\mu\nu} &= c' \bar{u}(p_2) \not{k} \frac{(-1 + C_1 P_R) i(\not{p}_2 + \not{k}) + M_t}{\zeta_1} \gamma^\nu u(p_1) \\
&= \frac{c'}{\zeta_1} \bar{u}(p_2) \left\{ M_t C_q P_L \not{k} \gamma^\nu + i(-1 + C_1 P_L) (2p_2 \cdot k + k^2) \gamma^\nu \right\}, \tag{10.78}
\end{aligned}$$

where we defined  $c' := -\frac{4g^2 s_w^2}{9}$ . Similarly, if we define

$$\begin{cases} \zeta_2 := \zeta((p_1 - k)^2) = M_t^2 C_2 + (-2p_1 \cdot k + k^2)(1 - C_2) \\ C_2 := C((p_1 - k)^2), \end{cases} \tag{10.79}$$

$$\begin{aligned}
k_\mu \mathcal{M}_2^{\mu\nu} &= c' \bar{u}(p_2) \gamma^\nu \frac{(-1 + C_2 P_R) i(\not{p}_1 - \not{k}) + M_t}{\zeta_2} \not{k} u(p_1) \\
&= c' \bar{u}(p_2) \left\{ M_t C_2 P_L \gamma^\nu \not{k} + i((-1 + C_2 P_L) (2p_1 \cdot k - k^2) \gamma^\nu) \right\} u(p_1). \tag{10.80}
\end{aligned}$$

$$\begin{aligned}
k_\mu \mathcal{M}^{\mu\nu} &= k_\mu \mathcal{M}_1^{\mu\nu} + k_\mu \mathcal{M}_2^{\mu\nu} \\
&= c' \bar{u}(p_2) \left\{ \frac{M_t C_1}{\zeta_1} P_L \not{k} \gamma^\nu + \frac{M_t C_2}{\zeta_2} P_L \gamma^\nu \not{k} \right. \\
&\quad \left. + i \left[ \frac{(-1 + C_1 P_L) (2p_2 \cdot k + k^2)}{\zeta_1} + \frac{(-1 + C_2 P_L) (2p_1 \cdot k - k^2)}{\zeta_2} \right] \gamma^\nu \right\} u(p_1). \tag{10.81}
\end{aligned}$$

If we now evaluate C exactly at the resonance, such that

$$C_1 = C_2 = C(-M_t^2) = i\tilde{\gamma} \quad \Rightarrow \quad \begin{cases} \zeta_1 = M_t^2 i\tilde{\gamma} + (2p_2 \cdot k + k^2)(1 - i\tilde{\gamma}) \\ \zeta_2 = M_t^2 i\tilde{\gamma} + (-2p_1 \cdot k + k^2)(1 - i\tilde{\gamma}), \end{cases} \tag{10.82}$$

$$\begin{aligned}
k_\mu \mathcal{M}^{\mu\nu} &= c' \bar{u}(p_2) \left\{ \frac{M_t i\tilde{\gamma}}{M_t^2 i\tilde{\gamma} + (2p_2 \cdot k + k^2)(1 - i\tilde{\gamma})} P_L \not{k} \gamma^\nu \right. \\
&\quad \left. + \frac{M_t i\tilde{\gamma}}{M_t^2 i\tilde{\gamma} + (-2p_1 \cdot k + k^2)(1 - i\tilde{\gamma})} P_L \gamma^\nu \not{k} \right. \\
&\quad \left. - \tilde{\gamma} M_t^2 \frac{2(p_1 + p_2) \cdot k}{[M_t^2 i\tilde{\gamma} + (2p_2 \cdot k + k^2)(1 - i\tilde{\gamma})] [M_t^2 i\tilde{\gamma} + (-2p_1 \cdot k + k^2)(1 - i\tilde{\gamma})]} (-1 + i\tilde{\gamma} P_L) \gamma^\nu \right\} u(p_1). \tag{10.83}
\end{aligned}$$

For finite  $\gamma$ , this does not vanish. The resummation thus again violates the Ward identity, at least if we use the on-shell relations (10.75). As a check, we can send  $\gamma \rightarrow 0$ . In this limit (10.83) vanishes. This should indeed be the case, for the Ward identity should be satisfied without the resummation.

We can now repeat the calculation but with the use of the relations (10.76) instead of (10.75). Doing this causes more terms to cancel, yet the answer

$$k_\mu \mathcal{M}^{\mu\nu} = \frac{c' M_t}{(1 - i\tilde{\gamma})^{3/2}} \left[ \left( \sqrt{1 - i\tilde{\gamma}} - 1 \right) + i\tilde{\gamma} P_L \right] \left\{ \frac{1}{p_2 \cdot k + k^2} \not{k} \gamma^\nu + \frac{1}{-2p_1 \cdot k + k^2} \gamma^\nu \not{k} \right\}, \tag{10.84}$$

is still nonzero. Note again that (10.84) vanishes for  $\gamma \rightarrow 0$ , as it should. We thus conclude that neither by using the relations (10.75) for the external unstable fermions, nor by using (10.76), does the resummation lead to a satisfied Ward identity.

# 11. The Complex Mass Scheme (CMS)

## 11.1. Definition

The complex mass scheme is a *renormalization scheme*. As will be explained in this chapter, it avoids the gauge invariance problem. One can think of the CMS as treating unstable particles analogous to the way the OSRS treats stable particles. Let us clarify this idea. The main idea behind the OSRS is that the renormalized mass  $M$  is determined by requiring  $p^2 = -M^2$  to be the pole position of the resummed propagator *for stable particles*. This is expressed by equation (6.14). The virtue of this scheme is that the renormalized mass  $M$  then coincides with the physical mass. *For unstable particles*, however, the self-energy acquires an imaginary part. Since the OSRS mass is required to be real, it does not correspond to the pole position of unstable particles. Moreover, as explained in section 9.2, neither does it equal their physical mass. So, whereas the OSRS is very convenient for dealing with stable particles, it is less so for unstable particles.

The CMS defines its renormalized mass  $\hat{m}$  in an analogous way: it requires  $p^2 = -\hat{m}^2$  to be the pole position of the resummed propagator *also for unstable particles*. That is,  $\hat{m}$  is (or equivalently, the counterterms are) defined by requiring

$$[p^2 + \hat{m}^2 - \Sigma(p^2, \hat{m}^2)] \Big|_{p^2 = -\hat{m}^2} = 0 \quad \Leftrightarrow \quad \Sigma(-\hat{m}^2, \hat{m}^2) = 0. \quad (11.1)$$

Since for unstable particles  $\Sigma$  is a complex function of its arguments, the mass  $\hat{m}$  will have to be complex to satisfy (11.1). It is therefore clear that it cannot correspond to a physical object. As emphasized in section 6.3, this is fine, for renormalized quantities do generally not carry any physical meaning. To be complete, the complex mass scheme defines the renormalization of the of the mass and the field strength by requiring

$$\begin{cases} \Sigma(-\hat{m}^2, \hat{m}^2) = 0 \\ \Sigma'(-\hat{m}^2, \hat{m}^2) = 0, \end{cases} \quad (11.2)$$

which can be thought of as an extension of the renormalization conditions of the OSRS (6.17). The second condition of (11.2) ensures that the propagator residue in the CMS is  $Z = 1$ . One has to keep in mind that the complex masses are to be used *everywhere* in the Feynman rules. In particular, the weak mixing angle also becomes complex, for

$$\cos^2(\theta_w) := c_w^2 = 1 - s_w^2 = \frac{\hat{m}_w^2}{\hat{m}_Z^2}, \quad (11.3)$$

where  $\hat{m}_w$  and  $\hat{m}_Z$  denote the complex masses of the  $W$ - and  $Z$ -boson. Also, one must not forget to include the appropriate counterterms when calculating diagrams to NLO or beyond. This holds true for any renormalization scheme; the only difference is that counterterms may now be complex where they were purely real (or purely imaginary) in the OSRS.

## 11.2. How the CMS avoids the gauge invariance problem

The main advantage of the CMS is that it avoids the whole gauge invariance problem by making it unnecessary to resum internal propagators. To understand this, we consider again the process shown in figure 9.3. In the CMS, the bare propagator of the internal particle A (which can be either stable or unstable) is given by

$$\Delta_0(s_A) = \frac{1}{i(2\pi)^4} \frac{1}{-s_A + \hat{m}^2}, \quad (11.4)$$

if A is scalar particle. Propagators of other particles share this denominator structure. If we now consider the corrections to this propagator shown in figure 9.4, then every 1PI-insertion yields an extra factor

$$\frac{\Sigma(-s_A, \hat{m}^2)}{-s_A + \hat{m}^2}. \quad (11.5)$$

As stated by equation 9.30, this extra factor does not spoil the perturbation expansion if its absolute value is much smaller than 1. The region of phase space that was problematic before is the region where  $s_A$  becomes close to  $\hat{m}^2$ . In this region it seems plausible that the small denominator may render the absolute value of (11.5) large, in spite of  $\Sigma$  being of order  $\alpha$ . To investigate this region, we assume

$$\left| \frac{s_A - \hat{m}^2}{\hat{m}^2} \right| \ll 1. \quad (11.6)$$

Then we can expand the absolute value of (11.5) around  $s_A = \hat{m}^2$ .

$$\begin{aligned} \left| \frac{\Sigma(-s_A, \hat{m}^2)}{s_A - \hat{m}^2} \right| &= \left| \frac{\hat{m}^2}{s_A - \hat{m}^2} \left\{ \frac{\Sigma(-\hat{m}^2, \hat{m}^2)}{\hat{m}^2} + \frac{\hat{m}^2 - s_A}{\hat{m}^2} \Sigma'(-\hat{m}^2, \hat{m}^2) \right. \right. \\ &\quad \left. \left. + \left( \frac{\hat{m}^2 - s_A}{\hat{m}^2} \right)^2 \hat{m}^2 \Sigma''(-\hat{m}^2, \hat{m}^2) + \dots \right\} \right| \\ &\stackrel{(11.2)}{=} \left| \frac{\hat{m}^2 - s_A}{\hat{m}^2} \hat{m}^2 \Sigma''(-\hat{m}^2, \hat{m}^2) \right| \\ &\sim \left| \frac{\hat{m}^2 - s_A}{\hat{m}^2} \alpha \right| \ll 1, \end{aligned} \quad (11.7)$$

where we used that  $\Sigma'' \sim \frac{\alpha}{\hat{m}^2}$  and, in the last step, (11.6) together with  $\alpha \ll 1$ . Therefore, we conclude that resummation is indeed unnecessary. Consequently, our physical observables are guaranteed to be gauge invariant order by order in perturbation theory<sup>1</sup>.

It may seem remarkable that the need for resummation disappears simply by adopting a convenient renormalization scheme. The reason for this is that the question whether resummation is necessary, depends on the terms in perturbation theory that are of higher order than the order  $n$  to which the physical observables are being calculated. In section 6.3 we explained that by adopting a different renormalization, these higher order terms become modified<sup>2</sup>. This

<sup>1</sup>Actually, for this to be true we also need the renormalization conditions (11.2) *themselves* to be gauge independent. This follows from the fact that  $\hat{m}^2$  - being the position of the pole of the full two-point function - is gauge independent[21].

<sup>2</sup>It was also explained that this happens *in a gauge invariant manner*. One can of course add terms of higher order in perturbation theory *by hand*, but this will generally violate the Ward identities; gauge invariance is guaranteed order by order by following the prescription to find physical observables by applying the Feynman rules, not when adding higher order terms by hand.

feature is being exploited here: by switching to the CMS, the higher order terms proportional to  $\alpha^m$  (thus  $m > n$ ) are altered in such a way that they *do* properly decrease with  $m$ . Thereby, perturbation theory is restored. The next section elaborates further on how these higher order terms are shuffled around if one switches to the CMS. In section 11.4 we shall confirm that the CMS does indeed fix the gauge invariance problem of the  $W$ -boson resonance of section 10.2 by checking the Ward identity.

### 11.3. Relation between the CMS and the $\bar{m}$ -scheme

The CMS is a renormalization scheme which is unusual by having a complex mass. As we discussed in the previous section, the advantage of the CMS is that ordinary perturbation theory still holds in the resonance region. This contrasts with renormalization schemes that adopt real masses. An example of a renormalization scheme of the latter type is the scheme in which the renormalized mass  $m$  equals the real mass  $\bar{m}$ . Recall from section 9.2 that  $\bar{m}$  is related to the complex CMS mass  $\hat{m}$  by

$$\hat{m}^2 = \bar{m}^2 - i\bar{m}\bar{\Gamma}. \quad (11.8)$$

We shall call this scheme in which  $m = \bar{m}$  the  $\bar{m}$ -scheme. Thus upon switching from the  $\bar{m}$ -scheme to the CMS, one avoids the problem that perturbation theory breaks down near the resonance. At the end of the previous section we argued that the reason for this is that terms of higher order in perturbation theory are shuffled around. In this we clarify how this shuffling takes place.

It is assumed for now that the masses under discussion belong to a scalar field  $\phi$ , and that we are dealing with a  $\phi^3$ -theory. The relations between the relevant Lagrangians are as follows

$$\mathcal{L}_0 = \mathcal{L}^{\bar{m}} + \Delta\mathcal{L}^{\bar{m}} = \mathcal{L}^{\text{cms}} + \Delta\mathcal{L}^{\text{cms}} \quad (11.9a)$$

$$= \mathcal{L}_{\text{quadr}}^{\bar{m}} + \mathcal{L}_{\text{int}}^{\bar{m}} = \mathcal{L}_{\text{quadr}}^{\text{cms}} + \mathcal{L}_{\text{int}}^{\text{cms}}. \quad (11.9b)$$

The notation is as introduced in chapter 6.  $\mathcal{L}_0$  denotes the bare Lagrangian;  $\mathcal{L}^{\bar{m}}$  and  $\mathcal{L}^{\text{cms}}$  are the renormalized Lagrangians of respectively the  $\bar{m}$ -scheme and the CMS;  $\Delta\mathcal{L}^{\bar{m}}$  and  $\Delta\mathcal{L}^{\text{cms}}$  denote the corresponding counterterms. The step from (11.9a) to (11.9b) is made by adsorbing the counterterms together with the non-quadratic parts of  $\mathcal{L}$  into  $\mathcal{L}_{\text{int}}$ . The quadratic parts of the renormalized Lagrangians are given by

$$\begin{cases} \mathcal{L}_{\text{quadr}}^{\bar{m}} = -\frac{1}{2}(\partial_\mu\phi)^2 - \frac{1}{2}\bar{m}^2(\phi)^2 \\ \mathcal{L}_{\text{quadr}}^{\text{cms}} = -\frac{1}{2}(\partial_\mu\phi)^2 - \frac{1}{2}\hat{m}^2(\phi)^2. \end{cases} \quad (11.10)$$

From (11.8), (11.9b) and (11.10) we then conclude that

$$\mathcal{L}_{\text{quadr}}^{\text{cms}} = \mathcal{L}_{\text{quadr}}^{\bar{m}} + \frac{1}{2}i\bar{m}\bar{\Gamma}\phi^2 \quad \text{and} \quad (11.11a)$$

$$\mathcal{L}_{\text{int}}^{\text{cms}} = \mathcal{L}_{\text{int}}^{\bar{m}} - \frac{1}{2}i\bar{m}\bar{\Gamma}\phi^2. \quad (11.11b)$$

In words: switching from the  $\bar{m}$ -scheme to the CMS consists of 1. adjusting the quadratic part  $\mathcal{L}_{\text{quadr}}$  to make the mass complex, as expressed by (11.11a) and 2. adding a compensating

counterterm, as expressed by (11.11b). It is important to realize that the counterterm  $-i\bar{m}\bar{\Gamma}\phi^2/2$  is treated as an interaction term and thus gives rise to a vertex in the Feynman rules. In contrast, the extra quadratic part  $i\bar{m}\bar{\Gamma}\phi^2/2$  in (11.11a) is *not* treated as an interaction term. Instead, it is adsorbed into  $\hat{m}^2$  and thus part of the CMS propagator

$$\Delta^{\text{CMS}}(k) = \frac{1}{i(2\pi)^4} \frac{1}{k^2 + \hat{m}^2} = \frac{1}{i(2\pi)^4} \frac{1}{k^2 + \bar{m}^2 - i\bar{m}\bar{\Gamma}}. \quad (11.12)$$

The reason that the CMS has a well-defined perturbation expansion is that its bare propagator (11.12) can be regarded as a resummed version of the (bare)  $\bar{m}$ -scheme propagator

$$\Delta^{\bar{m}}(k) = \frac{1}{i(2\pi)^4} \frac{1}{k^2 + \bar{m}^2}. \quad (11.13)$$

$\Delta^{\text{CMS}}$  being a resummed version of  $\Delta^{\bar{m}}$  can be understood by noting that

$$\Sigma(-\hat{m}^2, \bar{m}^2) = i\bar{m}\bar{\Gamma}. \quad (11.14)$$

This we shall discuss below. As explained in section 9.4, the resummation includes all propagator corrections that spoil perturbation theory near the resonance in the  $\bar{m}$ -scheme. The fact that all these corrections are contained in the bare propagator in the CMS is the reason that its perturbation expansion is well-defined everywhere in phase-space.

#### Proof of (11.14).

At this point it is important to realize what we precisely mean by  $\Sigma(-\hat{m}^2, \bar{m}^2)$ . Recall that in our notation,  $\Sigma(k^2, m^2)$  denotes the self-energy with incoming momentum  $k$ , calculated in the renormalization scheme that is characterized by having renormalized mass  $m$ .  $m$  is thus the mass being used in the internal propagators. Furthermore, the counterterms are also taken into account in the calculation of this self-energy. These counterterms are specific to the renormalization scheme. Therefore, the argument  $m^2$  of  $\Sigma(k^2, m^2)$  also specifies - implicitly - the counterterms that are used in the calculation of the self-energy. On a sidenote, in the next section we shall also use the notation  $\hat{\Sigma}(k^2, m^2)$ . This specifies the same self-energy, but calculated *without* taking any counterterms into account. Summarizing, we can say that the quantity under consideration,  $\Sigma(-\hat{m}^2, \bar{m}^2)$ , denotes the self-energy calculated in the  $\bar{m}$ -scheme, including counterterms and evaluated at momentum  $k^2 = \hat{m}^2$ .

We shall now show that (11.14) is valid. The strategy will be to *assume* that (11.14) is correct, then switch to the CMS and show that (11.14) gives rise to  $\Sigma(-\hat{m}^2, \hat{m}^2) = 0$ . Since this is the defining relation (11.1) of the CMS, (11.14) must indeed be the correct expression. We illustrate the procedure for the case that the parameters in the  $\bar{m}$ -scheme are renormalized to order  $\alpha^3$ . This means that all amplitudes can be calculated to this order. Since we are assuming (11.14), this means we know  $i\bar{m}\bar{\Gamma}$  to three-loop order. We can thus write

$$i\bar{m}\bar{\Gamma} = (i\bar{m}\bar{\Gamma})^{(1)} + (i\bar{m}\bar{\Gamma})^{(2)} + (i\bar{m}\bar{\Gamma})^{(3)}, \quad \text{where } (i\bar{m}\bar{\Gamma})^{(n)} \sim \alpha^n. \quad (11.15)$$

These terms are the counterterms that have to be added when switching from the  $\bar{m}$ -scheme to the CMS. To illustrate how we denote these counterterms in the Feynman rules, we wrote equation (11.15) in diagram language in figure 11.1. We shall neglect the other (real) counterterms that are already present in the  $\bar{m}$ -scheme. The reason is that these are irrelevant, for they are also present in the CMS scheme. The diagrams contributing to  $\Sigma(k^2, \bar{m}^2)$  are shown

Figure 11.1.:  $i\bar{m}\bar{\Gamma} = (i\bar{m}\bar{\Gamma})^{(1)} + (i\bar{m}\bar{\Gamma})^{(2)} + (i\bar{m}\bar{\Gamma})^{(3)}$

in figure 11.2. A propagator with a double line denotes  $\Delta^{\bar{m}}$ ; a dotted line denotes  $\Delta^{\text{CMS}}$ . Since the diagrams in figure 11.2 are truncated, the external lines do not carry any real meaning. Therefore, we wrote the external lines as solid lines, denoting neither  $\Delta^{\bar{m}}$ , nor  $\Delta^{\text{CMS}}$ . We will think here of  $\Delta^{\bar{m}}$  as the resummed version of  $\Delta^{\text{CMS}}$  instead of the other way around as before. This idea is depicted in figure 11.3, which shows the resummation leading to the result (11.12).

Now we switch to the CMS. To obtain contributions to the CMS version of the self-energy

*Symmetry factors are left implicit.*

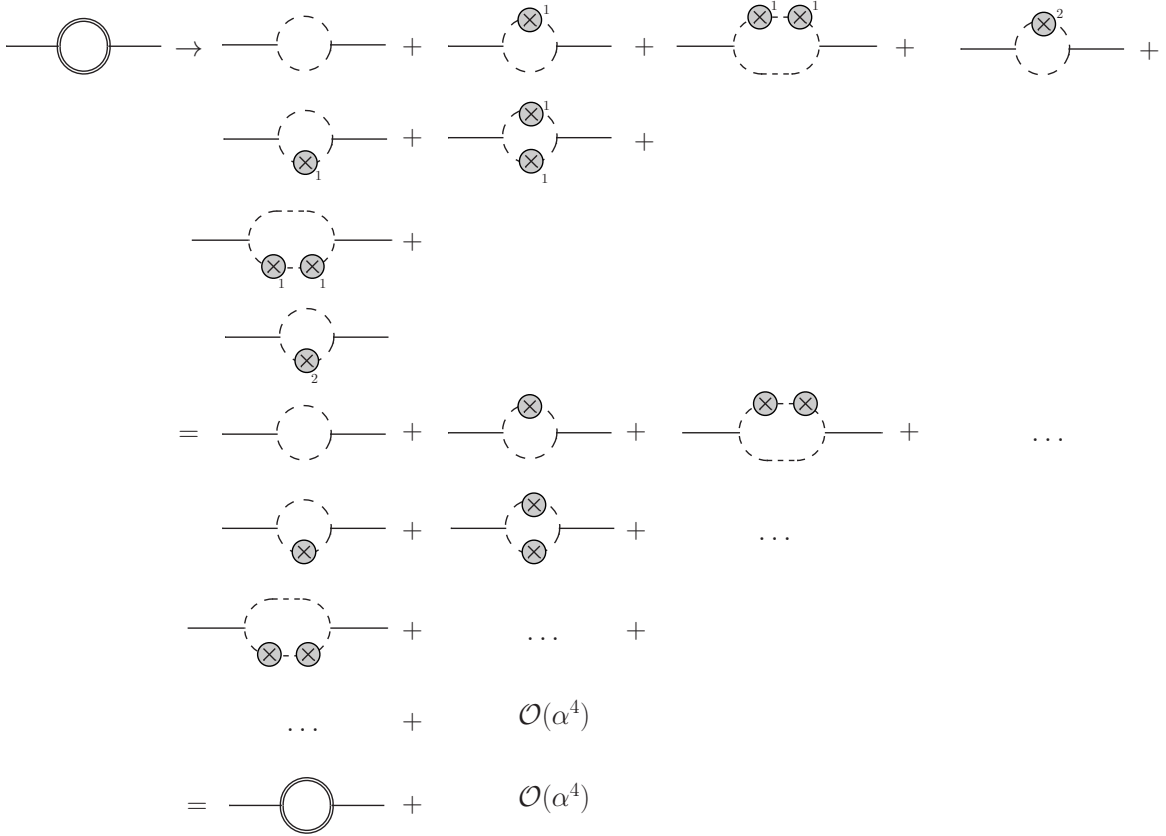
Figure 11.2.

Figure 11.3.:  $\Delta^{\bar{m}}$  as a resummed version of  $\Delta^{\text{CMS}}$

$\Sigma(k^2, \hat{m}^2)$ , we have to modify the diagrams contributing to  $\Sigma(k^2, \bar{m}^2)$  by 1. replacing the propagators  $\Delta^{\bar{m}} \rightarrow \Delta^{\text{CMS}}$  and 2. by supplementing these propagators with the counterterm vertices of figure 11.1 in all possible ways. This is done for one such diagram in the first step of figure 11.4. In principle, adding the counterterms is done with the restriction that we do not obtain diagrams of order  $\alpha^4$ . However, we are free to add (non-resonant) higher order terms. Therefore, after having applied the two modifications to a diagram, we can add more counterterms in such a way that we obtain the original diagram, but with every internal propagator  $\Delta^{\bar{m}}$  replaced by the propagator  $\Delta^{\text{CMS}}$  corrected by an infinite series of counterterms. By figure 11.3, this diagram is then equal to the original diagram to an accuracy of order  $\alpha^3$ . This idea is illustrated in the remaining two steps of figure 11.4. Therefore, upon switching to the CMS scheme the self-energy diagrams are not changed up to the order that we are doing perturbation theory (here  $\alpha^3$ ). This generalizes to any order in perturbation theory, which proves what was stated in chapter 6: amplitudes calculated in different renormalization schemes are the same *up to the order of perturbation theory that one is working at*. So we have established that the diagrams composing  $\Sigma(k^2, \bar{m}^2)$  do not change upon switching to the CMS (to the desired accuracy).

However, we also obtain some *extra* 1PI diagrams, namely the counterterms (figure 11.1 times  $(-1)$ ). These equal  $-i\bar{m}\bar{\Gamma}$ . Therefore, the self-energy  $\Sigma(k^2, \bar{m}^2)$  (evaluated at  $k^2 = -\hat{m}^2$ )





Comments:

- Symmetry factors are left implicit. Also, we drew some diagrams which are actually topologically equivalent; e.g. the third diagram on the first line is equivalent to the first diagram on the second line. Drawing them in this way is more instructive.
- These are amputated diagrams. Therefore, we drew the external lines as solid lines; these neither represent  $\Delta^{CMS}$  nor  $\Delta^{\hat{m}}$ .

Figure 11.4.: Transformation of a diagram upon switching to the CMS.

becomes in the CMS

$$\begin{aligned}
 \Sigma(-\hat{m}^2, \hat{m}^2) &= \Sigma(-\hat{m}^2, \bar{m}^2) - i\bar{m}\bar{\Gamma} + \mathcal{O}(\alpha^4) \\
 &\stackrel{(11.14)}{=} i\bar{m}\bar{\Gamma} - i\bar{m}\bar{\Gamma} + \mathcal{O}(\alpha^4) \\
 &= 0 + \mathcal{O}(\alpha^4),
 \end{aligned} \tag{11.16}$$

as required. This proves that (11.14) is indeed correct.

## 11.4. The W-boson resonance in the CMS

The aim of this section is to apply the CMS to the W-boson resonance, which was shown to violate the  $U(1)$  Ward identity in the RW scheme in section 10.2. We shall check whether this Ward identity is satisfied in the CMS, as it should be. Since ordinary perturbation theory works fine in the CMS, the calculation will be an ordinary tree-level calculation. It will turn out to be essentially the same as the tree-level calculation in the OSRS scheme (so *without* any

resummation). The latter satisfies the Ward identity, as was shown in section 10.2.1 by taking  $\gamma_w \rightarrow 0$ . To understand that the two calculations are essentially the same, we note that we can obtain the CMS calculation from the tree-level OSRS calculation by making the following modifications:

- the  $W$ -boson propagator to be used is now the bare CMS propagator

$$\Delta_{0,\mu\nu}^{\text{CMS}}(k) = \frac{1}{i(2\pi)^4} \frac{1}{k^2 + \hat{m}_W^2} \left( \eta_{\mu\nu} + \frac{k_\mu k_\nu}{\hat{m}_W^2} \right). \quad (11.17)$$

This is equal to the bare OSRS propagator ((10.17) with  $\gamma_w \rightarrow 0$ ), with the modification that the mass is now the complex CMS mass. Consequently, the  $W$ -propagators have to be modified by the simple replacement

$$M_W^2 \rightarrow \hat{m}_W^2. \quad (11.18)$$

Since the  $W$ -boson mass enters the calculation only (explicitly) through this propagator, this substitution can be made in the entire calculation.

- the constant  $s_w$  is to be modified, for it implicitly depends on  $M_W$ . The modification to be made is

$$s_w = 1 - \frac{M_W^2}{M_Z^2} \rightarrow 1 - \frac{\hat{m}_W^2}{M_Z^2}. \quad (11.19)$$

However,  $s_w$  is just an overall constant in the calculation. Therefore, it will not affect whether the Ward identity is satisfied or not.

Since the calculation is tree-level, counterterms do not play a role. In effect, the only relevant replacement to be made is thus (11.18). This will leave the tree-level OSRS result  $k_\mu \mathcal{M}^\mu = 0$  unaffected. Therefore we find the  $U(1)$  Ward identity is indeed satisfied in the CMS.

## 11.5. Unitarity in the CMS

In chapter 5 we presented the proof that the Standard Model is unitary by means of Cutkosky's cutting rules. What we did not mention was that in the proof we implicitly assumed to be dealing with stable particles only. This is reflected by the fact that the LSZ formalism - which assumes external particles to live infinitely long - cannot handle unstable particles. Yet by the Cutkosky rules *any* internal line can be cut, thus also external states corresponding to unstable particles can be produced. This issue has been addressed by Veltman [22]. He showed within *non-perturbative* quantum field theory that unitarity is satisfied under the condition that unstable particles are excluded from external states. In other words, the scattering matrix is unitary on the Hilbert space spanned by stable particles only;

$$i(\langle b|\mathcal{T}|a\rangle - \langle a|\mathcal{T}|b\rangle^*) = - \sum_{|c\rangle \in \text{stable states}} \langle c|i\mathcal{T}|a\rangle \langle c|i\mathcal{T}|b\rangle^* \quad \forall |a\rangle, |b\rangle \in \text{stable states}. \quad (11.20)$$

Thus if (11.20) is to be identified with a cutting equation, then it is one in which unstable propagators are not being cut.

The fact that the full theory is unitary implies that any valid perturbation theory should

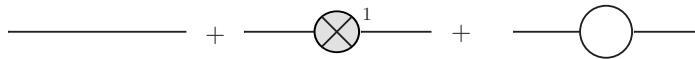


Figure 11.5.: All the order  $\alpha$  corrections to the two-point function reside in these three diagrams, not solely in the latter two.

yield results that are unitary up to the accuracy of the expansion. That is, equation (11.20) has to be satisfied up to the order of perturbation theory that is being considered. An important point to note here is that the perturbation theory is done in the coupling constant, or equivalently, in  $\alpha$ . Let us for the sake of the discussion count a  $\alpha^p$  counterterm as  $p$ -loops. If one then performs the usual diagrammatic expansion in the CMS, then it is *not* true that all  $n$ -loop diagrams (which are thus understood to also include the appropriate counterterms) precisely correspond to all the  $\alpha^n$ -terms in perturbation theory. The reason is that the CMS propagator contains  $i\bar{m}\bar{\Gamma}$  in its denominator. Since  $i\bar{m}\bar{\Gamma}$  is determined during the renormalization procedure, it is actually a function of  $\alpha$  satisfying  $i\bar{m}\bar{\Gamma} \sim \mathcal{O}(\alpha)$ . This means that within a single propagator are contained infinitely many higher order  $\alpha$ -corrections

$$\Delta^{\text{CMS}}(k) = \frac{1}{i(2\pi)^4} \frac{1}{k^2 + \hat{m}^2} = \frac{1}{i(2\pi)^4} \frac{1}{k^2 + \bar{m}^2} (1 + \mathcal{O}(\alpha)). \quad (11.21)$$

Indeed, as argued in section 11.3, the virtue of the CMS is precisely that the bare CMS propagator is inherently resummed. The upshot of this is that any  $n$ -loop diagram can contain  $\alpha^m$ -terms with  $m > n$ . For example, in the  $\phi^3$ -theory of section 11.3, all the order  $\alpha$ -corrections to the two point function are contained within the *three* diagrams shown in figure 11.5, not solely in the last two diagrams. The correct statement is that if one considers *all* diagrams up to  $n$ -loops, then these contain all terms up to  $\alpha^n$ -accuracy in perturbation theory. In this sense the diagrammatic expansion of the CMS defines a fine perturbation theory. Therefore, in the CMS equation (11.20) should be satisfied up to the accuracy of the perturbation expansion.

The aim of this section is to show that this is indeed the case. In order to do so, we will follow the proof presented by Denner and Lang [23]. They have proven (11.20) by formulating a generalized version of Cutkosky's cutting rules. The unitarity proof for stable particles, which uses the original Cutkosky's cutting rules, provides a nice starting point for their derivation. For convenience, in figure 11.6 we have repeated the diagram of chapter 5 summarizing these rules. The listed steps 1, 2a and 2b are not valid in the case of unstable particles in the CMS for the following reasons.

- 1 If one would make the same decomposition (5.5), then the property  $\Delta^\pm(x) = (\Delta^\mp)^*(x)$  (5.12) would no longer be satisfied. The reason is that the mass  $\hat{m}^2$  is now complex. Therefore, the approach we will take is to define a new decomposition into appropriate functions  $\Delta^\pm(x)$ , which satisfy both (5.5) and (5.12). With this decomposition, the largest time equation (LTE) (5.14) will again be satisfied.
- 2a) As highlighted by equation (11.11b), the CMS includes an imaginary counterterm as part of its Lagrangian. As a result,  $\mathcal{L}_{\text{int}} = \mathcal{L}_{\text{int}}^\dagger$  is not satisfied in the CMS. Therefore, we shall need some other means of establishing that circled regions can be interpreted as the complex conjugate of its reversed process.
- 2b) Since we shall now use other functions  $\Delta^\pm(x)$ , their Fouriertransforms do not equal (5.6) anymore. Therefore, cuts of propagators that correspond to unstable particles do not

$$1. \begin{cases} \Delta(x) = \theta(x)\Delta^+(x) + \theta(-x)\Delta^-(x) & (5.5) \\ \Delta^\pm(x) = (\Delta^\pm)^*(x) & (5.12) \end{cases}$$



**Largest Time Equation:**

$$D(a \rightarrow b) + \bar{D}(a \rightarrow b) = - \sum_{\text{other circulings}} D(a \rightarrow b) \quad (5.14)$$



**2.a)** Circled regions are the complex conjugate of their time-reversed process, e.g.  $\bar{D}(a \rightarrow b) = D^*(b \rightarrow a) = \langle a | iT | b \rangle$ .

This follows from  $\mathcal{L}_{\text{int}}^\dagger = \mathcal{L}_{\text{int}}$ .

**2.b)** Only cuts obeying the cut structure survive.

This is because  $\Delta^\pm(k) = 2\pi\theta(\pm k^0)\delta(k^2 - m^2)$  (5.6)

represents an on-shell particle with purely positive/negative energy.

**Unitarity:**

$$i(\langle b | \mathcal{T} | a \rangle - \langle a | \mathcal{T} | b \rangle^*) = - \sum_c \langle c | iT | a \rangle \langle c | iT | b \rangle^* \quad (5.17)$$

*Reminders on notation:*

- $D(a \rightarrow b)$  denotes a diagram contributing to the invariant amplitude of the process  $a \rightarrow b$ .
- $\bar{D}(a \rightarrow b)$  denotes the same diagram with all vertices circled.

Figure 11.6.: The steps of the unitarity proof.

represent physical particles with purely positive/negative energy. For this reason we shall need some way of establishing that only cuts survive that obey the cut structure.

Lastly, it also has to become clear what becomes of these cuts of unstable propagators, for according to (11.20) these should not contribute in the end. The following three subsections are devoted to discussing precisely the steps 1, 2a) and 2b). The final subsection addressed the question what becomes of the (cut structure satisfying) cuts of unstable propagators.

### 11.5.1. Decomposition of the CMS propagator

The  $\Delta^\pm(x)$  satisfying the requirements (5.5) and (5.12) are given by the Fourier transforms of

$$\Delta^\pm(k) = \pm \frac{1}{(2\pi)^4} \text{Im} \left[ \frac{1}{\hat{p}^0(p^0 \mp \hat{p}^0)} \right] \quad (11.22) \quad \text{where} \quad \hat{p}^0 := \sqrt{|\vec{p}|^2 + \hat{m}^2} \quad (11.23)$$

$$= \sqrt{|\vec{p}|^2 + \bar{m}^2 - i\bar{m}\bar{\Gamma}}.$$

In order to check (5.12), we define  $\hat{p}_R^0 := \text{Re}(\hat{p}^0)$  and  $\hat{p}_I^0 := \text{Im}(\hat{p}^0)$ . We can then write (11.22) explicitly as

$$\Delta^\pm(p) = \pm \frac{1}{(2\pi)^4} \frac{\hat{p}_I^0(p^0 \mp 2\hat{p}_R^0)}{\left[ \hat{p}_I^0 p^0 \mp (\hat{p}_R^0)^2 \pm (\hat{p}_I^0)^2 \right]^2 + \left[ \hat{p}_I^0 p^0 \mp 2\hat{p}_R^0 \hat{p}_I^0 \right]^2}. \quad (11.24)$$

From (11.24) it is easily checked that  $\Delta^+(p) = (\Delta^-)^*(-p)$ , which proves (5.12). Now we shall show that (11.22) does indeed define a correct decomposition (5.5). In order for (5.5) to be satisfied, we need for positive times that  $\Delta^{\text{CMS}}(t, \vec{x}) = \Delta^+(t, \vec{x})$ ; for negative times we need  $\Delta^{\text{CMS}}(t, \vec{x}) = \Delta^-(t, \vec{x})$ . That is, we require

$$\begin{cases} \Delta^{\text{CMS}}(|t|, \vec{x}) - \Delta^+(|t|, \vec{x}) = 0 \\ \Delta^{\text{CMS}}(-|t|, \vec{x}) - \Delta^-(-|t|, \vec{x}) = 0 \end{cases} \Leftrightarrow \int dp^0 [\Delta^{\text{CMS}}(p^0, \vec{p}) - \Delta^\pm(p^0, \vec{p})] e^{\mp ip^0|t|} = 0. \quad (11.25)$$

Now we check whether (11.22) does indeed satisfy (11.25).

$$\begin{aligned} & \int dp^0 [\Delta^{\text{CMS}}(p^0, \vec{p}) - \Delta^\pm(p^0, \vec{p})] e^{\mp ip^0|t|} \\ &= \frac{1}{i(2\pi)^4} \int dp^0 \left\{ \frac{1}{-(p^0)^2 + (\hat{p}^0)^2} \pm i \text{Im} \left[ \frac{1}{\hat{p}^0(p^0 \mp \hat{p}^0)} \right] \right\} e^{\mp ip^0|t|} \\ &= \frac{1}{i(2\pi)^4} \int dp^0 \left\{ \frac{1}{2\hat{p}^0} \left[ \frac{1}{p^0 + \hat{p}^0} - \frac{1}{p^0 - \hat{p}^0} \right] \pm \frac{1}{2} \left[ \frac{1}{\hat{p}^0(p^0 \mp \hat{p}^0)} - \frac{1}{(\hat{p}^0)^*(p^0 \mp (\hat{p}^0)^*)} \right] \right\} e^{\mp ip^0|t|}. \end{aligned} \quad (11.26)$$

Note that (11.26) displays two equations at once. In the first equation (concerning  $\Delta^+$ ), we can close the integration contour in the lower half of the complex plane. Note that, according to (11.23),  $\hat{p}^0$  lies in this lower half-plane. Therefore, of the four terms in (11.26), only the second and third contain poles in the lower half plane. The first and fourth term thus drop out. Similarly, in the other equation (concerning  $\Delta^-$ ), the contour has to be closed in the upper half of the complex plane. This results in the second and fourth term dropping out. We thus obtain

$$\int dp^0 [\Delta^{\text{CMS}}(p^0, \vec{p}) - \Delta^\pm(p^0, \vec{p})] e^{\mp ip^0|t|} = \frac{1}{i(2\pi)^4} \frac{1}{2\hat{p}^0} \int dp^0 \left( \mp \frac{1}{p^0 \mp \hat{p}^0} \pm \frac{1}{p^0 \mp \hat{p}^0} \right) e^{\mp ip^0|t|} = 0. \quad (11.27)$$

So (11.25) is indeed satisfied. This means that we can use our newly defined  $\Delta^\pm$  (11.22) in the generalized Feynman rules to encode propagators connecting uncircled vertices to circled

vertices. As before, this immediately gives rise to the Largest Time Equation (LTE) (5.14).

Since the cut propagators  $\Delta^\pm$  are now different from before, we cannot identify them as physical particles carrying purely positive/negative energy. However, at leading order in  $\frac{\bar{\Gamma}}{\bar{m}} \sim \alpha$ , we *can*. The reason is that if we take the limit  $\bar{\Gamma} \downarrow 0$ , we retrieve the expression for  $\Delta^\pm$  that we had for stable particles with mass  $\bar{m}$ . To see this is the case, we use the fact that the limit  $\bar{\Gamma} \downarrow 0$  is, according to (11.23), equivalent to  $\hat{p}_I^0 \uparrow 0 \Leftrightarrow (-\hat{p}_I^0) \downarrow 0$ . We then use (11.24) as starting point to take this limit.

$$\begin{aligned}
\lim_{\bar{\Gamma} \downarrow 0} \Delta^\pm(p) &= \mp \frac{1}{(2\pi)^4} \frac{1}{p^0 \mp 2\hat{p}_R^0} & \lim_{(-\hat{p}_I^0) \downarrow 0} \frac{-\hat{p}_I^0}{\left[\frac{\hat{p}_R^0(p^0 \mp \hat{p}_R^0)}{p^0 \mp 2\hat{p}_R^0}\right]^2 + (-\hat{p}_I^0)^2} \\
&\stackrel{(9.44)}{=} \mp \frac{1}{(2\pi)^4} \frac{1}{p^0 \mp 2\hat{p}_R^0} & \pi \delta\left(\frac{\hat{p}_R^0(p^0 \mp \hat{p}_R^0)}{p^0 \mp 2\hat{p}_R^0}\right) \\
&= \mp \frac{1}{(2\pi)^3} \frac{|p^0 \mp 2\hat{p}_R^0|}{p^0 \mp 2\hat{p}_R^0} & \frac{1}{2\hat{p}_R^0} \delta(p^0 \mp \hat{p}_R^0) \\
&= \mp \frac{1}{(2\pi)^3} \text{sgn}(p^0 \mp 2\hat{p}_R^0) \frac{1}{2\hat{p}_R^0} & \delta(p^0 \mp \hat{p}_R^0) \\
&= \frac{1}{(2\pi)^3} & \frac{1}{2\hat{p}_R^0} \delta(p^0 \mp \hat{p}_R^0) \\
&= \frac{1}{(2\pi)^3} & \theta(\pm p^0) \delta(p^2 + \bar{m}^2),
\end{aligned} \tag{11.28}$$

which is indeed the stable particle result.

### 11.5.2. Including the imaginary mass counterterm

Now that we have established the validity of the LTE, we address step 2a) of the unitarity proof. That is, we would like to be able to identify the circled regions of diagrams as the complex conjugate of that part of the region with all momenta reversed. As argued before, the presence of the imaginary counterterm makes that  $\mathcal{L}^{\text{int}}$  is not hermitian anymore. Thereby it spoils the desired identification. In this paragraph we explain how this difficulty can be overcome.

For illustrative purposes, we shall adopt a simple model at this point. It comprises a real scalar field  $\chi$  representing a *stable* particle with mass  $m_{\text{stable}}$ , coupled to a scalar field  $\phi$  representing an *unstable* particle. The coupling is through

$$\mathcal{L}_{\text{coupling}} = \frac{g}{2} \phi \chi^2. \tag{11.29}$$

We adopt the CMS for the unstable particle, whose propagator thus acquires the complex mass  $\hat{m}^2 = \bar{m}^2 - i\bar{m}\bar{\Gamma}$ . For convenience, we shall again ignore the real counterterms; the crucial

counterterm is the imaginary term

$$\mathcal{L}_{\text{CT}} = -\frac{1}{2}i\bar{m}\bar{\Gamma}\phi^2, \quad (11.30)$$

where  $\bar{\Gamma} = \mathcal{O}(\alpha)$  and  $\alpha \sim g^2$ . The two vertices of the theory are thus the ones given in figure 11.7.

$$\begin{aligned} \begin{array}{c} \diagup \\ \bullet \\ \diagdown \end{array} \text{---} &= i(2\pi)^4 g \\ \text{---} \textcircled{\times} \text{---} &= i(2\pi)^4 (-i\bar{m}\bar{\Gamma}) \end{aligned}$$

Figure 11.7.: The vertices of the toy model

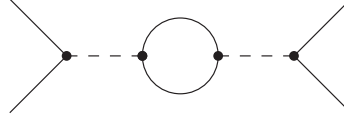


Figure 11.8.: A possible diagram  $\mathcal{F}^\tau$

Now we address the question how to cope with the imaginary counterterm (11.30). Suppose first we have a diagram containing *no* counterterm vertices, for example the one shown in figure 11.8. It contributes to an amplitude  $\mathcal{F}$  and we call this particular contribution - this diagram -  $\mathcal{F}^\tau$ . Since there are no counterterm vertices, we know that any circled region in this diagram can be identified as the complex conjugate of that region with reversed momenta. This is something that we are going to exploit. The trick is that a counterterm insertion can be generated as a derivative of an unstable propagator, as

$$\Delta^{\text{CMS}} i(2\pi)^4 (-i\bar{m}\bar{\Gamma}) \Delta^{\text{CMS}} \stackrel{(11.12)}{=} -\bar{m}\bar{\Gamma} \frac{\partial}{\partial \bar{m}\bar{\Gamma}} \Delta^{\text{CMS}}. \quad (11.31)$$

The diagrammatic equivalent of (11.31) is shown in figure 11.9. Multiple insertions can be

$$\bullet \text{---} \text{---} \textcircled{\times} \text{---} \bullet \quad \xrightarrow{k} \quad = \quad -\bar{m}\bar{\Gamma} \frac{\partial}{\partial \bar{m}\bar{\Gamma}} \bullet \text{---} \text{---} \bullet \quad \xrightarrow{k}$$

Figure 11.9.:  $\Delta^{\text{CMS}} i(2\pi)^4 (-i\bar{m}\bar{\Gamma}) \Delta^{\text{CMS}} = -\bar{m}\bar{\Gamma} \frac{\partial}{\partial \bar{m}\bar{\Gamma}} \Delta^{\text{CMS}}$ .

obtained by applying the differentiation multiple times;  $n$  insertions are obtained by acting with  $\frac{1}{n!}(-\bar{m}\bar{\Gamma})^n (\frac{\partial}{\partial \bar{m}\bar{\Gamma}})^n$  on the propagator. By this principle, *any* diagram can be generated from a diagram without any counterterm vertices. As an example, suppose that we are calculating an

amplitude  $\mathcal{F}$  in perturbation theory to order  $\alpha^3$ . Then a number of the contributing diagrams can be generated from  $\mathcal{F}^\tau$  (figure 11.8). These diagrams are the ones shown in front of the first equal sign in figure 11.10. The first two equalities of the figure show that, up to the required

$$\begin{aligned}
& \text{Diagram 1} + \text{Diagram 2} + \text{Diagram 3} + \text{Diagram 4} \\
& \text{Diagram 5} + \text{Diagram 6} + \dots \\
& \text{Diagram 7} + \dots \\
& \text{Diagram 8} \\
= & \text{Diagram 9} + \text{Diagram 10} + \text{Diagram 11} + \dots \\
& \text{Diagram 12} + \text{Diagram 13} + \text{Diagram 14} + \dots \\
& \text{Diagram 15} + \text{Diagram 16} + \text{Diagram 17} + \dots + \mathcal{O}(\alpha^4) \\
= & \text{Diagram 18} \text{ (in parentheses)} \text{ } \bigcirc \text{ } \text{Diagram 19} \text{ (in parentheses)} + \mathcal{O}(\alpha^4) \\
= & \sum_{n_{\tau_1}=0}^2 \frac{1}{n_{\tau_1}!} \left(-\bar{m}\bar{\Gamma} \frac{\partial}{\partial \omega_{\tau_2}}\right)^{n_{\tau_1}} \sum_{n_{\tau_2}=0}^2 \frac{1}{n_{\tau_2}!} \left(-\bar{m}\bar{\Gamma} \frac{\partial}{\partial \omega_{\tau_2}}\right)^{n_{\tau_2}} \mathcal{F}_\Omega^\tau \Big|_{\omega_{\tau_i}=0} + \mathcal{O}(\alpha^4)
\end{aligned}$$

Figure 11.10.: These diagrams can be generated from  $\mathcal{F}^\tau$  (figure 11.8).

accuracy, all these diagrams are obtained by inserting up to two full counterterm vertices in both unstable propagators of  $\mathcal{F}^\tau$ . To be able to express one such insertion at a specific propagator as a derivative of that specific propagator, we label the  $i$ -th unstable propagator of  $\mathcal{F}^\tau$  as  $\tau_i$ . Then, in every propagator  $\tau_i$ , we shift the width  $\bar{m}\bar{\Gamma} \rightarrow \bar{m}\bar{\Gamma} + \omega_{\tau_i}$ . The resulting diagram we call  $\mathcal{F}_\Omega^\tau$ . A counterterm insertion in the propagator  $\tau_i$  is then generated by applying the operator  $-\bar{m}\bar{\Gamma} \frac{\partial}{\partial \omega_{\tau_i}}$  to  $\mathcal{F}_\Omega^\tau$ . This means that all diagrams of figure 11.10 can be obtained by applying these kind of derivatives to  $\mathcal{F}_\Omega^\tau$  and setting  $\omega_{\tau_i} = 0$  afterwards. This is shown by the last equality in figure 11.10. Note that for this specific diagram  $\mathcal{F}^\tau$  we have to generate up to 2 counterterm insertions in every unstable propagator. The reason is that  $\mathcal{F}^\tau$  is a one-loop diagram, while we are doing perturbation theory to order  $\alpha^3$ . The difference between these numbers is  $m_\tau = 2$ . Thus

$$m_\tau := \text{P.T. order} - \# \text{ of loops in } \mathcal{F}^\tau. \quad (11.32)$$

By this procedure, we can generate *all* diagrams contributing to  $\mathcal{F}$  from *all* diagrams  $\mathcal{F}^\tau$  containing no counterterm vertices. The formal expression is

$$\mathcal{F} = \sum_\tau \prod_i \sum_{n_{\tau_i}=0}^{m_\tau} \frac{1}{n_{\tau_i}!} \left(-\bar{m}\bar{\Gamma} \frac{\partial}{\partial \omega_{\tau_i}}\right)^{n_{\tau_i}} \mathcal{F}_\Omega^\tau \Big|_{\omega_{\tau_i}=0}. \quad (11.33)$$



The LTE of the amplitude  $\mathcal{F}$  can now be obtained by writing the LTE's of  $\mathcal{F}_\Omega^\tau$  and subsequently applying the derivatives as prescribed by (11.33). The LTE of a diagram  $\mathcal{F}_\Omega^\tau$  contains diagrams whose vertices may be circled. Inside such a diagram, any unstable propagator with momentum  $k$  represents one of three expressions: if it connects two uncircled vertices it represents  $\Delta(k)$ ; if it connects two circled vertices it represents  $\Delta^*(-k)$ ; and if the propagator connects a circled vertex to an uncircled vertex - equivalently, if the propagator is being cut - it represent  $\Delta^\pm(k)$ . Note that we are using  $\Delta$  here as a shorthand for the CMS propagator  $\Delta^{\text{CMS}}$ . In the first case - if the propagator represents  $\Delta(k)$  - then differentiating that propagator will have the effect of inserting counterterms precisely as we just explained. If the propagator represents  $\Delta^*(-k)$  - the second case - then it lies inside a circled region. Since  $\mathcal{F}_\Omega^\tau$  contains no counterterm vertices, this circled region really is the complex conjugate of the region with reversed momenta. The effect of the differentiation as in (11.33) is then precisely to insert a complex conjugated counterterm vertex in this region, for

$$-\bar{m}\bar{\Gamma}\frac{\partial}{\partial\bar{m}\bar{\Gamma}}\Delta^*(-k) = \Delta^*(-k)i(2\pi)^4(-i\bar{m}\bar{\Gamma})^*\Delta^*(-k). \quad (11.34)$$

The diagrammatic equivalent of (11.34) is shown in figure 11.11. Thanks to (11.34), after having applied the derivative to a propagator inside a circled region, the region is still equal to its complex conjugate with reversed momenta. To illustrate these first two possibilities, we

$$-\bar{m}\bar{\Gamma}\frac{\partial}{\partial\bar{m}\bar{\Gamma}} \left( \bullet \xleftarrow{k} \bullet \right)^* = \left( \bullet \text{---} \text{---} \text{---} \left( \otimes \right) \text{---} \text{---} \bullet \right)^*$$

Figure 11.11.:  $-\bar{m}\bar{\Gamma}\frac{\partial}{\partial\bar{m}\bar{\Gamma}}\Delta^*(-k) = \Delta^*(-k)i(2\pi)^4(-i\bar{m}\bar{\Gamma})^*\Delta^*(-k)$ .

consider the LTE contribution of our example diagram  $\mathcal{F}^\tau$  (figure 11.8) that is shown in figure 11.12. Upon applying the derivatives according to (11.33), we obtain the diagrams on the RHS of the arrow in figure 11.12. These are precisely the diagrams that would arise from cutting the internal loop of all our *original* diagrams of figure 11.10 that *do* include counterterm vertices. Thanks to (11.34), the resulting circled regions - in this case the part of the diagram to the right of the cut - can now really be identified as the complex conjugate of these regions with reversed momenta. Thereby we have established step 2a) of the unitarity proof.

We did not adress the third case: what happens when an unstable propagator is being cut? This is the subject of the next two subsections.

Figure 11.12.: The transformation of a specific circling of  $\mathcal{F}^\tau$  under the differentiations (11.33)

### 11.5.3. Cutting an unstable propagator off resonance

In this paragraph we shall consider what becomes of a cut of an unstable propagator that is off resonance. More precisely, we shall see what becomes of a non-resonant cut propagator  $\Delta^\pm(p)$

in a diagram  $\mathcal{F}^\tau$  when it is acted upon with the derivatives of (11.33). By ‘off resonance’ we mean that we consider values of the cut propagator  $\Delta^\pm(p)$ ’s momentum for which

$$|p^0 \mp \sqrt{|\vec{p}|^2 + \bar{m}^2}|^2 \gg \bar{m}\bar{\Gamma}. \quad (11.35)$$

This means that we are far from the poles of  $\Delta^\pm(p)$ . Indeed, according to (11.22) these poles are located at  $p^0 = \pm\hat{p}^0 = \sqrt{|\vec{p}|^2 + \hat{m}^2}$ . An important point to note here is that a cut that violates the cut structure is always off resonance. The reason is that the corresponding  $\Delta^\pm(p)$  has  $\text{sgn}(p^0) = \mp 1$ , such that  $|p^0 \mp \sqrt{|\vec{p}|^2 + \bar{m}^2}|^2 \gtrsim \bar{m}^2 \gg \bar{m}\bar{\Gamma}$ . In this paragraph we shall show that these non-resonant cuts yield contributions that are of higher order in perturbation theory than the order under consideration. This will thus prove that cuts violating the cut structure can be ignored, thereby validating step 2b of the unitarity proof.

As argued before, the cut propagator  $\Delta^\pm(p)$  is a function of  $\bar{\Gamma}/\bar{m} \sim \alpha$ . Thereby, it contains contributions of all orders of perturbation theory. To make these more explicit, we shall expand  $\Delta^\pm(p)$  in  $\bar{\Gamma}/\bar{m}$ . Since we are off resonance, (11.28) tells us that the zeroth order term vanishes. Performing the expansion then yields

$$\begin{aligned} \Delta^\pm(p) &= -\frac{1}{(2\pi)^4} \frac{p^0 \mp 2\sqrt{|\vec{p}|^2 + \bar{m}^2}}{2\sqrt{|\vec{p}|^2 + \bar{m}^2}^3 (p^0 \mp \sqrt{|\vec{p}|^2 + \bar{m}^2})^2} \bar{m}\bar{\Gamma} + \mathcal{O}\left(\left(\frac{\bar{\Gamma}}{\bar{m}}\right)^3\right) \\ &:= \bar{m}\bar{\Gamma} f_\pm(\bar{m}\bar{\Gamma}). \end{aligned} \quad (11.36)$$

Since the term in the denominator satisfies  $(p^0 \mp \sqrt{|\vec{p}|^2 + \bar{m}^2})^2 \gg \bar{m}\bar{\Gamma}$  by (11.35),  $f_\pm(\bar{m}\bar{\Gamma})$  is analytic in  $\bar{m}\bar{\Gamma}$ .

Now we show that (11.36) becomes of higher order when acted upon with the derivatives (11.33). To this end, let us suppose we are doing perturbation theory to order  $n$ . We consider a contributing diagram  $\mathcal{F}^\tau$  with  $n - m_\tau$  loops; this is consistent with the definition (11.32) of  $m_\tau$ . Thus  $\mathcal{F}^\tau = \mathcal{O}(\alpha^{n-m_\tau})$ . Suppose that  $\mathcal{F}^\tau$  contains (at least) one propagator off resonance. We then consider  $\mathcal{F}_{\text{cut}}^\tau$ , which denotes the diagram  $\mathcal{F}^\tau$  with a cut through (one of) the off-resonant propagator(s). (11.33) then tells us that we have to apply  $m_\tau$  derivatives to the cut propagator (11.36) in  $\mathcal{F}_{\text{cut}}^\tau$ . The order of the resulting diagram  $\mathcal{F}_{\text{cut}}^{\tau, \text{res}}$  is then bounded from below as follows

$$\mathcal{O}\left(\mathcal{F}_{\text{cut}}^{\tau, \text{res}}\right) \geq \alpha^{n-m_\tau} \sum_{k=0}^{m_\tau} \frac{1}{k!} \left(-\xi \frac{\partial}{\partial \bar{m}\bar{\Gamma}}\right)^k \left(\bar{m}\bar{\Gamma} f_\pm(\bar{m}\bar{\Gamma})\right) \Big|_{\xi=\bar{m}\bar{\Gamma}} = \mathcal{O}(\alpha^{n+1}). \quad (11.37)$$

The last equality can be understood by noting that the summation actually represents a truncated Taylor expansion of  $\bar{m}\bar{\Gamma} f_\pm(\bar{m}\bar{\Gamma})$ . Explicitly,

$$\begin{aligned} 0 &= (\bar{m}\bar{\Gamma} - \xi) f_\pm(\bar{m}\bar{\Gamma} - \xi) \Big|_{\xi=\bar{m}\bar{\Gamma}} = \sum_{k=0}^{\infty} \frac{1}{k!} \left(-\xi \frac{\partial}{\partial \bar{m}\bar{\Gamma}}\right)^k \left(\bar{m}\bar{\Gamma} f_\pm(\bar{m}\bar{\Gamma})\right) \Big|_{\xi=\bar{m}\bar{\Gamma}} \\ &= \left\{ \sum_{k=0}^{m_\tau} \frac{1}{k!} \left(-\xi \frac{\partial}{\partial \bar{m}\bar{\Gamma}}\right)^k \left(\bar{m}\bar{\Gamma} f_\pm(\bar{m}\bar{\Gamma})\right) + \mathcal{O}(\alpha^{m_\tau+1}) \right\} \Big|_{\xi=\bar{m}\bar{\Gamma}}. \end{aligned} \quad (11.38)$$

In the second step we Taylor expanded  $(\bar{m}\bar{\Gamma} - \xi) f_\pm(\bar{m}\bar{\Gamma} - \xi)$  around  $\xi = 0$ ; in the last step we used  $\bar{\Gamma} \sim \alpha$ . Equation (11.38) implies that

$$\sum_{k=0}^{m_\tau} \frac{1}{k!} \left(-\xi \frac{\partial}{\partial \bar{m}\bar{\Gamma}}\right)^k \left(\bar{m}\bar{\Gamma} f_\pm(\bar{m}\bar{\Gamma})\right) \Big|_{\xi=\bar{m}\bar{\Gamma}} = \mathcal{O}(\alpha^{m_\tau+1}), \quad (11.39)$$

which in turn proves the last equality of (11.37). As promised, (11.37) shows that the cut of an unstable propagator off resonance gives a contribution of higher contribution in perturbation theory. Such cuts, including cut structure violating cuts, can thus be ignored.

#### 11.5.4. Cutting an unstable propagator near resonance

In the previous section it was shown that only cuts obeying the cut structure contribute. Thereby, we have succeeded in proving the steps 1, 2a and 2b of the unitarity proof. However, it is still not clear what is to become of cuts of unstable propagators that are close to resonance, i.e. whose momenta do not satisfy (11.35). According to the equation (11.20) proven by Veltman, only cuts of stable propagators should appear in the final cutting equation. In this paragraph we shall show that cuts of unstable propagators near resonance do indeed reduce to cuts of stable propagators.

##### Leading order cut

As a first step, we consider what becomes of a cut of an unstable propagator near resonance at leading order. Recalling that  $\Delta^\pm(p)$  is a function of  $\bar{\Gamma} \sim \alpha$ , we can find the leading order behaviour by taking the limit  $\bar{\Gamma} \downarrow 0$ .

$$\begin{aligned}
\text{---} \left[ \text{---} \right] \text{---} &= \Delta^\pm(p) \stackrel{(11.28)}{=} \frac{1}{(2\pi)^3} \theta(p^0) \delta(p^2 + \bar{m}^2) + \mathcal{O}(\alpha) = \frac{1}{(2\pi)^4} 2\pi \delta(2\omega_{\vec{p}}(p^0 \mp \omega_{\vec{p}})) + \mathcal{O}(\alpha) \\
&\stackrel{(9.44)}{=} \frac{1}{(2\pi)^4} \frac{2\bar{m}\bar{\Gamma}}{[-(p^0 \mp \omega_{\vec{p}})(p^0 \pm \omega_{\vec{p}})]^2 + (\bar{m}\bar{\Gamma})^2} + \mathcal{O}(\alpha) \\
&= \Delta^{\text{CMS}}(p) i(2\pi)^4 \frac{-2i\bar{m}\bar{\Gamma}}{(\Delta^{\text{CMS}})^*(p)} + \mathcal{O}(\alpha) \\
&= \Delta^{\text{CMS}}(p) i(2\pi)^4 (-2i) \text{Im}(\hat{\Sigma}) (\Delta^{\text{CMS}})^*(p) + \mathcal{O}(\alpha) \\
&\stackrel{\text{LTE}}{=} \text{---} \left[ \text{---} \right] \text{---} + \mathcal{O}(\alpha).
\end{aligned} \tag{11.40}$$

In going from the third to the fourth step we used that the the lowest order counterterm is designed to cancel the lowest order imaginary part of the self-energy, where we mean the self-energy calculated without using counterterms<sup>3</sup>; that is  $-i\bar{m}\bar{\Gamma} = -i\text{Im}(\hat{\Sigma})$ . Furthermore, the dots on both sides of the diagrams in (11.40) serve to emphasize that these diagrams are *not* amputated. Equation (11.40) shows that to leading order the cut of the bare unstable propagator equals the cut through its first loop correction, thus through *stable* particle propagators. This is precisely what is required by (11.20).

Note that both sides of (11.40) are of the same order in perturbation theory since we assume the propagator to be close to resonance, such that  $\Delta \sim g^{-2}$ . If we were off resonance, we would have  $\Delta \sim g^0$ , such that the loop cut in (11.40) would become  $\mathcal{O}(\alpha)$ . This is in agreement with the off-resonant result (11.36). We can thus summarize the two cases by

$$\text{---} \left[ \text{---} \right] \text{---} = \begin{cases} \mathcal{O}(\alpha) & \text{off resonance,} \\ \text{---} \left[ \text{---} \right] \text{---} + \mathcal{O}(\alpha) & \text{near resonance.} \end{cases} \tag{11.41}$$

<sup>3</sup>Recall that that we denote this ‘self-energy’ with a hat, i.e. as  $\hat{\Sigma}$ .

So in order to determine what expression to use for the cut at leading order, one has to determine whether the external momentum configuration of a diagram allows the propagator to become resonant. For example, suppose we want to calculate the imaginary part of the one-loop self-energy of the stable particle  $\Sigma_{\text{stable}}^{(1)}$ . We can utilize the LTE to do so. In cutting the internal unstable propagator to leading order we then have to distinguish cases as follows

$$\begin{aligned}
 i(2\pi)^4 2i\text{Im}(\Sigma_{\text{stable}}^{(1)}) &\stackrel{\text{LTE}}{=} \text{---} \text{---} \text{---} \text{---} \text{---} \text{---} \\
 &= \begin{cases} \mathcal{O}(\alpha^2) & \text{for } s \text{ below threshold,} \\ \text{---} \text{---} \text{---} \text{---} \text{---} \text{---} + \mathcal{O}(\alpha^2) & \text{for } s \text{ above threshold.} \end{cases} \quad (11.42)
 \end{aligned}$$

### Nesting resummed propagators

When considering diagrams of higher order, we need to take into account corrections to the leading order result (11.41). A way to do this would be - in principle - to explicitly perform an expansion of  $\Delta^\pm$  in higher orders of  $\bar{\Gamma}/\bar{m}$  and see what this becomes when we act upon it with the derivatives of (11.33). This we shall not do. In fact, we shall abandon the approach of generating counterterms by (11.33) altogether. Instead, we shall include all counterterms explicitly and reorganize our diagrams in a convenient way. Note that this leaves the steps 2a and 2b of the unitarity proof valid; we can still identify circled regions as the complex conjugated regions with reversed momenta and only cuts obeying the cut structure survive. Generating the counterterms by (11.33) was simply a means to prove so.

The approach we shall take is to combine several diagrams into diagrams with propagators that include corrections up to a certain order. By a slight abuse of notation, we shall call propagators that include all their corrections up to a certain order *dressed propagators*. Usually a dressed propagator is synonym for a resummed propagator, which includes corrections of all orders. The latter we shall explicitly refer to as *resummed propagators*. The distinction is not essential, for the difference between what we refer to as dressed and resummed propagators is of higher order in perturbation theory; still, it pays to be precise. The idea of grouping the diagrams into diagrams with dressed propagators is as follows. Suppose we perform a perturbation expansion to order  $\alpha^n$ . We thus consider diagrams with up to  $n$  loops/counterterms. Then for any diagram with at most  $n - 1$  loops/counterterms that has an internal propagator, there will be one or more higher order diagrams that are identical except for including a self-energy correction to that internal propagator. All these diagrams together can be written as the original diagram with the internal propagator replaced by a dressed propagator. As an example, suppose we are calculating the four-point function of four stable particles to order  $\alpha^2$ . We can summarize the following two contributing diagrams as follows

$$\begin{aligned}
 &\text{---} \text{---} \text{---} \text{---} \text{---} \text{---} + \text{---} \text{---} \text{---} \text{---} \text{---} \text{---} = \text{---} \text{---} \text{---} \text{---} \text{---} \text{---} \\
 &\text{with } \text{---} \text{---} \text{---} \text{---} \text{---} \text{---} := \text{---} \text{---} \text{---} \text{---} \text{---} \text{---} + \text{---} \text{---} \text{---} \text{---} \text{---} \text{---} . \quad (11.43)
 \end{aligned}$$

The summarizing diagram on the RHS can in turn be identified as a self-energy correction to the unstable propagator of the tree-level diagram. We can thus repeat the procedure and contain the RHS diagram of (11.43) in the tree-level diagram with a dressed unstable propagator (the first diagram after the equal sign in (11.44)). This dressed unstable propagator will thus contain a diagram that again contains a dressed propagator. By this procedure diagrams are thus summarized in terms of *nested* dressed propagators. In this way, all diagrams contributing to the four point function at order  $\alpha^2$  can be written as

$$\begin{aligned}
 \text{Diagram} &= \text{Diagram} + \text{Diagram} + \text{Diagram} + \text{Diagram} + \text{external leg permutations} + \\
 &+ \text{Diagram} + \text{other 2-loop diagrams} + \mathcal{O}(\alpha^3),
 \end{aligned}
 \tag{11.44}$$

with

$$\begin{aligned}
 \text{Dashed Propagator} &:= \text{Dashed Propagator} + \text{Dashed Propagator} + \text{Dashed Propagator} + \text{Dashed Propagator} + \text{Dashed Propagator} + \text{Dashed Propagator} + \text{Dashed Propagator} + \text{Dashed Propagator}, \\
 \text{Solid Propagator} &:= \text{Solid Propagator} + \text{Solid Propagator} + \text{Solid Propagator} + \text{Solid Propagator}.
 \end{aligned}
 \tag{11.45}$$

If we want, we can replace the dressed propagators by resummed propagators (where a self-energy of up to two loops/counterterms is used in the resummation), for their difference is  $\mathcal{O}(\alpha^3)$ . This idea we shall exploit later on. Note that equation (11.45) does indeed show that the dressed propagators are defined in terms of other dressed propagators. This is perfectly fine, for in order to determine the dressed propagators on the LHS of (11.45) up to  $n$  loops/counterterms, one only needs the dressed propagators on the RHS up to  $n - 1$  loops/counterterms. The dressed propagators are thus defined iteratively.

Now we can apply the LTE to all the diagrams. In order to do so, we shall *define* the cut through a dressed propagator as the sum of all allowed cuts through its composing diagrams. For the dressed propagators of equation (11.45), we thus define

$$\begin{aligned}
 \text{Dashed Propagator with Cut} &:= \sum_{\text{allowed cuts}} \left( \text{Dashed Propagator} + \dots + \text{Dashed Propagator} \right), \\
 \text{Solid Propagator with Cut} &:= \sum_{\text{allowed cuts}} \left( \text{Solid Propagator} + \dots + \text{Solid Propagator} \right).
 \end{aligned}
 \tag{11.46}$$

We have seen in the previous section that only cuts survive that satisfy the cut structure. We thus only have to consider single vertical cuts. This means that we can summarize all allowed cuts of all the diagrams that contribute to the amplitude, by all single vertical cuts through the diagrams written in terms of dressed propagators. For examples, the cuts of the diagrams of

(11.43) can be written as - neglecting the cuts through the left and right unstable propagator for the moment -

with (11.47)

Note that the cut through the internal bare unstable propagator is to be evaluated by (11.41). Similarly, all cuts through all diagrams contributing to the four point function can be written as all single vertical cuts through the diagrams shown in (11.44). The cuts through the dressed propagators are then given by (11.46).

We shall now rewrite the cut through a dressed unstable propagator. This is done by adding higher order terms to make it equal a resummed propagator. We let  $\Sigma$  be shorthand for the self-energy  $\Sigma^{(n)}(p^2, \hat{m}^2)$  evaluated up to order  $n$ , the order at which we are calculating our amplitude  $\mathcal{F}$ . Using  $n = 2$  for illustration, we rewrite the cut of the dressed propagator as follows

$$\begin{aligned}
\text{Diagram with cut through dressed propagator} &= \sum_{\text{allowed cuts}} \left( \text{Diagram 1} + \dots + \text{Diagram 2} \right) \\
&\stackrel{\text{LTE}}{=} -2i \text{Im} \left( \text{Diagram 1} + \dots + \text{Diagram 2} \right) \\
&= -2i \text{Im} \left( \text{Diagram 1} + \text{Diagram 3} + \text{Diagram 4} + \dots \right) \quad + \mathcal{O}(\alpha^3) \\
&= i(2\pi)^2 (-2i) \text{Im} \left[ \frac{1}{p^2 + \hat{m}^2 - \Sigma} \right] \quad + \mathcal{O}(\alpha^3) \\
&= i(2\pi)^2 (-2i) \frac{1}{p^2 + \hat{m}^2 - \Sigma} \text{Im} \left[ (p^2 + \hat{m}^2 - \Sigma)^* \right] \left( \frac{1}{p^2 + \hat{m}^2 - \Sigma} \right)^* \quad + \mathcal{O}(\alpha^3) \\
&= \frac{1}{p^2 + \hat{m}^2 - \Sigma} i(2\pi)^4 2i \text{Im} \left[ \Sigma + i\bar{m}\bar{\Gamma} \right] \left( \frac{1}{p^2 + \hat{m}^2 - \Sigma} \right)^* \quad + \mathcal{O}(\alpha^3) \\
&\stackrel{\text{LTE}}{=} (-1) \cdot \text{Diagram 5} \quad + \mathcal{O}(\alpha^3).
\end{aligned} \tag{11.48}$$

Note that  $\Sigma + i\bar{m}\bar{\Gamma}$  is the self-energy  $\Sigma(p^2, \hat{m}^2)$  *without* the counterterm  $-i\bar{m}\bar{\Gamma}$  (figure 11.1 times  $-1$ ), which is otherwise present in  $\Sigma(p^2, \hat{m}^2)$ . In the last step we defined the cut through  $\Sigma + i\bar{m}\bar{\Gamma}$  as the sum of all possible cuts through its composing diagrams. What we have accomplished by (11.48) is that we have rewritten the cut through a dressed propagator in terms of cuts through 1PI-diagrams, which is a simplification. As part of cuts of these 1PI-diagrams, we may again encounter cuts of dressed propagators. To calculate these we can again employ (11.48).

The procedure to calculate all cuts of an amplitude and thus the LHS of (11.20) is then

1. write all diagrams up to the desired accuracy in terms of dressed propagators,
2. apply all cuts to these diagrams that obey the cut structure,
3. to evaluate a cut of a dressed *stable* propagator, use its definition in terms of cuts of its composing diagrams, e.g. the first line of (11.46).
4. to evaluate a cut of a dressed *unstable* propagator, use (11.48).
5. Both the dressed stable propagator and  $\Sigma(p^2, \hat{m}^2) + i\bar{m}\bar{\Gamma}$  may again contain dressed propagators. To evaluate their cuts, apply steps 2, 3 and 4 iteratively, until
6. the desired accuracy has been reached. At this point, the cut of a dressed stable propagator just becomes the cut of bare stable propagator; the cut of an unstable propagator becomes (11.41).

In the last step, (11.41) guarantees that cuts of unstable propagators are either of higher order than the desired accuracy, or replaced by a cut through a loop of stable particles. Therefore, no cuts through unstable particles survive, which is precisely what is required by (11.20). Since all the ingredients of the unitarity proof (steps 1, 2a and 2b) are shown to be satisfied, this then proves that (11.20) is valid perturbatively in the CMS.

As an example, we apply this cutting procedure to produce all cuts up to order  $\alpha^2$  of the first diagram contributing to the four point function (11.44).

(11.49)

To evaluate the cuts of the self-energy diagrams, we use

(11.50)

To evaluate the cuts through the bare unstable propagators we now use (11.41). We shall assume  $s > (2m_{\text{stable}} + \bar{m})^2$ , such that the bare unstable propagators can become resonant. Therefore,

we have to use the second expression of (11.41) for their cut. The cuts of the diagram (11.49) then become

$$\begin{aligned}
 \text{Diagram} &= \text{Diagram}_1 + \text{Diagram}_2 + \text{Diagram}_3 + \text{Diagram}_4 \\
 &+ \text{Diagram}_5 + \text{Diagram}_6 + \text{Diagram}_7 \\
 &+ \text{Diagram}_8 + \text{Diagram}_9 + \text{Diagram}_{10} + \text{symm.} \quad ,
 \end{aligned}
 \tag{11.51}$$

where symmetry factors are again left implicit. This does indeed show that only cuts through stable propagators survive, which is in agreement with (11.20).



# 12. Effective Field Theory (EFT)

## 12.1. Introduction

We have seen in chapter 9 that ordinary perturbation theory in the coupling constant  $g$  breaks down for a diagram with a single internal propagator, when its momentum  $p_A$  is close to its mass  $m$ . This can be viewed as a consequence of the fact that in this phase space region  $g$  is not the only small parameter. Instead, there are *two* small parameters: both  $g$  and

$$\delta := \frac{-p_A^2 - m^2}{m^2}. \quad (12.1)$$

Ordinary perturbation theory in  $g$  expands an amplitude  $\mathcal{M}$  as

$$\mathcal{M} = f_0(\delta) + \alpha f_1(\delta) + \alpha^2 f_2(\delta) + \dots \quad (12.2)$$

The coefficient functions  $f_n$  are all of the same order in  $g$  so  $\alpha \sim g^2$  explicitly indicates the suppression of higher order terms. The problem with the expansion (12.2) is that when  $\delta$  becomes small, the coefficient functions  $f_n(\delta)$  may become large. For example, a correction to the propagator consisting of  $n$  sequential loops<sup>1</sup> has coefficient function  $f_n(\delta) \sim \frac{1}{\delta^{n+1}}$ . In the phase-space region where  $\delta$  is of the same order of  $\alpha$ , this term thus contributes to 12.2 as  $\alpha^n f_n(\delta) \sim \frac{1}{\delta} \left(\frac{\alpha}{\delta}\right)^n \sim \frac{1}{\delta}$ , which is independent of  $n$ . Therefore, all these terms (for any  $n$ ) have to be taken into account. This is done by resumming the propagator, which is implicitly done in the CMS.

Beneke, Chapovsky, Signer and Zanderigni have developed a different approach. They have constructed an effective field theory (EFT) to describe the unstable particle in the resonance region [24–26]. The purpose of this chapter is to explain this method. The idea of the EFT is to set up a perturbation expansion in  $g^2$  and  $\delta$  *simultaneously*, assuming that  $g^2 \sim \delta$ . As such, it is only expected to be valid in the region of phase-space where

$$g^2 \ll 1, \quad \delta \ll 1, \quad \text{and} \quad g^2 \sim \delta. \quad (12.3)$$

An amplitude is then expanded as

$$\begin{aligned} \mathcal{M} &\sim \sum_n \left(\frac{g^2}{\delta}\right)^n \left\{ 1(\text{LO}); g^2, \delta(\text{NLO}); g^4, g^2\delta, \delta^2(\text{NNLO}); \dots \right\} \\ &= h_0\left(\frac{g^2}{\delta}\right) + g^2 h_{1a}\left(\frac{g^2}{\delta}\right) + \delta h_{1b}\left(\frac{g^2}{\delta}\right) + g^4 h_{2a}\left(\frac{g^2}{\delta}\right) + g^2 \delta h_{2b}\left(\frac{g^2}{\delta}\right) + \delta^2 h_{2c}\left(\frac{g^2}{\delta}\right) + \dots \end{aligned} \quad (12.4)$$

If the perturbation expansion is set up correctly, gauge invariance and unitarity are taken care of automatically. There is an intermediate phase-space region where both expansions (12.2) and (12.4) are expected to give reliable results. This is the region where  $\delta$  is small and  $\frac{g^2}{\delta}$  is small

---

<sup>1</sup>For visualization: we mean the  $n$ -th term in figure 9.4, where each  $1PI$ -blob is to be replaced by a single loop.

(but not *very* small). This is the region where the two approaches can be matched, as will be explained in paragraph 12.3.4) of this chapter.

### Definition of the model

To introduce the essential ideas of the EFT without too many distracting complications, Beneke et al. introduce a toy model. It features an unstable scalar particle, described by a complex field  $\phi$  with renormalized mass  $m$ . The unstable particle couples by Yukawa interactions to two massless fermion fields  $\psi$  and  $\chi$ . The fields  $\phi$  and  $\psi$  are charged electromagnetically and thus couple to a  $U(1)$  gauge field  $A^\mu$ . The Lagrangian reads

$$\begin{aligned} \mathcal{L} = & - (D_\mu \phi)^\dagger (D^\mu \phi) - m^2 |\phi|^2 - \bar{\psi} \not{D} \psi - \bar{\chi} \not{D} \chi - \frac{1}{4} F_{\mu\nu} F^{\mu\nu} - \frac{1}{2} (\lambda \partial_\mu A^\mu)^2 \\ & + y \phi \bar{\psi} \chi + y^* \phi^\dagger \bar{\chi} \psi - \frac{\tilde{\lambda}}{4} (\phi^\dagger \phi)^2 + \mathcal{L}_{\text{CT}}. \end{aligned} \quad (12.5)$$

We define  $\alpha_g := \frac{g^2}{4\pi}$ ,  $\alpha_y := \frac{|y|^2}{4\pi}$ , and assume that  $\alpha_g \sim \alpha_y \sim \alpha$ . The  $\phi^4$ -term has to be included for renormalizability purposes. Since the relevant counterterm is of order  $\alpha^2$ , we can assume that  $\tilde{\lambda} \sim \alpha^2$ . As a result, the  $\phi^4$ -term only becomes relevant at NNLO in perturbation theory and can safely be ignored throughout this chapter. The gauge symmetry of the Lagrangian (12.5) (with  $\lambda = 0$ ), is the  $U(1)$  symmetry familiar from chapter 3

$$\left\{ \begin{array}{l} \phi \rightarrow e^{ig\xi(x)} \phi \\ \psi \rightarrow e^{ig\xi(x)} \psi \\ A_\mu \rightarrow A_\mu + \partial_\mu \xi(x). \end{array} \right. \quad (12.6)$$

The process of interest is  $\psi\bar{\chi} \rightarrow \psi\bar{\chi}$  forward scattering, which proceeds at tree-level through the production and decay of a virtual unstable scalar  $\phi$ . The tree-level diagram is shown in figure 12.1. The purpose of this chapter is to construct an EFT to capture this process in terms of a simultaneous expansion in  $\alpha$  and  $\delta$ , as in (12.4). We shall thus assume to be in the region of phase space described by (12.3), i.e. we shall assume that  $s := -p_A^2 = -(q_1 + q_2)^2$  is such that  $\delta = \frac{s-m^2}{m^2} \sim \alpha \ll 1$ . Before explaining how the EFT is constructed, we shall introduce a concept used in this construction: the expansion by regions.

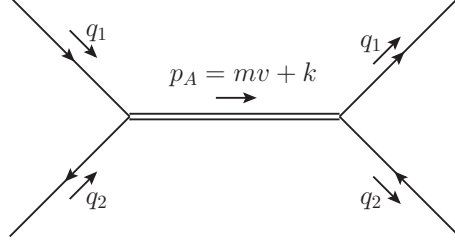
## 12.2. Expansion by regions

### 12.2.1. A simple example

The expansion by regions is a method to divide an integral into several integrals that are supposed to be easier - or more illuminating - to evaluate [27]. Before outlining the general procedure, we shall illustrate the method by a simple example, following a lecture by Thomas Becher [28]. This example is also meant to illustrate some of the reasoning why the method should be valid.

Consider the following one-dimensional integral

$$I = \int_0^\infty dk f(k), \quad \text{where} \quad f(k) := \frac{k}{(k^2 + m_1^2)(k^2 + m_2^2)} \quad \text{and} \quad m_1 \ll m_2. \quad (12.7)$$



Notation:

- the double line denotes the unstable scalar  $\phi$ .
- a solid line denotes a propagator of either a  $\psi$  or  $\chi$  fermion. By convention, in this chapter the upper fermion line always corresponds to  $\psi$  and the lower to  $\chi$ .

This notation here is very similar to the notation used in Feynman diagrams of the EFT. To avoid confusion, throughout this chapter we shall mention explicitly whether a diagram denotes a full theory diagram or an EFT diagram. This is a full theory diagram.

Figure 12.1.:  $\psi\bar{\chi} \rightarrow \psi\bar{\chi}$  forward scattering

In this case, the full integral can be calculated explicitly and subsequently approximated by using  $m_1 \ll m_2$ , as follows.

$$I = \frac{1}{m_2^2 - m_1^2} \int_0^\infty dk \left[ \frac{k}{k^2 + m_1^2} - \frac{k}{k^2 + m_2^2} \right] = \frac{\ln(\frac{m_1}{m_2})}{m_1^2 - m_2^2} \approx -\frac{\ln(\frac{m_1}{m_2})}{m_2^2}. \quad (12.8)$$

Suppose that we are not able to perform this full integral. Then we may exploit the hierarchy of scales  $m_1 \ll m_2$  before performing the integration, by expanding the integrand  $f(k)$  appropriately. This can be done by introducing a separator  $\Lambda$  satisfying  $m_1 \ll \Lambda \ll m_2$ , to divide the integration into two regions as

$$I = \int_0^\Lambda dk f(k) + \int_\Lambda^\infty dk f(k). \quad (12.9)$$

In the region  $0 < k < \Lambda$ , which we shall refer to as the *soft* region,  $f(k)$  can be expanded by using  $k^2 < m_2^2$ . We shall name the leading order term of this expansion  $f_{\text{soft}}(k)$ . Similarly, in the region  $\Lambda < k < \infty$  - the *hard* region - the scaling  $k^2 \gg m_1^2$  can be used to expand  $f(k)$ . The resulting LO term is called  $f_{\text{hard}}(k)$ . The integral (12.9) is thus rewritten as

$$I = \int_0^\Lambda dk f_{\text{soft}}(k) + \int_\Lambda^\infty dk f_{\text{hard}}(k), \quad \text{where} \quad \begin{cases} f_{\text{soft}}(k) = \frac{1}{m_2^2} \frac{k}{k^2 + m_1^2} \\ f_{\text{hard}}(k) = \frac{1}{k(k^2 + m_2^2)}. \end{cases} \quad (12.10)$$

So far nothing surprising has happened.

The surprising part - and the essence of the method - comes now. We extend the integration domains of both integrals of (12.10) to the *complete* original integration domain  $0 < k < \infty$ . That is

$$I \stackrel{?}{=} \int_0^\infty dk f_{\text{soft}}(k) + \int_0^\infty dk f_{\text{hard}}(k). \quad (12.11)$$

The question mark above the equal sign serves to indicate that we have no reason yet to believe that the sum of these integrals is indeed equal to  $I$ . First, we shall show that (12.11) does in fact hold true by explicit calculation. Afterwards we shall argue why this had to be the case. Note that the extension of the integration domains gives rise to a UV divergence in the first integral of (12.11) and an IR divergence in the second. The prescription of the method is to use dimensional regularization to regularize these divergencies. Since  $I$  is finite, these two divergencies must cancel against each other if (12.11) is to hold true. We now show that (12.11) indeed holds true by explicit calculation. To regularize the integrals, we shall work in  $1 + \epsilon$  dimensions.

$$\int_0^\infty d^{1+\epsilon}k f_{\text{soft}}(k) = \frac{1}{m_2^2} \int_0^\infty dk \frac{k^{1+\epsilon}}{k^2 + m_1^2}. \quad (12.12)$$

By the standard integral

$$\int_0^\infty dx \frac{x^{2\beta-1}}{(x^2 + m^2)^\alpha} = \frac{\Gamma(\beta)\Gamma(\alpha - \beta)}{\Gamma(\alpha)} \frac{1}{2(m^2)^{\alpha-\beta}}, \quad (12.13)$$

(12.12) becomes

$$\int_0^\infty d^{1+\epsilon}k f_{\text{soft}}(k) = \frac{1}{2m_2^2} \Gamma(1 + \frac{\epsilon}{2}) \Gamma(-\frac{\epsilon}{2}) m_1^\epsilon = -\frac{\mu^\epsilon}{m_2^2} \left[ \frac{1}{\epsilon} + \ln\left(\frac{m_1}{\mu}\right) + \mathcal{O}(\epsilon) \right]. \quad (12.14)$$

Similarly, we calculate

$$\begin{aligned} \int_0^\infty d^{1+\epsilon}k f_{\text{hard}}(k) &= \int_0^\infty \frac{dk}{k} \frac{k^\epsilon}{k^2 + m_1^2} = \frac{1}{m_2^2} \int_0^\infty dq \frac{q^{1-\epsilon}}{q^2 + m_2^2} \stackrel{(12.13)}{=} \frac{1}{2m_2^2} \Gamma(1 - \frac{\epsilon}{2}) \Gamma(\frac{\epsilon}{2}) m_2^\epsilon \\ &= \frac{\mu^\epsilon}{m_2^2} \left[ \frac{1}{\epsilon} + \ln\left(\frac{m_2}{\mu}\right) + \mathcal{O}(\epsilon) \right]. \end{aligned} \quad (12.15)$$

In the second step we made the substitution  $k \rightarrow q = \frac{1}{k}$ . Adding (12.14) and (12.15) together, we do indeed find that the poles in  $\epsilon$  vanish and that the finite parts add up to

$$\int_0^\infty dk f_{\text{soft}}(k) + \int_0^\infty dk f_{\text{hard}}(k) = -\frac{\ln(\frac{m_1}{m_2})}{m_2^2} \stackrel{(12.8)}{=} I. \quad (12.16)$$

This result may seem very magical - why would it be allowed to extend the integration regions the way we did? To understand this, we first assume that  $k$ ,  $m_1$  and  $m_2$  have mass dimension 1, as suggested by the notation. Then we note that the original integrand (12.7) involves two scales:  $m_1$  and  $m_2$ . On the other hand, the two integrands (12.11) that arise by applying the expansion by regions, only contain a single scale. The first integrand only contains the large mass  $m_2$  as a scale, whereas the second integrand only contains the small mass  $m_1$  as scale (the factor  $\frac{1}{m_2^2}$  can be pulled outside the integral). This is a result precisely of making the soft approximation ( $k \ll m_2^2$ ) and the hard approximation ( $k \gg m_1^2$ ) respectively. To understand

why the step from (12.10) to (12.11) is allowed, we consider the part that is added to  $I$  in this step

$$I_{\text{extra}} = \int_{\Lambda}^{\infty} dk f_{\text{soft}}(k) + \int_0^{\Lambda} dk f_{\text{hard}}(k). \quad (12.17)$$

The claim of the strategy of regions is that these two integrals cancel against each other when using dimensional regularization. The nice thing of (12.17) is that we now encounter  $f_{\text{soft}}(k)$  integrated over the hard region and  $f_{\text{hard}}(k)$  over the soft region. We can thus use the hard approximation in the first integral and the soft approximation in the second.

$$\begin{cases} \int_{\Lambda}^{\infty} d^{1+\epsilon}k f_{\text{soft}}(k) = \frac{1}{m_2^2} \int_{\Lambda}^{\infty} d^{1+\epsilon}k \frac{k}{k^2 + m_1^2} \stackrel{k^2 \gg m_1^2}{=} \frac{1}{m_2^2} \int_{\Lambda}^{\infty} d^{1+\epsilon}k \frac{1}{k} \sim \Lambda^{\epsilon} \\ \int_0^{\Lambda} d^{1+\epsilon}k f_{\text{hard}}(k) = \int_0^{\Lambda} d^{1+\epsilon}k \frac{1}{k(k^2 + m_2^2)} \stackrel{k^2 \ll m_2^2}{=} \frac{1}{m_2^2} \int_0^{\Lambda} d^{1+\epsilon}k \frac{1}{k} \sim \Lambda^{\epsilon}. \end{cases} \quad (12.18)$$

Here is what happened in words. Making the hard approximation in the first integral eliminates the remaining mass scale  $m_1$  from the integral. As a result, the only remaining mass scale in the integral is the cut-off  $\Lambda$ . For dimensional reasons, the integral thus has to be proportional to  $\Lambda^{\epsilon}$ . Similarly, making the soft approximation in the second integral eliminates the mass scale  $m_2$  from the integral. Since  $m_1$  was already eliminated as a scale from that integral, also here the only remaining mass scale is  $\Lambda$ . Again, the integral must consequently be proportional to  $\Lambda^{\epsilon}$  to attain the right mass dimension. The last step is to note that  $I_{\text{extra}}$  (12.17) is independent of  $\Lambda$ . The reason is that it is defined as the difference between the RHS of (12.11), which is independent of  $\Lambda$ , and (12.10), which is also independent of  $\Lambda$  (since  $I$  is). This means that the sum of the two integrals in (12.17) must be independent of  $\Lambda^{\epsilon}$ . Since we just found that both integrals are proportional to  $\Lambda^{\epsilon}$ , both integrals must cancel each other. This is why the expansion by regions works. Alternatively, one can note that the two integrals of (12.18) add up to  $m_2^{-2} \int_0^{\infty} d^{1+\epsilon}k k^{-1}$ , which is scaleless and therefore 0.

### 12.2.2. The general procedure

The integrals that we encounter in the calculation of Feynman diagrams are typically much harder to evaluate than our example (12.7). Their calculation may even be impossible. The expansion by regions may then simplify the integrands in such a way that the resulting integrals become possible to evaluate analytically. The general procedure prescribed by the method is as follows [27, 29–32].

1. Divide the integration domain into suitable regions. Since the domain is typically a multi-dimensional space - four-dimensional for a one-loop calculation - there are many regions that can in principle be identified. The relevant regions are usually determined in the context of the problem at hand, by considering the structure of the integrand and the limits of the integration variable in which singularities occur. Typically distinguished are the hard region, the soft region and (a) collinear region(s).
2. Expand the integrand in the appropriate way in every region. Then, integrate every expanded integrand *over the entire integration domain*, using dimensional regularization to regulate possible divergencies.

3. Take into account that any scaleless integral vanishes in dimensional regularization.

The sum of the integrals then equals the original integral, which is a very non-trivial result. For certain types of expansions the strategy has been proven to be correct. For other types of expansions very non-trivial checks have successfully been performed to show its correctness [33]. However, a general mathematical proof of the method does not exist [29].

## 12.3. Setting up the EFT

As explained in section 12.1, the aim of the EFT is to calculate amplitudes in an expansion in  $\alpha$  and  $\delta$  simultaneously. We thus wish to obtain the expansion (12.4) up to a certain order in  $\alpha$  and  $\delta$ , say to order  $n$ . The approach will be to construct a Lagrangian accomodating such an expansion. The first step is to construct the Lagrangian up to order  $n$ . This Lagrangian then dictates Feynman rules, by which the sought after amplitude can be found to order  $n$ . In other words, the expansion in  $\alpha$  and  $\delta$  is implemented at the level of the EFT Lagrangian. The purpose of this section is to construct that Lagrangian.

### 12.3.1. Identifying the relevant modes and factorization

#### The soft modes

The EFT shall not contain all the fields as they are present in the full theory Lagrangian (12.5). The reason is that the fields in (12.5) can give rise to factors in Feynman diagrams that scale differently with  $\delta$  for different momenta. For example, the scalar field  $\phi$  gives rise to the propagator  $\frac{1}{i(2\pi)^4} \frac{1}{P^2+m^2}$ , where  $P$  denotes the momentum. Let us suppose that the propagator is part of a loop, such that  $P$  can take any value. When  $-P^2$  is close to  $m^2$ , the propagator scales as  $\frac{1}{\delta}$ . When this is not the case, the propagator scales as  $\delta^0$ . To make this statement more precise, we decompose the momentum as

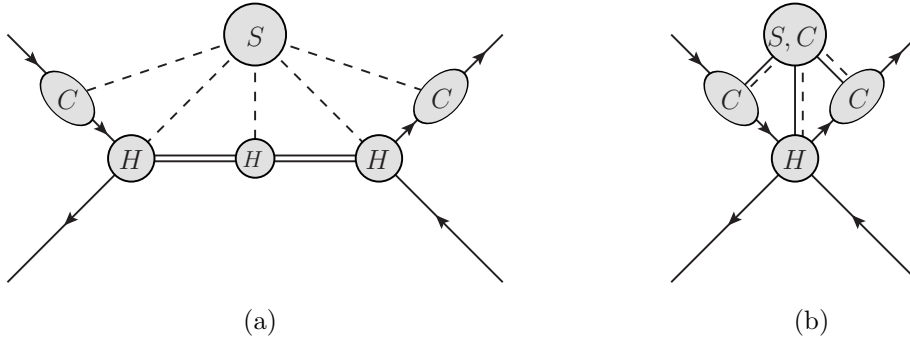
$$P = mv + k. \tag{12.19}$$

In (12.19)  $v$  is some unit vector satisfying  $v^2 = -1$ ;  $k = 0$  thus corresponds to  $P$  being on-shell. We call a fluctuation  $k$  soft if it scales as

$$k \sim m(\delta, \delta, \delta, \delta). \tag{12.20}$$

For soft fluctuations then, the propagator scales as  $\frac{1}{\delta}$ ; for other fluctuations - hard fluctuations - it scales as  $\delta^0$ . The point is that this possible difference in scaling is not manifest at the level of the full theory Lagrangian. Therefore, we associate a field  $\phi_v$  with only soft fluctuations. We shall call this the *soft* scalar mode, but keep in mind that we really refer to soft fluctuations around  $P = mv$ . The hard fluctuations are integrated out, such that the EFT only contains the soft mode  $\phi_v$  as a scalar field. How this integrating out of the hard fields is done is explained in paragraph 12.3.2.

The reason to integrate out the hard fluctuations can also be understood in a more intuitive way. If we interpret the process under consideration in a classical way, then we distinguish three stages: production of the scalar, propagation of the scalar and decay of the scalar. The timescale of both the production and decay is  $\frac{1}{m}$ , while the timescale of propagation is much larger:  $\frac{1}{\Gamma}$ . Production and decay are thus separated by a long time interval. Quantum mechanically this means that only fluctuations of the scalar with long wavelengths (soft momenta) can



Notation:

- The double line represents a  $\phi_v$ -propagator.
- The solid lines represent the fermions  $\psi_{c1}$  and  $\chi_{c2}$ .
- The  $H$ -vertices represent hard corrections.
- The  $C$ -vertices represent collinear corrections to the external fermions.
- The dotted lines emerging from the  $S$  represent possible loops by soft modes. These can be either  $\phi_v$ -lines, soft photons or soft fermions.
- Similarly, in figure 12.2b, the solid lines emerging from the  $S, C$ -blob represent possible collinear loops.

Figure 12.2.: Reduced topologies of scattering diagrams in the EFT

simultaneously resolve the details of the production and the decay. These modes have to be kept as a dynamical degree of freedom in the theory; they are represented by  $\phi_v$ . The hard modes on the other hand cannot ‘see’ the production and decay simultaneously. Therefore, we expect the hard modes only to yield corrections to production, propagation and decay *separately*. These corrections *factorize*: the total correction they give rise to is the product of their corrections to the production, propagation and decay of the scalar. This idea is depicted in figure 12.2a, which shows the corresponding reduced diagram topology that the EFT gives rise to. In figure 12.2a, the double line now represents the soft scalar field  $\phi_v$ ; the ‘H-vertices’ represent the mentioned hard corrections. The figure does indeed show that it is only the soft  $\phi_v$ -field that connects the production and decay, whereas the hard corrections factorize as corrections to production, propagation and decay. It turns out that some corrections do not factorize. These are very generally incorporated in the EFT as a 4-fermion vertex. Therefore the EFT also embodies diagrams with the reduced topology of figure 12.2b. These diagrams do not proceed via a resonant scalar and thus include all ‘background’ scattering processes.

Distinguishing soft and hard fluctuations of the scalar automatically leads us to distinguish soft and hard photons, as well as soft and hard fermions. The reason is that the scalar couples to photons and fermions in the full theory. To understand this, suppose that in the full theory a scalar near resonance - a soft scalar mode - emits or absorbs a photon (fermion). Then the scalar mode will only stay soft if the photon (fermion) is soft. Otherwise the scalar becomes a hard mode, which is not present as a dynamical field in the EFT. Consequently, the soft scalar  $\phi_v$  can only couple in the EFT to a soft photon field  $A_s^\mu$  and to soft fermion fields  $\psi_s$  and  $\chi_s$ . In obtaining the EFT from the full theory, hard photons and hard fermions are thus also integrated out. Again, this results in the EFT in hard corrections that are expected to factorize.

The part of the EFT Lagrangian that describes the soft modes  $\phi_v$ ,  $A_s^\mu$ ,  $\psi_s$  and  $\chi_s$ , and their interactions, is  $\mathcal{L}_{\text{HSET}}$ . The soft modes will thus provide quantum corrections in the EFT in the usual way: as loops with Feynman rules governed by  $\mathcal{L}_{\text{HSET}}$ . These loop corrections

coincide with the soft part of the full theory loop corrections, in the sense of the expansion by regions. The hard parts of the full theory loop corrections are represented in the form of hard corrections in the EFT. These corrections are introduced in the EFT Lagrangian as terms with coefficients that are in first instance unspecified. These coefficients are then determined by *matching* the EFT with the full theory. The matching procedure is discussed in more detail in section 12.3.4.

### The collinear modes

Besides the soft fermion mode we need to include another type of fermion mode in the EFT: a collinear fermion mode. To explain, we consider again the scattering process proceeding through a nearly resonant scalar. The scalar's momentum is thus  $p_A = mv + k$ , where  $k$  is soft. We work in the frame in which  $v = (1, 0, 0, 0)$ ; this would be the rest frame of the scalar if  $k$  were 0. To produce this nearly resonant scalar, the external fermions both need to have a large momentum component; they cannot be soft. If we rotate our reference frame such that the external fermions move approximately along the z-axis, then their momenta are given by

$$q_1 = \frac{1}{2} \begin{pmatrix} m \\ 0 \\ 0 \\ m \end{pmatrix} + k_1, \quad q_2 = \frac{1}{2} \begin{pmatrix} m \\ 0 \\ 0 \\ -m \end{pmatrix} + k_2, \quad \text{with } k_1, k_2 \text{ soft.} \quad (12.21)$$

As a short intermezzo, at this point we introduce *lightcone coordinates*. Inspired by (12.21), we define the vectors

$$n_+ := \begin{pmatrix} 1 \\ 0 \\ 0 \\ 1 \end{pmatrix}, \quad n_- := \begin{pmatrix} 1 \\ 0 \\ 0 \\ -1 \end{pmatrix}, \quad \text{satisfying} \quad \begin{cases} n_+^2 = n_-^2 = 0 \\ n_+ \cdot n_- = -2. \end{cases} \quad (12.22)$$

These vectors are thus lightlike. They can be used to express any four-vector  $r^\mu$  in lightcone coordinates as

$$r^\mu = (-n_- \cdot r) \frac{n_+^\mu}{2} + (-n_+ \cdot r) \frac{n_-^\mu}{2} + r_\perp^\mu, \quad (12.23)$$

where  $r_\perp^\mu$  represents a vector living in the two-dimensional plane perpendicular to  $n_+^\mu$  and  $n_-^\mu$ . Note that  $r^2 = -2n_+ \cdot r \, n_- \cdot r + r_\perp^2$ . In vector notation the vector  $r^\mu$  is written in lightcone coordinates as

$$r^\mu = \left( -\frac{n_- \cdot r}{2}, -\frac{n_+ \cdot r}{2}, \vec{r}_\perp \right). \quad (12.24)$$

The fact that only three slots are displayed in this vector, together with the vector arrow on the last entry serves to indicate that the coordinates are lightcone coordinates using the lightlike vectors 12.22 as basis.

The lightlike vectors (12.22) can now be used to write the external momenta (12.21) as

$$q_1 = m \frac{n_+}{2} + k_1, \quad q_2 = m \frac{n_-}{2} + k_2. \quad (12.25)$$



Furthermore, we note that

$$v = \frac{1}{2}(n_+ + n_-) \xrightarrow{p_A = q_1 + q_2} k = k_1 + k_2. \quad (12.26)$$

The point here is that we must allow for a  $\psi$  fermion field with momentum  $p_1$  that has one large component  $-\frac{n_- p_1}{2} \sim m$ , for this is required to describe the momentum of the external fermions. Similarly, a mode of the  $\chi$  fermion field has to be included that carries momentum  $p_2$  with the scaling  $-\frac{n_- p_2}{2} \sim m$ . Therefore, we introduce *collinear* fermion modes  $\psi_{c_1}$  and  $\chi_{c_2}$ , whose momenta  $p_1$  and  $p_2$  scale as<sup>2</sup>

$$p_1 \sim m(1, \delta, \delta^{1/2}), \quad p_2 \sim m(\delta, 1, \delta^{1/2}). \quad (12.27)$$

The scaling of the small components is chosen such that  $p_1^2 \sim p_2^2 \sim m^2 \delta$ . To understand the reason for this we note that the momenta of the external fermions satisfy  $q_1^2 = q_2^2 = 0$ . The external  $\psi$ -fermions can then interact with the soft photons that are present in the EFT (the  $\chi$ -fermion is neutral but treated similarly). Such a photon has momentum  $k$  scaling as (12.20). The interaction will cause the fermion to obtain a momentum with off-shellness  $-(q_1 + k)^2 \sim m^2 \delta$ . The small components of the collinear fermion modes (12.27) are thus chosen as to allow for such an off-shellness.

Having identified the collinear fermion modes, we now turn to its interaction with the photon field. As already mentioned,  $\psi_{c_1}$  can interact with soft photons. Indeed, such an interaction leaves the scaling (12.27) of the collinear fermion intact. However, there is a more general class of photons that leaves the collinear scaling (12.27) intact upon interaction: collinear photons  $A_{c_1}$  (or  $A_c$  for short; a field  $A_{c_2}$  is not present since  $\chi_{c_2}$  is neutral).

The Lagrangian describing the collinear fields  $\psi_{c_1}$ ,  $\chi_{c_2}$  and  $A_c$ , their interaction with each other, and their interaction with the soft photon field  $A_s$  is  $\mathcal{L}_{\text{SCET}}$ . It is given in paragraph 12.3.3. Its effect is also incorporated in the reduced diagram topologies of figure 12.2. Figure 12.2a shows that  $\psi_{c_1}$  fermions can couple to soft photons. The coupling of  $\psi_{c_1}$  to collinear photons is incorporated differently. The reason is that the exchange of such a collinear photon between the incoming and outgoing  $\psi_{c_1}$  ensures that internal scalar is not close to resonance anymore. Therefore, such a topology falls in the category of figure 12.2b. Collinear photons in 12.2a have to be emitted and adsorbed by the same  $\psi_{c_1}$  line. Therefore in figure 12.2a they only provide only loop corrections to the  $\psi_{c_1}$  propagator, which are represented by the C-corrections.

There is a drawback to working with the collinear fields  $\psi_{c_1}$  and  $\chi_{c_2}$ : it is not guaranteed that two such fields produce a scalar near resonance. What we would like to have in the EFT Lagrangian are terms  $a_1 \phi_v \bar{\psi}_{c_1} \chi_{c_2}$  and  $a_2 \phi_v^\dagger \psi_{c_1} \bar{\chi}_{c_2}$  describing the production respectively decay of the scalar. Focussing on the production, such a term allows a  $\psi_{c_1}$  with generic collinear momentum  $p_1$  to interact with a  $\chi_{c_2}$  with generic collinear momentum  $p_2$  to produce a scalar with momentum  $p_1 + p_2$ . The scalings (12.27) of  $p_1$  and  $p_2$  then make sure that the scalar momentum satisfies  $-(p_1 + p_2)^2 \sim m^2$ . So this quantity is *of the order of*  $m^2$ , but there is nothing to guarantee that it is *close to*  $m^2$ ; nothing guarantees that  $-(p_1 + p_2)^2 - m^2 \sim m^2 \delta^2$ . Yet this is required for the momentum of the  $\phi_v$ -field. Therefore these production and decay terms cannot be included in the EFT Lagrangian. A way to circumvent this problem is to distinguish collinear modes that differ from  $m \frac{n_+}{2}$  and  $m \frac{n_-}{2}$  by collinear fluctuations from those

---

<sup>2</sup>Note that we use the notation  $q_1, q_2$  for the momenta of the external fermions.  $p_1$  and  $p_2$  denote general momenta of the collinear fields  $\psi_{c_1}$  and  $\chi_{c_2}$ .

that differ only by soft fluctuations. To make this explicit, we write  $p_1$  and  $p_2$  analogous to (12.21) as

$$p_1 = m \frac{n_+}{2} + k_1, \quad p_2 = m \frac{n_-}{2} + k_2. \quad (12.28)$$

The fluctuation  $k$  of the produced scalar (defined by (12.19)) is then  $k = k_1 + k_2$ . If we use  $\psi_{c_1}$  and  $\chi_{c_2}$  fields, the fluctuations  $k_1$  and  $k_2$  can be collinear, hence  $k$  can be as well. To guarantee that  $K$  is soft, we only allow for *soft* fluctuations  $k_1$  and  $k_2$ . So as a second step, we integrate out the collinear fluctuations from  $\mathcal{L}_{\text{SCET}}$  to obtain a new Lagrangian  $\mathcal{L}_{\pm}$ .  $\mathcal{L}_{\pm}$  will then be a function of the fermion fields  $\psi_{n_+}$  and  $\chi_{n_-}$ , which are the fields that are associated with soft fluctuations in (12.28). As part of the procedure, collinear photons are also integrated out, leaving only soft photons. The collinear photon loops in figure 12.2 then disappear, leaving collinear corrections that appear in  $\mathcal{L}_{\pm}$  as higher order terms quadratic in  $\psi_{n_+}$ .

The final piece of the EFT Lagrangian is  $\mathcal{L}_{\text{int}}$ . It includes the terms governing the production and decay of the scalar (in terms of  $\psi_{n_+}$  and  $\chi_{n_-}$  fields), as well as the four-fermion term corresponding to figure 12.2b. The complete EFT Lagrangian is thus given by  $\mathcal{L}_{\text{EFT}} = \mathcal{L}_{\text{HSET}} + \mathcal{L}_{\pm} + \mathcal{L}_{\text{int}}$ . Each of these pieces is discussed in a following paragraph. Section 12.4 serves to illustrate how full theory diagrams are reproduced by the EFT.

### 12.3.2. Constructing $\mathcal{L}_{\text{HSET}}$

In this paragraph we shall construct  $\mathcal{L}_{\text{HSET}}$ : the part of the Lagrangian governing the soft scalar, soft photon and soft fermion modes. HSET is shorthand for ‘Heavy Scalar Effective Theory’. The idea of only considering the soft fluctuations of the massive scalar can be thought of as an extension of HQET, ‘Heavy Quark Effective Theory’ [34, 35]. It is an extension in the sense that the field is now a scalar field whose two point function has a complex pole position. In HQET, the terms quadratic in the soft mode of the massive particle are obtained by integrating out the hard modes from the full theory Lagrangian. Even though this is not the approach adopted here, we shall outline how this integrating out should work in this case. The first step would be to decompose the massive scalar field  $\phi$  in a soft mode  $\phi_v$  and a hard mode  $\phi_{\text{hard}}$ . The soft mode is related to the full field by

$$\phi_v(x) = e^{imv \cdot x} \mathcal{P}_+ \phi(x). \quad (12.29)$$

$\mathcal{P}_+$  is the operator that projects onto positive frequency modes; the exponential is there to extract the large component of  $\phi$ ’s momentum according to (12.19). The generating functional can then be written as

$$\mathcal{Z} = \int \mathcal{D}\phi_v^\dagger \mathcal{D}\phi_v \mathcal{D}\phi_{\text{hard}}^\dagger \mathcal{D}\phi_{\text{hard}} \exp \left( i \int d^4x \mathcal{L}[\phi_v^\dagger, \phi_v, \phi_{\text{hard}}^\dagger, \phi_{\text{hard}}] \right). \quad (12.30)$$

The integral over the hard fields is then carried out to yield

$$\mathcal{Z} \sim \int \mathcal{D}\phi_v^\dagger \mathcal{D}\phi_v \exp \left( i \int d^4x \mathcal{L}_{\text{HSET}}^{\phi\phi}[\phi_v^\dagger, \phi_v] \right), \quad (12.31)$$

where  $\mathcal{L}_{\text{HSET}}^{\phi\phi}$  is the part of the  $\mathcal{L}_{\text{HSET}}$  quadratic in  $\phi_v$ . If we ignore the coupling of  $\phi$  to  $A^\mu$  in  $\mathcal{L}$  (and the  $\phi^4$ -term, which is irrelevant up to NLO), then  $\mathcal{L}$  is purely quadratic in  $\phi$ . The integrals over the hard modes will thus be Gaussian integrals. One can show that integrating

out these fields is then equivalent to eliminating  $\phi_{\text{hard}}^\dagger$  and  $\phi_{\text{hard}}$  from  $\mathcal{L}$  by using the equation of motion for these fields. That is, the Lagrangian that results from this elimination is precisely  $\mathcal{L}_{\text{HSET}}^{\phi\phi}$  occurring in (12.31). The coupling with the soft photon field simply follows by replacing ordinary derivatives  $\partial$  by covariant ones  $D_s$ . Here  $D_s := \partial - igA_s$  only includes the soft photon field. The reason that we can incorporate the coupling with the photon in this simple manner is that both the separation into soft and hard modes and integrating out the hard modes are gauge invariant procedures [25].

As mentioned, integrating out the hard fields is not the approach adopted here. Instead, we shall find what the propagator of the soft mode  $\phi_v$  has to be and then construct the quadratic  $\phi_v$ -terms accordingly. As a starting point, we use a full theory propagator that we know defines a fine perturbation theory: the CMS propagator<sup>3</sup>

$$\Delta(P) = \frac{1}{i(2\pi)^4} \frac{1}{P^2 + \hat{m}^2}. \quad (12.32)$$

It may seem that this forces us to work in the CMS in the full theory. This is not the case: we can find  $\hat{m}^2$  in an arbitrary renormalization scheme with arbitrary mass  $m$ , by noting that  $\hat{m}^2$  is the complex pole of the full propagator. By plugging in the momentum decomposition (12.19) and writing  $k^\mu = (-v \cdot k)v^\mu + k_\perp^\mu$ , the propagator (12.32) can be written as

$$\begin{aligned} \Delta(P) &= \frac{1}{i(2\pi)^4} \frac{1}{-(v \cdot k)^2 + 2mv \cdot k + k_\perp^2 + m\Delta}, \quad \text{where } m\Delta := \hat{m}^2 - m^2, \\ &= \frac{1}{i(2\pi)^4} \frac{1}{\bar{\omega}} \left( \frac{1}{2m(v \cdot k - m + \sqrt{m^2 + m\Delta + k_\perp^2})} - \frac{1}{2m(v \cdot k - m - \sqrt{m^2 + m\Delta + k_\perp^2})} \right), \\ &\quad \text{where } \bar{\omega} := \left[ 1 + \frac{m\Delta + k_\perp^2}{m^2} \right]^{-\frac{1}{2}}. \end{aligned} \quad (12.33)$$

Now, only the first denominator corresponds to the soft mode, for only this term has a pole at  $-v \cdot k \sim m\delta$  (note that  $m\Delta \sim m^2\alpha \sim m^2\delta$ ). The second term on the other hand has a pole at  $-v \cdot k \sim m$ . Consequently, it cannot correspond to a soft mode. Indeed, this negative frequency is projected out by  $\mathcal{P}_+$  in (12.29). We thus construct  $\mathcal{L}_{\text{HSET}}^{\phi\phi}$  so as to reproduce the first denominator structure of (12.33). Again promoting the derivatives  $\partial \rightarrow D_s$ , the sought after Lagrangian is

$$\begin{aligned} \mathcal{L}_{\text{HSET}}^{\phi\phi} &= -2m\phi_v^\dagger \left( -iv \cdot D_s - m + \sqrt{m^2 + m\Delta + (-iD_{s\perp})^2} \right) \phi_v \\ &= -2m\phi_v^\dagger \left( -iv \cdot D_s + \frac{\Delta^{(1)}}{2} \right) \phi_v - 2m\phi_v^\dagger \left( \frac{(-iD_{s\perp})^2}{2m} - \frac{[\Delta^{(1)}]^2}{8m} + \frac{\Delta^{(2)}}{2} \right) \phi_v + \dots \end{aligned} \quad (12.34)$$

The factor  $m$  in front is to ascertain that  $\phi_v$  has mass dimension one, the canonical mass dimension of a scalar field.

In the second line of (12.34) we expanded in  $\alpha$  and  $\delta$ . This is exactly the purpose of the EFT: the expansion is done at the level of the Lagrangian. The number of terms that one

<sup>3</sup>actually, it is sufficient to work in a renormalization scheme that has the same mass as the CMS, but arbitrary field renormalization. Such a scheme also gives rise to the propagator (12.32) and still defines a valid perturbation theory in  $\alpha$ , for equation (11.7) works without setting  $\Sigma'(-\hat{m}^2, \hat{m}^2)$  to zero.

needs in the expansion is determined by the required accuracy of the amplitude that one wishes to calculate. In this chapter we shall not go beyond NLO, and thus only need the LO term (the first term) and the NLO term (the second term). Determining the scaling of the various terms proceeds by simple *power counting*. In the following we shall leave out the masses in the scalings; the relevant scaling here is in  $\alpha \sim \delta$ , not in the mass dimension. To illustrate the powercounting we shall determine the scaling of the various quantities present in (12.34). First of all,  $v \cdot k$  in (12.33) represents a soft fluctuation, hence it scales as  $\delta$ . Since the integration measure  $d^4k \sim \delta^4$ , the real space propagator scales as  $\delta^4 \cdot \delta^{-1} = \delta^{-3}$ . This means that the field  $\phi_v$  scales as  $\delta^{3/2}$ . Furthermore,  $v \cdot k \sim \delta$  implies  $v \cdot D \sim \delta$  and hence  $A_s \sim \delta$ . The scalings of other quantities are determined according to similar arguments; they are listed in table 12.1. Furthermore, in 12.34 we have decomposed  $\Delta$  as  $\Delta = \sum_{i=1} \Delta^{(i)}$ , where  $\Delta^{(i)} \sim \alpha^i \sim \delta^i$ . The determination of these *matching coefficients* is carried out below.

The scalar propagator in the EFT is determined from the LO term in (12.34). The terms suppressed in  $\alpha$  and  $\delta$  are treated as vertices in the theory, as in a proper perturbation theory in  $\alpha$  and  $\delta$ . The propagator thus reads

$$\Delta(k) = \frac{1}{i(2\pi)^4} \frac{1}{2m(v \cdot k + \Delta^{(1)}/2)}. \quad (12.35)$$

In the  $\bar{m}$  renormalization scheme defined in section 11.3, we have  $m\Delta^{(1)} = \hat{m}^2 - \bar{m}^2 \stackrel{(9.19)}{=} -i\bar{m}\bar{\Gamma}$ , such that this propagator can be thought of as a fixed width propagator. One should note that we are not reproducing the factor  $\bar{\omega}^{-1}$  in (12.33). To account for this extra normalization, in calculating a truncated Green's function one has to multiply by a factor  $\bar{\omega}^{-1/2}$  for every external  $\phi_v$ .

The complete  $\mathcal{L}_{\text{HSET}}$  is simply found by supplying (12.34) with the the standard terms for the soft photon and fermion modes. Up to NLO, the result is

$$\begin{aligned} \mathcal{L}_{\text{HSET}} = & -2m\phi_v^\dagger \left( -iv \cdot D_s + \frac{\Delta^{(1)}}{2} \right) \phi_v - 2m\phi_v^\dagger \left( \frac{(-iD_{s\perp})^2}{2m} - \frac{[\Delta^{(1)}]^2}{8m} + \frac{\Delta^{(2)}}{2} \right) \phi_v \\ & - \frac{1}{4} F_{s\mu\nu} F_s^{\mu\nu} - \bar{\psi}_s \not{D}_s \psi_s - \bar{\chi}_s \not{\partial} \chi_s, \end{aligned} \quad (12.36)$$

where  $F_s^{\mu\nu} := \partial^\mu A_s^\nu - \partial^\nu A_s^\mu$ .

### Determination of $\Delta = \hat{m}^2 - m^2$

$\Delta$  can be determined from the self-energy of the full theory. To determine  $\Delta$  we use the fact that  $\hat{m}^2$  corresponds to the complex pole position of the full propagator. Thus  $\hat{m}^2$  satisfies

$$-\hat{m}^2 + m^2 - \Sigma(-\hat{m}^2, m^2) = 0 \quad \Rightarrow \quad m\Delta = \Sigma(-\hat{m}^2, m^2). \quad (12.37)$$

However, there is a catch here. In the foregoing we constructed the quadratic  $\phi_v$ -terms of  $\mathcal{L}_{\text{HSET}}$  to reproduce the CMS propagator of the full theory, which equals the full theory's bare

		$\partial$	$\sim$	$\delta$
$\phi_v$	$\sim$	$\Delta^{(n)}$	$\sim$	$\alpha^n$
$A_s$	$\sim$	$C^{(0)}$	$\sim$	1
$\psi_s, \chi_s$	$\sim$	$C^{(1)}$	$\sim$	$\alpha$
$\psi_{n+}, \chi_{n-}$	$\sim$	$D^{(0)}$	$\sim$	$\alpha$

Table 12.1.: Power counting for the quantities appearing in  $\mathcal{L}_{\text{HSET}}$ ,  $\mathcal{L}_{\pm}$ , and  $\mathcal{L}_{\text{int}}$

propagator with the pole shifted by an amount  $m\Delta$ . However, the two point function of the effective theory is not formed solely by these terms: the EFT also features loop corrections due to the coupling of  $\phi_v$  with the soft photon  $A_s$  and the soft fermions  $\psi_s$  and  $\chi_s$ . The correct statement is that the complete EFT two point function - containing both the loop corrections and the corrections from  $\mathcal{L}_{\text{HSET}}^{\phi\phi}$  - must reproduce the CMS propagator of the full theory. Since the loop corrections in the EFT correspond to the soft parts of the full theory loop corrections (expanded by the strategy of regions), the matching coefficient  $\Delta$  in  $\mathcal{L}_{\text{HSET}}^{\phi\phi}$  must only reproduce the hard part of the full theory self-energy. The proper statement is thus that we need

$$m\Delta = \Sigma_h(-\hat{m}^2, m^2). \quad (12.38)$$

To determine  $\Delta$ , we expand the hard part of the self-energy around  $\Sigma_h(-m^2, m^2)$ . To separate the different scales that are contained in the self-energy, we use the notation  $\Sigma_h(-m^2, m^2) = \sum_n \Sigma_h^{(n,0)}$ , where it is understood that  $\Sigma_h^{(n,l)} \sim \alpha^n$ . The expansion then proceeds according to  $\Sigma_h(-s, m^2) = \sum_{n,l} (-\delta)^l \Sigma_h^{(n,l)}$ , with  $\Sigma_h^{(n,l)} := \frac{1}{l!} \frac{d^l}{(dp^2)^l} \Sigma_h^{(n,0)}(p^2, m^2)|_{p^2=-m^2}$ . After the expansion, (12.37) reads

$$m\Delta = (\Sigma_h^{(1,0)} + \Sigma_h^{(2,0)} + \dots) + \frac{\Delta}{m} (\Sigma_h^{(1,1)} + \Sigma_h^{(2,1)} + \dots) + \left(\frac{\Delta}{m}\right)^2 (\Sigma_h^{(1,2)} + \Sigma_h^{(2,2)} + \dots) + \dots \quad (12.39)$$

To solve for  $m\Delta$ , we use  $\Delta = \sum_i \Delta^{(i)}$  and solve for  $\Delta^{(i)} \sim \alpha^i$  iteratively. The result is

$$m\Delta^{(0)} = 0, \quad m\Delta^{(1)} = \Sigma_h^{(1,0)}, \quad m\Delta^{(2)} = \Sigma_h^{(2,0)} + \Sigma_h^{(1,1)} \Sigma_h^{(1,0)}, \quad \dots \quad (12.40)$$

This can be continued to any order desired.

### 12.3.3. The Lagrangian of the collinear modes

The collinear fermion and photon modes introduced in paragraph 12.3.1, together with their interaction with each other and with the soft photon field, are described by  $\mathcal{L}_{\text{SCET}}$ . This is the Lagrangian appearing in ‘Soft Collinear Effective Theory’. For its construction we refer to [36–38]. Here we just quote the Lagrangian to leading power in  $\delta$ .

$$\begin{aligned} \mathcal{L}_{\text{SCET}} = & -\bar{\psi}_{c1} \left( n_+ \cdot D + \not{D}_{\perp c} \frac{1}{n_- \cdot D_c - i\epsilon} \not{D}_{\perp c} \right) \frac{\not{n}_-}{2} \psi_{c1} + \dots \\ & - \bar{\chi}_{c2} \left( n_- \cdot \partial + \not{\partial}_{\perp} \frac{1}{n_+ \cdot \partial - i\epsilon} \not{\partial}_{\perp} \right) \frac{\not{n}_+}{2} \chi_{c2} + \dots - \frac{1}{4} F_{c\mu\nu} F_c^{\mu\nu}. \end{aligned} \quad (12.41)$$

In (12.41), the notation is that  $D_c := \partial - igA_c$  and  $n_{\pm} \cdot D := n_{\pm} \cdot \partial - ign_{\pm} \cdot A_c - ign_{\pm} \cdot A_s$ . Integrating out the collinear fluctuations from the collinear fermion fields yields [25]

$$\mathcal{L}_{\pm} = -\bar{\psi}_{n_+} n_+ \cdot D_s \frac{\not{n}_-}{2} \psi_{n_+} - \bar{\chi}_{n_-} n_- \cdot \partial \frac{\not{n}_+}{2} \chi_{n_-} \quad (12.42)$$

to leading order in  $\delta$ .

### 12.3.4. Constructing $\mathcal{L}_{\text{int}}$

As explained in paragraph 12.3.1, by using the fields  $\psi_{n_+}$  and  $\chi_{n_-}$  the production and decay of the field  $\phi_v$  from and into two fermions can be implemented in the Lagrangian. Together with

the four-fermion vertex of figure 12.2b, these production and decay terms are included in  $\mathcal{L}_{\text{int}}$ . This final piece of the EFT Lagrangian reads

$$\mathcal{L}_{\text{int}} = Cy\phi_v\bar{\psi}_{n_+}\chi_{n_-} + Cy^*\phi_v^\dagger\bar{\chi}_{n_-}\psi_{n_+} + D\frac{yy^*}{m^2}(\bar{\psi}_{n_+}\chi_{n_-})(\bar{\chi}_{n_-}\psi_{n_+}). \quad (12.43)$$

The constants  $C$  and  $D$  are matching coefficients. In the EFT they represent hard corrections of the full theory, for the soft corrections of the full theory are reproduced in the EFT by loops of the present soft fields.

### The matching procedure

The matching coefficients are determined by requiring that renormalized, on-shell Green's functions, calculated in the full theory and in the EFT, agree to a certain accuracy in  $\alpha$  and  $\delta$ . Determinating the coefficients this way is called *matching*. Suppose we wish to find a matching coefficient to order  $n$  in  $\alpha$  and  $\delta$ . The matching procedure then proceeds as follows. First one computes the renormalized, on-shell Green's functions in the full theory to order  $\alpha^n$ . Since this Green's function is renormalized, it is UV-finite. On-shell in the full theory means that the momentum  $P$  of an external scalar line satisfies  $-P^2 = \hat{m}^2 = m^2 + m\Delta$ . One then expands this amplitude around  $-P^2 = m^2$ . The expansion parameter is thus  $\frac{\Delta}{m} \sim \delta$ . In the expansion one only keeps up to  $N^n$  LO-terms in the simultaneous expansion in  $\alpha$  and  $\delta$ . The amplitude then has to be multiplied by the (full theory) residue factors. These too are to be renormalized, put on-shell and expanded around  $P^2 = m^2$  in the same way.

Subsequently one computes the same quantities in the EFT, except this time one does not renormalize<sup>4</sup>. Again, on-shell means for the scalar that  $-P^2 = \hat{m}^2$ . Also, the residue factors of the effective theory have to be taken into account, including the  $\bar{\omega}^{-1/2}$  factor for every external  $\phi_v$  line. By demanding that the two quantities agree to  $N^n$  LO, the matching coefficients are determined.

### Matching C

We shall now illustrate the matching procedure by obtaining the matching coefficient  $C$  to NLO. The LO expression for  $D$  will be deduced in the next paragraph. The first step is to calculate renormalized on-shell three-point function of the fields  $\psi$ ,  $\chi$  and  $\phi$  to first order in  $\alpha$  in the full theory. It is given by

$$\Gamma = \text{tree} + \text{loop} + \text{counterterm} = y + \Gamma^{\text{1-loop}} + \delta_y^{(1)}, \quad (12.44)$$

where the third diagram denotes the counterterm  $\delta_y^{(1)}$  renormalizing the UV divergence of  $\Gamma$  to order  $\alpha$ . In the calculation of  $\Gamma^{\text{1-loop}}$ , one should use the on-shell condition  $-P^2 = m^2 + m\Delta$ , but when expanding this around  $-P^2 = m^2$  only the LO in this expansion has to be taken into account since  $\Gamma^{(1)} \sim \alpha$ . Therefore we only need  $\Gamma^{(1)}$  evaluated at  $-P^2 = m^2$ . Furthermore,

<sup>4</sup>Loops in the EFT *can* exhibit UV divergencies, which can be thought of as follows. Renormalized full theory loops, which are UV-finite, can be expanded in hard and soft contributions according to the method of regions. Since the full theory is UV finite, so is its hard part. The soft part however may exhibit a UV-divergency, which is canceled by an IR-divergency of the hard integral. Roughly speaking, the EFT loops correspond to these soft loops, whereas the matching coefficient corresponds to the hard integrals. Therefore, the UV divergencies of the EFT loops will be canceled by poles of the matching coefficients. Since this is the case, one can also choose to renormalize both the matching coefficients and the UV divergencies of the EFT loops, as long as one renormalizes both in the same way. Any remaining poles correspond to IR divergencies of the EFT loops, as well as to IR divergencies of the full theory.

the renormalized full theory residues  $R_\psi$ ,  $R_\chi$  and  $R_\phi$  have to be calculated. These too must be expanded around  $-P^2 = m^2$ , where again only terms are kept that are up to NLO in  $\alpha$  and  $\delta$ .

The next step is to evaluate the same quantities in the EFT. Denoting the EFT diagrams by

$$\Gamma_{\text{eff}} := \text{[tree diagram]} + \text{[loop diagram]} = y(C^{(0)} + C^{(1)}) + \Gamma_{\text{eff}}^{1\text{-loop}} \quad (12.45)$$

and the residues by  $R_{\text{eff}\psi}$ ,  $R_{\text{eff}\chi}$  and  $R_{\text{eff}\phi}$ , the matching equation reads

$$\sqrt{R_\psi}\sqrt{R_\chi}\sqrt{R_\phi}\Gamma = \bar{\omega}^{-1/2}\sqrt{R_{\text{eff}\psi}}\sqrt{R_{\text{eff}\chi}}\sqrt{R_{\text{eff}\phi}}\Gamma_{\text{eff}}. \quad (12.46)$$

Solving (12.46) to LO straightforwardly yields  $C(0) = 1$ . Subsequently (12.46) is solved to NLO to obtain  $C^{(1)}$ . The involved loop diagrams exhibit IR divergencies, so an IR regulator has to be used in their evaluation. Any IR regulator is fine as long as the same regularization is used in the calculation of both the full theory and EFT diagrams. The matching coefficients are then guaranteed to be independent of the applied regularization scheme [25]. Here we adopt dimensional regularization. This has the advantage that the EFT loop diagrams vanish on-shell due to begin scaleless integrals. Therefore  $\Gamma_{\text{eff}}^{1\text{-loop}} = 0$  and  $R_{\text{eff}\psi} = R_{\text{eff}\chi} = R_{\text{eff}\phi} = 1$ . It is convenient to expand the full theory loop  $\Gamma^{1\text{-loop}}$  and the full theory one-loop self-energies (needed for the calculation of the full theory residues) in a soft and hard part according to the strategy of regions. Since these quantities are calculated on-shell, the soft integrals vanish due to being scaleless. Indeed, this has to the case, for these soft parts correspond to the EFT loops which also vanish. The matching equation (12.46) thus simplifies to

$$\sqrt{R_{h\psi}}\sqrt{R_{h\chi}}\sqrt{R_{h\phi}}\Gamma_h = \bar{\omega}^{-1/2}y[1 + C^{(1)}], \quad (12.47)$$

where the subscript  $h$  of a quantity serves to indicate that any loops required in the calculation of that quantity is to be replaced by its hard part according to the expansion by regions. Equation (12.47) illustrates what we claimed before: the matching coefficient represents hard corrections of the full theory. The calculation of  $\Gamma_h^{1\text{-loop}}$  is performed in appendix B. The resulting hard three-point function to NLO is

$$\Gamma_h = y \left( 1 + \alpha_g \bar{\mu}^\epsilon \left[ -\frac{4}{\epsilon^2} + \frac{2}{\epsilon} - 2 - \frac{\pi^2}{12} \right] \right) + \delta_y^{(1)}. \quad (12.48)$$

This gives rise to the following result for  $C(1)$  [25]

$$C^{(1)} = \alpha_y \left[ \ln \left( \frac{m^2}{\mu^2} \right) - \frac{1}{4} - \frac{i\pi}{2} \right] + \alpha_g \left[ -\frac{4}{\epsilon^2} - \frac{2}{\epsilon} \left( \ln \left( \frac{m^2}{\mu^2} \right) - \frac{5}{2} \right) - \frac{1}{2} \ln^2 \left( \frac{m^2}{\mu^2} \right) + \frac{7}{4} \ln \left( \frac{m^2}{\mu^2} \right) - \frac{15}{4} - \frac{\pi^2}{12} \right]. \quad (12.49)$$

We note that  $\Gamma_h$  - and therefore also  $C^{(1)}$  - contains a *double* pole in  $\epsilon$ . Since  $\Gamma_s$  vanishes if all external lines are taken on-shell, this means that  $\Gamma$  contains a double pole in that case. If one would keep the scalar *off-shell*,  $\Gamma$  would only exhibit single poles. This can be verified by either the explicit full theory calculation, or by using the expansion by regions  $\Gamma = \Gamma_h + \Gamma_s$ .  $\Gamma_s$  only vanishes on-shell; off-shell it features a double pole that precisely cancels the double pole of

$\Gamma_h$ . We shall witness this cancellation at the level of the EFT in the calculation of the forward scattering amplitude in section 12.7. There the double pole of  $\Gamma_h$  is present inside the matching coefficient  $C^{(1)}$ , whereas  $\Gamma_s$  is represented by the loop calculated within the EFT. We shall see that the double poles cancel, which indeed has to be the case, for the scalar is essentially kept off-shell in the calculation. So the double poles in  $\epsilon$  are - for the case that that one takes the scalar off-shell - an artefact of the strategy of regions.

## 12.4. How the full theory is reproduced by the EFT: two example diagrams

The EFT is designed to reproduce full theory amplitudes to a certain accuracy in a simultaneous expansion in  $\alpha$  and  $\delta$ . The aim of this section is to illustrate by two examples how full theory diagrams are represented in the full theory.

There is a factor complicating the comparison, which coincides precisely with the reason that the EFT is useful: a term of a certain order in  $\alpha$  and  $\delta$  in an EFT amplitude can correspond to a collection of full theory diagrams of all orders in  $\alpha^n$ . Indeed, as discussed in section 12.1, a correction to the scalar propagator in the full theory that consists of *any* number  $n$  of sequential loops, is of leading order in the simultaneous expansion of  $\alpha$  and  $\delta$ . Indeed, such a correction scales as  $\frac{1}{\delta} \cdot \left(\frac{\alpha}{\delta}\right)^n \sim \frac{1}{\delta}$ , just as the bare propagator in the full theory. This was accounted for in paragraph 12.3.2 by constructing  $\mathcal{L}_{\text{HSET}}^{\phi\phi}$  in such a way that the EFT two-point function matches the CMS propagator of the full theory. Since one can think of the CMS propagator as being inherently resummed, as explained in chapter 11, it contains all these corrections. As a result, the matching coefficient  $\Delta^{(1)}$  (to name one) accounts for an infinite number of diagrams in the full theory. Therefore, we can say that there is not a one-to-one correspondence between diagrams in the full theory and corrections in the EFT. However, there is nothing wrong with saying that any full theory diagram must be accounted for somehow by the EFT. In this paragraph we therefore consider how two full theory diagrams are represented in the EFT.

### 12.4.1. The full theory tree-level diagram

First we consider the tree-level scattering diagram of figure 12.1 in the full theory. To understand how this tree-level diagram is reproduced in the EFT, we ignore the terms in the EFT that correspond to full theory self-energy corrections. As discussed in paragraph 12.3.2, full theory self-energy corrections are accounted for in the EFT by the matching coefficient  $\Delta$ , so for this example we think of  $\Delta = 0$  in  $\mathcal{L}_{\text{HSET}}$ .

Leaving out the external spinors, the full theory tree-level diagram reads

$$\mathcal{M}_{\text{full theory}}^{\text{tree}} = y \frac{1}{p_A^2 + m^2} y^*. \quad (12.50)$$

To separate the different orders of  $\delta$  present in (12.50), we plug in  $p_A = mv + k = mv - (v \cdot k)v + k_\perp$  and expand in  $k \sim \delta$ .

$$\begin{aligned} \mathcal{M}_{\text{full theory}}^{\text{tree}} &= y \frac{1}{2mv \cdot k + k_\perp^2 - (v \cdot k)^2} y^* \\ &= y \frac{1}{2mv \cdot k} y^* - y \frac{1}{2mv \cdot k} k_\perp^2 \frac{1}{2mv \cdot k} y^* + \frac{yy^*}{4m^2} + \mathcal{O}(\delta). \end{aligned} \quad (12.51)$$



Note that the first term is of order  $\frac{1}{\delta}$ , whereas the second and third terms are of order  $\delta^0$ . In the EFT (with  $\Delta = 0$ ), the first term is reproduced by the  $\phi_v$ -propagator together with the LO production vertex  $y$  and the LO decay vertex  $y^*$ . That is, the first term is reproduced by the diagram of figure 12.1 in the EFT. The second term is reproduced by the same EFT diagram but with one insertion of the  $(-i\partial_\perp)^2$  correction present in (12.36). The third term does not involve a  $\phi_v$  propagator. Therefore its topology of the type of figure 12.2b. This contribution must consequently be reproduced by the four-fermion term with coefficient  $D$  that is present in  $\mathcal{L}_{\text{int}}$  (12.43). Equation (12.51) thus tells us that we need  $D = \frac{1}{4} + \mathcal{O}(\alpha, \delta)$  and that this LO part of  $D$  gives rise to a NLO contribution to the forward scattering amplitude.

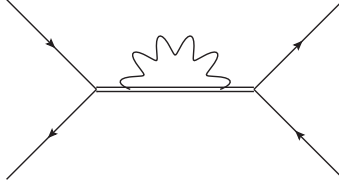


Figure 12.3.: Self-energy correction to the tree-level scattering diagram in the full theory.

### 12.4.2. Full theory self-energy correction and ordering into gauge invariant pieces

Gauge invariance in the EFT is guaranteed because every step in the construction of the EFT preserves gauge invariance [25]. In particular, integrating out the hard modes from the full theory Lagrangian (12.5) leaves the resulting Lagrangian  $\mathcal{L}_{\text{EFT}}$  invariant under the same symmetry. More specifically, the  $U(1)$  symmetry (12.6) of the full theory Lagrangian (12.5) implies that the effective Lagrangian  $\mathcal{L}_{\text{EFT}}$  is invariant under the transformations

$$\left\{ \begin{array}{l} \phi_v \rightarrow e^{ig\xi_s(x)}\phi_v \\ \psi_s \rightarrow e^{ig\xi_s(x)}\psi_s \\ \psi_{n_+} \rightarrow e^{ig\xi_s(x)}\psi_{n_+} \\ A_\mu \rightarrow A_\mu + \partial_\mu\xi_s(x). \end{array} \right. \quad (12.52)$$

This implies that the matching coefficients  $\Delta$ ,  $C$  and  $D$  are also gauge invariant. Furthermore, since the EFT defines a proper perturbation theory in  $\alpha$  and  $\delta$ , the fact that  $\mathcal{L}_{\text{EFT}}$  exhibits the symmetry (12.52) *for every*  $\alpha$  and  $\delta$  implies that gauge invariance should hold perturbatively. Therefore EFT amplitudes are gauge independent order by order in the simultaneous expansion in  $\alpha$  and  $\delta$ . This is in contrast with the full theory, which is suited only for a perturbation theory in  $\alpha$ . For example, consider the one-loop full theory self-energy  $\Sigma^{1\text{-loop}}(-s, m^2)$ . If one would expand this in  $\delta$ , the leading order term is the on-shell self-energy  $\Sigma^{(1,0)}$ , which is gauge invariant. However, the higher order terms  $\Sigma^{(1,1)}$ ,  $\Sigma^{(1,2)}$ , etc are *not*; they can depend on the gauge fixing parameter  $\lambda$  [25]. The power of the EFT is that it orders full theory quantities that are gauge dependent into gauge independent objects. The following example illustrates this ordering.

This example concerns the one-loop self-energy correction to the tree-level scattering diagram

in the full theory. It is shown in figure 12.3 and reads

$$\mathcal{M}_{\text{full theory}}^{\text{SE corr.}} = y \frac{1}{m^2 \delta} \Sigma^{1\text{-loop}}(-s, m^2) \frac{1}{m^2 \delta} y^*. \quad (12.53)$$

To relate this to the EFT, we use the strategy of regions to write the self-energy as

$$\Sigma^{1\text{-loop}}(-s, m^2) = \Sigma_s^{1\text{-loop}}(-s, m^2) + \Sigma_h^{1\text{-loop}}(-s, m^2). \quad (12.54)$$

The part of (12.53) with the soft self-energy loop is reproduced by the same loop in the EFT (formed by a soft photon  $A_s$  and the soft scalar  $\phi_v$ ). To understand how the hard part is reproduced we decompose it as in section 12.3.2.

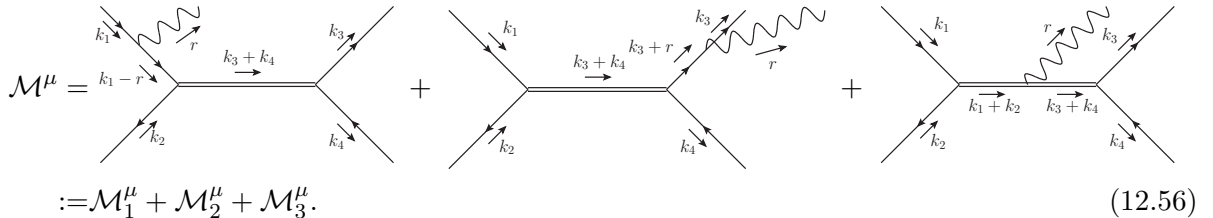
$$\Sigma_h^{1\text{-loop}}(-s, m^2) = \sum_l (-\delta)^l \Sigma_h^{(1,l)}, \quad \text{yielding}$$

$$\mathcal{M}_{\text{full theory}}^{\text{SE corr.}} = y \frac{1}{m^2 \delta} \Sigma_h^{(1,0)} \frac{1}{m^2 \delta} - y \frac{\Sigma_h^{(1,1)}}{m^2} \frac{1}{m^2 \delta} y^* + y \frac{\Sigma_h^{(1,2)}}{m^4} y^* + \mathcal{O}(\delta). \quad (12.55)$$

The first term is accounted for in the EFT by the presence of  $m\Delta^{(1)}$  in the  $\phi_v$ -propagator. As stated before, it is not *only* the first term of (12.55) that the  $\phi_v$ -propagator accounts for, but it *does* account for it. Indeed, according to (12.40)  $\Sigma_h^{(1,0)}$  defines  $\Delta^{(1)}$ . Since  $\Sigma_h^{(1,0)} = \Sigma^{(1,0)}$  (which is a result of  $\Sigma_s^{(1,0)}$  being a scaleless integral) and since  $\Sigma^{(1,0)}$  is gauge invariant,  $\Delta^{(1)}$  is gauge invariant, as it should be. In the second term of (12.55) one propagator has canceled due to the expansion of the self-energy. Therefore, this gauge dependent  $\Sigma_h^{(1,1)}$  correction is accounted for in the EFT as a hard correction to the production/decay vertex. It is thus accounted for by the gauge independent  $C^{(1)}$  in  $\mathcal{L}_{\text{int}}$  (12.43). It enters the expression for  $C^{(1)}$  in the matching procedure outlined in paragraph 12.3.4 through the residue  $R_{h\phi}$ . In the matching, the gauge dependence of  $R_{h\phi}$  cancels the gauge dependence of  $\Gamma_h$  to yield a gauge independent coefficient  $C^{(1)}$ . Similarly, in the third term of (12.55) both propagators have canceled, meaning that the gauge dependent  $\Sigma^{(1,2)}$  correction is accounted for by the gauge independent four-fermion coefficient  $D$  in  $\mathcal{L}_{\text{int}}$ . Note that this term is of higher order than the third term of (12.51) and only represents a NNLO contribution to the forward scattering diagram.

## 12.5. Checking the Ward identity at tree-level

If the EFT does indeed define a proper perturbation theory in  $\alpha$  and  $\delta$ , then amplitudes should satisfy the Ward identity order by order. In this section we check the Ward identity for the scattering process with the extra emission of a soft photon, that is for  $\psi\bar{\chi} \rightarrow \psi\bar{\chi}\gamma$ , at tree-level. The contributing diagrams are



$$\mathcal{M}^\mu = \mathcal{M}_1^\mu + \mathcal{M}_2^\mu + \mathcal{M}_3^\mu. \quad (12.56)$$

The momenta in the diagrams refer to the momenta of the EFT fields. So the external  $\psi_{n+}$  carries momentum  $k_1$ , meaning that the full theory  $\psi$  would carry momentum  $q_1 = m \frac{n+}{2} + k_1$

etc. The LO Feynman rules in the EFT, derived from the Lagrangians (12.36), (12.42) and (12.43), are given by

$$\begin{aligned}
\begin{array}{c} \xrightarrow{k} \\ \hline \hline \end{array} &= \frac{1}{i(2\pi)^4} \frac{1}{2mv \cdot k + m\Delta^{(1)}}, \\
\begin{array}{c} \xrightarrow{k} \\ \hline \end{array} &= \frac{1}{i(2\pi)^4} \frac{1}{in_+ \cdot k} \frac{\not{k}_+}{2}, \\
\begin{array}{c} \phantom{\xrightarrow{k}} \\ \hline \hline \text{---} \mu \\ \hline \hline \end{array} &= i(2\pi)^4 2mgv^\mu, \\
\begin{array}{c} \phantom{\xrightarrow{k}} \\ \hline \text{---} \mu \\ \hline \hline \end{array} &= i(2\pi)^4 ign_+^\mu \frac{\not{k}_-}{2}. \tag{12.57}
\end{aligned}$$

The fermion lines drawn in (12.57) are understood to correspond to the  $\psi_{n_+}$  field. The two expressions appearing as the denominator of the scalar propagator are abbreviated as

$$\begin{cases} D_{12} := 2mv \cdot (k_1 + k_2) + m\Delta^{(1)} \\ D_{34} := 2mv \cdot (k_3 + k_4) + m\Delta^{(1)}. \end{cases} \tag{12.58}$$

The on-shell conditions for the external fermions are found from the Lagrangian  $\mathcal{L}_\pm$  (12.42) to be

$$n_+ \cdot k_1 = n_- \cdot k_2 = n_+ \cdot k_3 = n_- \cdot k_4 = 0. \tag{12.59}$$

Furthermore, the external spinors satisfy the relations [36]

$$\frac{\not{k}_+}{2} \frac{\not{k}_-}{2} u(k_1) = u(k_1), \quad \bar{v}(k_2) \frac{\not{k}_+}{2} \frac{\not{k}_-}{2} = \bar{v}(k_2), \quad \frac{\not{k}_+}{2} \frac{\not{k}_-}{2} u(k_3) = u(k_3), \quad \bar{v}(k_4) \frac{\not{k}_+}{2} \frac{\not{k}_-}{2} = \bar{v}(k_4). \tag{12.60}$$

The first diagram of (12.56) contributes to the Ward identity as

$$r_\mu \mathcal{M}_1^\mu = i(2\pi)^4 |y|^2 \frac{1}{in_+ \cdot (k_3 + k_4 - k_2)} igr_\mu n_+^\mu \frac{1}{D_{34}} \bar{v}(k_2) \frac{\not{k}_+}{2} \frac{\not{k}_-}{2} u(k_1) \bar{u}(k_3) v(k_4). \tag{12.61}$$

The spinor structure of (12.61) simplifies by (12.60) to  $\mathcal{F} = \bar{v}(k_2) u(k_1) \bar{u}(k_3) v(k_4)$ . To simplify (12.61) further, we use  $r = k_1 + k_2 - k_3 - k_4$  together with (12.59). Collecting prefactors as  $c := i(2\pi)^4 g |y|^2$  we obtain

$$\begin{aligned} r_\mu \mathcal{M}_1^\mu &= c \frac{n_+ \cdot (k_2 - k_4)}{n_+ \cdot (k_4 - k_2)} \frac{1}{D_{34}} \mathcal{F} \\ &= -c \mathcal{F} \frac{1}{D_{34}}. \end{aligned} \tag{12.62}$$

Similarly, the second and third diagrams of (12.56) contribute to the Ward identity as

$$\begin{aligned} r_\mu \mathcal{M}_2^\mu &= i(2\pi)^4 |y|^2 \frac{1}{D_{12}} \frac{1}{in_+ \cdot (k_1 + k_2 - k_4)} igr_\mu n_+^\mu \bar{v}(k_2) u(k_1) \bar{u}(k_3) \frac{\not{k}_+}{2} \frac{\not{k}_-}{2} v(k_4). \\ &= c \frac{n_+ \cdot (k_2 - k_4)}{n_+ \cdot (k_2 - k_4)} \frac{1}{D_{12}} \mathcal{F} \\ &= c \mathcal{F} \frac{1}{D_{12}}, \end{aligned} \tag{12.63}$$

$$\begin{aligned}
r_\mu \mathcal{M}_3^\mu &= i(2\pi)^4 |y|^2 \frac{1}{D_{34}} 2m g r_\mu v^\mu \frac{1}{D_{12}} \mathcal{F} \\
&= c\mathcal{F} \frac{1}{D_{12}} \frac{1}{D_{34}} [2m g v \cdot (k_1 + k_2 - k_3 - k_4)] \\
&= c\mathcal{F} \frac{1}{D_{12}} \frac{1}{D_{34}} [D_{12} - D_{34}] \\
&= c\mathcal{F} \left( \frac{1}{D_{34}} - \frac{1}{D_{12}} \right).
\end{aligned} \tag{12.64}$$

The Ward identity then reads

$$\begin{aligned}
r_\mu \mathcal{M}^\mu &= r_\mu \mathcal{M}_1^\mu + r_\mu \mathcal{M}_2^\mu + r_\mu \mathcal{M}_3^\mu \\
&= c\mathcal{F} \left( -\frac{1}{D_{34}} + \frac{1}{D_{12}} + \frac{1}{D_{34}} - \frac{1}{D_{12}} \right) \\
&= 0.
\end{aligned} \tag{12.65}$$

So the Ward identity is indeed satisfied for this process at tree-level.

## 12.6. Unitarity in the EFT

As stated in section 11.5, Veltman has shown that a *full* quantum field theory is unitary if unstable particles are excluded from asymptotic states. The resulting equation (11.20) reads for the case of forward scattering

$$2i\text{Im}(\langle a|\mathcal{T}|a\rangle) = - \sum_{|c\rangle \in \text{stable states}} |\langle c|\mathcal{T}|a\rangle|^2. \tag{12.66}$$

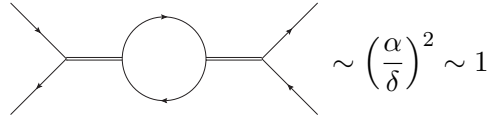
Equation (12.66) is valid for any  $\alpha$  and any  $\delta$  in the full theory. Consequently, the fact that the EFT finds the full theory amplitudes properly expanded in  $\alpha$  and  $\delta$  implies that (12.66) must hold *order by order* for amplitudes that are calculated in the EFT.

In chapter 5 we proved unitarity for a field theory containing only stable particles. There unitarity followed from Cutkosky's cutting rules, which were derived under the assumption that the (non-quadratic part of) Lagrangian is hermitian. The EFT Lagrangian  $\mathcal{L}_{\text{EFT}}$  is *not* hermitian, for the matching coefficients are complex. Indeed,  $\Delta^{(1)}$  has a nonvanishing imaginary part since according to (12.40) it follows from  $\Sigma^{(1,0)}$ . Equation (12.49) shows that the same is true for  $C^{(1)}$ . Therefore, Cutkosky's cutting rules are not valid in the EFT.<sup>5</sup> The fact that unitarity (12.66) still holds anyway is precisely due to the imaginary parts of the matching coefficients. For example, the LO contribution to the RHS of the unitarity condition (12.66) comes from

$$\left| \begin{array}{c} \text{---} \diagdown \\ \text{---} \diagup \\ \text{---} \text{---} \end{array} \right|^2 \sim \left( \frac{\alpha}{\delta} \right)^2 \sim 1. \tag{12.67}$$

<sup>5</sup>  $\mathcal{L}_{\text{EFT}}$  not being hermitian is in fact not the *only* problem encountered when trying to define cutting rules in the EFT. Another difficulty is that the  $\phi_v$ -propagator  $\Delta(k)$  is linear in its momentum  $k$ , as shown by equation (12.35). This means that it can not be decomposed into a  $\Delta^+(k)$  and  $\Delta^-(k)$  in the way that the standard scalar propagator can.

If there were valid cutting equations in the EFT, one would probably expect this to correspond to the cut through the internal loop of

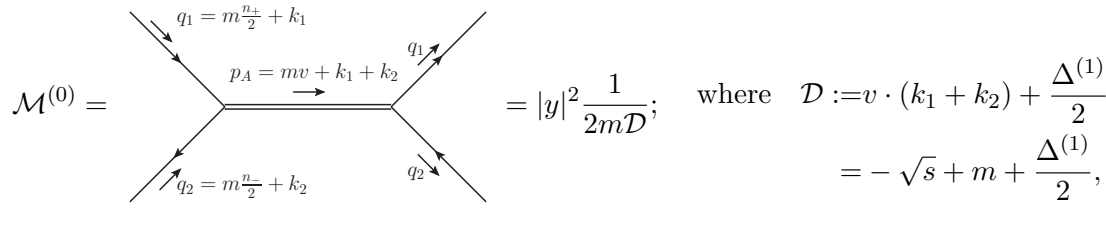


$$\sim \left(\frac{\alpha}{\delta}\right)^2 \sim 1. \quad (12.68)$$

However, this diagram vanishes in the EFT, for the corresponding intergral is scaleless. Instead, the LO contribution to the LHS of (12.66) comes from the imaginary part of the tree-level scattering diagram (the diagram shown in equation (12.69)), which also scales as  $\frac{\alpha}{\delta} \sim 1$ . The reason that the tree-level diagram contributes to the LHS is precisely that the matching coefficient  $\Delta^{(1)}$  (which appears in the  $\phi_v$ -propagator (12.35)) contains an imaginary piece. This illustrates that although the cutting equations do not hold in the EFT, the unitarity equation (12.66) *does* hold perturbatively in the EFT.

## 12.7. Calculating quantum corrections: the forward scattering amplitude to NLO

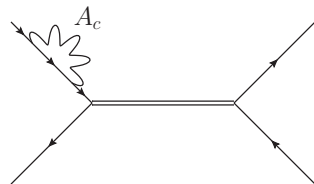
To illustrate how the computation of quantum corrections proceeds in the EFT, we shall now calculate the forward scattering amplitude up to NLO. The LO diagram in the EFT reads



$$\mathcal{M}^{(0)} = \dots = |y|^2 \frac{1}{2m\mathcal{D}}; \quad \text{where } \mathcal{D} := v \cdot (k_1 + k_2) + \frac{\Delta^{(1)}}{2} = -\sqrt{s} + m + \frac{\Delta^{(1)}}{2}, \quad (12.69)$$

where  $s = -(q_1 + q_2)^2$  as usual.

There are three types of NLO corrections: collinear corrections to the external fermions, hard corrections, and loop corrections. The collinear corrections can be calculated in two ways: either by using the collinear fermion fields  $\psi_{c_1}$  and  $\chi_{c_2}$  with the Lagrangian  $\mathcal{L}_{\text{SCET}}$  (12.41), or by using the fields  $\psi_{n_+}$  and  $\chi_{n_-}$  with the Lagrangian  $\mathcal{L}_{\pm}$  (12.42). In the first approach, the corrections occur as loops involving the collinear photon fields  $A_c$  attaching on the external fermions, e.g. as



Since the external fermions are on-shell, these corrections lead to scaleless integrals. The collinear corrections thus vanish.

The remaining corrections are shown in figure 12.4. First we calculate the hard corrections. It is convenient to express these corrections in terms of the LO amplitude  $\mathcal{M}^{(0)}$ . The

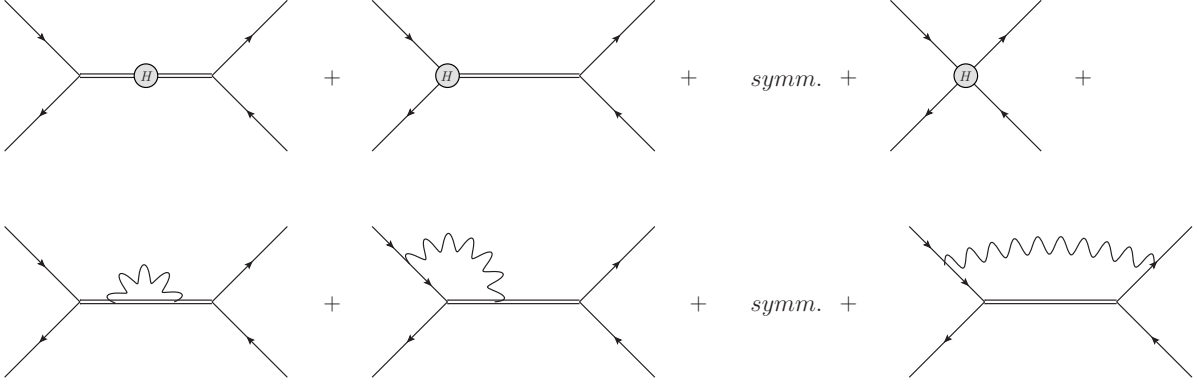


Figure 12.4.: NLO corrections in the EFT.

first hard correction - the hard correction to the propagator - follows from the insertion of the second term of  $\mathcal{L}_{\text{HSET}}$  (12.36), resulting in

$$\mathcal{M}^{(0)} \cdot \frac{1}{2m\mathcal{D}} \left( (k_{1\perp} + k_{2\perp})^2 + \frac{[\Delta^{(1)}]^2}{4} - m\Delta^{(2)} \right) = \mathcal{M}^{(0)} \left( \frac{[\Delta^{(1)}]^2}{8m\mathcal{D}} - \frac{\Delta^{(2)}}{2\mathcal{D}} \right), \quad (12.70)$$

where we assumed that  $n_+$  and  $n_-$  are chosen such that  $k_{1\perp} = k_{2\perp} = 0$ . The vertex corrections consist of an insertion of the coefficient  $C^{(1)}$ . The final hard correction comes as a non-resonant scattering topology of figure 12.2b. As explained in paragraph 12.4.1, to obtain a NLO correction to the scattering amplitude one needs the expression for the corresponding coefficient  $D = \frac{1}{4}$ . By adding these corrections to the propagator correction (12.70) the sum of the hard corrections is found to be

$$\mathcal{M}_{\text{hard corr.}}^{(1)} = \mathcal{M}^{(0)} \cdot \left( 2C^{(1)} + \frac{\mathcal{D}}{2m} + \frac{[\Delta^{(1)}]^2}{8m\mathcal{D}} - \frac{\Delta^{(2)}}{2\mathcal{D}} \right). \quad (12.71)$$

Then there are the three soft photon loops. Since the loops represent an order  $\alpha$ -correction, they are evaluated using the LO Feynman rules (12.57). The last loop correction of figure 12.4 vanishes. The reason is that the photon couples to two external  $\psi_{n_+}$  fields. The Feynman rules then imply that the loop vanishes by  $n_+^2 = 0$ . The remaining two loop corrections are evaluated in appendix C. The result is

$$\mathcal{M}_{\text{loop corr.}}^{(1)} = \mathcal{M}^{(0)} \cdot \alpha_g \bar{\mu}^\epsilon \left( \frac{2\mathcal{D}}{\mu} \right)^\epsilon \left( \frac{8}{\epsilon^2} - \frac{4}{\epsilon} + 4 + \frac{5\pi^2}{6} \right). \quad (12.72)$$

The double pole in  $\epsilon$  in (12.72) arises from the EFT loop correction to the production and decay vertex. It is an artefact of the expansion of the full theory loop correction  $\Gamma$  into a hard part  $\Gamma_h$  and a soft part  $\Gamma_s$ .  $\Gamma = \Gamma_h + \Gamma_s$  does not contain a double pole in  $\epsilon$  (at least with the scalar off-shell, which is what we need for the scattering amplitude), but  $\Gamma_h$  and  $\Gamma_s$  do contain cancelling double poles. Indeed, equation (12.48) shows the double pole of  $\Gamma_h$ . In the EFT this double pole is present in the hard matching coefficient  $C^{(1)}$  and thus enters the hard corrections (12.71). The soft part  $\Gamma_s$  of the full theory loop is reproduced by the EFT loop; its double pole is thus the one encountered in (12.72). Adding the hard corrections (12.71) and loop corrections

(12.72) together, we do indeed find that the double poles cancel.

$$\begin{aligned}
\mathcal{M}^{(1)} &= \mathcal{M}_{\text{hard corr.}}^{(1)} + \mathcal{M}_{\text{loop corr.}}^{(1)} \\
&= \mathcal{M}^{(0)} \cdot \left\{ \alpha_g \left[ 3 + \ln \left( \frac{2m\mathcal{D}}{m^2} \right) \right] \left[ \frac{2}{\epsilon} + \ln \left( \frac{2m\mathcal{D}}{\mu^2} \right) \right] + \alpha_g \left[ -7 \ln \left( \frac{2m\mathcal{D}}{m^2} \right) - \frac{3}{2} \ln \left( \frac{m^2}{\mu^2} \right) - \frac{7}{2} + \frac{2\pi^2}{3} \right] \right. \\
&\quad \left. + \alpha_y \left[ 2 \ln \left( \frac{m^2}{\mu^2} \right) - \frac{1}{2} - i\pi \right] + \frac{[\Delta^{(1)}]^2}{8m\mathcal{D}} - \frac{\Delta^{(2)}}{2\mathcal{D}} + \frac{\mathcal{D}}{2m} \right\}
\end{aligned} \tag{12.73}$$

The remaining single pole in  $\epsilon$  is a collinear singularity associated with the initial (massless)  $\psi_{n_+}$  particle. This is analogous to the collinear singularity associated with an initial state quark in QCD. In that case, according to the factorization theorem, the amplitude would have to be convolved with the corresponding parton distribution function (PDF) to obtain the cross section. By renormalizing the PDF one can do away with the single pole of (12.73). Equation (12.73) does not make all the factors  $\alpha$  and  $\delta$  explicit. The  $\delta$  factors are contained within  $\mathcal{D}$ , which is also present in  $\mathcal{M}^{(0)}$ ; both these statements follow from equation (12.69). Furthermore, recall that  $\Delta^{(i)} \sim \alpha^i$ .

# 13. Comparing the NWA, CMS and EFT

## 13.1. Advantages and drawbacks

In this thesis we have discussed several methods to describe scattering processes that possibly proceed through the production and decay of an unstable particle. Three of them were found to respect the gauge invariance and unitarity of the theory: the narrow-width approximation (NWA) of section 9.5, the complex mass scheme (CMS) of chapter 11, and the effective field theory (EFT) of chapter 12. In this section we list the advantages and disadvantages of each of these approaches; the next section illustrates the accuracies of the methods for single-top production.

### 13.1.1. NWA

- ⊕ **Ease of implementation.** The NWA is very straightforward to implement; the unstable particle is essentially approximated to be stable, such that the total scattering process factorizes into the production and decay of the particle.
- ⊖ **Possibility to include background.** Background processes - diagrams contributing to the scattering process that do not involve a single internal propagator of the unstable particle - cannot be taken into account. Or at least, the interference between resonant processes and background cannot be taken into account, for the NWA only prescribes how to approximate the Breit-Wigner shape that arises by considering resonant processes only.
- ⊖ **Accuracy.** As long as (interference with) background does not play an important role, the NWA is expected to predict observables that are insensitive to or integrated over  $s_A$  (the invariant mass of the unstable particle) with an error of  $\mathcal{O}(\Gamma/m)$ . Corrections in the coupling constant  $\alpha$  to the production and decay of the particle can be taken into account, but there is no way to reduce the  $\mathcal{O}(\Gamma/m)$  error made by taking the limit  $\frac{\Gamma}{m} \downarrow 0$ .
- ⊖ **Difficulty of loop calculations.** Loop corrections to the production and decay of the unstable particle are the usual loop corrections and thus of the normal difficulty.

Summarizing, if background processes are unimportant, the NWA is a suitable approximation for observables that do not depend on the invariant mass of the unstable particles, for a required precision of  $\mathcal{O}(\Gamma/M)$  or lower. In particular, this makes the NWA suitable for Higgs production, since the width of the Higgs  $\Gamma_H/M_H \sim 3 \cdot 10^{-5}$  is very small, as showcased in table 9.1.

### 13.1.2. CMS

- ⊕ **Ease of implementation.** As the CMS is a specific choice of a renormalization scheme, its implementation is straightforward.
- ⊕ **Validity throughout phase space.** The CMS is valid in the entire phase space and thus readily applicable to any kinematical configuration.



- ⊕ **Possibility to include background.** Background processes - including their interference with resonant diagrams - can be included without problems.
- ⊕ **Accuracy.** The accuracy of observables is determined by the order of perturbation theory and can thus consistently be improved in principle.
- ⊖ **Difficulty of loop calculations.** The loop calculations are equal to standard loop calculations with the complication of complex masses and complex counterterms. At NLO this is not a major complication. On the other hand, NNLO calculations are presently difficult.
- ⊖ **Summation of large logarithms  $\ln\left(\frac{m}{\Gamma}\right)$ .** The summation of these logarithms cannot be performed in the CMS [26].

Its ease of implementation makes the CMS the weapon of choice for NLO computations. Indeed, it is implemented in automated one-loop computations [39, 40]. When going beyond NLO, or when the summation of large logarithms is desired, the EFT may be preferable.

### 13.1.3. EFT

- ⊖ **Ease of implementation.** Setting up the effective theory is not as straightforward. The EFT depends on the desired observable and requires the matching of the EFT to the full theory in standard perturbation theory.
- ⊖ **Validity throughout phase space.** The EFT is - by construction - only valid in the region of phase space close to the resonance. Although outside this region standard perturbation theory is valid, in practice it can be inconvenient to distinguish between different regions of phase space.
- ⊕ **Possibility to include background.** Background processes - including their interference with resonant diagrams - can be included without problems.
- ⊕ **Accuracy.** The accuracy of observables is determined by the order of perturbation theory (in  $\alpha$  and  $\delta$ ) and can thus consistently be improved in principle.
- ⊕ **Difficulty of loop calculations.** In contrast to the CMS, the calculations in the EFT are minimal in the sense that only terms are calculated that are strictly necessary to obtain a certain accuracy in  $\alpha$  and  $\delta$ . This makes the loop calculations in the EFT simpler. For example, if one calculates the full theory NLO three-point function  $\Gamma$  (12.44) in the toy model of chapter 12, one finds integrals yielding hypergeometric functions. These can be considered more complicated than the hard part (12.48) and soft part (12.72) of  $\Gamma$ . These parts are the ones needed for the EFT calculation: the hard part is encountered in matching the EFT to the full theory and the soft part in calculating loop corrections in the EFT.
- ⊕ **Summation of large logarithms  $\ln\left(\frac{m}{\Gamma}\right)$ .** The summation of these logarithms *can* be performed in the EFT [26].

Summarizing, the EFT is more elaborate to apply than the CMS, but promising for NNLO calculations, or when the summation of large logarithm is desired. In these cases the EFT seems preferable over the CMS.

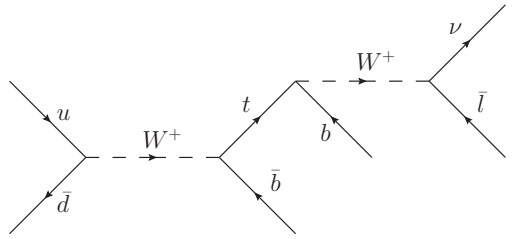
## 13.2. Accuracies for single-top production

In this section the accuracy of the NWA, the CMS and the EFT is compared for single-top production. The top quark is so shortlived that it does not have time to form a bound state [41]. Therefore its production and decay can be treated as that of any virtual particle in perturbative calculations. We discuss results obtained by the different approaches in two papers.

In 2000 van der Heide et al. calculated the cross section for processes involving single-top production at tree-level [42]. The subsequent decay of the top assumed is  $t \rightarrow b + \bar{l} + \nu$ . Three partonic subprocesses involving a single top that are considered are

- the “W-gluon fusion” process  $u + g \rightarrow t + d + b \rightarrow b + \bar{l} + \nu + d + b$ ,
- the “flavor excitation” process  $u + b \rightarrow t + d \rightarrow b + \bar{l} + \nu + d$ ,
- the “s-channel” process  $u + \bar{d} \rightarrow t + \bar{b} \rightarrow b + \bar{l} + \nu + \bar{b}$ .

To obtain an impression of the contributing diagrams: a typical tree-level diagram for the “s-channel” process is



but also many background processes exist that contribute to  $u + \bar{d} \rightarrow b + \bar{l} + \nu + \bar{b}$  without producing a top. Van der Heide et al. calculated the cross section for these processes *including* background processes numerically in the CMS and compared the results to the cross sections that were found by only considering resonant contributions (so *without* background) in the NWA. The results are displayed in table 13.1. The second column shows the cross section calculated with the restriction that the invariant mass  $m_{\nu\bar{l}b}$  of the decay products of the top lies within 20 GeV of the top mass. Table 13.1 shows that for the “W-gluon fusion” and “flavor excitation” processes the NWA agrees well with the full result. The relative error does indeed seem to be of order  $\frac{\Gamma_t}{m_t} \approx \frac{1}{87}$ , which is expected since the considered cross section is integrated over  $m_{\nu\bar{l}b}$ . On the other hand, the cross section for the “s-channel” process is strongly underestimated by the NWA. The reason seems to be that background processes provide a significant contribution to this process, indicated by the fact that the second column shows a cross section much smaller than the total cross section.

In 2013, Papanastasiou et al. considered single top production to NLO [40]. The examined process is similar

$$pp \rightarrow W^+ J_b J_{\text{light}} + X, \quad (13.1)$$

where  $J_b$  denotes a jet emerging from a b-quark and  $J_{\text{light}}$  a jet emerging from a light quark

process	$\sigma_{\text{tot}}$	$ m_{\nu\bar{b}} - m_t  < 20 \text{ GeV}$	NWA
W-gluon fusion	$15.0 \pm 0.4 \text{ fb}$	$14.3 \pm 0.3 \text{ fb}$	$14.5 \pm 0.1 \text{ fb}$
flavor excitation	$87 \pm 1 \text{ fb}$	$85 \pm 2 \text{ fb}$	$87 \pm 1 \text{ fb}$
s-channel	$46 \pm 1 \text{ fb}$	$32.3 \pm 0.3 \text{ fb}$	$29.0 \pm 0.2 \text{ fb}$

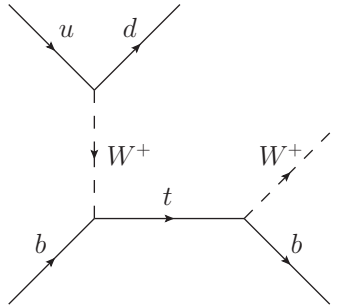
(a) At the Tevatron (2 TeV).

process	$\sigma_{\text{tot}}$	$ m_{\nu\bar{b}} - m_t  < 20 \text{ GeV}$	NWA
W-gluon fusion	$4.6 \pm 0.2 \text{ pb}$	$4.5 \pm 0.4 \text{ pb}$	$4.6 \pm 0.1 \text{ pb}$
flavor excitation	$13.1 \pm 0.3 \text{ pb}$	$13.0 \pm 0.4 \text{ pb}$	$13.3 \pm 0.1 \text{ pb}$
s-channel	$685 \pm 19 \text{ fb}$	$479 \pm 16 \text{ fb}$	$432 \pm 4 \text{ fb}$

(b) At the LHC (14 TeV).

Table 13.1.: Single top production at tree level [42].

(e.g. a d-quark). A typical resonant tree-level diagram of the partonic subprocess is



The “s-channel” process, for which the background turned out to be important in the above, is not included. The full cross sections (including background) are calculated to LO and to NLO using numerical methods adopting the CMS. In addition, the cross section found by including only resonant diagrams (diagrams involving a single top) are calculated to NLO using both the NWA and the EFT.

First the total cross section is considered, calculated with the restriction that the invariant mass of the reaction products  $M(W^+, J_b)$  lies in the window around the top mass  $140 < M(W^+, J_b) < 200 \text{ GeV}$ . The results are displayed in table 13.2. The conclusion is that all three approaches agree to within 1% for the total cross section.

Also considered was the differential cross section, as a function of  $M(W^+, J_b)$ . The results

method	LO	NLO
CMS [pb]	$4.184(1)^{+8.5\%}_{-12.3\%}$	$4.115(5)^{+0.5\%}_{+4.6\%}$
NWA [pb]	$4.223(1)^{+8.8\%}_{-12.2\%}$	$4.138(1)^{+0.9\%}_{+2.6\%}$
% diff	+0.9	+0.6
EFT [pb]	$4.154(1)^{+8.8\%}_{-12.2\%}$	$4.074(1)^{+0.3\%}_{+4.0\%}$
% diff	-0.7	-1.0

Numbers in brackets are Monte Carlo integration uncertainties, whereas the percentages indicate scale uncertainties. “% diff” indicates the relative difference with the CMS result.

Table 13.2.: Single top production to NLO at the LHC (8TeV) [40]

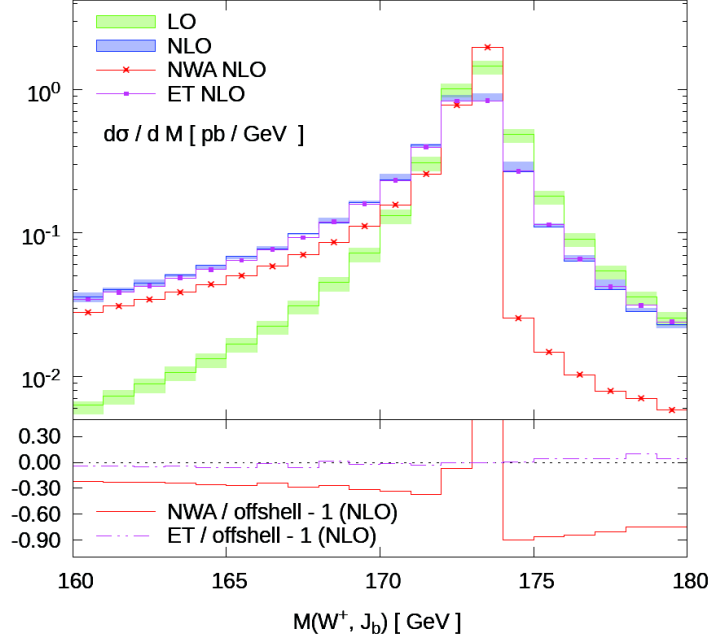


Figure 13.1.: Differential cross section for single top production at the LHC (8TeV) [40].

of the different approaches are shown in figure 13.1. There are several things to note here. The first is that the difference between the full LO and NLO calculations is rather large below the resonance ( $M(W^+, J_b) < M_t$ ). The large correction is due to real emission from the production and decay process of the top. This can be concluded from the fact that the NLO NWA curve agrees fairly well with the full NLO result for  $M(W^+, J_b) < M_t$ . To understand this, we note that at LO, the NWA calculation returns a spike at  $M(W^+, J_b) = M_t$ . The reason is that at LO the invariant mass of the top  $s_A$  equals  $M(W^+, J_b)$  and that the NWA implies that only  $s_A = M_t$  is allowed. The same argument applies to virtual corrections in the NWA. Therefore, any contribution to the NLO NWA differential cross section for  $M(W^+, J_b) \neq M_t$  is due to real corrections. The fact that the full NLO result agrees fairly well with the NLO NWA result for  $M(W^+, J_b) < M_t$  thus indicates that the large correction is due to real emission from the production or decay of the top. Another distinct feature of figure 13.1 is that whereas the NWA NLO curve agrees fairly well with the full NLO result below the resonance, above the resonance it is completely off. Above we argued that all contributions to the NLO NWA curve in this region are real corrections to the production or decay of the top. Since real emission from the decay of the top is impossible for  $M(W^+, J_b) > M_t$  (for it would require  $s_A > M_t$ ), the entire NLO NWA differential cross section in this region is due to real corrections to the production of the top. In contrast, in the full calculation this region receives contributions already at LO, both from diagrams containing a (slightly) off-shell top as well as from background processes. This explains the large difference between the full NLO and NWA NLO result for  $M(W^+, J_b) > M_t$ . The large difference confirms the expectation that the NWA is *not* a good approximation for observables that depend on  $M(W^+, J_b)$ . In this respect it is interesting to note that the NWA underestimates the differential cross section for  $M(W^+, J_b) \neq M_t$  and overestimates it for  $M(W^+, J_b) = M_t$ . The difference between the under- and overestimation is such that the *total* cross section (the differential cross section integrated over  $M(W^+, J_b)$ ) *does* agree fairly well with the full NLO cross section, as established in table 13.2. Finally, figure 13.1 shows that the

NLO EFT computation agrees very well with the full computation. Note that the plot only comprises values of  $|\delta| \approx \left| \frac{(M(W^+, J_b))^2 - M_t^2}{M_t^2} \right| \leq 0.14$ . Since the EFT is derived for  $|\delta| \ll 1$ , outside the plot range the EFT is expected to become unreliable.

## 14. Conclusion

This thesis has given an account of unstable particles and the complications they bring in a quantum field theory. Subject of discussion have been their masses and decay rates, gauge invariance and unitarity in their presence, and how to obtain accurate predictions for physical observables in a theory involving unstable particles. Since unstable particles give rise to resonant processes that dominate physical observables, understanding their influence in quantitative way is essential. Indeed, in order to test the Standard Model, the theoretical accuracy of its predictions have to match the experimental accuracy reached by particle colliders. In theories describing physics beyond the Standard Model, the notion of unstable particles is likely to be even more important. Indeed, any new particle that the 13 TeV LHC run may find hints of - or more generally, any new particle that is going to be found in the future - is very likely to be unstable. Once again, testing predictions of these new physics theories requires a careful treatment of their unstable particles.

## A. Calculation of $I(k^2, m_1^2, m_2^2)$

The integral is defined as

$$I(k^2, m_1^2, m_2^2) := \frac{1}{(2\pi)^n} \int d^n q \frac{1}{[(q + \frac{1}{2}k)^2 + m_1^2 - i\eta] [(q - \frac{1}{2}k)^2 + m_2^2 - i\eta]}, \quad (\text{A.1})$$

where it is understood that  $\eta > 0$  and that we take the limit  $\eta \downarrow 0$ . The integrand can be rewritten as one denominator using Feynman's trick (10.39). This results in

$$I(k^2, m_1^2, m_2^2) = \frac{1}{(2\pi)^n} \int_0^1 dx \int d^n q \frac{1}{[Q^2 + M^2]^2}, \quad (\text{A.2})$$

$$\text{where } \begin{cases} Q^2 = q + k(x - \frac{1}{2}) \\ M^2 = m_2^2 + x(m_1^2 - m_2^2) + k^2 x(1 - x) - i\eta. \end{cases} \quad (\text{A.3})$$

The integral over  $q$  is evaluated by using (10.41). Putting  $n = 4 + \epsilon$ , we obtain

$$I(k^2, m_1^2, m_2^2) = \frac{i}{(4\pi)^2} \Gamma(-\frac{\epsilon}{2}) \mu^\epsilon (f(x, s) - i\eta)^{\epsilon/2},$$

$$\text{where } f(x, s := -k^2) := \frac{m_2^2 + x(m_1^2 - m_2^2) - sx(1 - x)}{4\pi\mu^2}. \quad (\text{A.4})$$

By using (10.65) to expand  $\Gamma(-\frac{\epsilon}{2})$ , this becomes

$$I(k^2, m_1^2, m_2^2) = -\frac{i\mu^\epsilon}{8\pi^2} \left[ \frac{1}{\epsilon} + \frac{1}{2}\gamma_E + \frac{1}{2} \int_0^1 dx \ln(f(x, s) - i\eta) \right]. \quad (\text{A.5})$$

It is important to investigate whether  $f(x, s)$  can become negative in the integration domain. The reason is that the logarithm has a branch cut along the negative real axis, such that the  $-i\eta$  prescription implies

$$\ln(f(x, s) - i\eta) = \begin{cases} \ln|f| & \text{if } f > 0 \\ \ln|f| - i\pi & \text{if } f < 0. \end{cases} \quad (\text{A.6})$$

Inspection shows that  $f(x, s)$ , which is an upward opening parabola in  $x$ , becomes negative for some values of  $x$  if  $\lambda(s, m_1^2, m_2^2) > 0 \Leftrightarrow (s < (m_1 - m_2)^2 \vee s > (m_1 + m_2)^2)$ , where  $\lambda(x, y, z) := x^2 + y^2 + z^2 - 2xy - 2xz - 2yz$ . In this case, the roots are given by  $x_\pm = \frac{1}{2s} [s + m_2^2 - m_1^2 \pm \lambda^{1/2}]$ . From this one can derive that  $f(x, s)$  only becomes negative *in the integration domain* if  $s > (m_1 + m_2)^2$ , and if so in the region  $0 < x_- < x < x_+ < 1$ . As a result, the integral over the logarithm is

$$\frac{1}{2} \int_0^1 dx \ln(f(x, s) - i\eta) = \frac{1}{2} \int_0^1 dx \ln|f(x, s)| - i\pi \frac{\lambda^{1/2}}{2s} \theta(s - (m_1 + m_2)^2). \quad (\text{A.7})$$

The integral left to calculate is then

$$\frac{1}{2} \int_0^1 dx \ln |f(x, s)| = \frac{1}{2} \ln \left| \frac{s}{4\pi\mu^2} \right| + \frac{1}{2} \int_0^1 dx \ln |(x-A)^2 - D|,$$

where  $A := \frac{1}{2}(1+B)$ ,  $B := \frac{m_2^2 - m_1^2}{s}$ , and  $D := \frac{\lambda}{4s^2}$ . (A.8)

The integral on the right hand side of (A.8) can be evaluated as follows.

$$\begin{aligned} \frac{1}{2} \int_0^1 dx \ln |(x-A)^2 - D| &= \frac{1}{2} \int_{-A}^{-A+1} \ln |x^2 - D| \\ &= \frac{1}{2} \left\{ [x \ln |x^2 - D|]_{-\frac{1}{2}(1+B)}^{\frac{1}{2}(1-B)} - \int_{-\frac{1}{2}(1+B)}^{\frac{1}{2}(1-B)} dx \frac{2x^2}{x^2 - D} \right\}. \end{aligned} \quad (\text{A.9})$$

The first term of (A.9) gives

$$[x \ln |x^2 - D|]_{-\frac{1}{2}(1+B)}^{\frac{1}{2}(1-B)} = \frac{1}{2s} \left[ s \ln \left( \frac{m_1 m_2}{s} \right) + (m_2^2 - m_1^2) \ln \left( \frac{m_2}{m_1} \right) \right]; \quad (\text{A.10})$$

the second can be rewritten as

$$J := - \int_{-\frac{1}{2}(1+B)}^{\frac{1}{2}(1-B)} dx \frac{2x^2}{x^2 - D} = - \left( 1 + D \int_{-\frac{1}{2}(1+B)}^{\frac{1}{2}(1-B)} dx \frac{1}{x^2 - D} \right). \quad (\text{A.11})$$

To evaluate the integral in (A.11), we distinguish two cases.

1.  $D = \frac{\lambda}{4s^2} > 0 \Leftrightarrow (s < (m_1 - m_2)^2 \vee s > (m_1 + m_2)^2)$ .

In this case we substitute  $x = \sqrt{D} \cdot y$ , such that  $J$  becomes

$$\begin{aligned} J &= -1 - \sqrt{D} \int_{\frac{1}{2\sqrt{D}}(1+B)}^{\frac{1}{2\sqrt{D}}(1-B)} dy \frac{1}{y^2 - 1} \\ &= -1 - \frac{\sqrt{D}}{2} \int_{\frac{1}{2\sqrt{D}}(1+B)}^{\frac{1}{2\sqrt{D}}(1-B)} dy \left[ \frac{1}{y-1} - \frac{1}{y+1} \right] \\ &= -1 - \frac{\sqrt{D}}{2} \left[ \ln |y-1| - \ln |y+1| \right]_{\frac{1}{2\sqrt{D}}(1+B)}^{\frac{1}{2\sqrt{D}}(1-B)} \\ &= -1 - \frac{\lambda^{1/2}}{4s} \left\{ \ln \left| \frac{s + m_1^2 - m_2^2 - \lambda^{1/2}}{s + m_1^2 - m_2^2 + \lambda^{1/2}} \right| + \ln \left| \frac{s - m_1^2 + m_2^2 - \lambda^{1/2}}{s - m_1^2 + m_2^2 + \lambda^{1/2}} \right| \right\}. \end{aligned} \quad (\text{A.12})$$

2.  $D = \frac{\lambda}{4s} < 0 \Leftrightarrow (m_1 - m_2)^2 < s < (m_1 + m_2)^2$ .

In this case we substitute  $x = \sqrt{-D} \cdot y$ , such that  $J$  becomes

$$\begin{aligned} J &= -1 + \sqrt{-D} \int_{\frac{1}{2\sqrt{-D}}(1+B)}^{\frac{1}{2\sqrt{-D}}(1-B)} dy \frac{1}{y^2 + 1} \\ &= -1 + \sqrt{-D} \left[ \text{Arctan}(y) \right]_{-\frac{1}{2\sqrt{-D}}(1+B)}^{\frac{1}{2\sqrt{-D}}(1-B)} \\ &= -1 + \frac{\sqrt{-\lambda}}{2s} \left\{ \text{Arctan} \left( \frac{s + m_1^2 - m_2^2}{\sqrt{-\lambda}} \right) + \text{Arctan} \left( \frac{s - m_1^2 + m_2^2}{\sqrt{-\lambda}} \right) \right\}. \end{aligned} \quad (\text{A.13})$$



Putting everything together yields the final result

$$\begin{aligned}
I(k^2 = -s^2, m_1^2, m_2^2) &= \frac{-i\mu^\epsilon}{8\pi^2} \left\{ \frac{1}{\epsilon} + \frac{1}{2}\gamma_E + \frac{1}{2}\ln\left(\frac{m_1 m_2}{4\pi\mu^2}\right) + \frac{m_1^2 - m_2^2}{2s}\ln\left(\frac{m_1}{m_2}\right) - 1 \right. \\
&\quad \left. + h(s, m_1^2, m_2^2) - i\pi\frac{\lambda^{1/2}}{2s}\theta(s - (m_1 + m_2)^2), \right. \tag{A.14}
\end{aligned}$$

where

$$h(s, m_1^2, m_2^2) := \frac{|\lambda|^{1/2}}{2s} \begin{cases} \text{Arctan}\left(\frac{s + m_1^2 - m_2^2}{\sqrt{-\lambda}}\right) + \text{Arctan}\left(\frac{s - m_1^2 + m_2^2}{\sqrt{-\lambda}}\right) & \text{for } (m_1 - m_2)^2 < s < (m_1 + m_2)^2, \\ -\frac{1}{2} \left\{ \ln\left|\frac{s + m_1^2 - m_2^2 - \lambda^{1/2}}{s + m_1^2 - m_2^2 + \lambda^{1/2}}\right| + \ln\left|\frac{s - m_1^2 + m_2^2 - \lambda^{1/2}}{s - m_1^2 + m_2^2 + \lambda^{1/2}}\right| \right\}, & \text{for } (s < (m_1 - m_2)^2 \vee s > (m_1 + m_2)^2). \end{cases} \tag{A.15}$$

## B. Calculation of $\Gamma_h^{1\text{-loop}}$

In this appendix we calculate the hard part of the one-loop correction to the  $\psi\bar{\chi}\phi$  three-point function of the full toy theory used in section 12. The diagram is shown in figure B.1. We

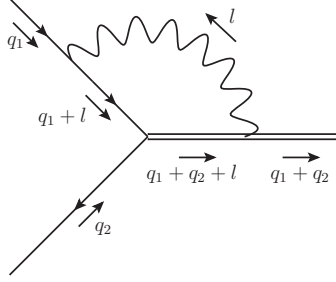


Figure B.1.: One-loop correction to the full theory three-point function  $\Gamma$

shall assume the two external fermions to be on-shell such that  $\bar{v}(q_2)\not{q}_2 = \not{q}_1 u(q_1) = 0$ . The Feynman rules can be derived from the full theory Lagrangian (12.5). The resulting amplitude reads (using the Feynman gauge for the photon propagator)

$$\begin{aligned} \Gamma^{1\text{-loop}} &= \frac{ig^2 y}{i(2\pi)^n} \bar{v}(q_2) \int d^n l \frac{-i(\not{q}_1 + \not{l})}{(q_1 + l)^2} \gamma_\mu \frac{\eta^{\mu\nu}}{l^2} (2q_1 + 2q_2 + l)_\nu \frac{1}{(q_1 + q_2 + l)^2 + m^2} u(q_1) \\ &= -\frac{ig^2 y}{(2\pi)^n} \bar{v}(q_2) \int d^n l \frac{l^2 + 2l \cdot q_1 + 4l \cdot q_2 + 4q_1 \cdot q_2}{l^2(l^2 + 2l \cdot q_1)(l^2 + 2l \cdot q_1 + 2l \cdot q_2 + 2q_1 \cdot q_2 + m^2)} u(q_1). \end{aligned} \quad (\text{B.1})$$

In the following the spinors  $\bar{v}(q_2)$  and  $u(q_1)$  are left implicit.

Now the hard approximation is made according to the strategy of regions. This comprises using the scalings

$$l \sim m(1, 1, \vec{1}) \quad \text{and} \quad \begin{cases} q_1 = m \frac{n_+}{2} + k_1 \\ q_2 = m \frac{n_-}{2} + k_2 \end{cases}, \quad \text{with} \quad k_1, k_2 \sim m(\delta, \delta, \vec{\delta}). \quad (\text{B.2})$$

We then keep only the terms that are of leading order in  $\delta$  in the numerator and denominator of (B.1). This effectively means neglecting  $k_1$  and  $k_2$ . Since this implies that  $(q_1 + q_2)^2 = m^2(\frac{n_+}{2} + \frac{n_-}{2})^2 = -m^2$ , this amounts to putting the scalar on-shell. Indeed, for an on-shell scalar we have that  $\Gamma_s^{1\text{-loop}} = 0$ , implying that  $\Gamma^{1\text{-loop}} = \Gamma_h^{1\text{-loop}}$  for an on-shell scalar. Defining

$l_{\pm} := n_{\pm} \cdot l$ , the hard part of (B.1) is

$$\begin{aligned}
\Gamma_h^{1\text{-loop}} &= -\frac{ig^2y}{(2\pi)^n} \int d^n l \frac{l^2 + ml_+ + 2ml_- - 2m^2}{l^2(l^2 + ml_+)(l^2 + ml_+ + ml_-)} \\
&= -\frac{ig^2y}{(2\pi)^n} \left\{ 2 \int d^n l \frac{1}{l^2(l^2 + ml_+)} - \int d^n l \frac{1}{l^2(l^2 + ml_+ + ml_-)} \right. \\
&\quad \left. - 2m^2 \int d^n l \frac{1}{l^2(l^2 + ml_+)(l^2 + ml_+ + ml_-)} \right\} \\
&:= I_{h1} + I_{h2} + I_{h3}.
\end{aligned} \tag{B.3}$$

These three integrals can be evaluated using Feynman parameters (10.39). The first integral then reads

$$I_{h1} = -\frac{ig^2y}{(2\pi)^n} \int_0^1 dx \int d^n l \frac{1}{(l + xm \frac{n_+}{2})^2} = 0. \tag{B.4}$$

The reason that this vanishes is that the integral over  $l$  becomes scaleless upon shifting  $l \rightarrow l - xm \frac{n_+}{2}$ .

The second integral gives

$$\begin{aligned}
I_{h2} &= \frac{ig^2y}{(2\pi)^n} \int_0^1 dx \int d^n l \frac{1}{[(l + xm \frac{n_+}{2} + xm \frac{n_-}{2})^2 - x^2 m^2]^2} \\
&\stackrel{(10.41)}{=} -y \frac{g^2}{(4\pi)^2} \mu^\epsilon (4\pi)^{-\epsilon/2} \left(\frac{m}{\mu}\right)^\epsilon \Gamma(-\frac{\epsilon}{2}) \int_0^1 dx x^\epsilon \\
&= -y \alpha_g \mu^\epsilon (4\pi)^{-\epsilon/2} \left(\frac{m}{\mu}\right)^\epsilon \Gamma(1 - \frac{\epsilon}{2}) \left(-\frac{2}{\epsilon(1+\epsilon)}\right),
\end{aligned} \tag{B.5}$$

where in the last step we used  $\alpha_g = \frac{g^2}{(4\pi)^2}$ .

To calculate  $I_{h3}$ , we use Feynman parameters (10.39) to combine two denominators twice, resulting in

$$\begin{aligned}
\frac{1}{A_1 A_2 A_3} &= \int_0^1 dx \frac{1}{A_1} \frac{1}{[xA_2 + (1-x)A_3]^2} \\
&= 2 \int_0^1 dx \int_0^1 dy \frac{y}{[(1-y)A_1 + yA_3 + xy(A_2 - A_3)]^3}.
\end{aligned} \tag{B.6}$$

$$\begin{aligned}
I_{h3} &\stackrel{(B.6)}{=} 4m^2 \frac{ig^2y}{(2\pi)^n} \int_0^1 dx \int_0^1 dy \int d^n l \frac{y}{[(1-y)l^2 + y(l^2 + ml_+) + xym l_-]^3} \\
&= 4m^2 \frac{ig^2y}{(2\pi)^n} \int_0^1 dx \int_0^1 dy y \int d^n l \frac{1}{[(l + ym \frac{n_+}{2} + xym \frac{n_-}{2})^2 - m^2 y^2 x]^3} \\
&\stackrel{(10.41)}{=} -2y \frac{g^2}{(4\pi)^2} \mu^\epsilon (4\pi)^{-\epsilon/2} \left(\frac{m}{\mu}\right)^\epsilon \Gamma(1 - \frac{\epsilon}{2}) \int_0^1 dx x^{\epsilon/2-1} \int_0^1 dy y^{\epsilon-1} \\
&= -y \alpha_g \mu^\epsilon (4\pi)^{-\epsilon/2} \left(\frac{m}{\mu}\right)^\epsilon \Gamma(1 - \frac{\epsilon}{2}) \frac{4}{\epsilon^2}.
\end{aligned} \tag{B.7}$$

Using  $\Gamma(1+z) = e^{-\gamma_E z + \frac{\pi^2}{12} z^2} + \mathcal{O}(z^3)$ ,

(B.8)

we find

$$\begin{aligned} \Gamma_h^{1\text{-loop}} = I_{h1} + I_{h2} + I_{h3} &= -y\alpha_g \mu^\epsilon (4\pi)^{-\epsilon/2} e^{\gamma_E \epsilon/2} \left(\frac{m}{\mu}\right)^\epsilon e^{\frac{\pi^2}{48} \epsilon^2} \left[ \frac{4}{\epsilon^2} - \frac{2}{\epsilon(1+\epsilon)} \right] \\ &= y\alpha_g \bar{\mu}^\epsilon \left[ -\frac{4}{\epsilon^2} + \frac{2}{\epsilon} - 2 - \frac{\pi^2}{12} \right], \end{aligned}$$
(B.9)

where we defined  $\bar{\mu}^\epsilon := \mu^\epsilon (4\pi)^{-\epsilon/2} e^{\gamma_E \epsilon/2}$ .

## C. Calculation of loop corrections in the EFT

This appendix is devoted to the calculation of the EFT loop corrections to the forward scattering amplitude  $\mathcal{M}_{\text{loop corr.}}^{(1)}$  encountered in section 12.7. The Feynman rules are given by equation (12.57).

The self-energy correction is

$$\mathcal{M}_{\text{SE loop}}^{(1)} = \text{Diagram} \quad . \quad (\text{C.1})$$

The drawn momenta are the momenta of the EFT fields. Thus the scalar field with momentum  $k$  would in the full theory correspond to a scalar with momentum  $P = mv + k$ . Furthermore, it is understood that  $k = k_1 + k_2$  and  $\mathcal{D} = v \cdot k + \frac{\Delta^{(1)}}{2}$ .

$$\begin{aligned} \mathcal{M}_{\text{SE loop}}^{(1)} &= \frac{\mathcal{M}^{(0)}}{i(2\pi)^n} (2mg)^2 \frac{1}{2m\mathcal{D}} \int d^n l \frac{v_\mu \eta^{\mu\nu} v_\nu}{l^2 (2mv \cdot l + 2m\mathcal{D})} \\ &= -\frac{\mathcal{M}^{(0)}}{i(2\pi)^n} \frac{2mg^2}{\mathcal{D}} J_1, \end{aligned} \quad (\text{C.2})$$

where the integral  $J_1$  reads

$$\begin{aligned} J_1 &= \int d^n l \frac{1}{l^2 (2mv \cdot l + 2m\mathcal{D})} \\ &\stackrel{(10.39)}{=} \int_0^1 dx \int d^n l \frac{1}{[(1-x)l^2 + x(2mv \cdot l + 2m\mathcal{D})]^2} \\ &= \int_0^1 dx \frac{1}{(1-x)^2} \int d^n l \frac{1}{[(l + \frac{x}{1-x}mv)^2 + \frac{x}{1-x}2m\mathcal{D} + \frac{x^2}{(1-x)^2}m^2]^2}. \end{aligned} \quad (\text{C.3})$$

Upon shifting  $l \rightarrow l - \frac{x}{1-x}mv$  this can be evaluated by (10.41) to give (in  $n = 4 + \epsilon$  dimensions)

$$\begin{aligned} J_1 &= i\pi^{n/2} \Gamma\left(-\frac{\epsilon}{2}\right) (2m\mathcal{D})^{\epsilon/2} \int_0^1 dx x^{\epsilon/2} (1-x)^{-2-\epsilon} \left[1 - x\left(1 - \frac{m}{2\mathcal{D}}\right)\right]^{\epsilon/2} \\ &= i\pi^{n/2} \frac{2\mathcal{D}}{m} (2\mathcal{D})^\epsilon \Gamma(-1-\epsilon) \Gamma\left(1 + \frac{\epsilon}{2}\right). \end{aligned} \quad (\text{C.4})$$

The self-energy correction (C.2) then becomes

$$\mathcal{M}_{\text{SE loop}}^{(1)} = -\mathcal{M}^{(0)} \alpha_g \mu^\epsilon (4\pi)^{-\epsilon/2} \left(\frac{2\mathcal{D}}{\mu}\right)^\epsilon \left[4\Gamma(-1-\epsilon) \Gamma\left(1 + \frac{\epsilon}{2}\right)\right]. \quad (\text{C.5})$$

The loop correction to the vertex is (leaving the external spinors implicit)

$$\begin{aligned}
\mathcal{M}_{\text{vertex loop}}^{(1)} &= \text{Diagram} \\
&= \frac{\mathcal{M}^{(0)}}{i(2\pi)^n} 2im g^2 \int d^n l \frac{1}{in_+ \cdot (k_1 + l)} \frac{\not{k}_+ \not{k}_- n_+^\mu \eta_{\mu\nu} v^\nu}{2} \frac{1}{l^2} \frac{1}{2mv \cdot (k + l) + m\Delta^{(1)}}. \quad (\text{C.6})
\end{aligned}$$

This expression can be simplified by using that  $v = \frac{n_+}{2} + \frac{n_-}{2}$ ,  $\frac{\not{k}_+ \not{k}_-}{2} u(k_1) = u(k_1)$  and the fact that the external fermions are on-shell, i.e.  $n_+ \cdot k_1 = 0$ .

$$\mathcal{M}_{\text{vertex loop}}^{(1)} = -\frac{\mathcal{M}^{(0)}}{i(2\pi)^n} m^2 g^2 J_2, \quad (\text{C.7})$$

where the integral  $J_2$  is

$$\begin{aligned}
J_2 &= \int d^n l \frac{1}{mn_+ \cdot l} \frac{1}{l^2} \frac{1}{2m(v \cdot l + \mathcal{D})} \\
&\stackrel{(\mathcal{B}, \mathcal{Y})}{=} 2 \int_0^1 dx dy \int d^n l \frac{y}{[(1-y)l^2 + ymn_+ \cdot l + xy(mn_- \cdot l + 2m\mathcal{D})]^3} \\
&= 2 \int_0^1 dx dy \frac{y}{(1-y)^3} \int d^n l \frac{1}{[(l + \frac{y}{1-y} m \frac{n_+}{2} + x \frac{y}{1-y} m \frac{n_-}{2})^2 + x \frac{y}{1-y} 2m\mathcal{D} + x \frac{y^2}{(1-y)^2} m^2]^3} \\
&\stackrel{(\infty', \Delta, \infty)}{=} i\pi^{n/2} \Gamma(1 - \frac{\epsilon}{2}) (2m\mathcal{D})^{\epsilon/2-1} \int_0^1 dx x^{\epsilon/2-1} \int_0^1 dy y^{\epsilon/2} (1-y)^{\epsilon/2-1} [1 - y(1 - \frac{m}{2\mathcal{D}})]^{\epsilon/2-1} \\
&= \frac{i\pi^{n/2}}{m^2} (2\mathcal{D})^\epsilon \frac{2}{\epsilon} \Gamma(-\epsilon) \Gamma(1 + \frac{\epsilon}{2}). \quad (\text{C.8})
\end{aligned}$$

The vertex correction (C.7) then becomes

$$\mathcal{M}_{\text{vertex loop}}^{(1)} = -\mathcal{M}^{(0)} \alpha_g \mu^\epsilon (4\pi)^{-\epsilon/2} \left( \frac{2\mathcal{D}}{\mu} \right)^\epsilon \left[ \frac{4}{\epsilon} \Gamma(-\epsilon) \Gamma(1 + \frac{\epsilon}{2}) \right]. \quad (\text{C.9})$$

By combining (C.5) and (C.9) we can find the sum of the loop of the EFT corrections

$$\begin{aligned}
\mathcal{M}_{\text{loop corr.}}^{(1)} &= \mathcal{M}_{\text{SE loop}}^{(1)} + 2\mathcal{M}_{\text{vertex loop}}^{(1)} \\
&= -\mathcal{M}^{(0)} \alpha_g \mu^\epsilon (4\pi)^{-\epsilon/2} \left( \frac{2\mathcal{D}}{\mu} \right)^\epsilon \left[ \frac{8}{\epsilon} \Gamma(-\epsilon) \Gamma(1 + \frac{\epsilon}{2}) + 4\Gamma(-1 - \epsilon) \Gamma(1 + \frac{\epsilon}{2}) \right]. \quad (\text{C.10})
\end{aligned}$$

By using  $z\Gamma(z) = \Gamma(1+z)$ , together with (B.8), (C.10) can be written as

$$\begin{aligned}
\mathcal{M}_{\text{loop corr.}}^{(1)} &= \mathcal{M}^{(0)} \alpha_g \mu^\epsilon (4\pi)^{-\epsilon/2} e^{\gamma_E \epsilon/2} \left( \frac{2\mathcal{D}}{\mu} \right)^\epsilon e^{\frac{5\pi^2}{48} \epsilon^2} \left[ \frac{8}{\epsilon^2} - \frac{4}{\epsilon(1+\epsilon)} \right] \\
&= \mathcal{M}^{(0)} \alpha_g \bar{\mu}^\epsilon \left( \frac{2\mathcal{D}}{\mu} \right)^\epsilon \left[ \frac{8}{\epsilon^2} - \frac{4}{\epsilon} + 4 + \frac{5\pi^2}{6} \right]. \quad (\text{C.11})
\end{aligned}$$

# Bibliography

1. De Wit, B., Laenen, E. & Smith, J. *Field Theory in Particle Physics* 2013.
2. Peskin, M. E. & Schroeder, D. V. *An Introduction to Quantum Field Theory* (Westview Press, 1995).
3. Veltman, M. *Diagrammatica* (Cambridge University Press, 1994).
4. Cutkosky, R. Singularities and discontinuities of Feynman amplitudes. *J. Math. Phys.* **1**, 429–433 (1960).
5. Denner, A. Techniques for the calculation of electroweak radiative corrections at the one-loop level and results for W-physics at the LEP200. *Fortschritte der Physik* **41**, 307–420 (1993).
6. Quadt, A. Top quark physics at hadron colliders. *European Physical Journal C* **48**, 835–1000 (2006).
7. Heinemeyer, S. *et al.* Handbook of LHC Higgs Cross Sections: 3. Higgs Properties. arXiv: 1307.1347 [hep-ph] (2013).
8. CMS Collaboration. Constraints on the Higgs boson width from off-shell production and decay to Z-boson pairs. *Phys. Lett. B* **736**, 64 (2014).
9. Olive (Particle Data Group) *et al.* 2014 Review of Particle Physics. *Chinese Physics C* **38**, 090001 (2014).
10. Bohm, A. R. & Harshman, N. On the Mass and Width of the Z-boson and Other Relativistic Quasistable Particles. *Nucl. Phys. B* **581**, 91–115 (2000).
11. Willenbrock, S. & Valencia, G. On the definition of the Z boson mass. *Phys. Lett. B* **259**, 373–376 (1991).
12. Sirlin, A. Observations concerning mass renormalization in the electroweak theory. *Phys. Letters B* **267**, 240–242 (1991).
13. Sirlin, A. Theoretical Considerations Concerning the  $Z^0$  Mass. *Physical Review Letters* **67**, 2127–2130 (1991).
14. Stuart, R. G. Gauge invariance, analyticity and physical observables at the  $Z^0$  resonance. *Phys. Letters B* **262**, 113–119 (1991).
15. Veltman, H. Mass and width of unstable gauge bosons. *Z. Phys. C* **62**, 35–51 (1994).
16. The LEP Collaborations: ALEPH, DELPHI, L3 and OPAL. Electroweak parameters of the  $Z^0$  resonance and the standard model. *Phys. Lett. B* **276**, 247–253 (1992).
17. Beenakker, W. *et al.* The fermion-loop scheme for finite-width effects in  $e^+e^-$  annihilation into four fermions. *Nucl. Phys. B* **500**, 255–298 (1997).
18. Baur, U. & Zeppenfeld, D. Finite width effects and gauge invariance in radiative W production and decay. *Phys. Rev. Letters* **75**, 1002–1005 (1995).
19. Vermaseren, J. New features of FORM. arXiv: math-ph/0010025 (2000).

20. Argyres, E. N. *et al.* Stable calculations for unstable particles: restoring gauge invariance. *Physics Letters B* **358**, 339–346 (1995).
21. Kronfeld, A. S. The Perturbative pole mass in QCD. *Phys. Rev. D* **58**, 051501 (1998).
22. Veltman, M. Unitarity and causality in a renormalizable field theory with unstable particles. *Physica* **29**, 186 (1963).
23. Denner, A. & Lang, J. The Complex-Mass Scheme and Unitarity in perturbative Quantum Field Theory. arXiv: [hep-ph/1406.6280](https://arxiv.org/abs/hep-ph/1406.6280) (2014).
24. Beneke, M., Chapovsky, A. P., Signer, A. & Zanderighi, G. Effective theory approach to unstable particle production. *Phys. Rev. Lett.* **93**, 011602 (2004).
25. Beneke, M., Chapovsky, A., Signer, A. & Zanderighi, G. Effective theory calculation of resonant high-energy scattering. *Nucl. Phys.* **B686**, 205–247 (2004).
26. Beneke, M. Unstable-particle effective theory. *Nucl. Part. Phys. Proc.* **261-262**, 218–231 (2015).
27. Beneke, M. & Smirnov, V. Asymptotic expansion of Feynman integrals near threshold. *Nucl. Phys.* **B522**, 321–344 (1998).
28. Becher, T. *Soft-Collinear Effective Theory. Part 1: The strategy of regions* <[https://people.phys.ethz.ch/~banfi/gaugetheory/Becher/SCET\\_I.pdf](https://people.phys.ethz.ch/~banfi/gaugetheory/Becher/SCET_I.pdf)>.
29. Jantzen, B. Foundation and generalization of the expansion by regions. *JHEP* **1112**, 076 (2011).
30. Smirnov, V. A. & Rakhmetov, E. R. The regional strategy in the asymptotic expansion of two-loop vertex Feynman diagrams. *Theor. Math. Phys.* **120**, 870 (1999).
31. Smirnov, V. A. Problems of the strategy of regions. *Phys. Lett. B* **465**, 226 (1999).
32. Smirnov, V. A. *Applied Asymptotic Expansion in Momenta and Masses* ISBN: 879-3-540-42334-8 (Springer, 2002).
33. Anastasiou, C., Duhr, D. & Dulat, F. Real-virtual contribution to the inclusive Higgs at  $N^3LO$ . *JHEP* **1312**, 088 (2013).
34. (eds Ellis, R. K., Hill, C. T. & Lykken, J. D.) *Proc. Theoretical Advanced Study Institute* (World Scientific, 1992), 589.
35. Grinstein, B. The static quark effective theory. *Nucl. Phys. B* **339**, 253–576 (1990).
36. Bauer, C. W., Fleming, S., Pirjol, D. & Stewart, I. An effective field theory for collinear and soft gluons: Heavy to light decays. *Phys. Rev. D* **63**, 114020 (2001).
37. Bauer, C. W., Fleming, S., Pirjol, D. & Stewart, I. W. Soft-Collinear Factorization in Effective Field Theory. *Phys. Rev. D* **65**, 054022 (2002).
38. Beneke, M., Chapovsky, A. P., Diehl, M. & Feldmann, T. Soft-collinear effective theory and heavy-to-light currents beyond leading power. *Nucl. Phys. B* **643**, 431 (2002).
39. Ossola, G., Papadopoulos, C. G. & Pittau, R. CutTools: A Program Implementing the OPP reduction method to compute one-loop amplitudes. *JHEP* **0803**, 042 (2008).
40. Papanastasiou, A. S., Federix, R., Frixione, S., Hirschi, V. & Maltoni, F. Single-top  $t$ -channel production with off-shell and non-resonant effects. *Phys. Lett.* **B726**, 223–227 (2013).
41. Bigi, I. I. Y., Dokshitzer, Y. L., Khoze, V. A., Kuhn, J. H. & Zerwas, P. M. Production and Decay Properties of Ultraheavy Quarks. *Phys. Lett.* **B181**, 157 (1986).



42. Van der Heide, J., Laenen, E., Phaf, L. & Weinzierl, S. Helicity amplitudes for single top production. *Phys. Rev.* **D62**, 074025 (2000).